FAA-75-3

REPORT NO. FAA-RD-75-31

SIDELOBE SUPPRESSION MODE PERFORMANCE OF ATCRBS WITH VARIOUS ANTENNAS

Jovan Zatkalik
Dipak L. Sengupta
Chen-To Tai

FEBRUARY 1975

INTERIM REPORT

Prepared for
U.S. DEPARTMENT OF TRANSPORTATION
FEDERAL AVIATION ADMINISTRATION
Systems Research and Development Service
Washington DC 20591

TECHNICAL REPORT STANDARD TITLE PAGE

1. Report No.	2. Government Accession No.	3. Recipient's Catalog No.
FAA-RD-75-31		

4. Title and Subtitle
SIDELOBE SUPPRESSION MODE PERFORMANCE OF ATCRBS WITH VARIOUS ANTENNAS

5. Report Date
February 1975

6. Performing Organization Code

7. Author(s)
Jovan Zatkalik, Dipak L. Sengupta, and Chen-To Tai*

8. Performing Organization Report No.
DOT-TSC-FAA-75-3

9. Performing Organization Name and Address
The University of Michigan
College of Engineering
Dept. of Electrical and Computer Engineering
Radiation Laboratory
Ann Arbor MI 48105

10. Work Unit No.
FA519/R5119

11. Contract or Grant No.
DOT-TSC-717

12. Sponsoring Agency Name and Address
U.S. Department of Transportation
Federal Aviation Administration
Systems Research and Development Service
Washington DC 20591

13. Type of Report and Period Covered
Interim Report
July 1973-June 1974

14. Sponsoring Agency Code

15. Supplementary Notes
*Under contract to: U.S. Department of Transportation
Transportation Systems Center
Kendall Square
Cambridge MA 02142

16. Abstract

The SLS mode performance of terminal and enroute ATCRBS using existing and various improved antennas in the presence of perfectly dielectric flat ground are investigated theoretically. Necessary analytical expressions for various quantities characterizing the system performance have been derived. A computer program has been developed for the computation and tabulation of these quantities as functions of the elevation angle of the observation point for different combinations of heights of the directional and omnidirectional antennas. For each antenna combination results are given for the following seven quantities: the P1 and P2 pulse intensities, the pulse ratio P1/P2, the mainbeam killing and sidelobe punch-through zones in space, the effective azimuth beamwidth, the number of replies and the coverage diagram. Short discussions of results are given wherever appropriate.

17. Key Words	18. Distribution Statement
Sidelobe Suppression, Sidelobe, 'Punch Through', Antennas, Vertical Lobing, Main Beam Killing	DOCUMENT IS AVAILABLE TO THE PUBLIC THROUGH THE NATIONAL TECHNICAL INFORMATION SERVICE, SPRINGFIELD, VIRGINIA 22161

19. Security Classif. (of this report)	20. Security Classif. (of this page)	21. No. of Pages	22. Price
Unclassified	Unclassified	160	

Form DOT F 1700.7 (8-69)

Preface

This report investigates the SLS performance of the present ATCRBS linear array antenna and of the various ATCRBS Improvement Antennas in terminal and enroute configurations. The improvement antennas were developed by Hazeltine, Texas Instruments and Westinghouse under contract to the Transportation Systems Center. The NADIF Fix was developed by NAFEC as a possible enroute improvement antenna prior to those developed under contract and is included in these investigations. These antennas represent solutions to the vertical lobing problem caused by the relatively narrow vertical aperture of the present ATCRBS antenna. The report is a preliminary attempt at theoretically quantifying the performance of each antenna so that improvements, if any, may be properly assessed.

We are pleased to acknowledge the benefit of several discussions with Mr. Frank LaRussa and Dr. Rudy Kalafus of DOT/TSC, Cambridge. We also acknowledge the valuable counsel and suggestions by Professor Ralph E. Hiatt. We wish to acknowledge with thanks the work of Dr. Mohammed Hidayet who prepared the computer programming for this report.

TABLE OF CONTENTS

Table of Contents (cont'd)

LIST OF ILLUSTRATIONS

List of Illustrations (cont'd)

List of Illustrations (cont'd)

List of Illustrations (cont'd)

List of Illustrations (cont'd)

LIST OF TABLES

1. INTRODUCTION

1.1 Preliminary Remarks

This is the first technical report on contract DOT-TSC-717 entitled "Volumetric Study in Support of ATCRBS". The effects of ground on the interrogator sidelobe suppression (SLS) mode performance of ATCRBS using various antennas are theoretically investigated in the present report.

The basic principle of the interrogator sidelobe suppression system used in ATCRBS is well-known and is discussed in the open literature [1], [2], [3]. It mainly depends on the ability of the transponder logic to recognize the P1 and P2 pulses, radiated by the interrogator directional and omnidirectional antennas respectively, to compare their amplitudes, to decide whether their ratio is above or below some predetermined threshold levels and to inhibit the transponder replies if the latter occurs. Consider an ideal case when the free space elevation plane patterns of the two interrogator antennas are identical and their phase centers coincide. In this situation, with appropriate levels of the radiated P1 and P2 pulses and with proper threshold level at the transponder, the received pulse ratio P1/P2 at the transponder will always stay above the threshold level within the mainbeam region and below the threshold level within the sidelobe region. Consequently the transponder logic will operate in the desirable fashion at all elevation angles.

However, in reality, the phase centers of the two antennas seldom coincide. As a result, even with ideally matched free space elevation plane patterns of directional and omnidirectional antennas, the presence of ground causes strong lobing structures in the patterns which are not matched with each other. Thus the received pulse ratio P1/P2 is no longer a constant but varies strongly with the elevation angle θ of the transponder. The variation of the pulse ratio may be of such an amount that critical threshold levels are reached causing the transponder logic to operate in an undesirable fashion, thereby giving rise to mainbeam killing and sidelobe punch-through (false target) zones. Between these two

extreme zones in space there lies the effective zone where the transponder will reply at a rate depending on the interrogator pulse repetition frequency, the interrogator antenna scanning rate, and the effective azimuth beamwidth of the interrogator antenna.

1.2 Outline of the Report

The purpose of the present report is to investigate theoretically the effects of ground on the interrogator sidelobe suppression mode of operation of the ATCRBS for nine different interrogator antennas and for various combinations of heights of directional and omnidirectional antennas located above a flat infinite ground. The basic theoretical formulations of various quantities of interest are given in Section 2. The quantities of interest are the intensities of the radiated pulses at a far field point where a transponder is located, the received pulse ratio at the transponder, the potential mainbeam killing and sidelobe punch-through zones in space, the effective azimuth beamwidth of the interrogator directional antenna, the effective number of replies from the transponder and the coverage diagram.

The various antennas along with their free space elevation plane patterns are discussed in Section 3. The reflection coefficient of the ground as a function of the elevation angle is also discussed in Section 3.

Section 4 gives the numerical results and discussions of the various quantities of interest.

A general discussion of the results along with our conclusions are given in Section 5.

1.3 Basic Assumptions

It is appropriate to give here the basic assumptions and approximations on which the present investigation is based. These should be noted when applying the results to an actual system. The theoretical formulations used make the following assumptions and approximations:

1.3.1 The directional and omnidirectional interrogator antennas have definite phase centers located generally at different heights above ground. Over the entire range of elevation angles of interest the free space field patterns

are equiphase with respect to the corresponding phase centers with possible jumps by $\pm \pi$ at some particular angles.

1.3.2 For most of the antennas, the free space directional and omnidirectional elevation plane patterns are ideally matched with the exceptions of the NADIF-fix antenna with the Westinghouse omni and the NADIF-fix antenna with the existing "small" omni (called the NADIF-fix II and the NADIF-fix III antennas, respectively).

1.3.3 The elevation pattern profile at different azimuth section is the same. This implies that the elevation pattern profile in the region of the azimuthal sidelobe is of the same shape as in the region of the mainbeam. Consequently if $f(\theta)$ is the elevation pattern profile in the plane of symmetry of the mainbeam, then $Lf(\theta)$ will be the elevation pattern profile of the azimuthal sidelobe, where L is the sidelobe level relative to the maximum of the mainbeam (note that $0 < |L| \leq 1$).

1.3.4 The nominal or 3 dB beamwidths of the azimuthal plane pattern of the directional antennas are independent of the elevation angle θ. For small elevation angles (say $\theta \leq 5^{o}$) this assumption is quite acceptable.

1.3.5 For most of the antennas the elevation plane patterns are available. For the purpose of computational simplicity we have developed approximate analytical expressions for these patterns by an interpolation procedure based on Woodward and Lawson's aperture synthesis method [4].

1.3.6 The ground is flat and smooth and is a pure dielectric with permittivity $\epsilon = 3$.

1.3.7 The mainbeam killing takes place whenever the P1 and P2 pulse amplitudes at the transponder satisfy the relation $P1(dB) - P2(dB) \leq 9\,dB$.

1.3.8 In the azimuthal sidelobe region, sidelobe punch-through occurs whenever the two pulses at the transponder satisfy the relation $P1(dB) - P2(dB) \geq 0$.

2. BASIC THEORETICAL FORMULATIONS

2.1 The Intensities of P1 and P2 Pulses

The ATCRBS directional and omnidirectional antennas, mounted on a tower, are represented schematically in Fig. 1. The antenna system is located

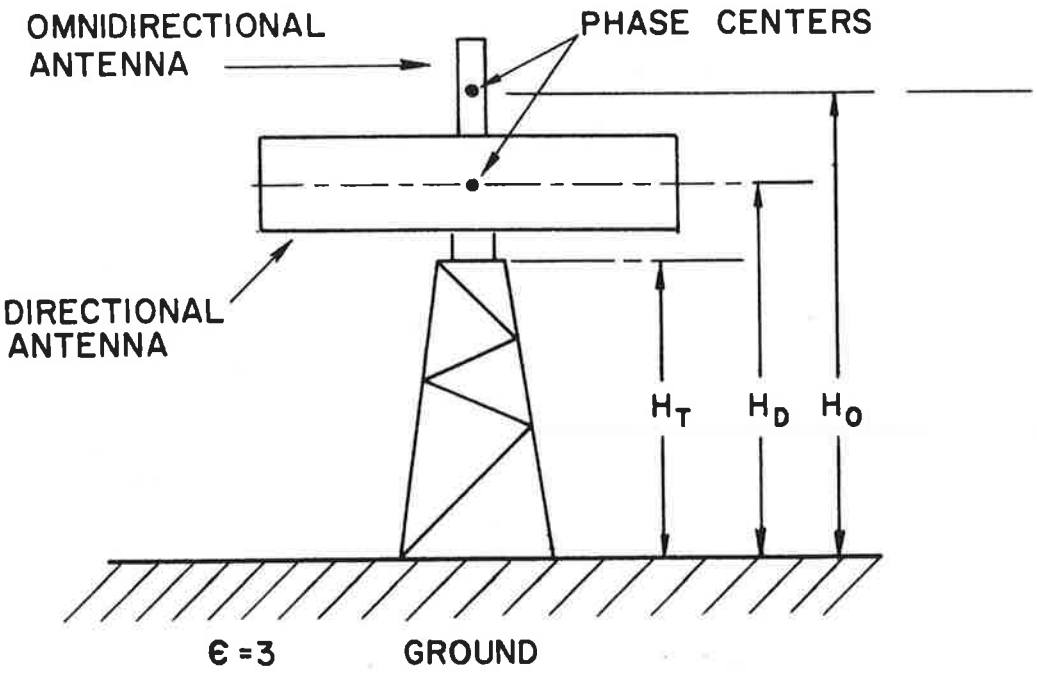

FIG. 1: ATCRBS directional and omnidirectional antennas located above ground.

above an infinite planar ground which is assumed to be a pure dielectric with relative dielectric constant equal to 3. It is also assumed that the phase centers of the directional and omnidirectional antennas lie on a vertical line. The horizontal displacement between the antenna phase centers will not be considered because it can be shown that a small horizontal displacement, compared with the target distance, has no effect on the SLS mode of operation.

Suppose that the phase center of an antenna with normalized free space elevation plane for field pattern $f(\theta)$ is located at a height Z above ground. After applying the standard procedure, as shown in Fig. 2, we obtain the following

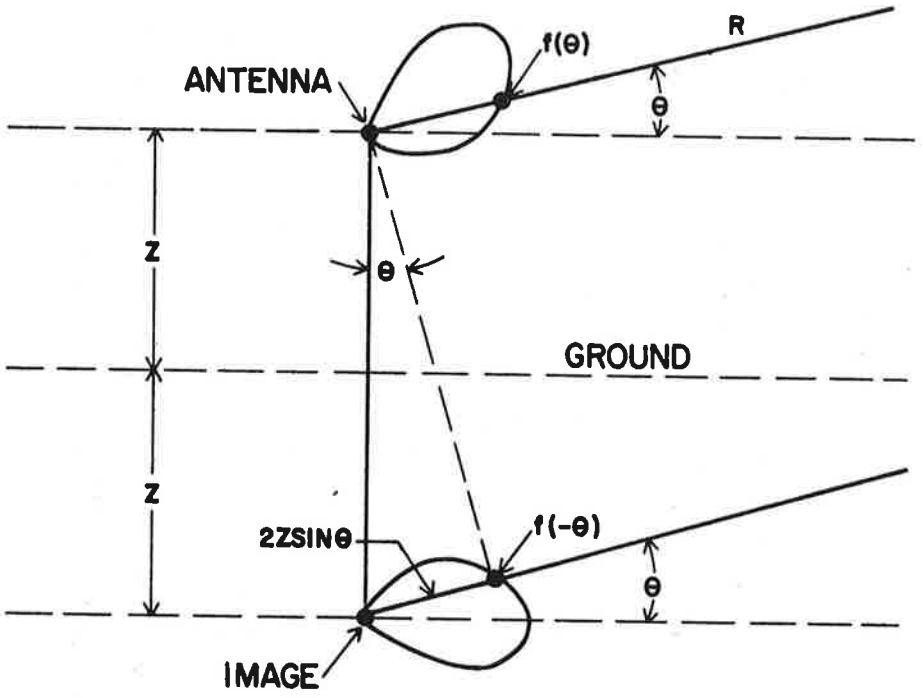

FIG. 2: Geometrical representation of an antenna and its image.

expression for the electric field at a distant point $M(R, \theta)$, located in the plane of symmetry of the azimuthal pattern which is taken to be $\phi = 0^{o}$.

$$E(\theta) = \frac{\sqrt{30WG}}{R} e^{-j\beta R} \left[f(\theta) + \rho(\theta) f(-\theta) e^{-j2\beta Z \sin\theta} \right], \qquad (1)$$

where

W is the power radiated by the antenna

G is the maximum gain of the antenna

$\rho(\theta)$ is the reflection coefficient of the ground for the appropriate polarization

$\beta = 2\pi/\lambda$ is the free space propagation constant.

In the present case $\rho(\theta)$ is a real quantity and we obtain the magnitude of the complex expression given by Eq. (1) as follows:

$$|E(\theta)| = \frac{\sqrt{30WG}}{R}\left\{\left[f(\theta)\right]^2 + 2\rho(\theta)\, f(\theta)\, f(-\theta)\cos(2\beta Z \sin\theta) + \left[\rho(\theta)\, f(-\theta)\right]^2\right\}^{1/2}. \tag{2}$$

The intensities of the P1 and P2 pulses at the far field point $M(R,\theta)$ are defined to be the magnitudes of the far electric fields, given by Eq. (2), produced by the directional and omnidirectional antennas, respectively, and located at appropriate heights above ground. After substituting the appropriate values for $f(\theta)$ and Z in Eq. (2), we obtain the following two expressions for the respective pulse amplitudes:

$$P1(\theta) = \frac{\sqrt{30W_dG_d}}{R}\left\{\left[f_d(\theta)\right]^2 + 2\rho(\theta)\, f_d(\theta)\, f_d(-\theta)\cos(2\beta H_d \sin\theta) + \left[\rho(\theta)\, f_d(-\theta)\right]^2\right\}^{1/2}$$

$$= AF_d(\theta)\ , \tag{3}$$

$$P2(\theta) = \frac{\sqrt{30W_0G_0}}{R}\left\{\left[f_0(\theta)\right]^2 + 2\rho(\theta)\, f_0(\theta)\, f_0(-\theta)\cos(2\beta H_0 \sin\theta) + \left[\rho(\theta)\, f_0(-\theta)\right]^2\right\}^{1/2}$$

$$= \frac{A}{K_0} F_0(\theta)\ , \tag{4}$$

where

$$A = \frac{\sqrt{30W_dG_d}}{R} \tag{5}$$

W_d is the power radiated by the directional antenna

G_d is the maximum gain of the directional antenna in free space

W_0, G_0 are the similar quantities for the omnidirectional antenna

$$K_0 = \left(\frac{W_d G_d}{W_0 G_0}\right)^{1/2} \tag{6}$$

$f_d(\theta)$ and $f_0(\theta)$ are the free space elevation plane patterns of the directional and omnidirectional antennas respectively

$F_d(\theta)$ and $F_0(\theta)$ are the elevation plane patterns of the directional and omnidirectional antennas in the presence of ground and are as defined by Eqs. (3) and (4).

From Eqs. (3) and (4) we obtain the following expression for the pulse ratio $P1(\theta)/P2(\theta)$ at the far field point $M(R, \theta)$:

$$\frac{P1(\theta)}{P2(\theta)} = K_0 F_d(\theta)/F_0(\theta) \tag{7}$$

Instead of representing the absolute value of the pulse ratio given by Eq. (7), it is found to be more convenient to use the normalized pulse ratio which is defined as follows:

$$\frac{1}{K_0}\,\frac{P1(\theta)}{P2(\theta)} = \frac{F_d(\theta)}{F_0(\theta)} \tag{7a}$$

or, expressed in dB, the normalized pulse ratio is given by:

$$\text{normalized pulse ratio} = 20 \log_{10} \frac{F_d(\theta)}{F_0(\theta)} = 20 \log_{10} \frac{P1(\theta)}{P2(\theta)} - 20 \log_{10} K_0 \tag{7b}$$

In the ideal situation when the phase centers of the two antennas coincide and if their free space elevation plane patterns are identical, then Eq. (7) reduces to the following:

$$\frac{P1(\theta)}{P2(\theta)} = K_0 \tag{8}$$

Equation (8) indicates that in the ideal situation the pulse ratio is a constant equal to K_0 in the vertical plane $\phi = 0^o$. We shall call the quantity K_0 the nominal pulse ratio. From Eq. (6) it is found that with given G_d and G_0, the nominal pulse ratio can be adjusted to the desired value by using the appropirate values for the radiated powers W_d and W_0. For an observation point in the mainbeam of the directional antenna, the common value of the nominal pulse ratio, as recommended by the U.S. National Aviation Standards, is 18dB.

The expressions given above are valid for the far field point located within the azimuthal mainbeam of the directional antenna. For a field point located within the azimuthal sidelobe region of the directional antenna, the above expressions can also be used provided $f_d(\theta)$ is replaced by $Lf_d(\theta)$ where L is the sidelobe level compared to the mainbeam amplitude (note: in general $0 \leq |L| \leq 1$). For example, if the field point is located in the azimuthal sidelobe region, Eq. (7) should be modified to:

$$\frac{P1(\theta)}{P2(\theta)} = LK_0 \frac{F_d(\theta)}{F_0(\theta)} \quad , \qquad \text{in the azimuthal sidelobe region.} \qquad (9)$$

2.2 The Pulse Ratio: $P1(\theta)/P2(\theta)$

As discussed in Section 2.1, the pulse ratio at a far field point varies with the elevation angle at that point. Using Eqs. (3) and (4) we write explicitly the following general expression for the pulse ratio, for a point located in the azimuthal mainbeam.

$$\frac{P1(\theta)}{P2(\theta)} = K(\theta) = K_0 \frac{F_d(\theta)}{F_0(\theta)}$$

$$= K_0 \frac{\left\{\left[f_d(\theta)\right]^2 + 2\rho(\theta) f_d(\theta) f_d(-\theta) \cos(2\beta H_d \sin\theta) + \left[\rho(\theta) f_d(-\theta)\right]^2\right\}^{1/2}}{\left\{\left[f_0(\theta)\right]^2 + 2\rho(\theta) f_0(\theta) f_0(-\theta) \cos(2\beta H_0 \sin\theta) + \left[\rho(\theta) f_0(-\theta)\right]^2\right\}^{1/2}} \qquad (10)$$

At a certain angle θ the deviation of the pulse ratio $K(\theta)$ from its nominal value K_0 is an important parameter which characterizes the quality of a given antenna. We shall discuss this further in later sections.

For observation point located in the azimuthal sidelobe region, the pulse ratio is given by $LK(\theta)$, where $K(\theta)$ is given by Eq. (10). As discussed in Section 2.1, the pulse ratio within the mainbeam as well as in the sidelobe region will be normalized with respect to the nominal pulse ratio.

2.3 Mainbeam Killing and Sidelobe Punch-Through Zones

In order to define and obtain the mainbeam killing and sidelobe punch-through zones in space, let us introduce some conventions based on the standards for the beacon system. In the mainbeam region it is normally supposed that the P1 pulse amplitude is sufficiently greater than that of the P2 pulse, as shown in Fig. 3. Under this condition the transponder disab ling logic does not operate and

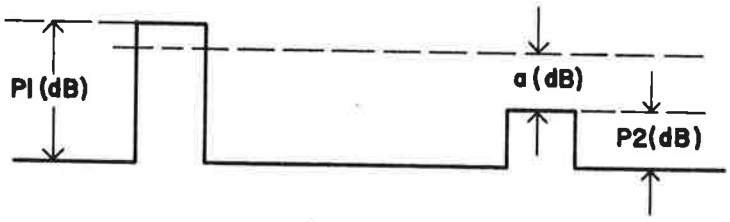

FIG. 3: P1 and P2 pulse levels within the azimuthal mainbeam region (normal condition).

regular replies are obtained. Let us assume that transponder disabling logic operates whenever the following relationship holds:

$$P1(dB) - P2(dB) \leq a\,dB \ , \tag{11}$$

where the quantity a is called the mainbeam killing threshold.

In the sidelobe region it is usually assumed that the P2 pulse amplitude is sufficiently greater than the P1 pulse amplitude as represented in Fig. 4.

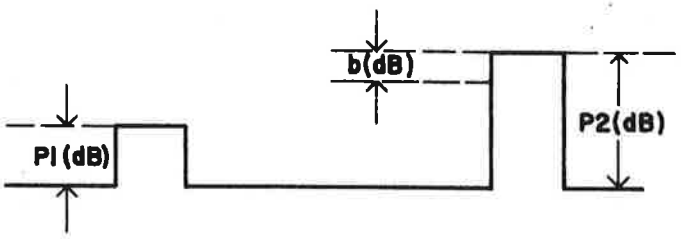

FIG. 4: P1 and P2 pulse levels within the azimuthal sidelobe region (normal condition).

Under this condition the transponder logic suppresses all replies. Let us assume that the transponder replies whenever the following relationship holds:

$$P2(dB) - P1(dB) \leq b\,dB \ , \qquad (12)$$

where the quantity b is called the sidelobe punch-through threshold.

The choice of the two threshold values a and b will influence considerably the extents of the mainbeam killing and sidelobe punch-through regions in space. Let us consider the three regions with respect to the P1 and P2 pulses as shown in Fig. 5, where it is assumed that the level of the P2 pulse is constant and that

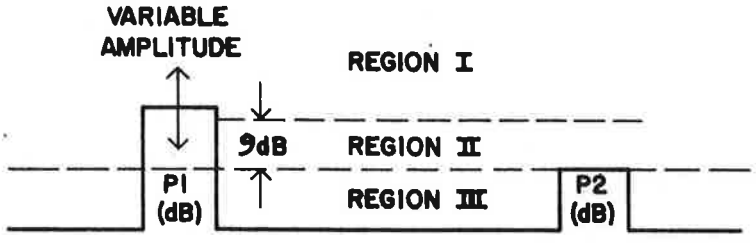

FIG. 5: Different regions for defining the threshold levels.

of the P1 pulse is variable. The region I corresponds to the condition P1(dB) - P2(dB) > 9 dB and according to the National Standards the transponder should reply with high probability in this region. In region II, where $0 \leq$ P1(dB) - P2(dB) $\leq$ 9 dB the transponder may or may not reply. In region III where P1(dB) - P2(dB) < 0 the transponder replies are suppressed with high probability.

Evidently the National Standards do not define any sharp transitions between the above three regions. For our purpose, in order to avoid the probabilistic approach, we must choose each of the thresholds a and b as definite boundaries between the regions with corresponding probabilities of reply as 0 and 1. We shall assume that the mainbeam killing threshold level is that of the boundary between the regions I and II in Fig. 5 and the sidelobe punch-through threshold level is that of the boundary between regions II and III, i.e., a = 9 dB and b = 0 dB. This choice of the threshold levels would give indications of the mainbeam killing and sidelobe punch-through zones for the worst case. A more realistic choice may be a = b = 4.5 dB. We shall later discuss the effects of this latter choice for some special cases.

The mainbeam killing zones in space represent the zones of elevation angle θ in a given vertical plane in the azimuthal mainbeam region where the pulse ratio at the transponder is less than or equal to the appropriate threshold level. They are defined by the following inequality:

$$\frac{P1(\theta)}{P2(\theta)} \leq a \quad ; \tag{13a}$$

expressed in dB, Eq. (13a) is modified to the following:

$$P1(dB) - P2(dB) \leq a\,(dB) \quad . \tag{13b}$$

After using Eqs. (7) and (13b), an expression is obtained for the mainbeam killing zones whenever the normalized pulse ratio satisfies the relation:

$$20 \log_{10} F_d(\theta) - 20 \log_{10} F_0(\theta) \leq a(dB) - 20 \log_{10} K_0 \quad . \tag{14}$$

Equation (14) indicates that the extent and the number of zones depend on the nominal pulse ratio K_0 for a given threshold level a.

The sidelobe punch-through zones represent the zones of elevation angle θ in a given vertical plane in the azimuthal sidelobe region where the pulse ratio is above the threshold level b. If the sidelobe level is L, then these zones are defined by:

$$L \frac{P1(\theta)}{P2(\theta)} \geq b \tag{15}$$

i.e., $LK(\theta) \geq b$. Sidelobe punch-through zones occur whenever the normalized pulse ratio in the sidelobe region satisfies the following relation:

$$20 \log_{10} F_d(\theta) - 20 \log_{10} F_0(\theta) > L + b(dB) - 20 \log_{10} K_0 \tag{16}$$

where the sidelobe level is expressed as $-L$ dB.

2.4 Effective Azimuth Beamwidth and Number of Replies

In order to obtain the number of replies from a transponder the azimuthal plane patterns of the interrogator antennas must be considered. For simplicity let us assume that the three dimensional pattern of the directional antenna in free space may be represented by:

$$f_{dt}(\theta, \phi) = f_d(\theta)\, \psi_d(\phi) \ , \tag{17}$$

where $f_d(\theta)$ is the free space elevation plane pattern of the directional antenna, discussed earlier, in the plane $\phi = 0^\circ$ and $\psi_d(\phi)$ is the azimuthal plane pattern. In the presence of ground, eq. (17) is modified to the following:

$$F_{dt}(\theta, \phi) = F_d(\theta)\psi_d(\phi) \ , \tag{18}$$

where F_d is as defined before (Eq. 3).

The omnidirectional antenna is assumed to be ideally isotropic in the azimuthal plane and its three-dimensional pattern in the presence of ground is represented by:

$$F_{0t}(\theta,\phi) = F_0(\theta) \quad , \tag{19}$$

where F_0 is as defined before (Eq. 4).

The intensities of the P1 and P2 pulses at a field point (R,θ,ϕ) are given by the following:

$$P1(\theta,\phi) = AF_{dt}(\theta,\phi) = AF_d(\theta)\psi_d(\phi) = P1(\theta)\psi_d(\phi) \quad , \tag{20}$$

$$P2(\theta,\phi) = \frac{A}{K_0} F_{0t}(\theta,\phi) = \frac{A}{K_0} F_0(\theta) = P2(\theta) \quad , \tag{21}$$

where $P1(\theta)$ and $P2(\theta)$ are given by Eqs. (3) and (4).

For some given elevation angle θ, the azimuth plane sketch of the $P1(\theta,\phi)$ and $P2(\theta,\phi)$ amplitudes as functions of ϕ are shown in Fig. 6. Another isotropic

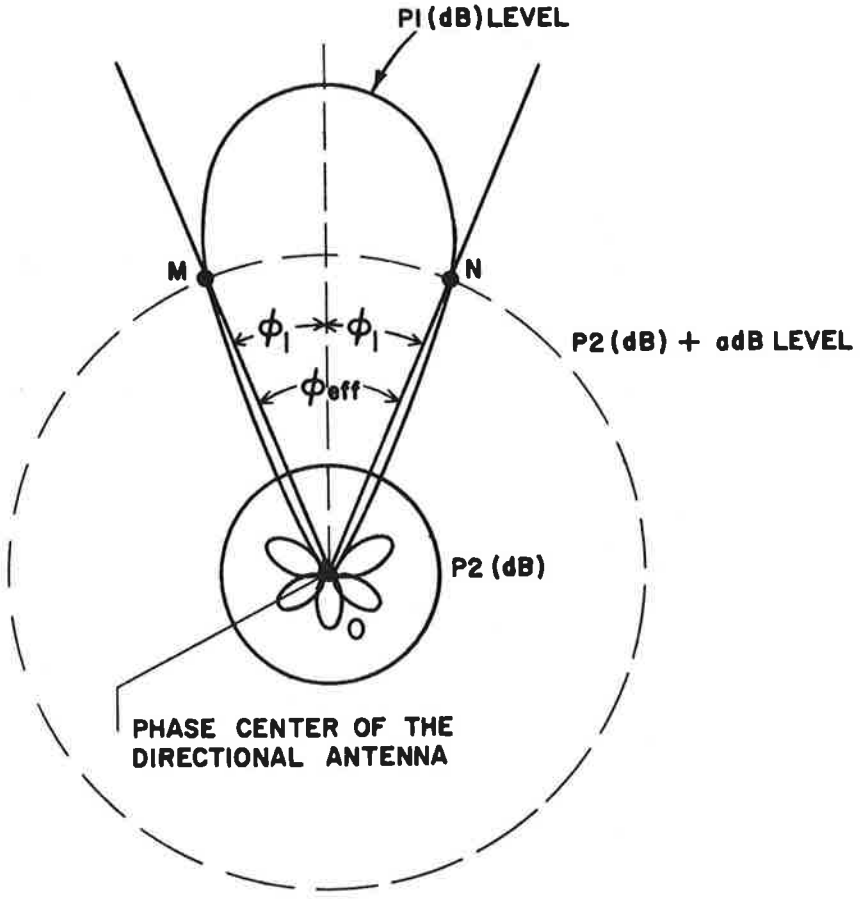

FIG. 6: Diagram showing the effective azimuthal beamwidth

level curve of value P2(dB) + a dB, where a is the mainbeam killing threshold level, is also shown in Fig. 6. The angle MON is defined to be the effective azimuth beamwidth (ϕ_{eff}). Targets within MON will reply and those outside will not. Let us write

$$\phi_{eff} = 2\phi_1 \quad , \tag{22}$$

where ϕ_1 is as shown in Fig. 6 and is the positive solution of the equation:

$$20 \log_{10} P1(\theta, \phi_1) = 20 \log P2(\theta) + a(dB) \quad . \tag{23}$$

By using Eqs. (20) and (21), Eq. (23) is modified as follows:

$$20 \log_{10} \psi_d(\phi_1) = -20 \log \frac{P1(\theta)}{P2(\theta)} + a(dB) = -20 \log K(\theta) + a(dB) \quad . \tag{24}$$

It is now assumed that the azimuth plane pattern $\psi_d(\phi)$ has the form of a universal Gaussian curve and is given by

$$\psi_d(\phi) = \exp\left[-1.39(\phi/\phi_0)^2\right] \tag{25}$$

where ϕ_0 is the total half-power beamwidth of the pattern. After introducing Eq. (25) into Eq. (24) we obtain the following for the effective azimuthal beamwidth:

$$\phi_{eff} = 2\phi_0 \sqrt{\frac{20 \log K(\theta) - a(dB)}{12.0735}} \quad . \tag{26}$$

The number of replies from the transponder is now defined as follows:

$$N = f_i \frac{\phi_{eff}}{\Omega} \quad , \tag{27}$$

where

f_i is the interrogator pulse repetition rate
Ω is the angular scanning rate in deg/sec.

Both the effective azimuthal beamwidth and the number of replies have practical meaning for targets which are relatively close to the interrogating station

2.5 Coverage Diagram

In general, the maximum range of a beacon system is a statistical quantity depending on the acceptable probability of detection and tolerable probability of false alarm. For the purpose of the present investigation, we shall adopt the following convention which seems to be appropriate for practical purposes. Let R_0 denote the maximum free space range of a beacon system for some given and convenient probabilities of detection and false alarm. It is assumed that the free space range R_0 is given as a known parameter of the beacon system. If $P1(\theta)_{min}$ is the minimum detectable P1 pulse signal according to the above criteria, then we obtain from Eq. (3) the following expression for the range:

$$R(\theta) = \frac{\sqrt{30 W_d G_d}}{P1(\theta)_{min}} F_d(\theta) , \tag{28}$$

where

$$F_d(\theta) = \left\{ \left[f_d(\theta) \right]^2 + 2\rho(\theta) f_d(\theta) f_d(-\theta) \cos(2\beta H_d \sin\theta) + \left[\rho(\theta) f_d(-\theta) \right]^2 \right\}^{1/2} , \tag{29}$$

where R is now expressed as a function of θ. The maximum free space range of the system is evidently given by:

$$R_0 = \frac{\sqrt{30 W_d G_d}}{P1_{min}} . \tag{30}$$

Thus the range as a function of θ is given by the following:

$$R(\theta) = R_0 F_d(\theta) \tag{31}$$

where $F_d(\theta)$ is given by Eq. (29).

The coverage diagram for a given system is obtained from Eq. (31).

3. ANTENNA PATTERNS AND GROUND CHARACTERISTICS

In the present chapter we discuss the free space far field pattern characteristics of various ATCRBS antennas that are considered in the present investigation. The reflecting properties of ground which play a considerable role in the ultimate performance of the beacon system are also discussed briefly.

3.1 Antennas Under Study

Performance of the beacon system using nine different antennas is studied in the present investigation. These antennas are the Westinghouse array antenna [4], Texas Instruments reflector antenna [5], Hazeltine open array antenna [6], the existing "hog-trough" antenna [7], Hazeltine E-scan antenna [8], enroute Texas Instruments Fix (TI Fix) antenna [5], enroute NADIF Fix with Texas Instruments omni antenna (NADIF Fix I) [5], enroute NADIF Fix with Westinghouse omni antenna (NADIF Fix II) [4], and enroute NADIF Fix with existing small omni antenna (NADIF Fix III) [7]. All these antennas are described in the references cited. The elevation plane patterns of these antennas are available. For the purpose of the present investigation we have developed approximate analytical expressions for the nine antennas by using Woodward and Lawson's pattern synthesis technique [9].

3.2 Free Space Patterns of Various Terminal and Enroute ATCRBS Directional Antennas

In this section we give the synthesized analytical expressions developed for the vertical plane patterns of the nine ATCRBS directional antennas mentioned in Section 3.1.

3.2.1 Westinghouse Array Antenna [4]

The Westinghouse improved ATCRBS directional antenna is a rotating planar array 8 feet high by 26 feet 8 inches wide. The array aperture is made up of 480 dipole radiating elements arranged in 32 columns of 15 elements each. The columns of dipoles are spaced 10 inches (0.83λ) apart. The dipoles in each column are spaced 6.4 inches apart. The array is designed to provide an

elevation coverage up to 30 degrees and have an azimuth beamwidth of 2.3 degrees at 1.03 GHz.

The elevation plane pattern of the antenna is assumed to be that produced by the central array of 15 dipoles. The excitation coefficients of the elements of the central array, as given in [4], are shown in Table 1.

TABLE 1: EXCITATION COEFFICIENTS OF THE CENTRAL ARRAY OF THE WESTINGHOUSE ARRAY ANTENNA

Element No. (n)	Amplitude (a_n)	Phase in degrees (ψ_n)
7	0.8108	-91.27
6	0.6346	-47.04
5	0.2644	-151.88
4	1.1086	-64.65
3	0.4554	13.02
2	1.7039	-135.06
1	4.3738	-64.85
0	5.4201	00.00
-1	4.3738	64.85
-2	1.7039	135.06
-3	0.4554	-13.02
-4	1.1086	64.65
-5	0.2644	151.88
-6	0.6346	47.04
-7	0.8108	91.27

The excitation coefficients are symmetrical in amplitude and antisymmetrical in phase with respect to the central (n = 0) element, so that the pattern in the plane of the array can be expressed in the form of a real trigonometric polynomial with eight terms. Let the array be represented as shown in Fig. 7. The electric field intensity at some far field point $M(R, \theta)$ is given by the following:

$$E(\theta) = \frac{\text{constant}}{R} f(\theta) \left[\sum_{n=-7}^{7} a_n \exp(j\psi_n) \exp -j\beta(R - nd \sin\theta) \right] , \qquad (32)$$

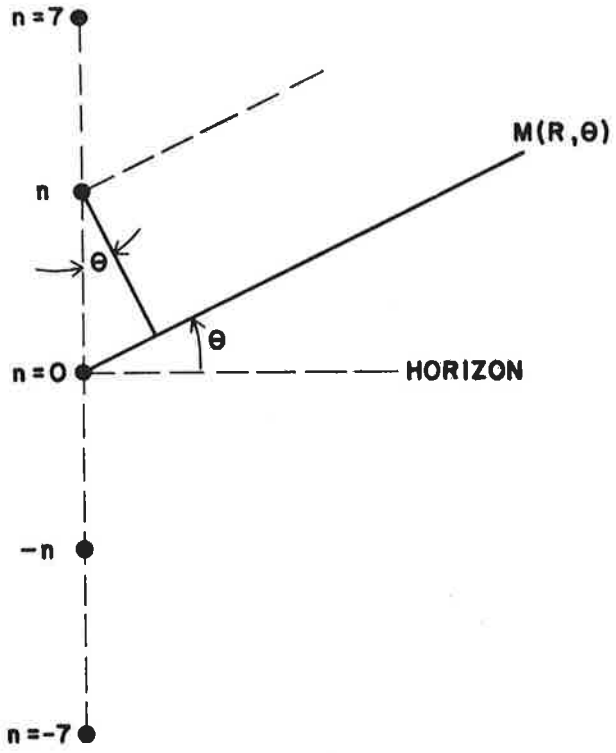

FIG. 7: Schematic representation of the vertical array.

where

a_n, ψ_n are the amplitude and phase of the nth element,

$f(\theta)$ is the element pattern which in the present case is given by

$$f(\theta) = \frac{\sin(\frac{\pi}{2}\cos\theta)\cos(\frac{\pi}{2}\sin\theta)}{\cos\theta} \quad , \tag{33}$$

d is the spacing between elements.

After using the symmetry of the excitation coefficients in Eqs. (32), the following expression is obtained for the normalized free space elevation plane pattern of the antenna:

$$f_d(\theta) = \frac{1}{15.86} \frac{\sin(\frac{\pi}{2}\cos\theta)\cos(\frac{\pi}{2}\sin\theta)}{\cos\theta} \left[5.4201 + \sum_{n=1}^{7} a_n \cos(n\beta d \sin\theta + \psi_n)\right] , \quad (34)$$

where a_n and ψ_n are as given in Table I. A plot of $f_d(\theta)$ vs θ is shown in Fig. 8.

3.2.2 Texas Instruments Reflector Antenna [5]

The Texas Instruments directional antenna uses a doubly curved reflector with an aperture 10 feet high and 30 feet wide. For better shaping of the vertical plane pattern three feed horns are used. With the help of Woodward and Lawson's [9] aperture synthesis technique we have developed an analytical expression to approximate the vertical plane pattern given in [5]. According to the sampling theorem [9, 10], the maximum spacing between the sampling points must not exceed λ/ℓ in the $\sin\theta$ space, where ℓ (= 10 feet) is the vertical dimension of the aperture and λ is the free space wavelength (λ = 11.484 inches at f = 1.03 GHz). Taking one of the sampling points to be $\theta = 0^o$, we have the following relation for all the sampling points:

$$\theta_n = \arcsin(n\lambda/\ell) \quad . \quad (35)$$

The values of θ_n and the corresponding values of the pattern function $f_d(\theta_n)$ taken from the pattern given in [5] are shown in Table 2. For the sampling points below -9^o and above 51.3^o, all values of $f_d(\theta_n)$ are taken to be zero.

According to the Woodward-Lawson formula we now obtain the following analytical expression for the pattern:

$$f_d(\theta) = \sum_{n=-2}^{10} f_{d_1}(\theta_n) \frac{\sin(\frac{\pi\ell}{\lambda}\sin\theta - n\pi)}{(\frac{\pi\ell}{\lambda}\sin\theta - n\pi)} \quad (36a)$$

where the coefficients $f_{d_1}(\theta_n)$ are given in Table 2. In the present case ℓ = 10', λ = 11.464". Introducing these values into Eq. (36a), the following is obtained:

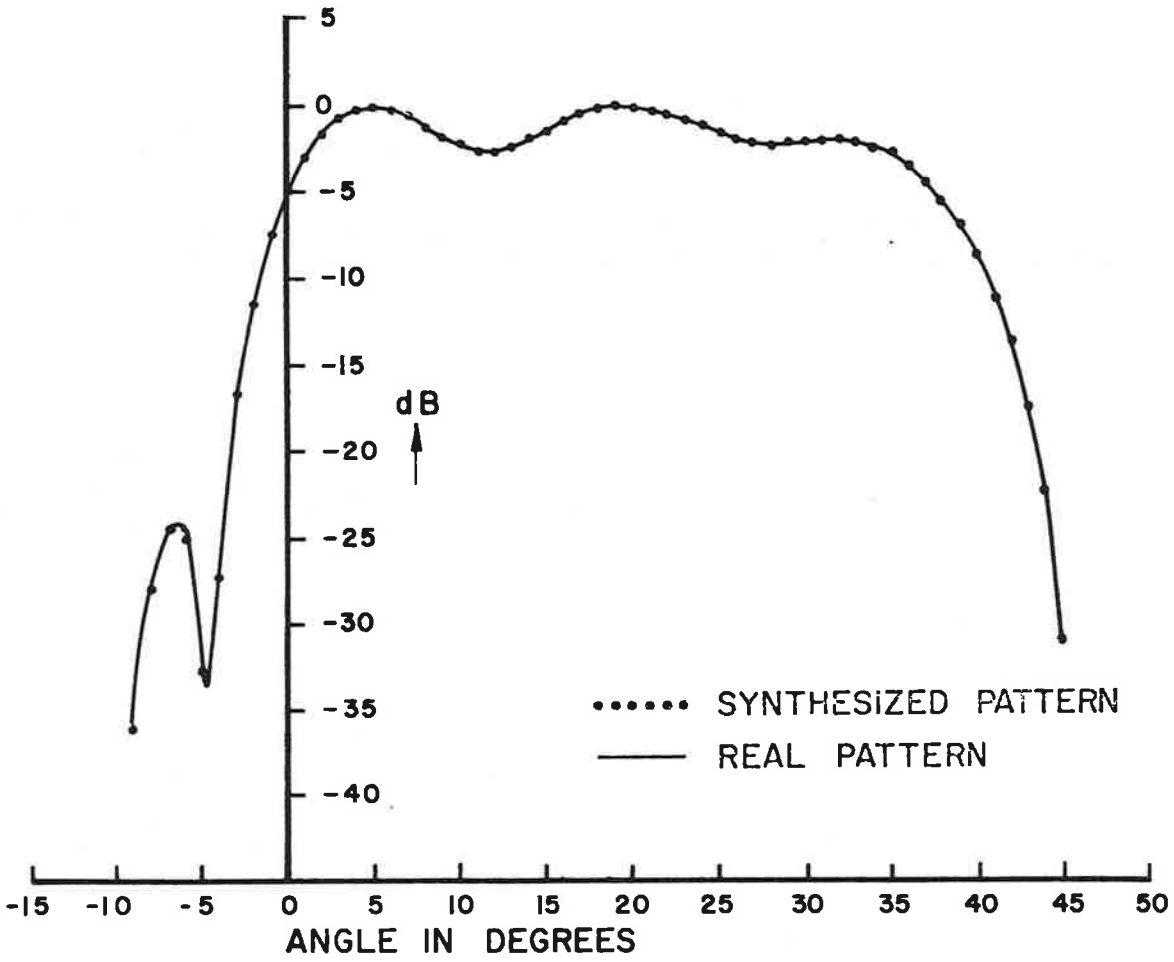

FIG. 8: Normalized free space elevation plane pattern of the Westinghouse array antenna.

TABLE 2: SAMPLED VALUES OF THE PATTERN FUNCTION FOR THE TEXAS INSTRUMENTS REFLECTOR ANTENNA

n	θ_n^o	$f_{d_1}(\theta_n)$
-2	-9	0.084
-1	-4.5	0.080
0	0	0.5
1	4.5	1
2	9	0.8
3	13.6	0.86
4	18.3	0.79
5	23.1	0.86
6	28.1	0.96
7	32.3	0.54
8	38.9	0.23
9	44.5	0.12
10	51.3	0.06

$$f_d(\theta) = \sum_{n=-2}^{n=10} f_{d_1}(\theta_n) \frac{\sin \pi\left(\frac{\sin\theta}{0.07846} - n\right)}{\pi\left(\frac{\sin\theta}{0.07846} - n\right)} \qquad (36b)$$

The plot of the synthesized pattern given by Eq. (36) is given in Fig. 9, where the exact pattern given in [5] is also shown for comparison. The agreement between the real and the synthesized pattern is considered to be quite satisfactory.

3.2.3 Hazeltine Open Array Antenna [6]

The Hazeltine open array directive antenna consists of a 4-foot high by 28-foot wide antenna array. It contains 36 columns of dipoles with each full column containing 8 dipoles. Using the same procedure as discussed in Section 3.2.2, we obtain the following expression for the pattern of the antenna:

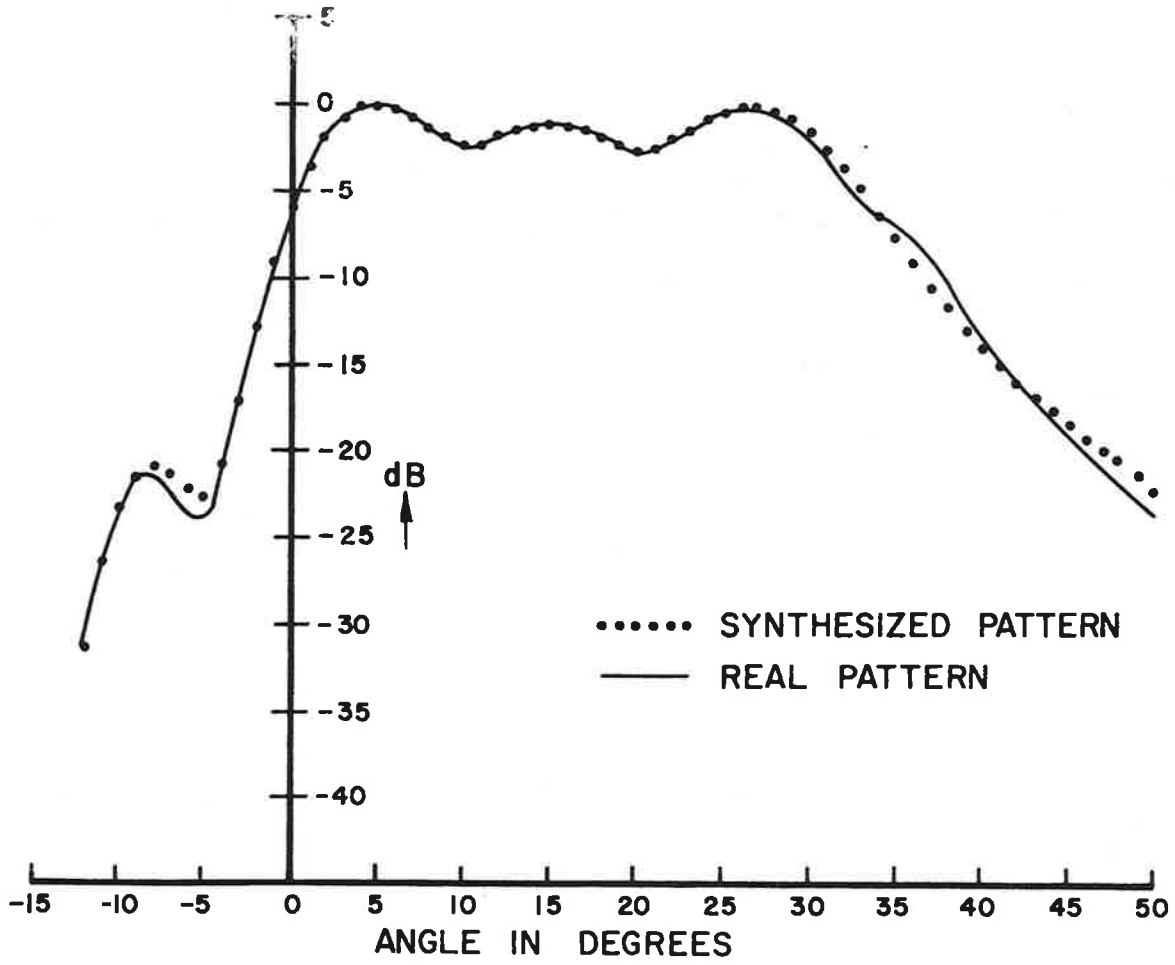

FIG. 9: Normalized free space elevation plane pattern of the Texas Instruments reflector antenna.

$$f_\theta(\theta) = \sum_{n=0}^{3} f_{d_1}(\theta_n) \frac{\sin \pi\left(\frac{\sin\theta}{0.2250} - n\right)}{\pi\left(\frac{\sin\theta}{0.2250} - n\right)} \quad , \tag{37}$$

where θ_n and $f_{d_1}(\theta_n)$ are given in Table 3.

TABLE 3: SAMPLED VALUES OF THE PATTERN FUNCTION FOR THE HAZELTINE OPEN ARRAY ANTENNA

n	θ_n^o	$f_{d_1}(\theta_n)$
0	0	0.500
1	13	1.000
2	26.75	0.885
3	42.4	0.530

A plot of the synthesized pattern given by Eq. (37) along with the real pattern given in [6] are shown in Fig. 10.

3.2.4 Existing Hog-Trough Antenna [7]

The existing antenna consists of an array with an aperture about 2 feet high and 28 feet wide. The analytic expression obtained to approximate its given pattern [7] is given by:

$$f_d(\theta) = \sum_{n=-2}^{n=+2} f_{d_1}(\theta_n) \frac{\sin \pi\left(\frac{\sin\theta}{0.47767} - n\right)}{\pi\left(\frac{\sin\theta}{0.47767} - n\right)} \quad , \tag{38}$$

where θ_n and $f_{d_1}(\theta_n)$ are shown in Table 4.

A plot of the synthesized pattern given by Eq. (38) and the real pattern [7] are shown in Fig. 11. The approximation is found to be satisfactory.

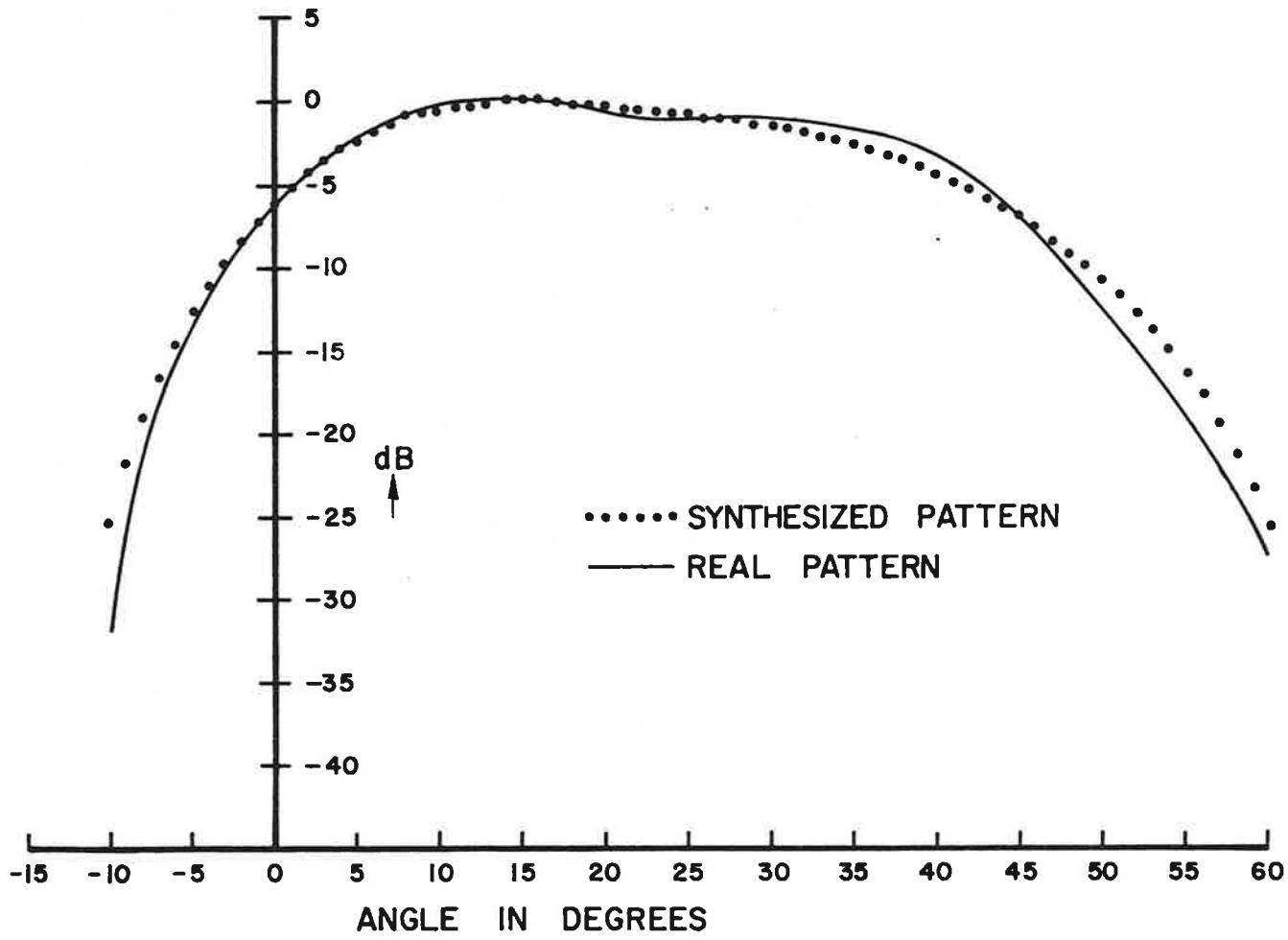

FIG. 10: Normalized free space elevation plane pattern of Hazeltine open array antenna.

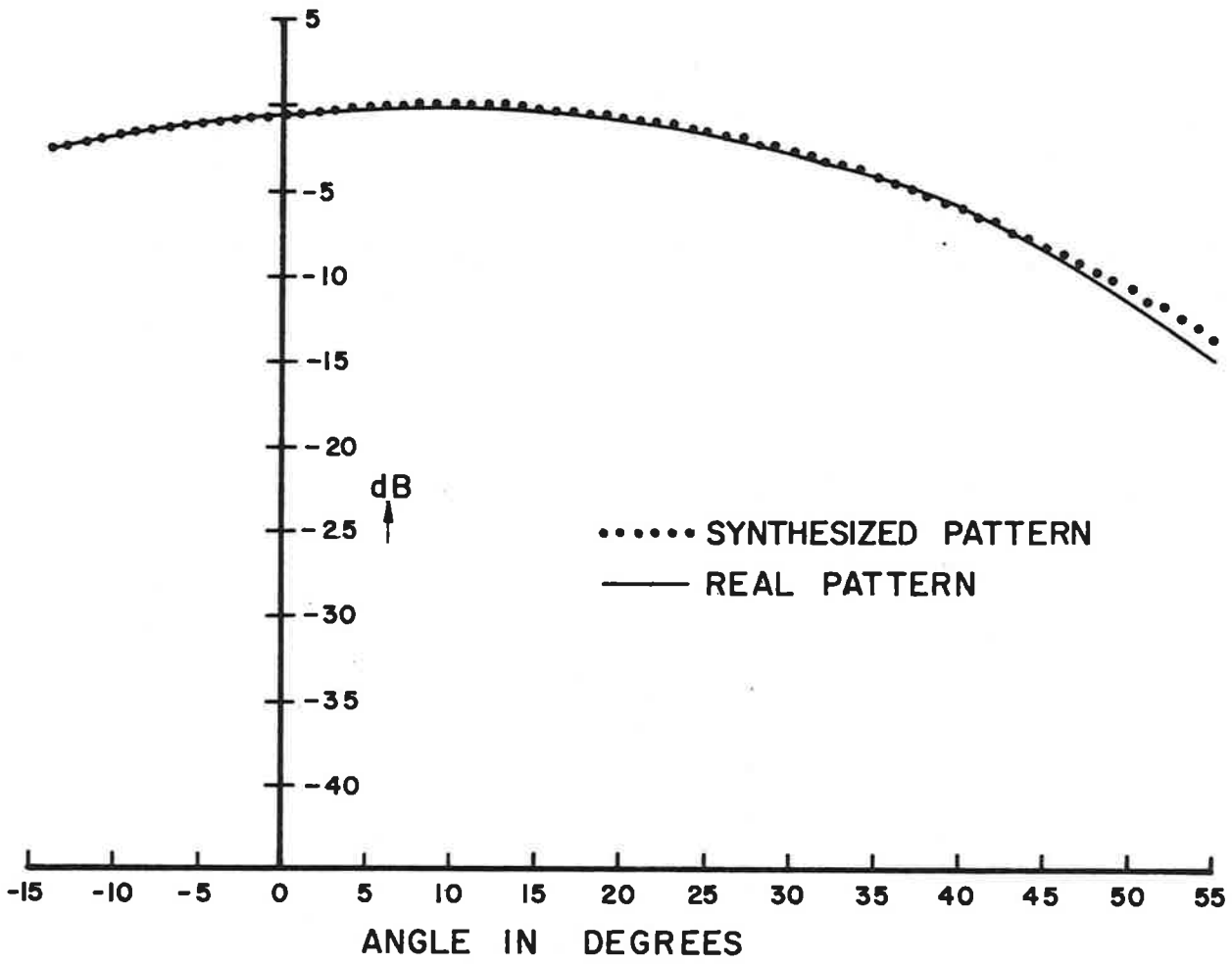

FIG. 11: Normalized free space elevation plane pattern of the existing "hog-trough" antenna.

TABLE 4: SAMPLED VALUES OF THE PATTERN FUNCTION FOR THE EXISTING ANTENNA

n	θ_n^o	$f_{d_1}(\theta_n)$
-2	-72.8	0.084
-1	-28.55	0.51
0	0	0.9661
1	28.55	0.780
2	72.8	0.045

3.2.5 Hazeltine E-scan Antenna [8, 7]

A description of the Hazeltine E-scan antenna may be found in [8]. It is a circular-cylindrical array of 224 columns; each column contains 16 strip-line dipole radiating elements. The vertical aperture is 8 feet long. The approximate analytical expression for its real pattern [7] is given by the following:

$$f_d(\theta) = \sum_{n=-3}^{n=6} f_{d_1}(\theta_n) \frac{\sin \pi \left(\frac{\sin \theta}{0.11942} - n \right)}{\pi \left(\frac{\sin \theta}{0.11942} - n \right)} , \qquad (39)$$

where the coefficients θ_n and $f_{d_1}(\theta_n)$ are given in Table 5.

TABLE 5: SAMPLED VALUES OF THE PATTERN FUNCTION FOR THE HAZELTINE E-SCAN ANTENNA

n	θ_n^o	$f_{d_1}(\theta_n)$
-3	-21	0.079
-2	-13.8	0.072
-1	-6.85	0.03
0	0.00	0.530
1	6.85	0.915
2	13.8	0.945
3	21	0.845
4	28.55	0.845
5	36.7	0.315
6	45.8	0.034

A plot of the synthesized pattern given by Eq. (39) and the real pattern [7] are shown in Fig. 12.

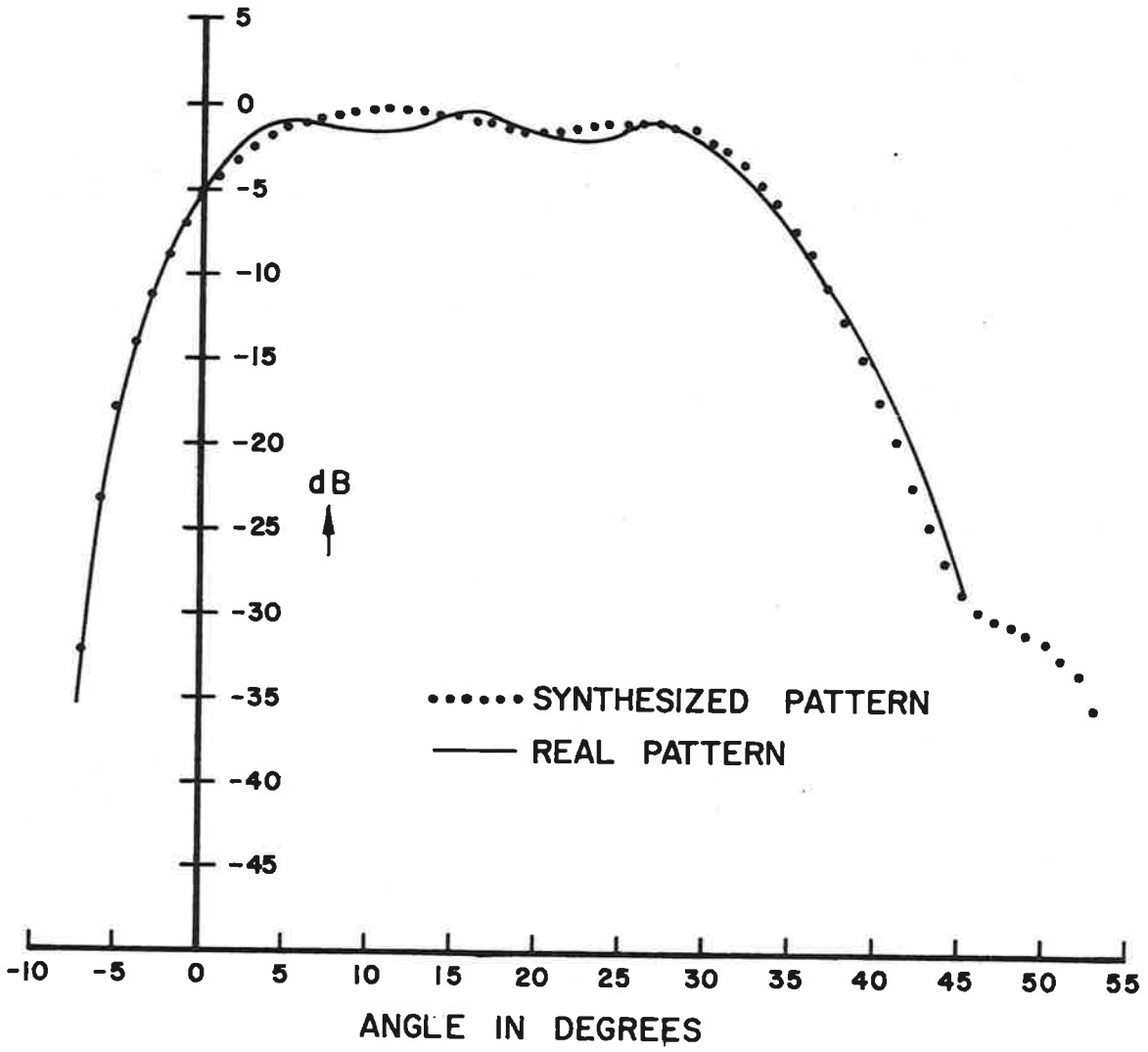

FIG. 12: Normalized free space elevation plane pattern of Hazeltine E-scan antenna.

3.2.6 Enroute Texas Instruments Fix Antenna (TI Fix) [5]

For the purpose of synthesizing the vertical plane pattern of the enroute Texas Fix antenna, an equivalent vertical aperture ℓ is assumed to be given by the expression

$$\ell \sim 68.8\lambda/\theta_H \tag{40}$$

where θ_H is the vertical plane half-power beamwidth in degrees. In the present case [5] $\theta_H \sim 4^o$.

The synthesized analytical expression for the real pattern [5, 7] is given by

$$f_d(\theta) = \sum_{n=-2}^{12} f_{d_1}(\theta_n) \frac{\sin \pi\left(\frac{\sin\theta}{0.0583} - n\right)}{\pi\left(\frac{\sin\theta}{0.0583} - n\right)} \tag{41}$$

where the coefficients θ_n and $f_{d_1}(\theta_n)$ are given in Table 6.

TABLE 6: SAMPLED VALUES OF THE PATTERN FUNCTION FOR ENROUTE TEXAS INSTRUMENTS FIX ANTENNA

n	θ_n^o	$f_{d_1}(\theta_n)$
-2	-6.7	0.010
-1	-3.33	0.039
0	0	0.561
1	3.33	0.990
2	6.7	0.482
3	10.1	0.450
4	13.5	0.435
5	17	0.420
6	20.5	0.355
7	24.1	0.417
8	27.8	0.342
9	31.65	0.350
10	35.7	0.334
11	39.9	0.240
12	44.4	0.120

A plot of the synthesized pattern given by Eq. (41) and the real pattern [5,7] are shown in Fig. 13.

3.2.7 Enroute NADIF-Fix Antennas (NADIF-Fix I, II and III) [5, 7]

The three enroute NADIF-Fix antennas use the same directional antenna but different omnidirectional antennas. The equivalent vertical aperture of the directional NADIF-Fix antennas are taken to be the same as that of the Texas Instruments Fix antenna discussed in 3.2.6 and is given by Eq. (40). Consequently the synthesized analytical expression for the vertical plane pattern is given by Eq. (41), and the coefficients f_{d_1} and θ_n are as given in Table 7.

TABLE 7: SAMPLED VALUES OF THE PATTERN FUNCTION FOR ENROUTE NADIF FIX ANTENNAS

n	θ_n^o	$f_{d_1}(\theta)$
-2	-6.7	0.01
-1	-3.3	0.094
0	0	0.635
1	3.33	0.990
2	6.7	0.530
3	10.1	0.542
4	13.5	0.515
5	17	0.515
6	20.5	0.430
7	24.5	0.465
8	27.8	0.437
9	31.65	0.302
10	35.7	0.302
11	39.9	0.217
12	44.4	0.153

A plot of the synthesized pattern given by Eq. (41) and the real pattern [7] are shown in Fig. 14.

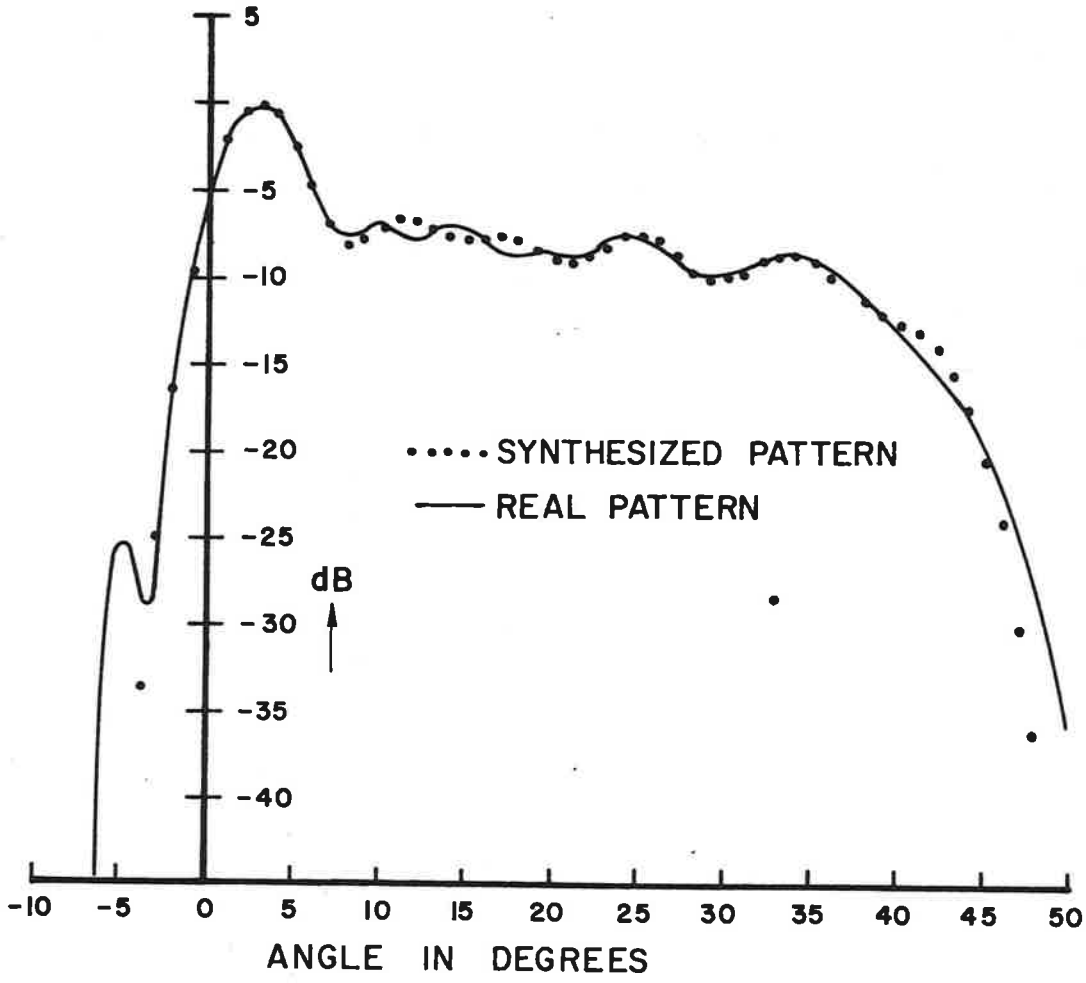

FIG. 13: Normalized free space elevation plane pattern of the enroute Texas Instruments Fix antenna.

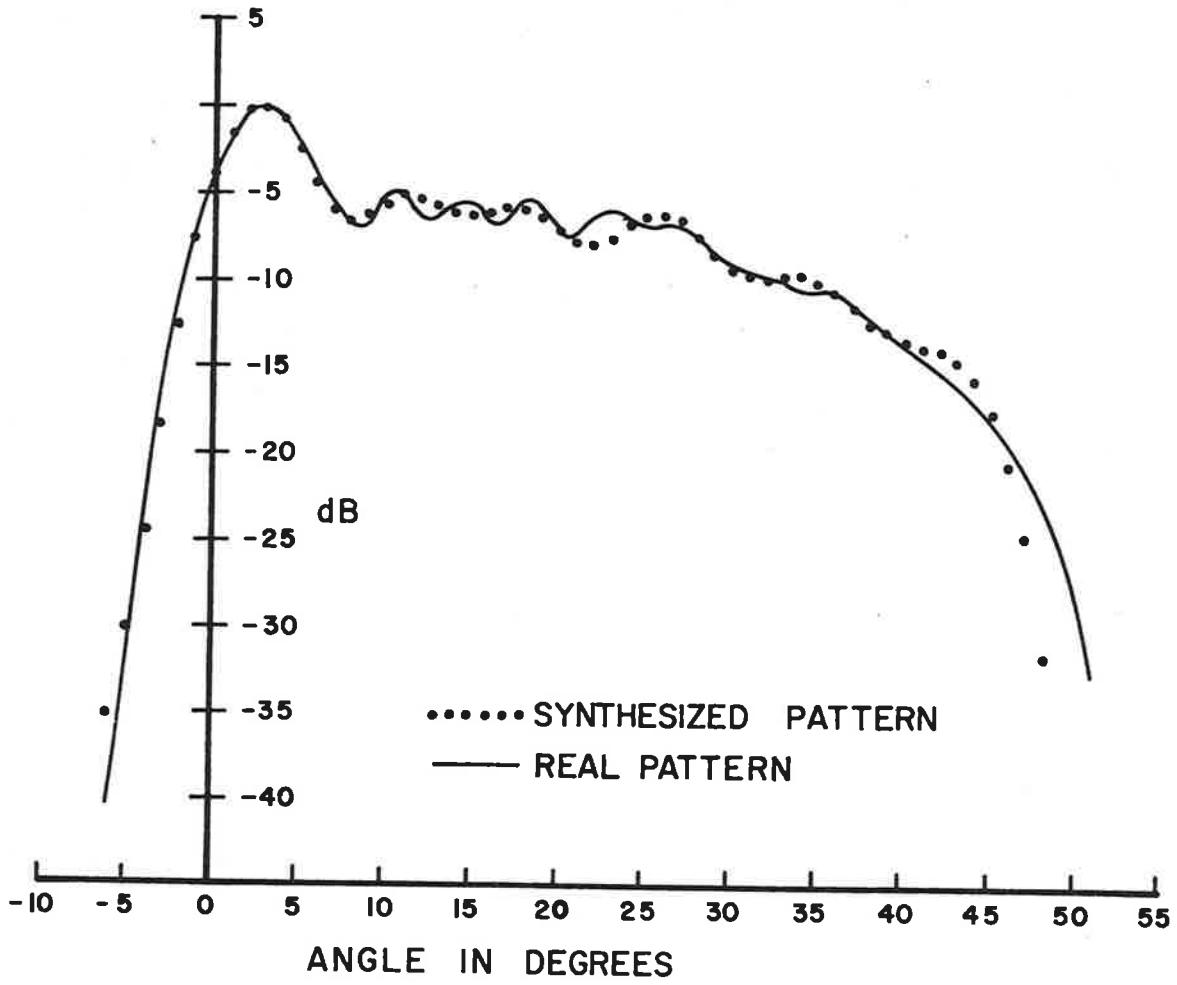

FIG. 14: Normalized free space elevation plane pattern of NADIF Fix antennas.

3.3 Free Space Elevation Plane Patterns of Omnidirectional Antennas

Most of the omnidirectional antennas are designed such that their free space vertical plane patterns match with the vertical plane patterns of the corresponding directional antennas. The exceptions are the NADIF Fix antennas where the elevation plane patterns of the directional and omnidirectional antennas differ appreciably; this is especially true for the NADIF Fix II antenna with Westinghouse omni antenna and NADIF Fix III antenna with the existing omni antenna. Thus for the first seven antennas it will be assumed that the free space elevation plane patterns of the omnidirectional antenna is identical with that of the corresponding directional antenna, i.e., $f_d(\theta) = f_0(\theta)$. This assumption leads to simpler expressions and better saving of the computer time. For NADIF Fix II antenna, $f_0(\theta)$ is assumed to be identical to $f_d(\theta)$ of the Westinghouse antenna and for NADIF Fix III antenna, $f_0(\theta)$ is identical to $f_d(\theta)$ of the existing directional antenna. As explained later, the computer program developed can handle the cases when $f_d(\theta) = f_0(\theta)$ and $f_d(\theta) \neq f_0(\theta)$.

3.4 The Reflection Coefficient $\rho(\theta)$

It is assumed that the ground is a plane smooth surface of infinite extent and is a pure dielectric with relative permittivity $\epsilon = 3$. According to Fresnel formulas [10], the reflection coefficient for the case of vertical polarization is given by

$$\rho(\theta) = \frac{3\sin\theta - \sqrt{3-\cos^2\theta}}{3\sin\theta + \sqrt{3-\cos^2\theta}} = \frac{3\sin\theta - \sqrt{2+\sin^2\theta}}{3\sin\theta + \sqrt{2+\sin^2\theta}} \quad . \tag{42}$$

Equation (42) indicates that $\rho(\theta)$ is a real quantity for all angles θ. The reflection coefficient as a function of θ is shown in Fig. 15. $\rho(\theta)$ is negative from $\theta = 0^\circ$ to the Brewster angle $\theta = 30^\circ$ and above the Brewster angle it is positive with a maximum value of 0.27 at $\theta = 90^\circ$.

3.5 Summary of the Important Parameters

As mentioned earlier, the SLS mode performance of the ATCRBS using all the antennas, discussed in the previous sections, are investigated in the

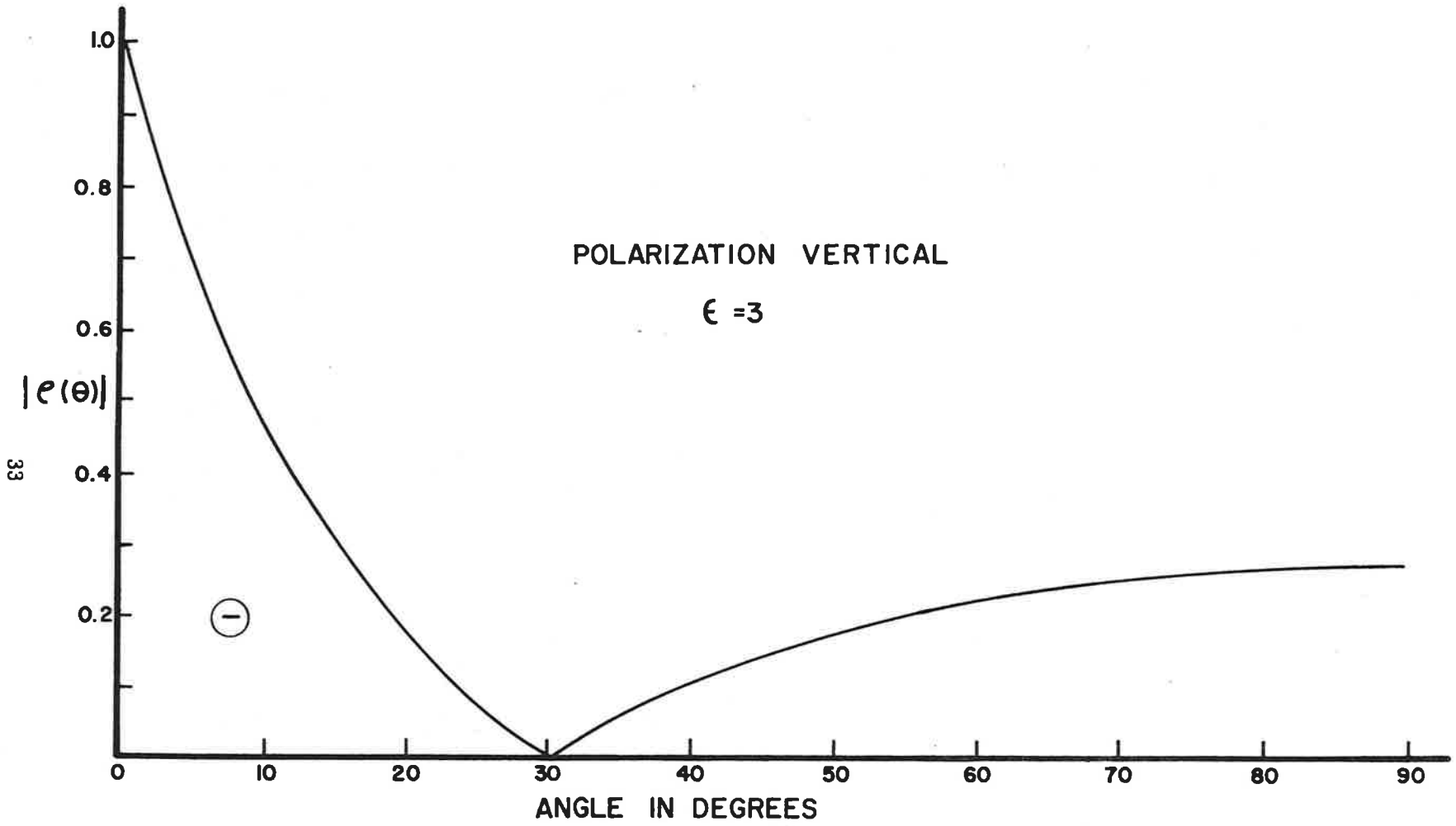

FIG. 15: The reflection coefficient of flat ground as a function of θ.

present study. In each case the appropriate antenna pattern functions are used to obtain the desired performance parameters described in Section 2. In addition to the pattern functions, the following parameters characterize each system studied:

H_d is the height of the phase center of the directional antennas expressed in feet

H_0 is the height of the phase center of the omnidirectional antennas expressed in feet

K_0 is the nominal pulse ratio in dB, usually taken to be 18 dB

ϕ_0 is the total azimuthal half-power beamwidth of the directional antennas in degrees

α_g is the field gradient at the horizon and is defined to be the rate of decay of the field in dB per 1^o below the horizon

R_0 is the free space range expressed in nautical miles

λ is the free space wavelength; λ = 11.464 inches at 1.03 GHz.

f_i is the pulse repetition frequency (pulses per second)

Ω is the scanning rate in degrees per second.

The various antenna systems to be studied, along with the important parameters characterizing each system are shown in Table 8.

TABLE 8: SOME IMPORTANT PARAMETERS OF THE ANTENNA SYSTEMS

	Antenna Type	H_d	H_0	ϕ_0	α_g	K_0	R_0	f_i	Ω
Terminal	Westinghouse Array	34	42	2.25	2.5	18	40	360	90
	Texas Inst. Reflector	34	43	2.36	3.4	18	40	360	90
	Hazeltine Open Array	33	37	2.30	1.6	18	40	360	90
	Existing Hog-Trough	41	43	2.27	0.37	18	40	360	90
	Hazeltine E-Scan	16	16	2.33	2.4	18	40	360	90
Enroute	Westinghouse Array	82	90	2.25	2.5	18	200	360	36
	Texas Inst. Reflector	82	91	2.36	3.4	18	200	360	36
	Existing Hog-Trough	108	110	2.27	0.37	18	200	360	36
	Texas Instruments Fix	92	112	2.2	5.0	18	200	360	36
	NADIF Fix I	92	112	1.53	5.0	18	200	360	36
	NADIF Fix II	92	111	1.53	5.0	18	200	360	36
	NADIF Fix III	92	110	1.53	5.0	18	200	360	36

All the terminal antennas, except the Hazeltine open array and the E-scan antennas are mounted on a 27' tower. The Hazeltine antennas are mounted on a 17' tower. All the enroute antennas are mounted on a 75' tower.

4. NUMERICAL RESULTS AND DISCUSSIONS

In the present chapter we give the numerical results obtained for the various quantities of interest characterizing the performance of the ATCRBS using different antennas. Short discussions of results are given wherever appropriate.

4.1 The Computer Program

A computer program has been developed to obtain numerical and/or graphical results for the various quantities described in Section 2. The program can accommodate antenna systems where $f_d(\theta) = f_0(\theta)$ and $f_d(\theta) \neq f_0(\theta)$. The computer output consists of the following:

4.1.1 Free space elevation plane patterns of various ATCRBS antennas (tabulated numerical results).

4.1.2 $P1(\theta)$, $P2(\theta)$ in dB as functions of the elevation angle θ (graphical).

4.1.3 Pulse ratio $K(\theta) = P1(\theta)/P2(\theta)$ in dB as a function of θ normalized to the free space nominal value K_0 (graphical).

4.1.4 Effective azimuth beamwidth ϕ_{eff} (tabulated).

4.1.5 Number of replies as a function of θ (graphical).

From the above results the mainbeam killing and sidelobe punch-through zones and the coverage diagram for each antenna system are prepared using the method described in Section 2.

The program can handle arbitrary combinations of H_d and H_o, arbitrary nominal pulse ratio K_0, any value of f_i and Ω and for any chosen range of the elevation angle θ.

It should be noted that the computer program is capable of supplying simultaneously similar sets of data for the ISLS mode of operation of the beacon system. The complete program is given in Appendix A.

4.2 Numerical Results for Terminal Installations

In this section numerical results are given for the terminal ATCRBS using different antenna systems. The method of obtaining some of the diagrams is described in more detail only for the Westinghouse antenna which is considered first. Since the method of obtaining the diagrams is the same, the discussion will not be repeated for the other antenna systems.

4.2.1 Westinghouse Array Antenna

In this case the tower height $H_T = 27'$. The heights of the phase centers of the directional and omnidirectional antennas are, respectively, $H_d = 34'$ and $H_o = 42'$. The vertical aperture of the antenna is about 8'. The elevation plane free space patterns of the two antennas are assumed to be identical and are given by Fig. 8.

Figure 16 shows the $P1(\theta)$, $P2(\theta)$ in dB as functions of θ where the 0 dB level is adjusted to coincide with the maximum $P1(\theta)$ level in the free space case. The corresponding free space curves are also shown in Fig. 16 for comparison. Note that the P1 and P2 curves are displaced from each other by the nominal pulse ratio of 18 dB. Because of the different heights of the two phase centers, the lobing structures in the $P1(\theta)$, $P2(\theta)$ curves are different. For example, the first minimum of $P1(\theta)$ is located at $\theta = 0.8^o$ while that of the $P2(\theta)$ is at $\theta = 0.65^o$; the corresponding depths of the minima are, respectively, -8.3 dB and -9.8 dB with respect to their free space values. The oscillations in the curves about the free space values are less than ± 1 dB for $\theta > 3^o$ and for $\theta > 5^o$ the two curves assume their free space values.

Figure 17 shows the pulse ratio as a function of θ normalized to the nominal free space value K_0. The maximum and minimum departure from the nominal value is found to be +9.7 dB and -9.5 dB respectively. The oscillations quickly attenuate and for $\theta > 4.5^o$ the pulse ratio assumes the free space value.

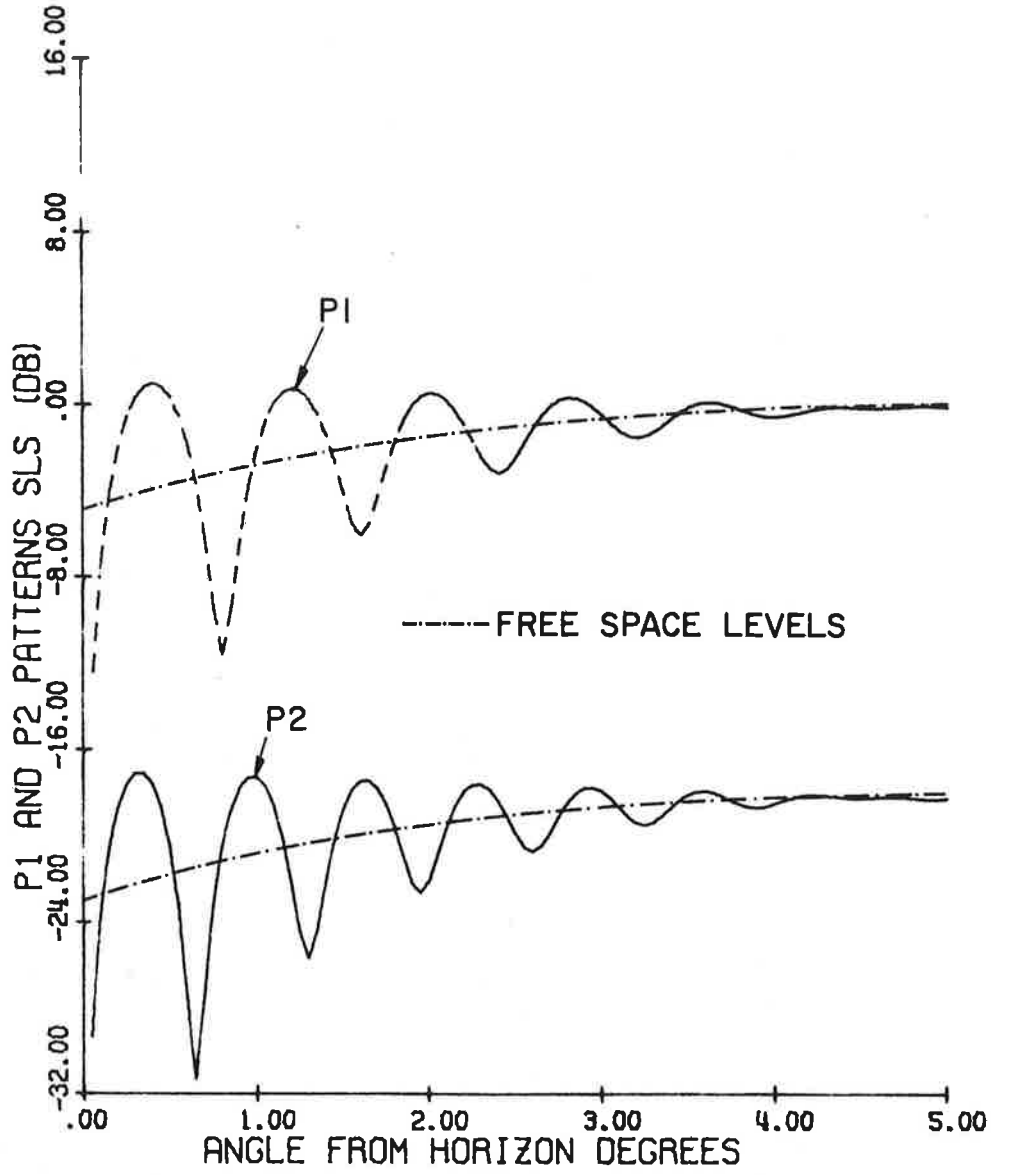

FIG. 16: P1 and P2 pulses as functions of θ.

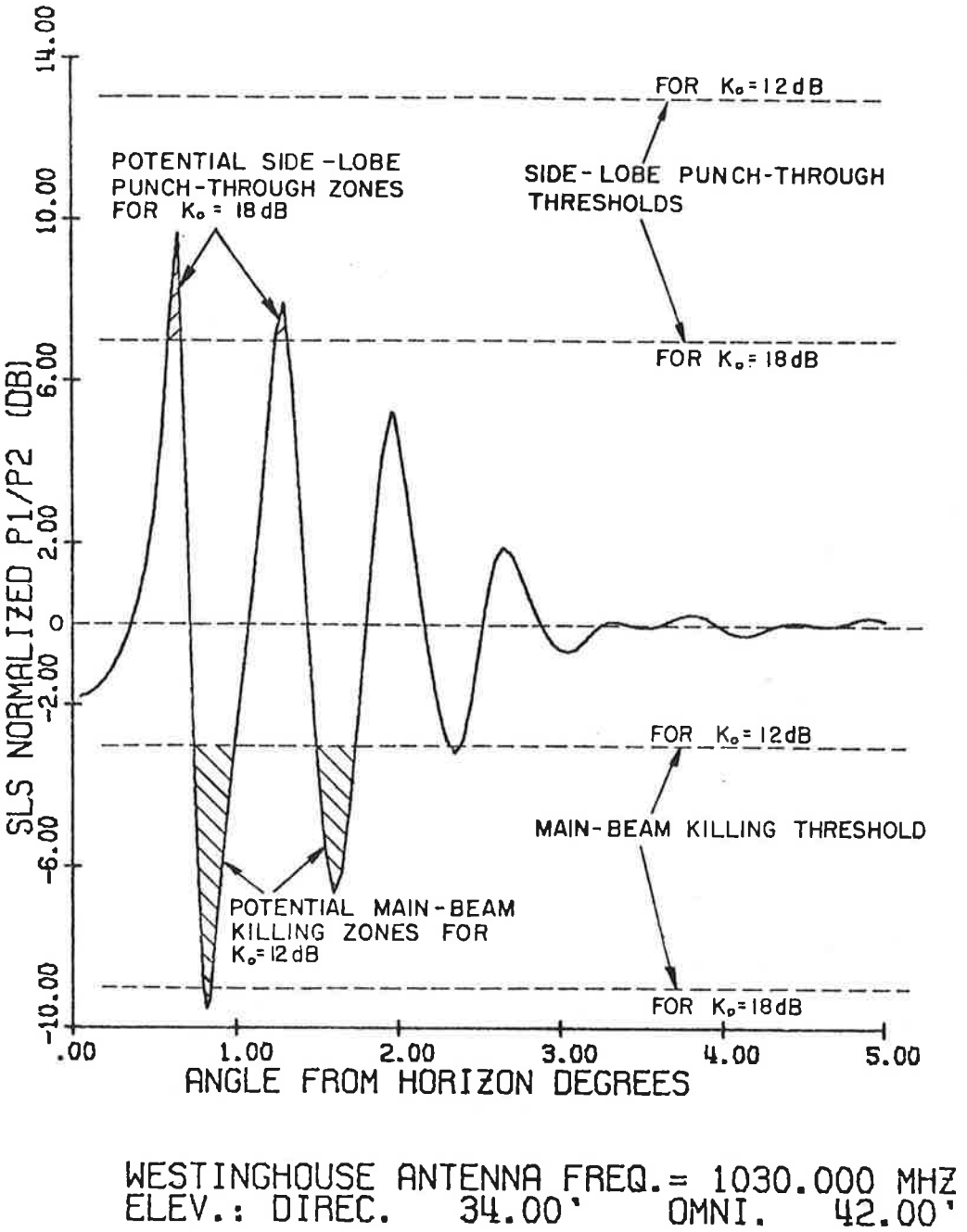

FIG. 17: Normalized pulse ratio as a function of θ.

The mainbeam killing and sidelobe punch-through zones for the antenna are obtained from the normalized pulse ratio curve shown in Fig. 17. The various level lines shown in the figure are used for this purpose. It is appropriate to give here a short explanation regarding this. As discussed in Section 2.3 the mainbeam killing zones in space are those regions of space where the pulse ratio falls below a threshold level a (dB) (Eq. 13b). For a pulse ratio curve normalized to the nominal free space value K_0 dB the mainbeam killing threshold occurs at $(a - K_0)$ dB (see Eq. 14). Thus with a = 9 dB and for K_0 = 18 dB and 12 dB, the threshold levels occur at (9 - 18) = -9 dB and (9 - 12) = -3 dB respectively as shown in Fig. 17.

The sidelobe punch-through zones in space are those regions in space where the pulse ratio rises above the sidelobe punch-through level b, defined earlier. For a pulse ratio curve normalized to the nominal free space value of K_0 dB, if the azimuth sidelobe level of the antenna is -L dB, the sidelobe punch-through level occurs at $(b + L - K_0)$ dB. With b = 0 dB, and L = 25 dB the punch-through threshold levels occur at (0 + 25 - 18) = 7 dB and (0 + 25 - 12) = 13 dB for K_0 = 18 dB and 12 dB respectively, as shown in Fig. 17.

Figure 18a shows the potential mainbeam killing and sidelobe punch-through regions as functions of the nominal pulse ratio K_0. These zones have been obtained from Fig. 17 using the appropriate level lines with a = 9 dB and b = 0 dB. The range of K_0 used in Fig. 18 is between 10 dB and 20 dB. From Fig. 18 it is found in general that the number and extent of the mainbeam killing zones are reduced with increase of the nominal pulse ratio K_0 for a given threshold level a. For the present antenna, the mainbeam killing zones disappear for $K_0 \geq 18.4$ dB. However, the number and extent of the potential sidelobe punch-through zones increase with increase of the nominal pulse ratio. For the present antenna, the sidelobe punch-through zones disappear for $K_0 \leq 15.3$ dB. As can be seen from Fig. 18, for $15.3\text{ dB} \leq K_0 \leq 18.4$ dB, both zones exist.

Figure 18b shows the potential mainbeam killing and sidelobe punch-through zones for the same antenna, but calculated with the two threshold levels adjusted

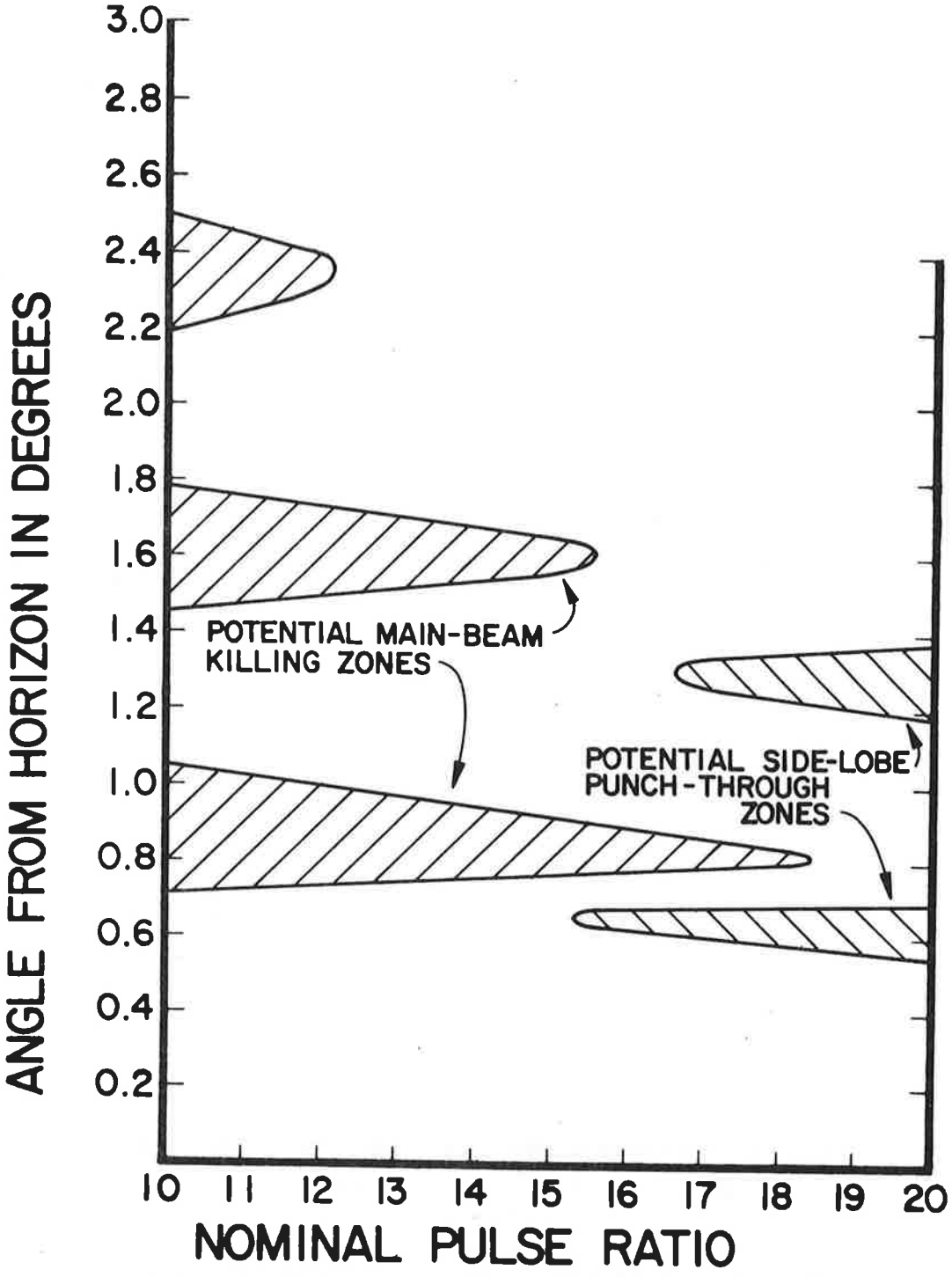

FIG. 18a: Mainbeam killing and sidelobe punch-through zones as functions of the nominal pulse ratio for the Westinghouse array antenna. $H_d = 34'$, $H_o = 42'$, f = 1030 MHz, a = 9dB, b = 0dB, L = -25dB.

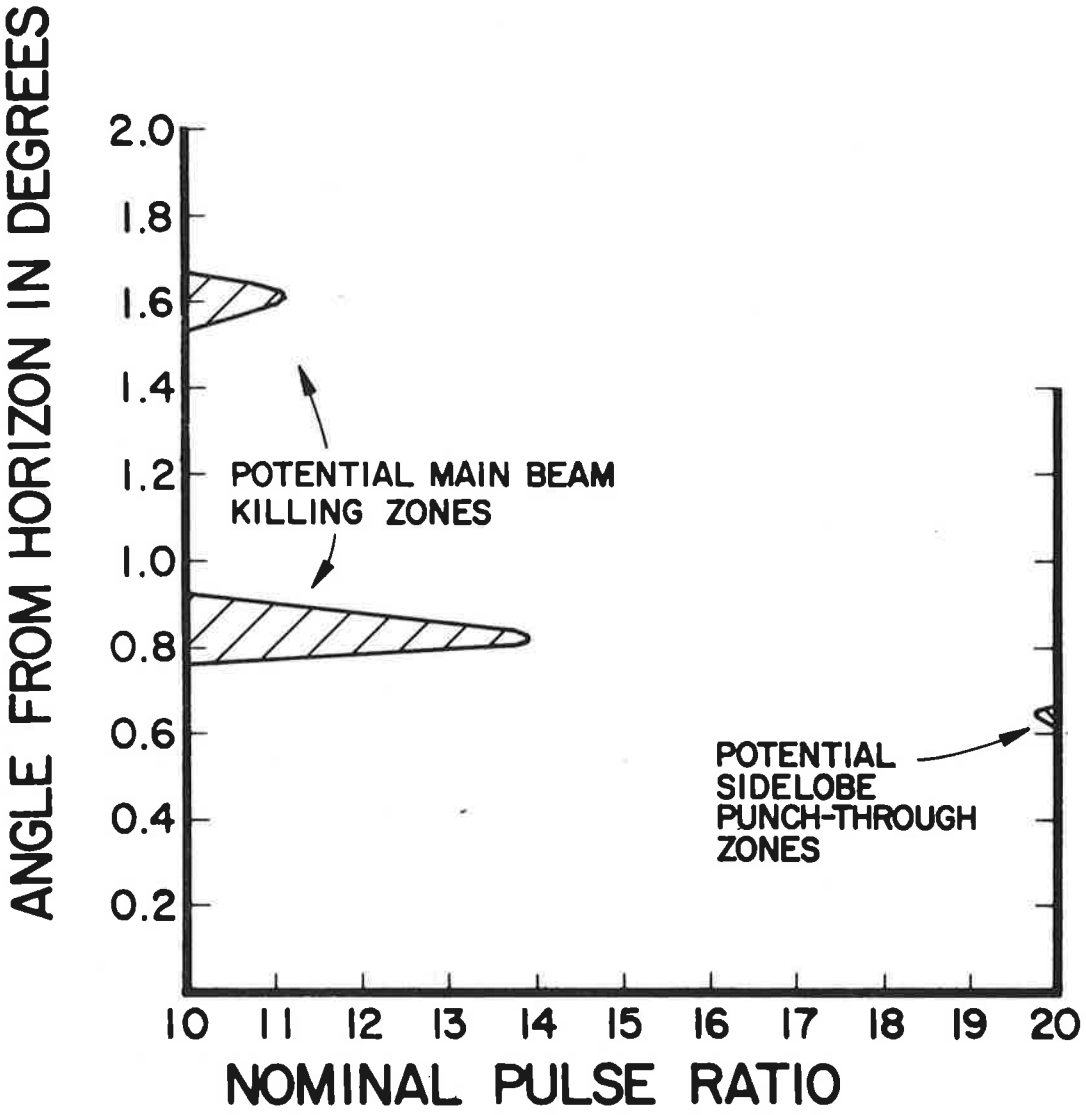

FIG. 18b: Mainbeam killing and sidelobe punch-through zones as functions of the nominal pulse ratio for the Westinghouse array antenna. $H_d = 34'$, $H_o = 42'$, f = 1030 MHz, a = b = 4.5 dB, L = -25 dB.

such that $a = b = 4.5$ dB. As compared to Fig. 17, it is found that in this case the number and extent of the zones are much reduced. Observe that for this value of the threshold levels, both the zones disappear for $14\,\text{dB} \leq K_0 \leq 19.8\,\text{dB}$.

Figure 19 shows the effective azimuth beamwidth as a function of θ, for the threshold level a = 9 dB and nominal pulse ratio $K_0 = 18$ dB. Figure 19 indicates that the effective beamwidth is a damped oscillatory function of θ with a maximum value of 5.6° and a minimum value of 0° which occurs at an angle θ which corresponds to the mainbeam killing (Fig. 18) zone for $K_0 = 18$ dB. For $\theta > 3^\circ$ the oscillations are stabilized and finally beyond about 4.5° the effective beamwidth assumes its free space value which is about 3.9°. It should be mentioned that the effective azimuth beamwidth concept has its real meaning for targets which are relatively close to the station so that replies can be received in an azimuth range which is broader than the 3 dB beamwidth region.

Figure 20 shows the number of replies as a function of the angle θ, based on Eq. (27) with $f_i = 360$ pulses/sec and $\Omega = 90$ deg/sec (15 r.p.m). Since the number of replies is an integer, Fig. 20 is obtained by taking the first integer which is less than or equal to the solution obtained from Eq. (27). In systems with digital data processing, the number of replies may be considered to be a good figure of merit of a given beacon antenna. For the antenna considered here Fig. 20 indicates that for $\theta \gtrsim 3.5^\circ$, the number of replies assumes a constant value of about 15.

Figure 21 shows the coverage diagram for the antenna, normalized to the maximum free space range of 40 nautical miles. The coverage diagram has been prepared with the conventional 4/3 radius of the earth to take into account the normal refraction in the lower atmosphere. For this antenna the maximum range of 45 NM occurs at $\theta = 0.4^\circ$ at the first maximum; at the deepest minimum, which appears at $\theta = 0.8^\circ$, the range is minimum and is equal to 10.5 NM. Above $\theta = 4.5^\circ$ the coverage diagram assumes its free space value.

4.2.2 Texas Instruments Reflector Antenna

The tower height for this antenna is 27' and the heights of the phase centers of the directional and omnidirectional antennas are $H_d = 34'$ and $H_o = 43'$ respectively, so that the vertical displacement between the two phase centers is 9'.

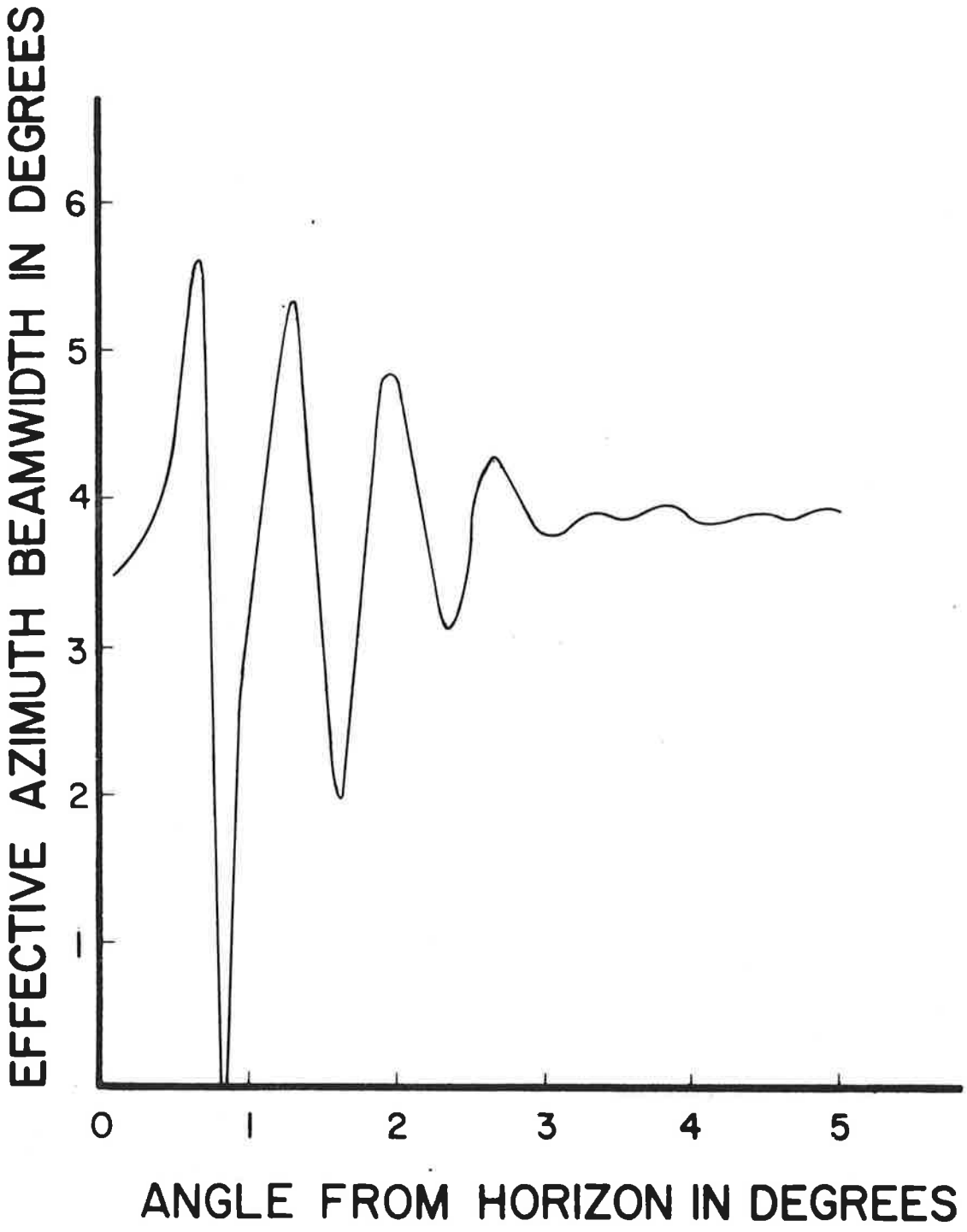

FIG. 19: Effective azimuth beamwidth as a function of the angle from the horizon for the Westinghouse array antenna. H_d = 34', H_o = 42', f = 1030 MHz, nominal pulse ratio K_o = 18dB.

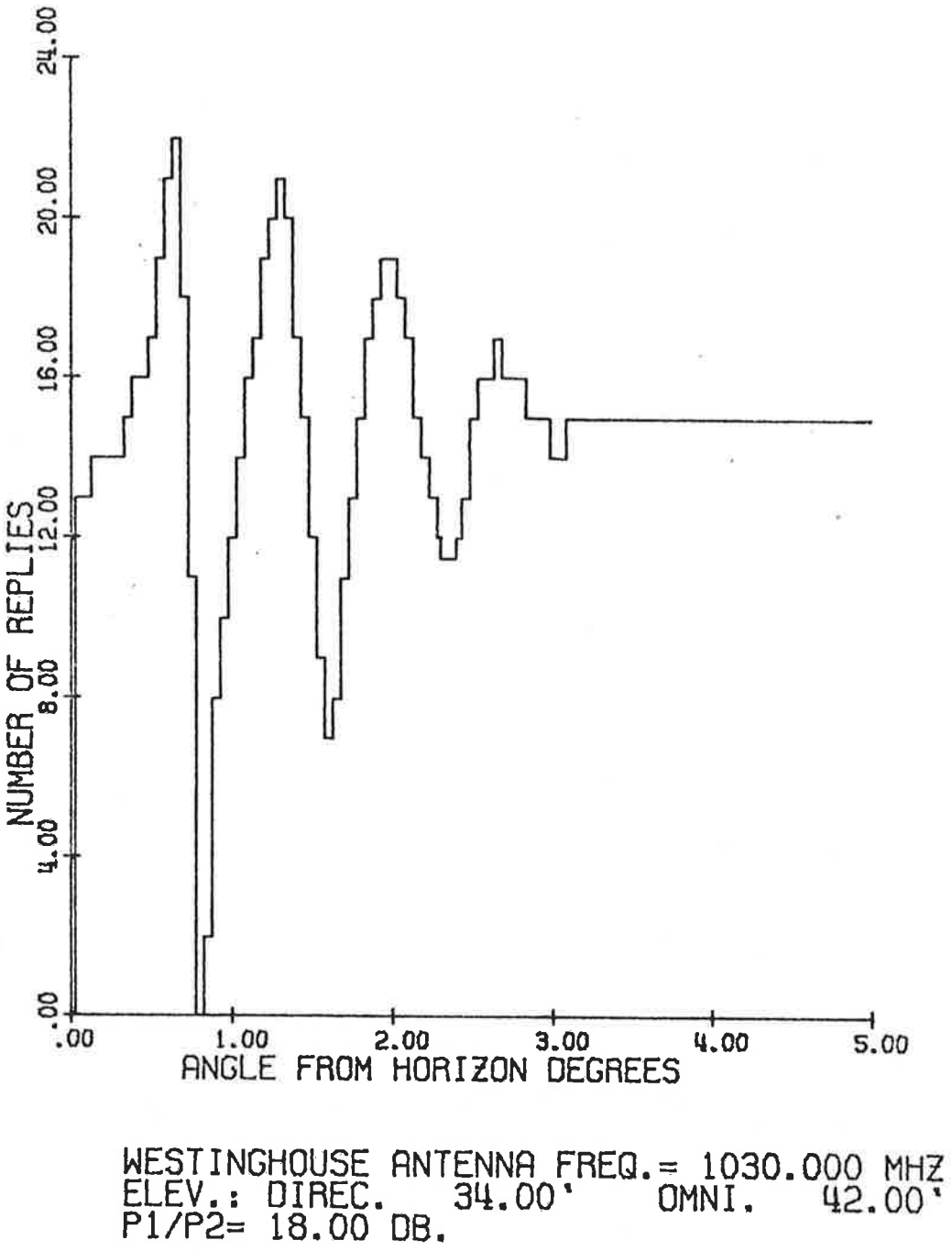

FIG. 20: Number of replies as a function of angle from the horizon.

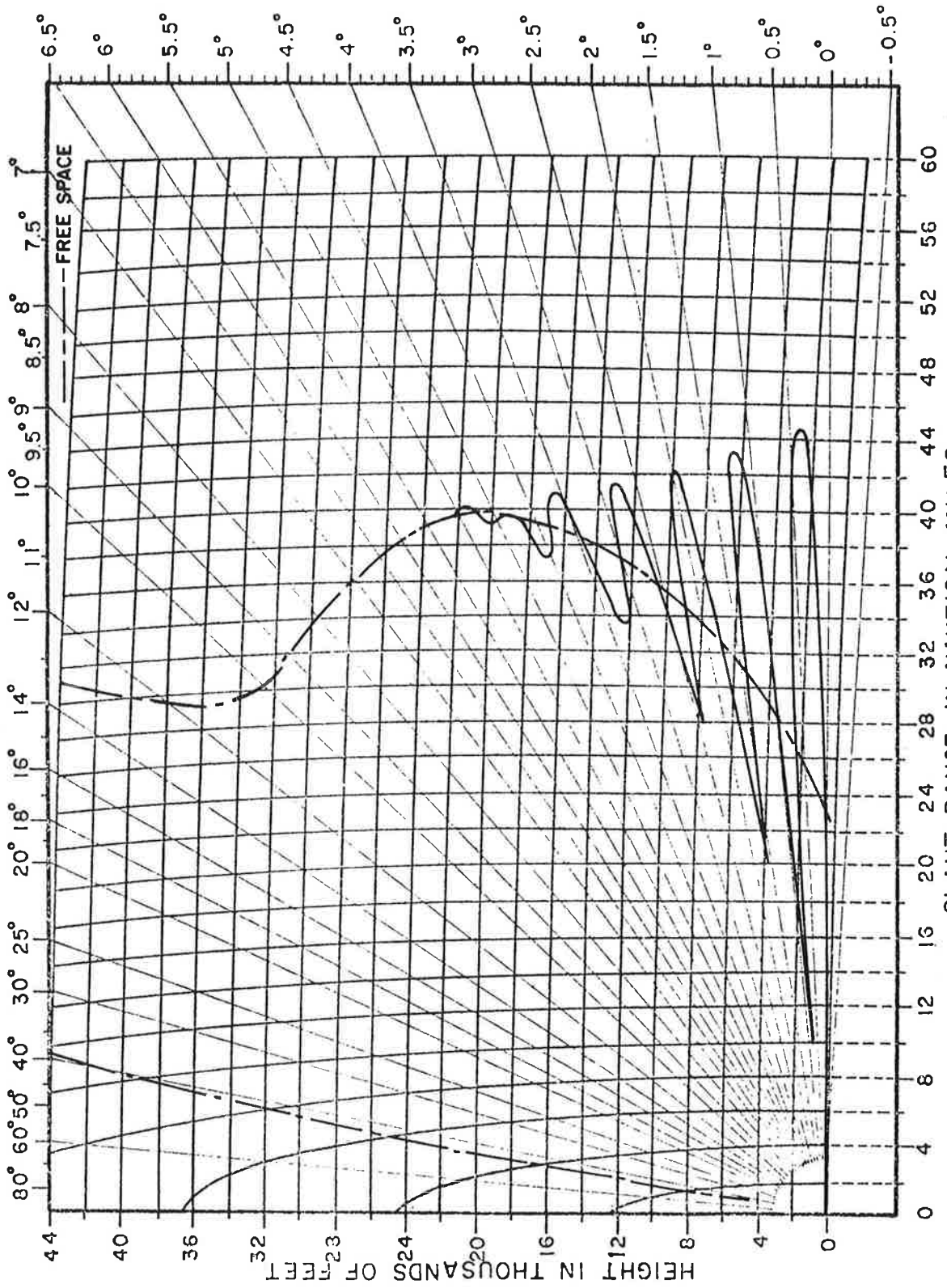

FIG. 21: Coverage diagram for the Westinghouse array antenna. $H_d = 34'$, $H_o = 42'$, f = 1030 MHz, **maximum** free space range = 40 nautical miles.

Figure 22 shows the $P1(\theta)$, $P2(\theta)$ as functions of θ where the 0 dB level is adjusted to coincide with the maximum $P1(\theta)$ level in the free space case. As shown in Fig. 22, the position and depth of the first minimum in the $P1(\theta)$ curve are 0.8^{o} and -7.2 dB relative to the free space value at the same elevation angle. The corresponding values of the $P2(\theta)$ curve are 0.65^{o} and -8.3 dB respectively. The corresponding values of the first maxima are 0.4^{o} and +5.3 dB for the $P1(\theta)$ curve and 0.3^{o} and +5.3 dB for the $P2(\theta)$ curve. For $\theta \geq 4.5^{o}$ the two curves assume their free space values.

Figure 23 shows the normalized pulse ratio as a function of θ. It can be seen from Fig. 23 that the maximum and minimum departures of the pulse ratio from the free space minimal value are +8.5 dB and -8.6 dB respectively. The oscillations are negligible for $\theta \geq 3^{o}$.

The mainbeam killing and sidelobe punch-through zones as functions of the nominal pulse free space ratio are shown in Fig. 24. It is assumed that the sidelobe level of the antenna is L = -25 dB. It is found that mainbeam killing zones exist for $K_0 \leq 17.5$ dB and the sidelobe punch-through zones exist for $K_0 \geq 15.7$ dB. Thus for $15.7 \leq K_0 \leq 17.5$ both zones exist.

Figure 25 shows the effective azimuth beamwidth as a function of θ, for the threshold level a = 9 dB and nominal pulse ratio K_0 = 18 dB. The effective beamwidth assumes its maximum value of 5.7^{o} at $\theta = 0.6^{o}$ and minimum value of 0.9^{o} at $\theta = 0.8^{o}$. After several damped oscillations, the effective azimuth beamwidth assumes its free space value of about 4^{o}.

The number of replies as a function of θ is shown in Fig. 26. The maximum value of N is 22 at $\theta = 0.6^{o}$ and the minimum value is 3 at $\theta = 0.8^{o}$, while the free space value of the number of replies is N = 16.

Figure 27 shows the coverage diagram for the antenna normalized to the free space maximum range of 40 nautical miles. As shown in Fig. 27, the first maximum range of 39.3 NM occurs at $\theta - 0.4^{o}$ and the minimum range of 11 NM at $\theta = 0.8^{o}$.

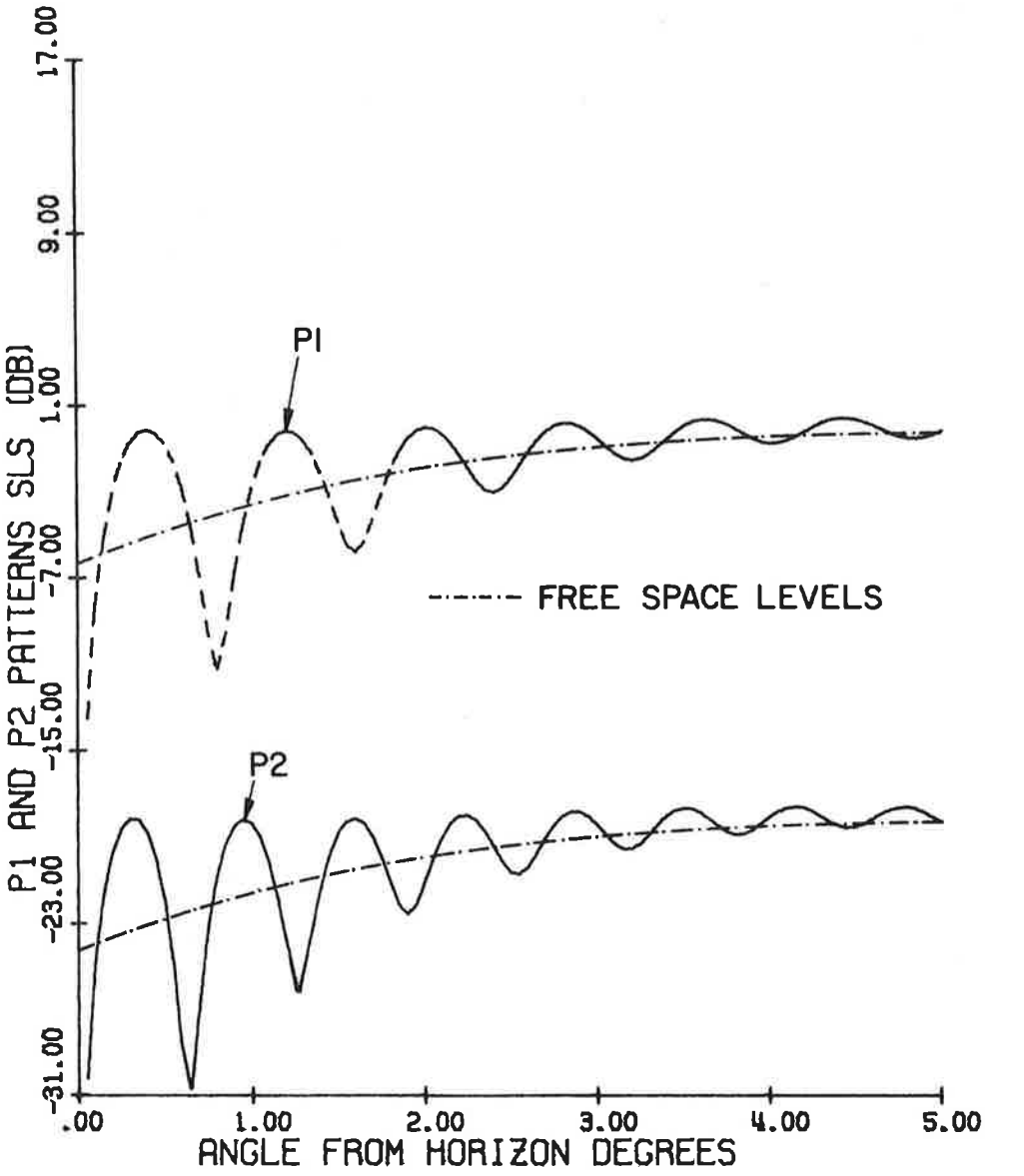

FIG. 22: P1 and P2 pulses as functions of θ.

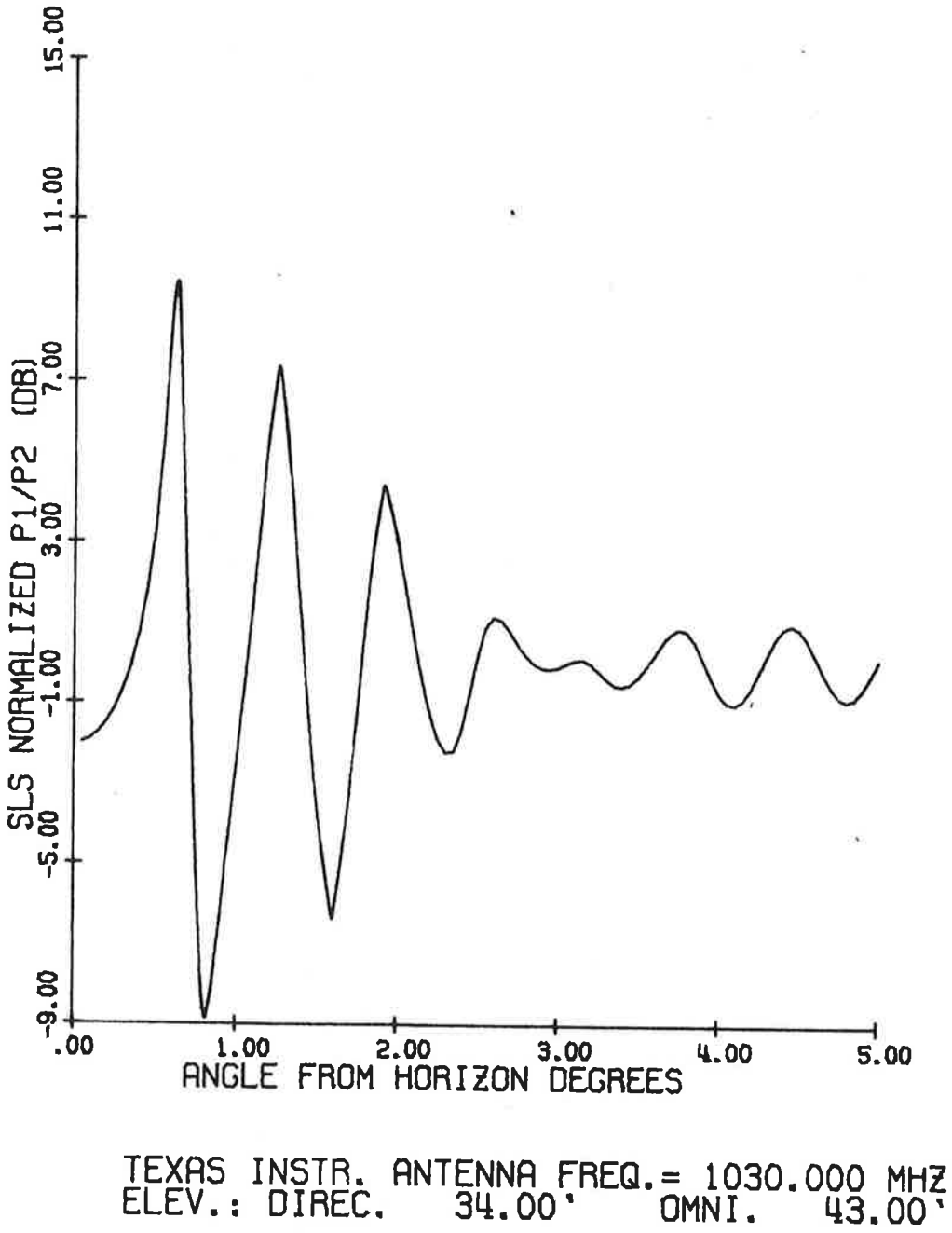

FIG. 23: Normalized pulse ratio as a function of θ.

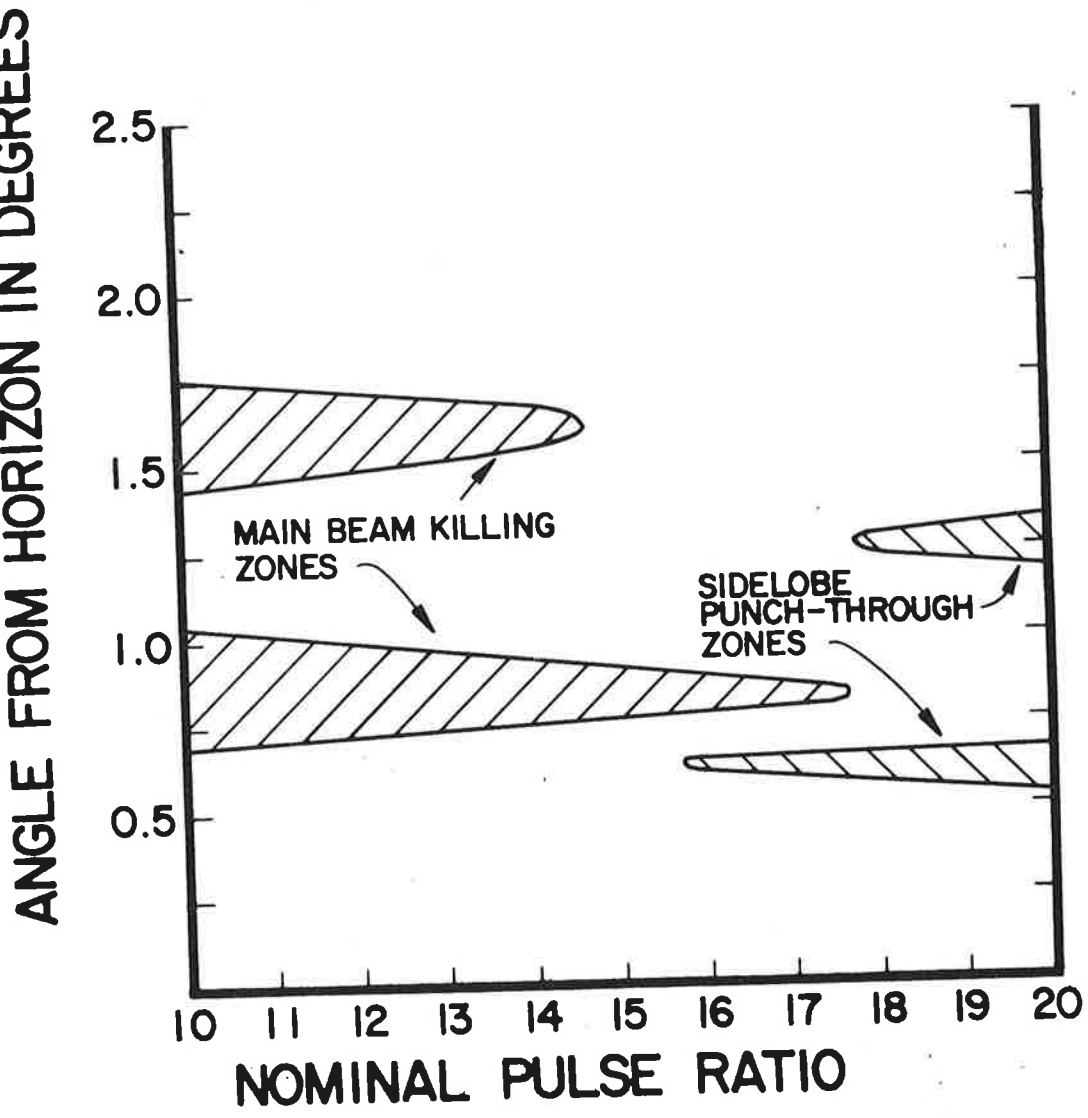

FIG. 24: Mainbeam killing and sidelobe punch-through zones as functions of the nominal pulse ratio for the Texas Instruments reflector antenna. $H_d = 34'$, $H_o = 43'$, f = 1030 MHz, a = 9 dB, b = 0 dB, L = -25 dB.

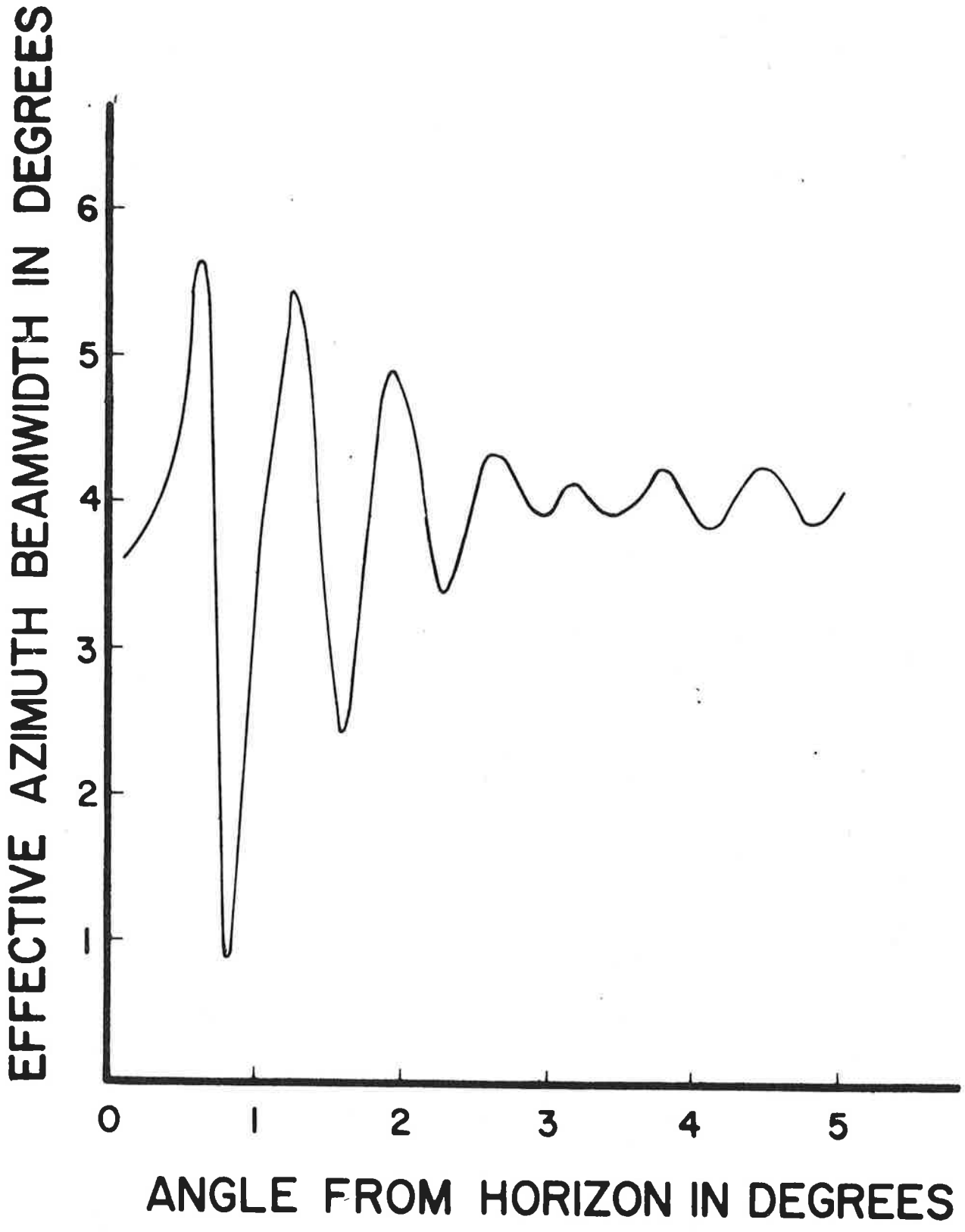

FIG. 25: Effective azimuth beamwidth as a function of angle from the horizon for the Texas Instruments reflector antenna. $H_d = 34'$, $H_o = 43'$, f = 1030 MHz, nominal pulse ratio $K_o = 18$dB.

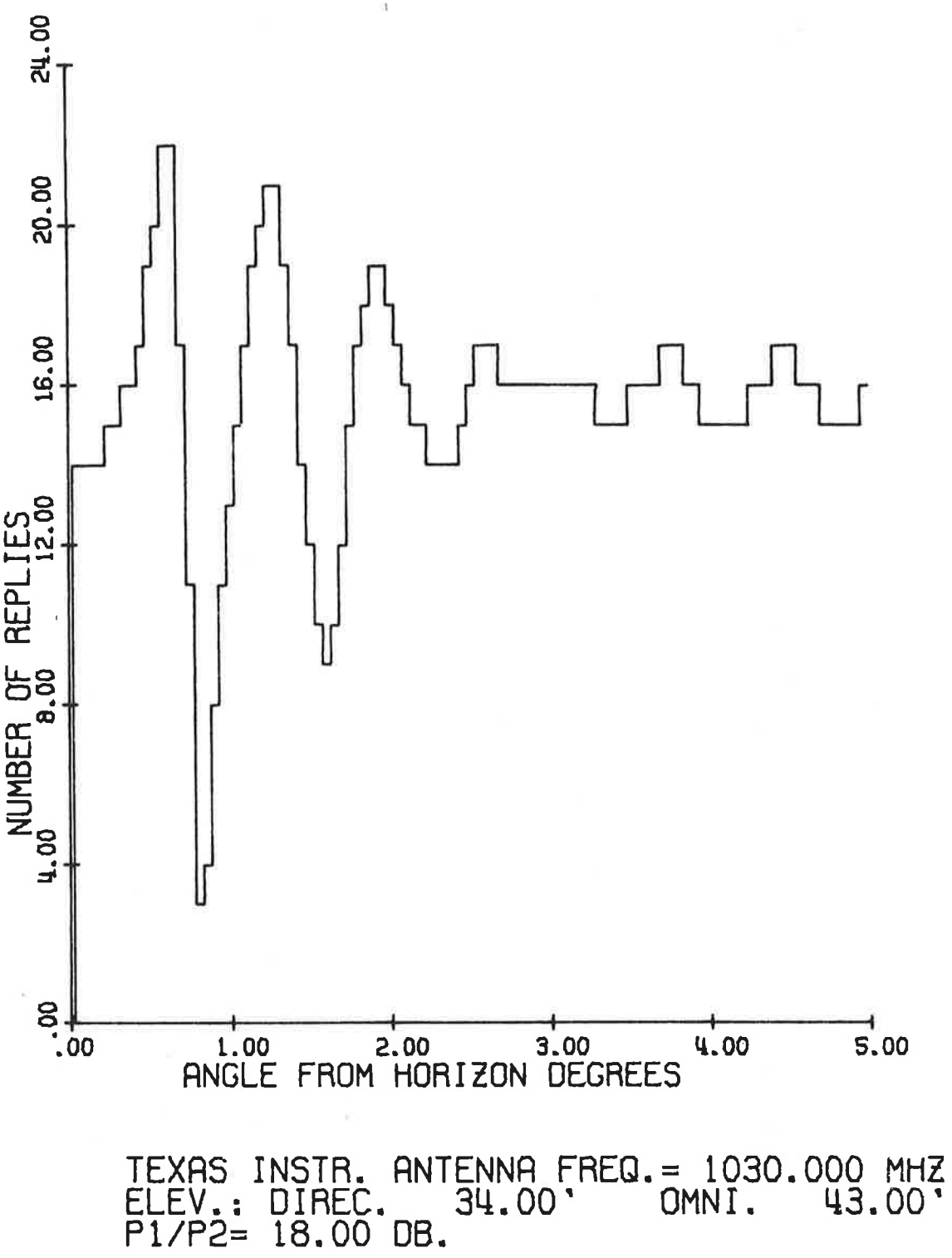

FIG. 26: Number of replies as a function of angle from the horizon.

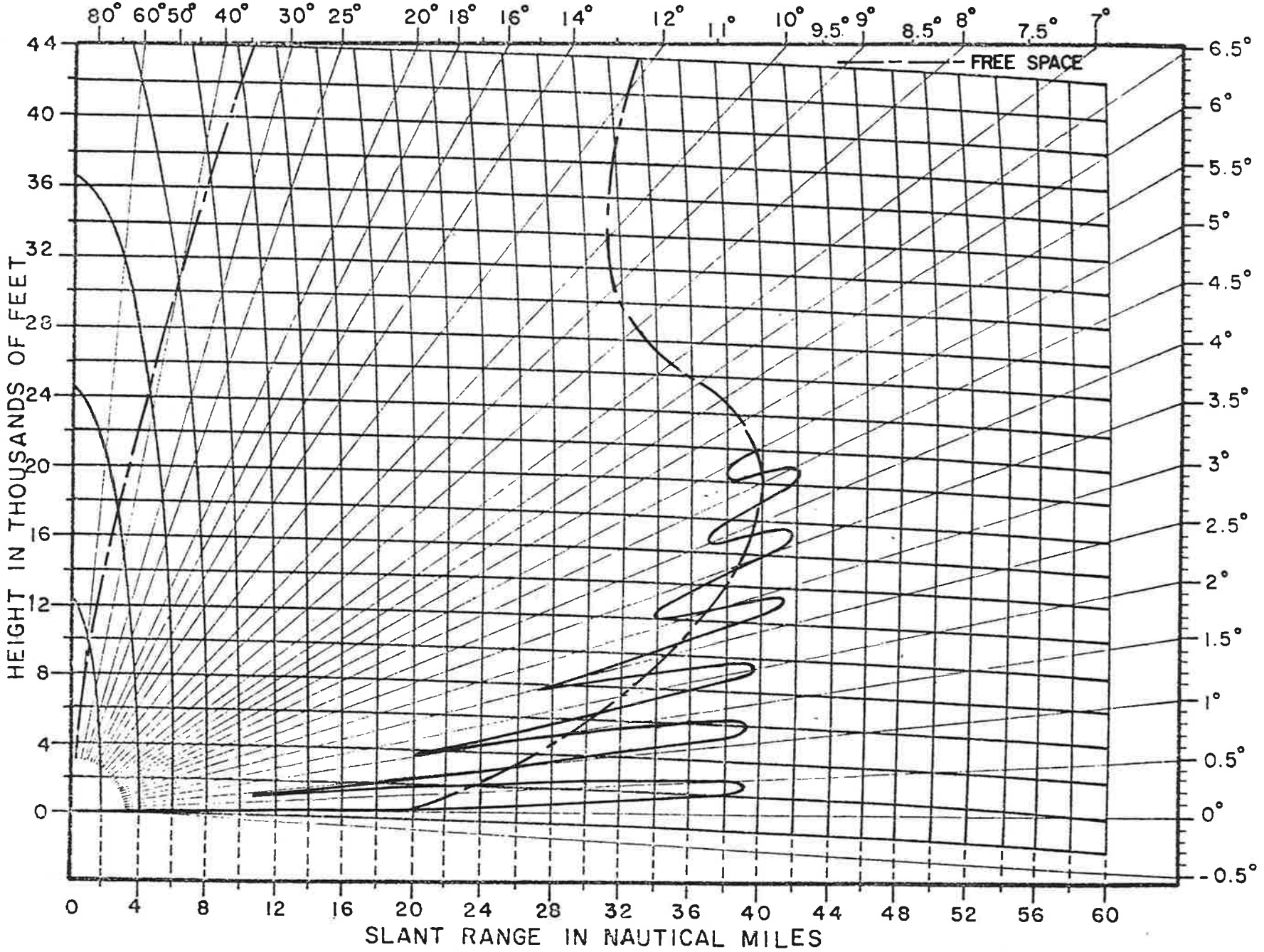

FIG. 27: Coverage diagram of the Texas Instruments reflector antenna. H_d = 34', H_o = 43', f = 1030 MHz, maximum free space range = 40 nautical miles.

4.2.3 Hazeltine Open Array Antenna

The tower height for this antenna is 27'. The heights of the phase centers of the directional and omnidirectional antennas are respectively $H_d = 33'$ and $H_o = 37'$. The two phase centers are displaced vertically by 4'. The vertical aperture of the antenna is 4'.

Figure 28a shows the $P1(\theta)$, $P2(\theta)$ pulses as functions of θ where the 0 dB level is adjusted to coincide with the maximum $P1(\theta)$ level in the free space case. The deepest minimum for the $P1(\theta)$ pulse occurs at an angle $\theta = 0.65^{\circ}$ with the level of -13.34dB with respect to the free space level at the same angle. The corresponding values for the $P2(\theta)$ pulse are 0.58° and -13.5dB. The positions and levels of the first maxima are 0.3° and +4.5dB for the $P1(\theta)$ pulse and 0.28° and +4.6dB for the $P2(\theta)$ pulse. The oscillations of the patterns around the free space values are not so quickly damped out as in the case of the previous two antennas. For this reason the $P1(\theta)$ and $P2(\theta)$ curves in the extended region $5^{\circ} \leq \theta \leq 10^{\circ}$ are shown in Fig. 28b. For $\theta > 10^{\circ}$ the curves assume their free space values.

The pulse ratio $P1(\theta)/P2(\theta)$ as a function of θ is shown in Fig. 29a. The maximum and minimum departures of the pulse ratio from its nominal free space values are+9.8dB and -9.9dB respectively. Figure 29b shows the pulse ratio variation in the range $5^{\circ} \leq \theta \leq 10^{\circ}$.

The mainbeam killing and sidelobe punch-through zones as functions of nominal pulse ratio are shown in Fig. 30. It is found from Fig. 30 that the mainbeam killing zones exist for $K_0 \leq 18.9$dB and the sidelobe punch-through zones exist for $K_0 \geq 15.2$dB. Both the zones exist for $15.2\text{dB} \leq K_0 \leq 18.9\text{dB}$. The antenna sidelobe level is assumed to be L = -25.dB. For the range of values shown in Fig. 30 there are seven mainbeam killing and five sidelobe punch-through zones.

The effective azimuth beamwidth as a function of θ is shown in Fig. 31 for the range $0 \leq \theta \leq 5^{\circ}$. The effective azimuth beamwidth attains its maximum value

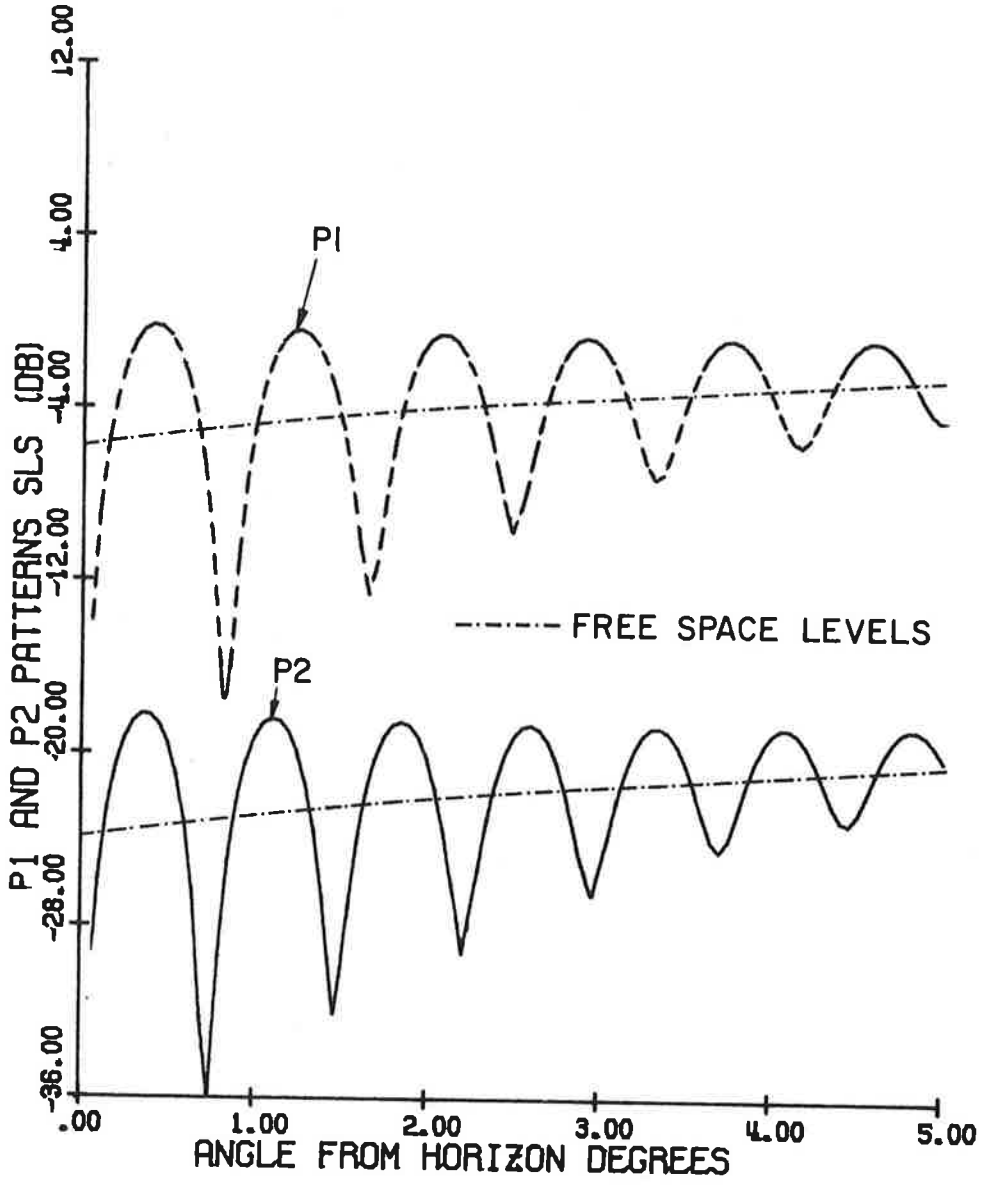

FIG. 28a: P1 and P2 pulses as functions of θ.

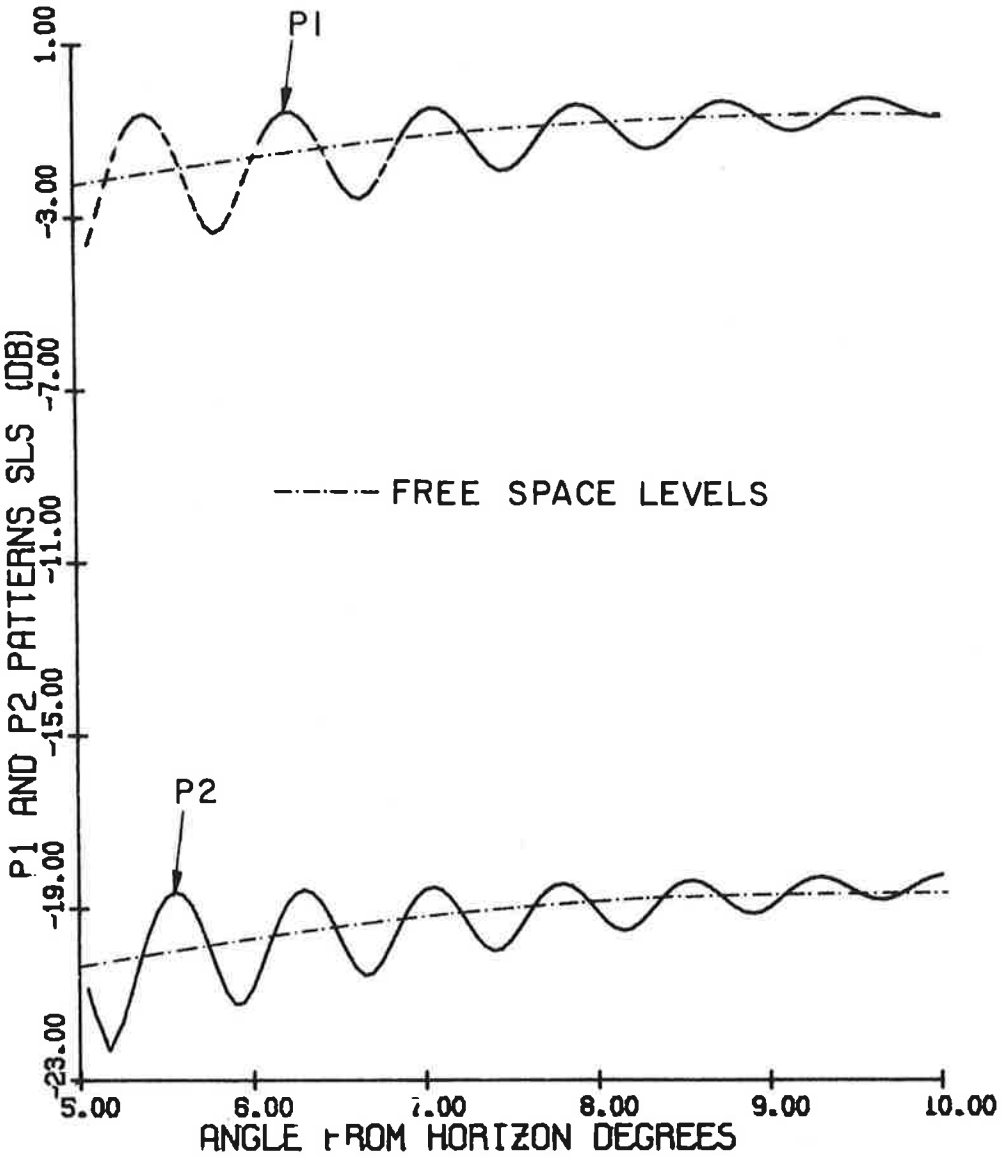

FIG. 28b: P1 and P2 pulses as functions of θ.

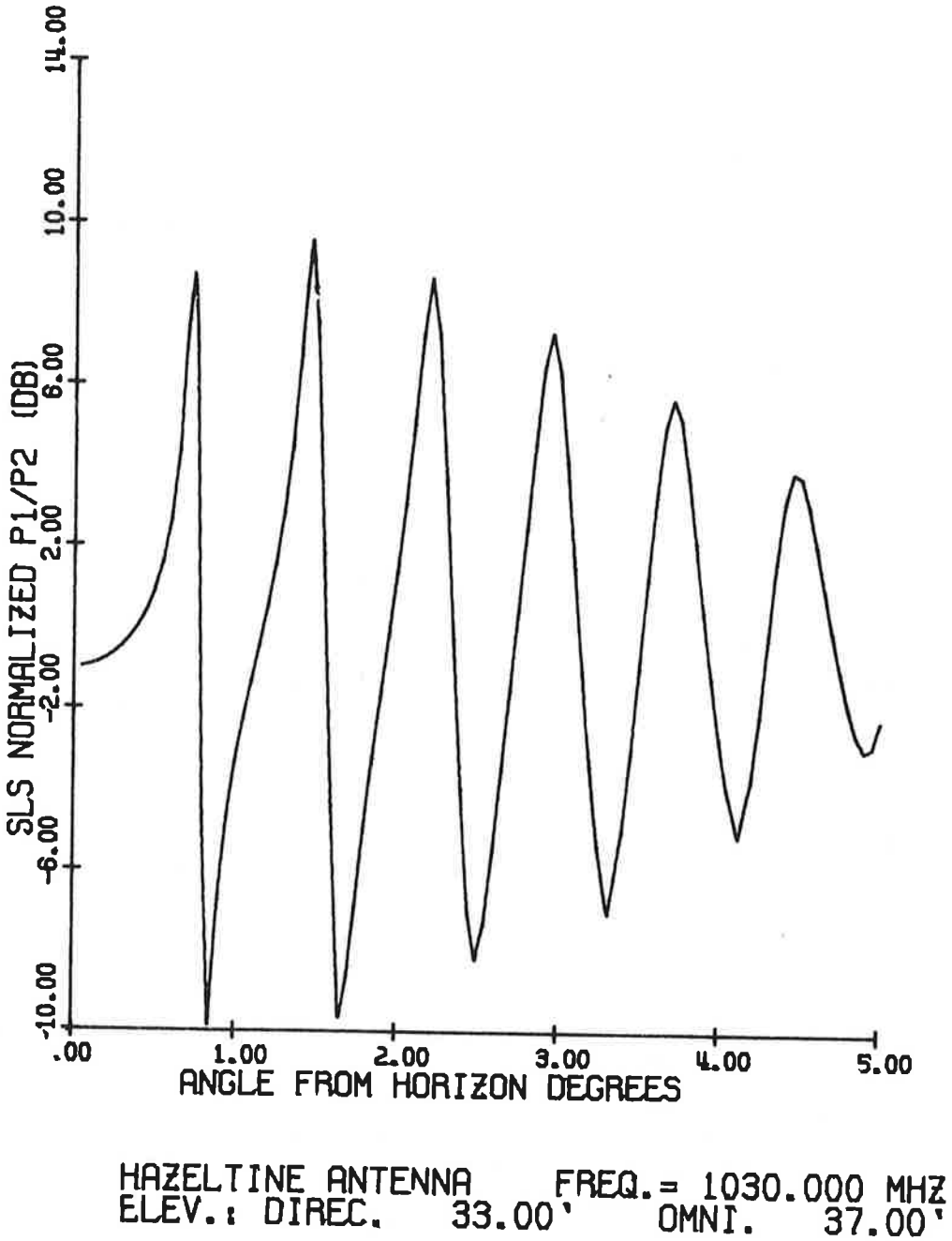

FIG. 29a: Normalized pulse ratio as a function of θ.

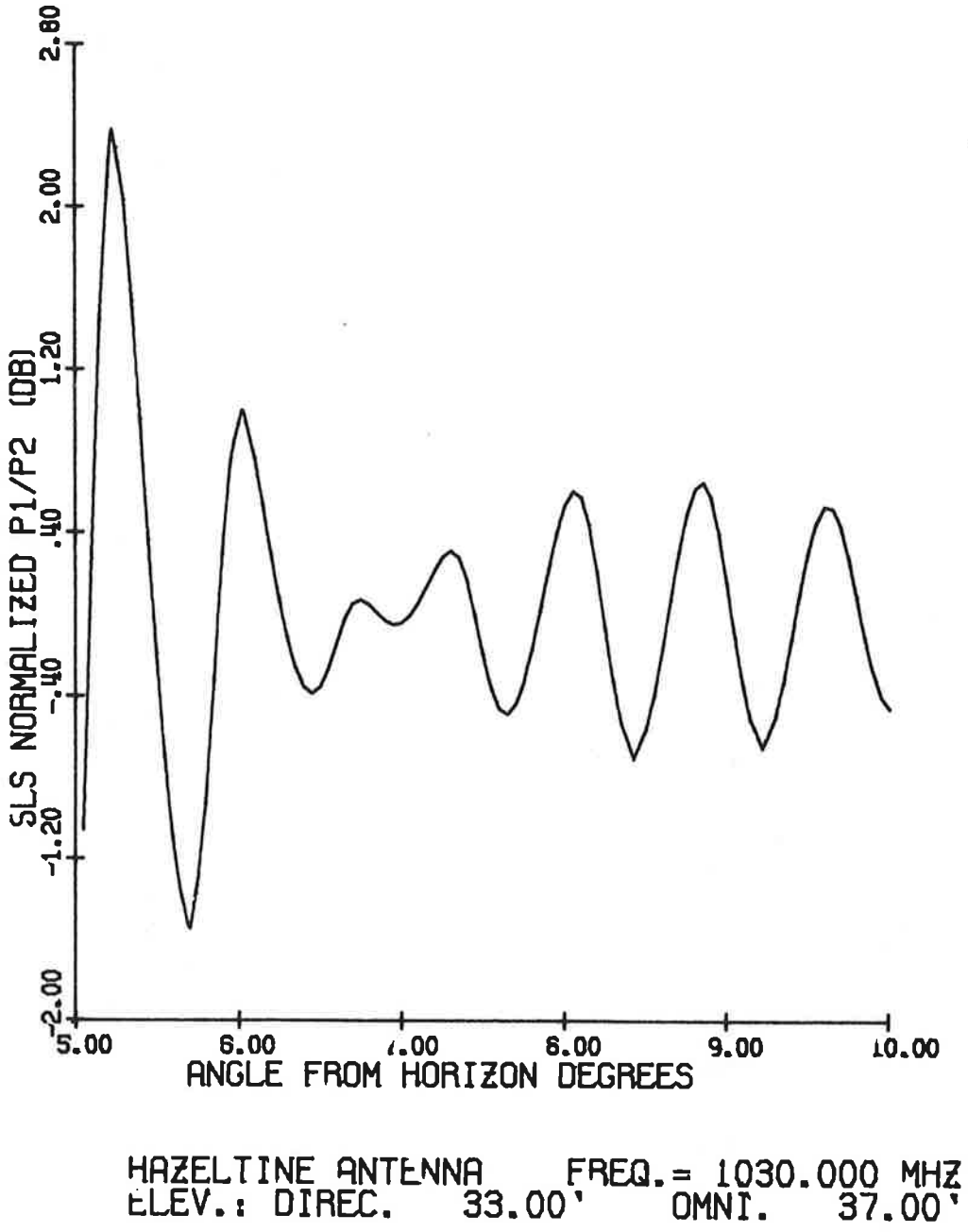

FIG. 29b: Normalized pulse ratio as a function of θ.

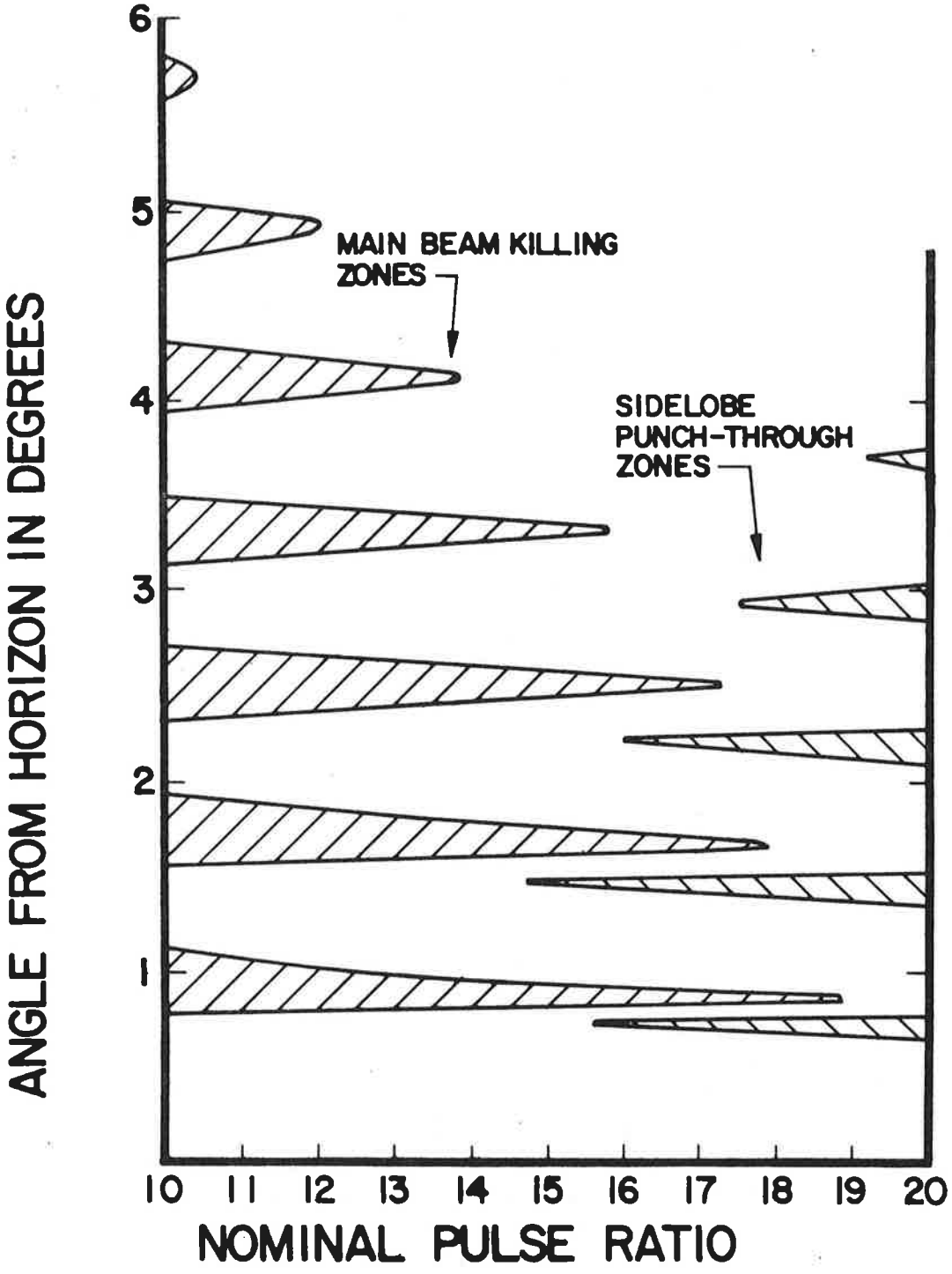

FIG. 30: Mainbeam killing and sidelobe punch-through zones as functions of the nominal pulse ratio for the Hazeltine open array antenna. $H_d = 33'$, $H_o = 37'$, $f = 1030$ MHz, $a = 9$dB, $b = 0$dB, $L = -25$dB.

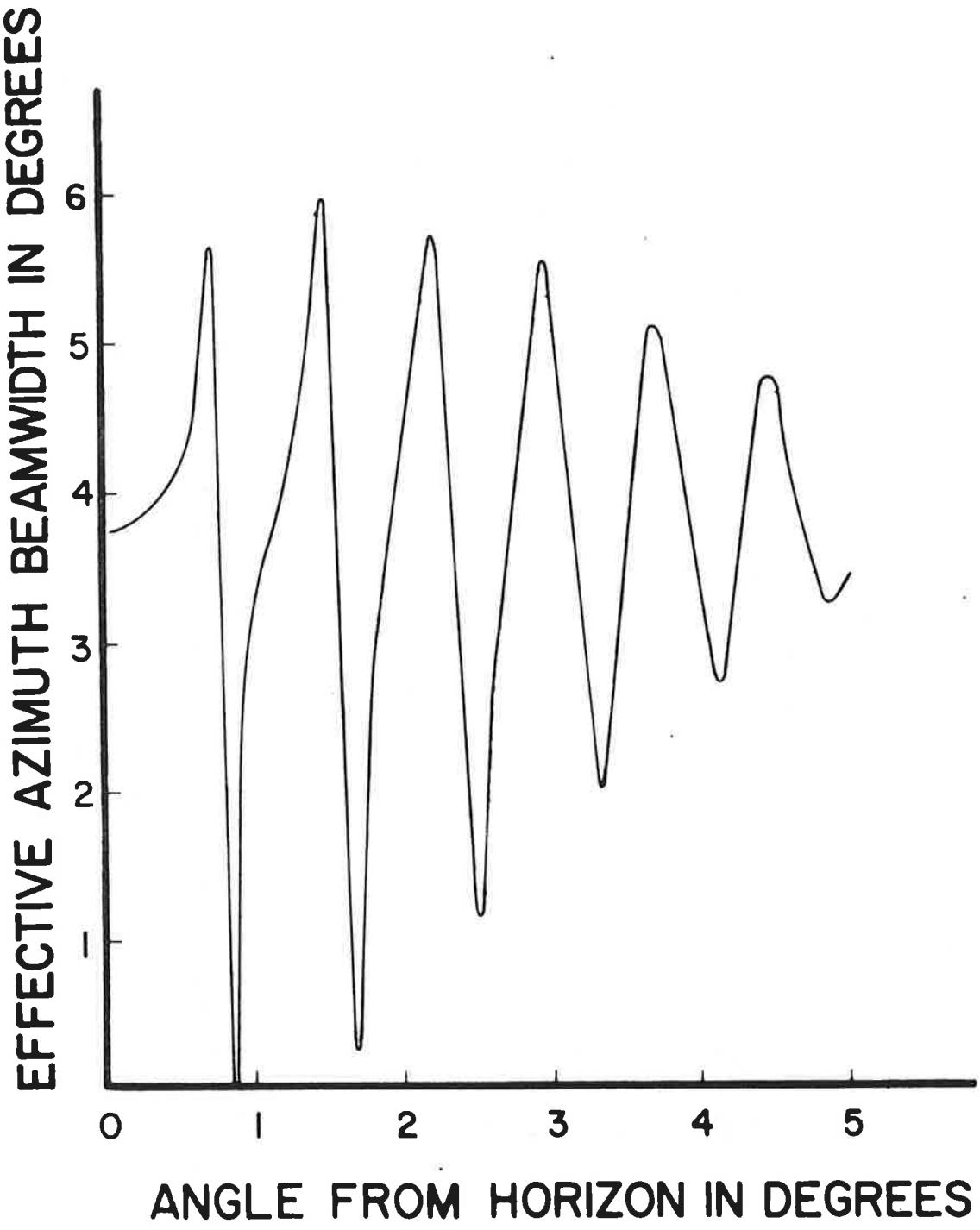

FIG. 31: Effective azimuth beamwidth as a function of angle from the horizon for the Hazeltine open array antenna. H_d = 34', H_o = 37', f = 1030 MHz, nominal pulse ratio K_o = 18 dB.

5.9^{o} at $\theta = 1.5^{o}$ and the minimum value of 0^{o} at $\theta = 0.85^{o}$. The curve oscillates around the free space value of about 4^{o} with decreasing amplitudes.

The number of replies as a function of θ are shown in Fig. 32 for the range of angle $0 \leq \theta \leq 5^{o}$. The number of replies varies from a maximum N = 23 to a minimum of 0 for $\theta = 0.65^{o}$ and $\theta = 1.3^{o}$. The free space value is about 15.

The coverage diagram is shown in Fig. 33. It is found from Fig. 33 that the deepest minimum range is 5.6 NM at $\theta = 0.65^{o}$; the first maximum range is about 39.3 NM at $\theta = 0.3^{o}$. The coverage diagram oscillates around the free space curve for elevation angles up to $\theta = 10^{o}$. For $\theta > 10^{o}$ the coverage diagram assumes practically its free space values.

4.2.4 The Existing Hog-Trough Antenna

The tower height for this antenna is 27'. The heights of the phase centers of the directional and omnidirectional antennas are 41' and 43' respectively. The two phase centers of the antenna are displaced vertically by 2'. The vertical aperture of the antenna is about 2'.

Figure 34a shows the P1(θ), P2(θ) pulses as functions of θ where the 0 dB level refers to the maximum P1(θ) level in the free space case. Because of the relatively small fall-off gradient of the free space pattern at the horizon, the lobing structures of the P1(θ) and P2(θ) are much more pronounced in the present case. The oscillations are found to be appreciable for values of θ up to about 20^{o}. Figures 34b - 34d show the variations of P1(θ) and P2(θ) pulses for three more regions of θ, $5^{o} \leq \theta \leq 10^{o}$, $10^{o} \leq \theta \leq 15^{o}$ and $15^{o} \leq \theta \leq 20^{o}$. The oscillations in the curves are found to be appreciable up to $\theta = 20^{o}$.

Figures 35a - 35d show the pulse ratio as a function of θ for four different ranges of θ.

Figure 36 shows the mainbeam killing and sidelobe punch-through zones within the range of θ given by $0 \leq \theta \leq 5^{o}$ as functions of the nominal pulse ratio. Within the range of values shown in Fig. 36, both the zones exist for $10.8\,\text{dB} \leq K_{0} \leq 22\,\text{dB}$. It is anticipated that both zones exist for this antenna for $\theta > 5^{o}$. If desired, they may be obtained from the corresponding pulse ratio curves.

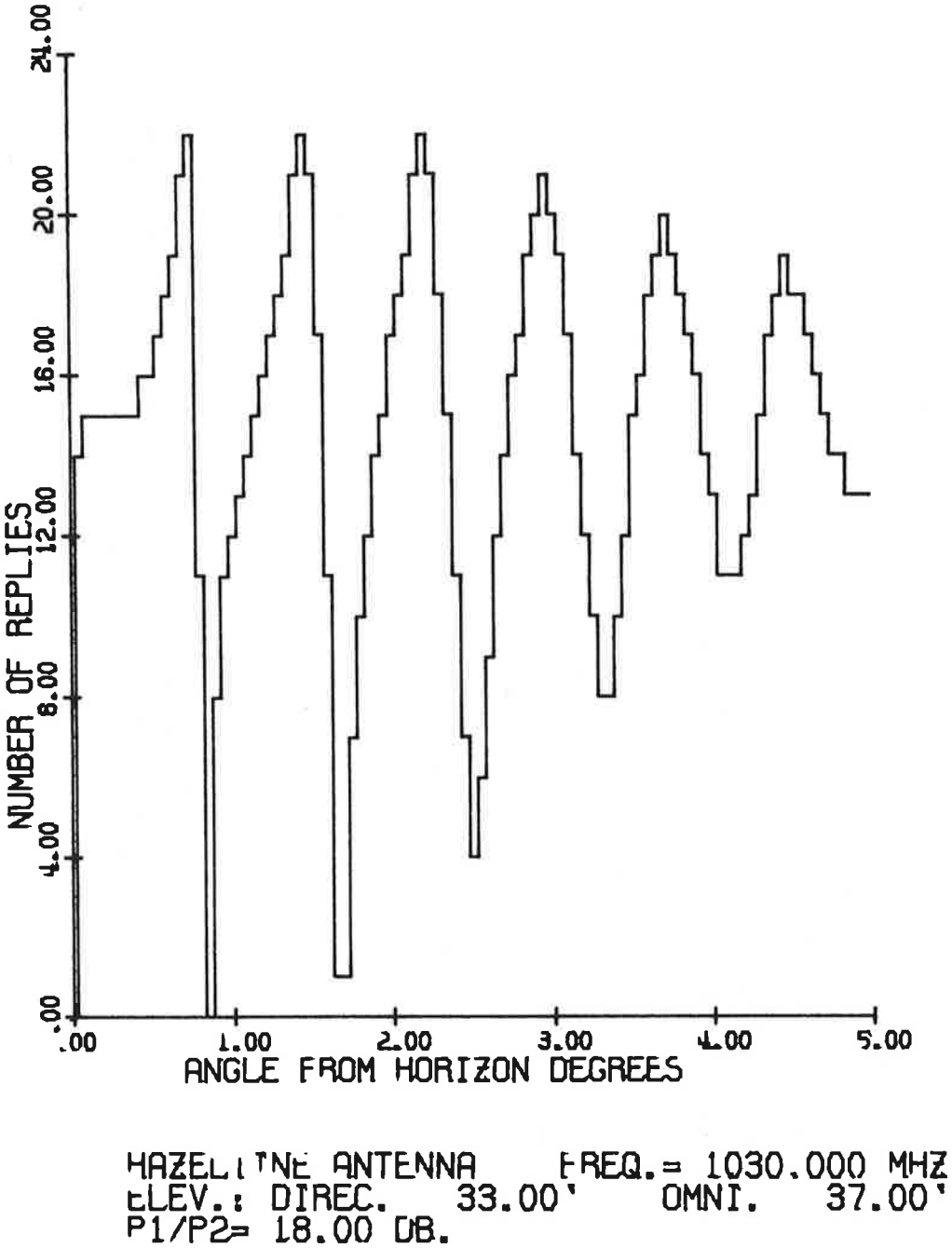

FIG. 32a: Number of replies as a function of angle from the horizon.

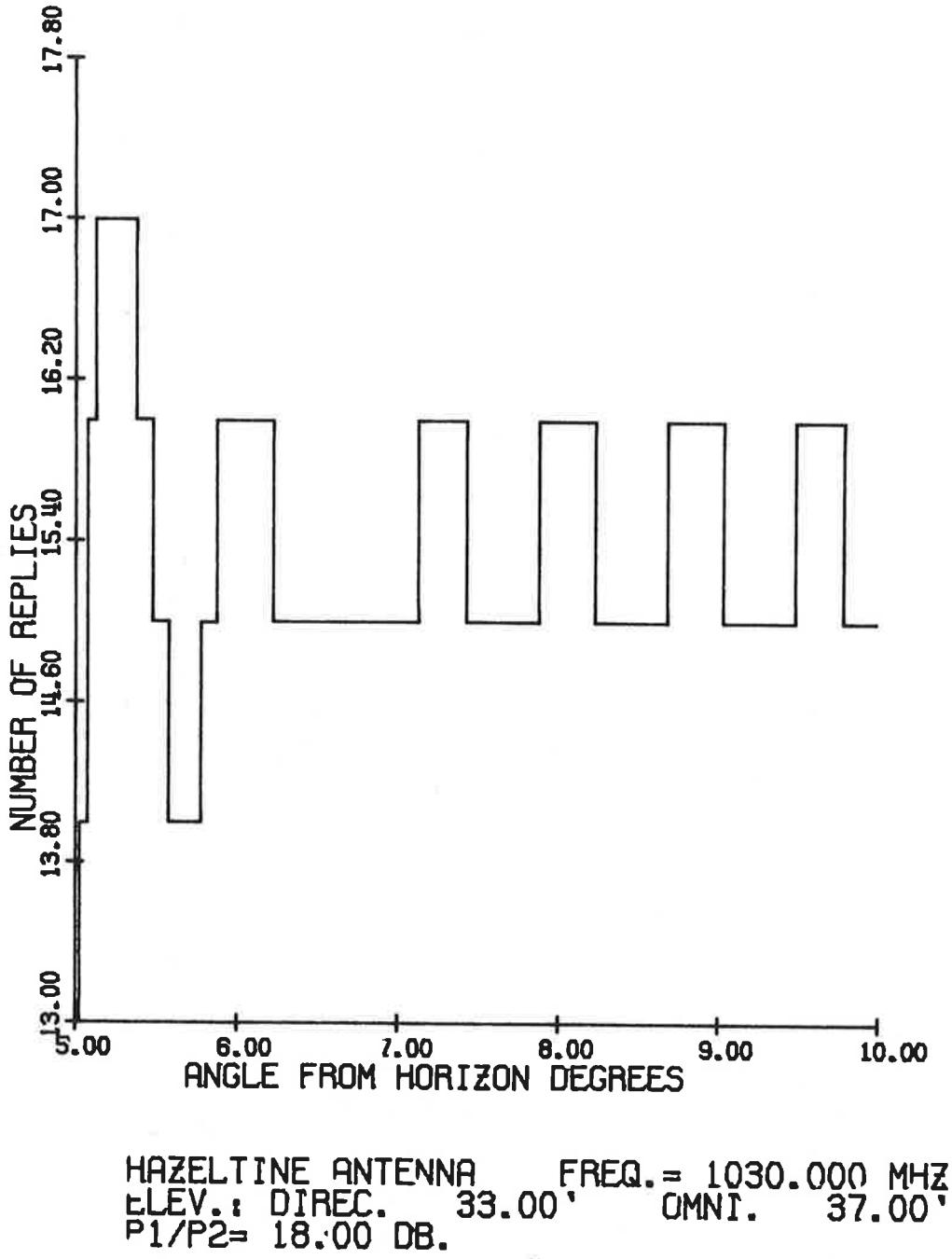

FIG. 32b: Number of replies as a function of angle from the horizon.

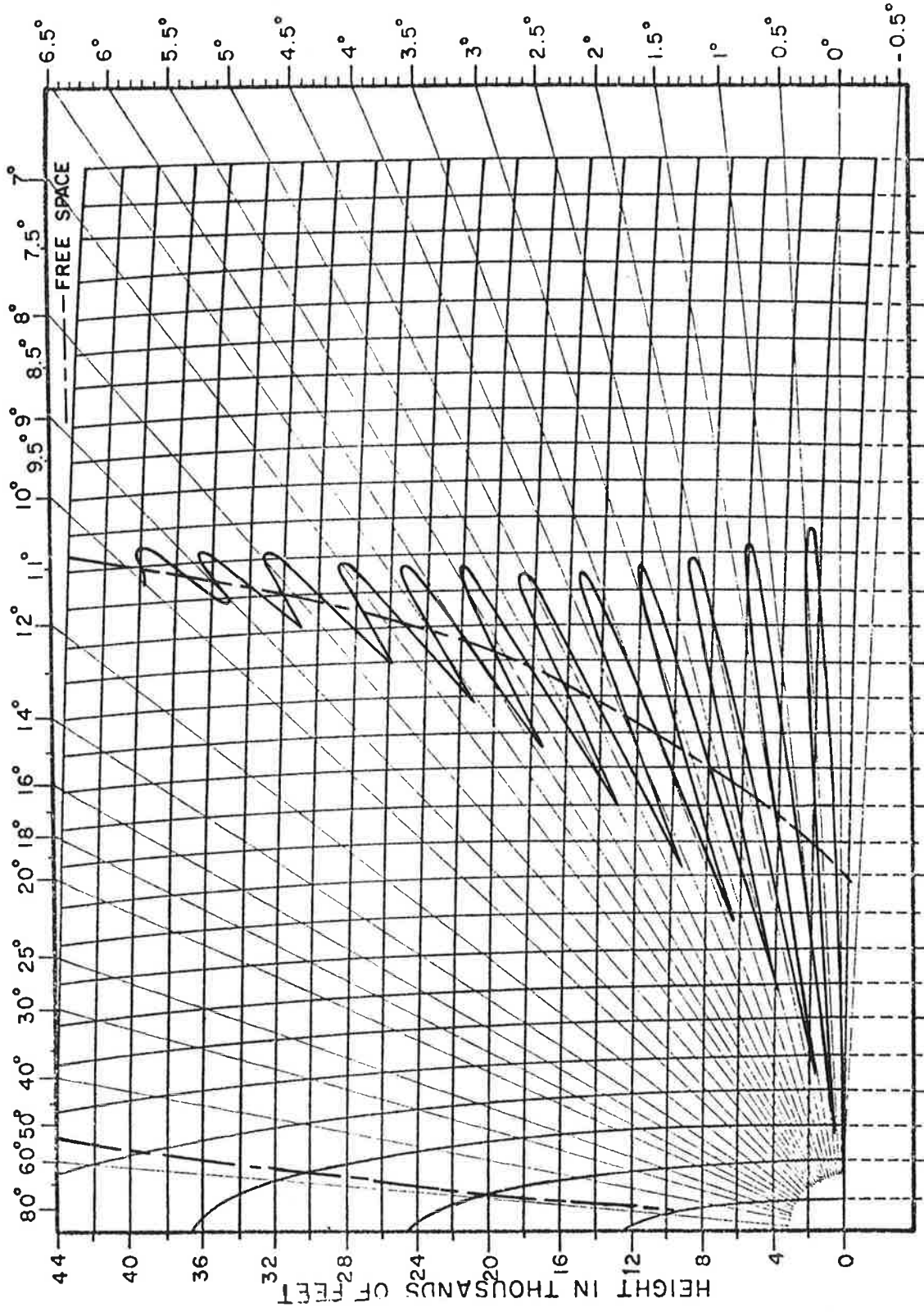

FIG. 33: Coverage diagram for the Hazeltine open array antenna. H_d = 34', H_o = 37', f = 1030 MHz, maximum free space range = 40 nautical miles.

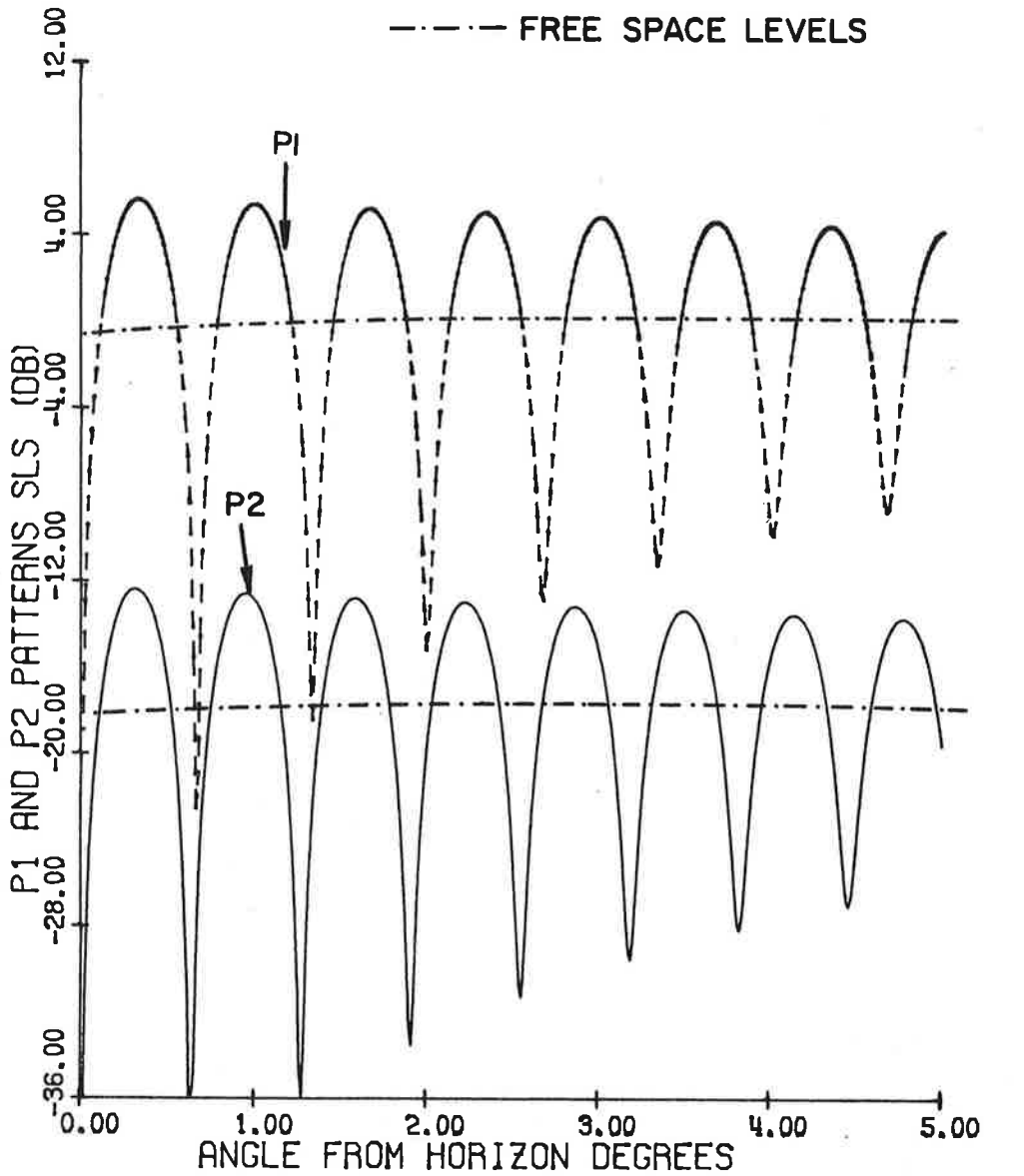

FIG. 34a: P1 and P2 pulses as functions of θ.

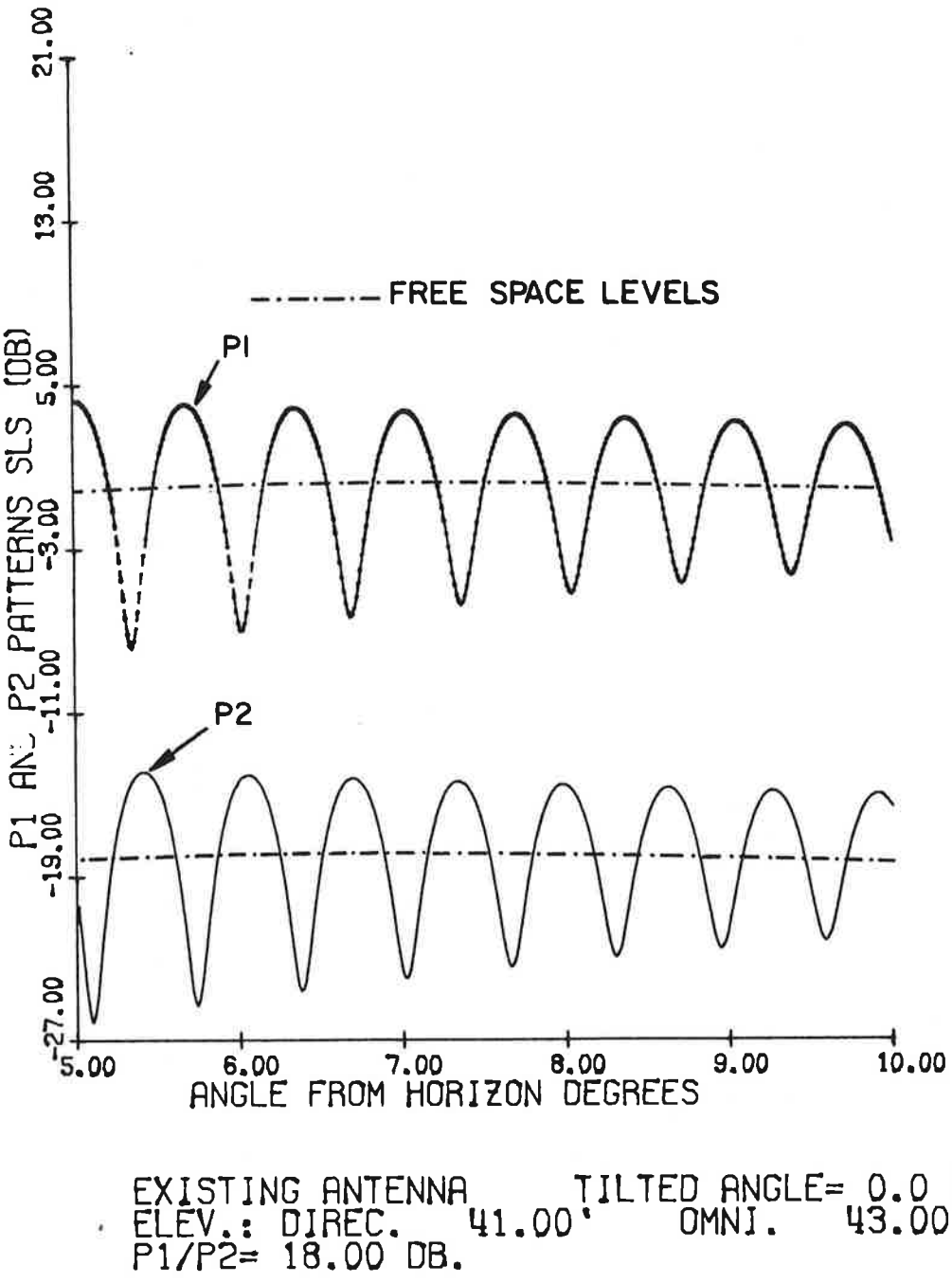

FIG. 34b: P1 and P2 pulses as functions of θ.

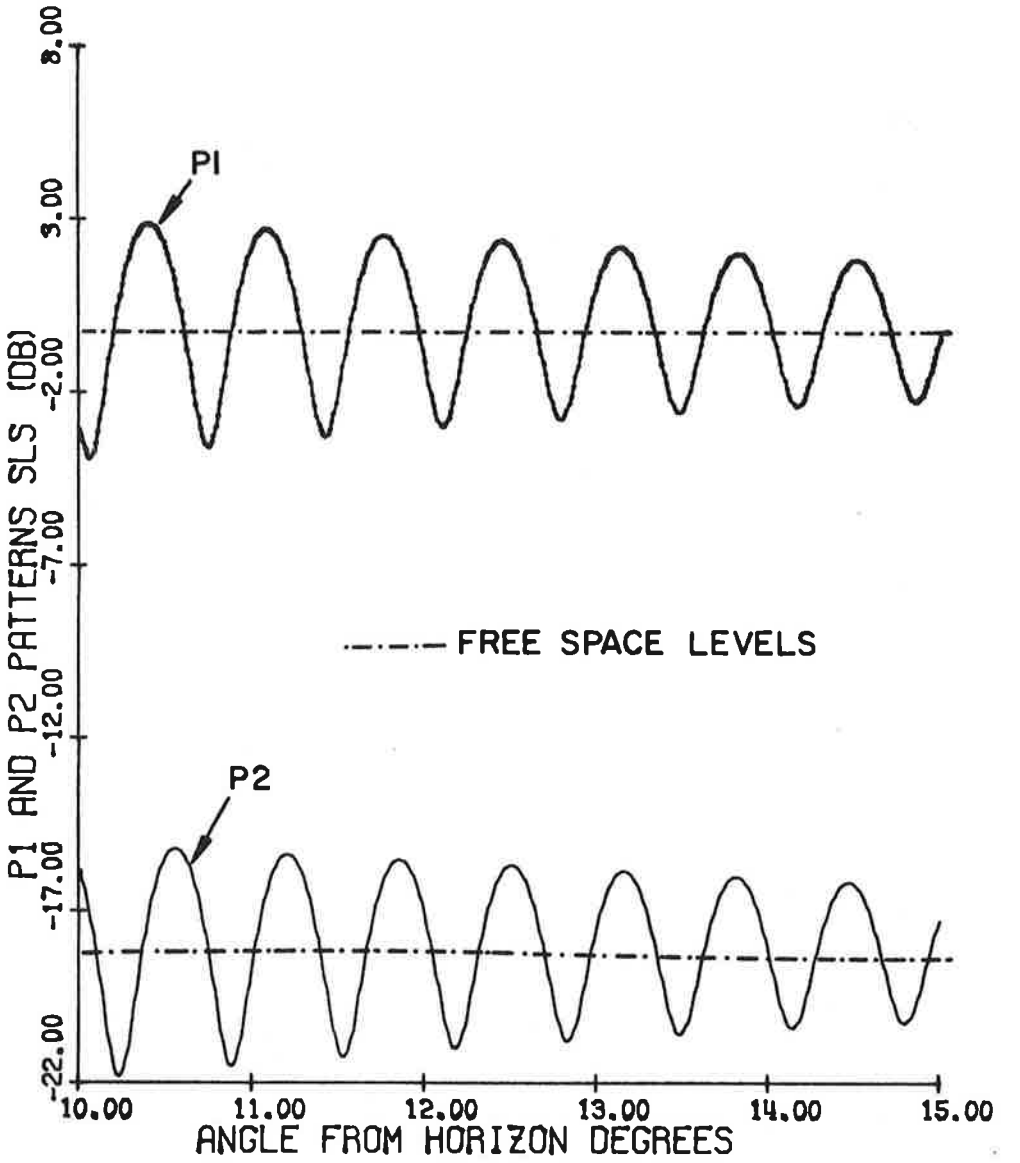

FIG. 34c: P1 and P2 pulses as functions of θ.

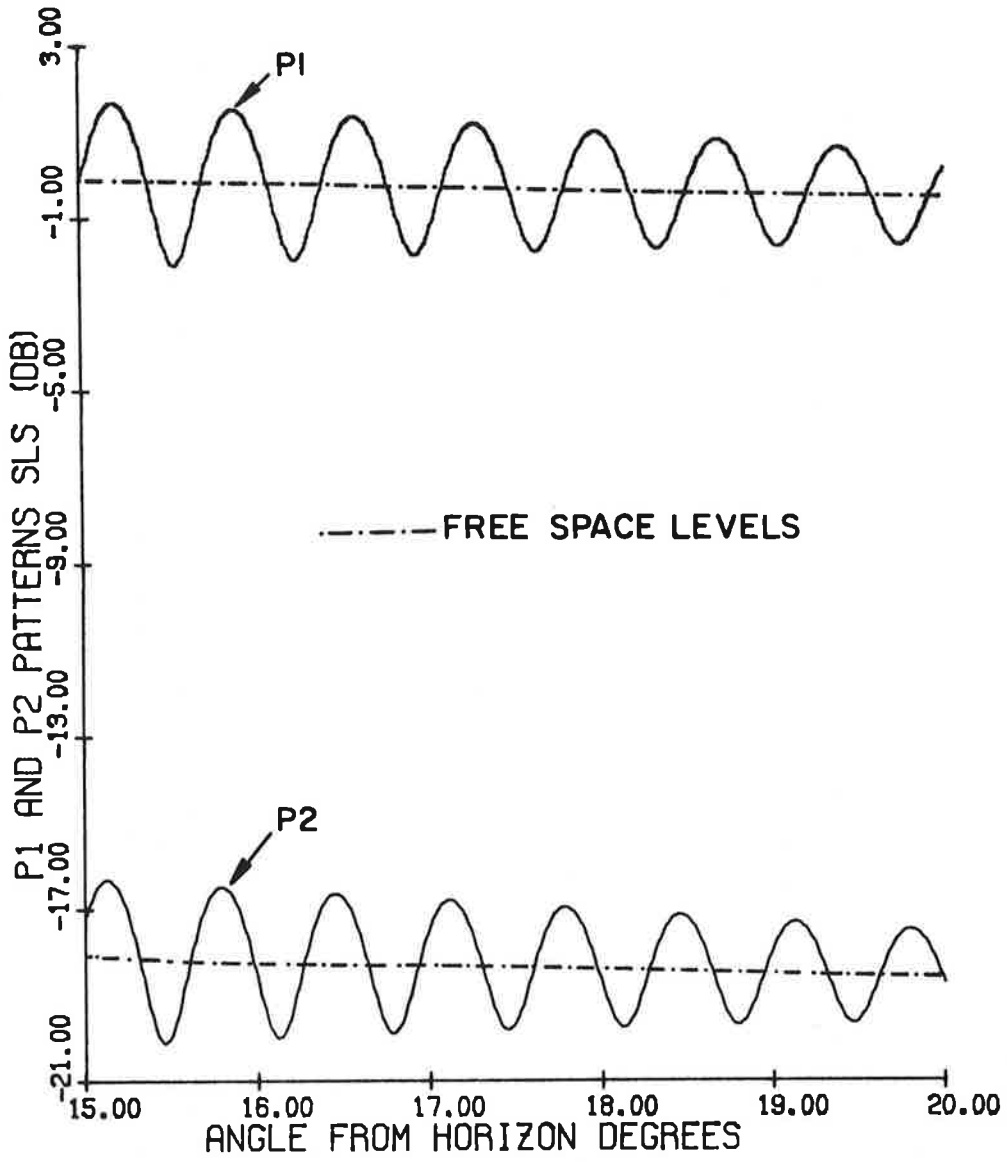

FIG. 34d: P1 and P2 pulses as functions of θ.

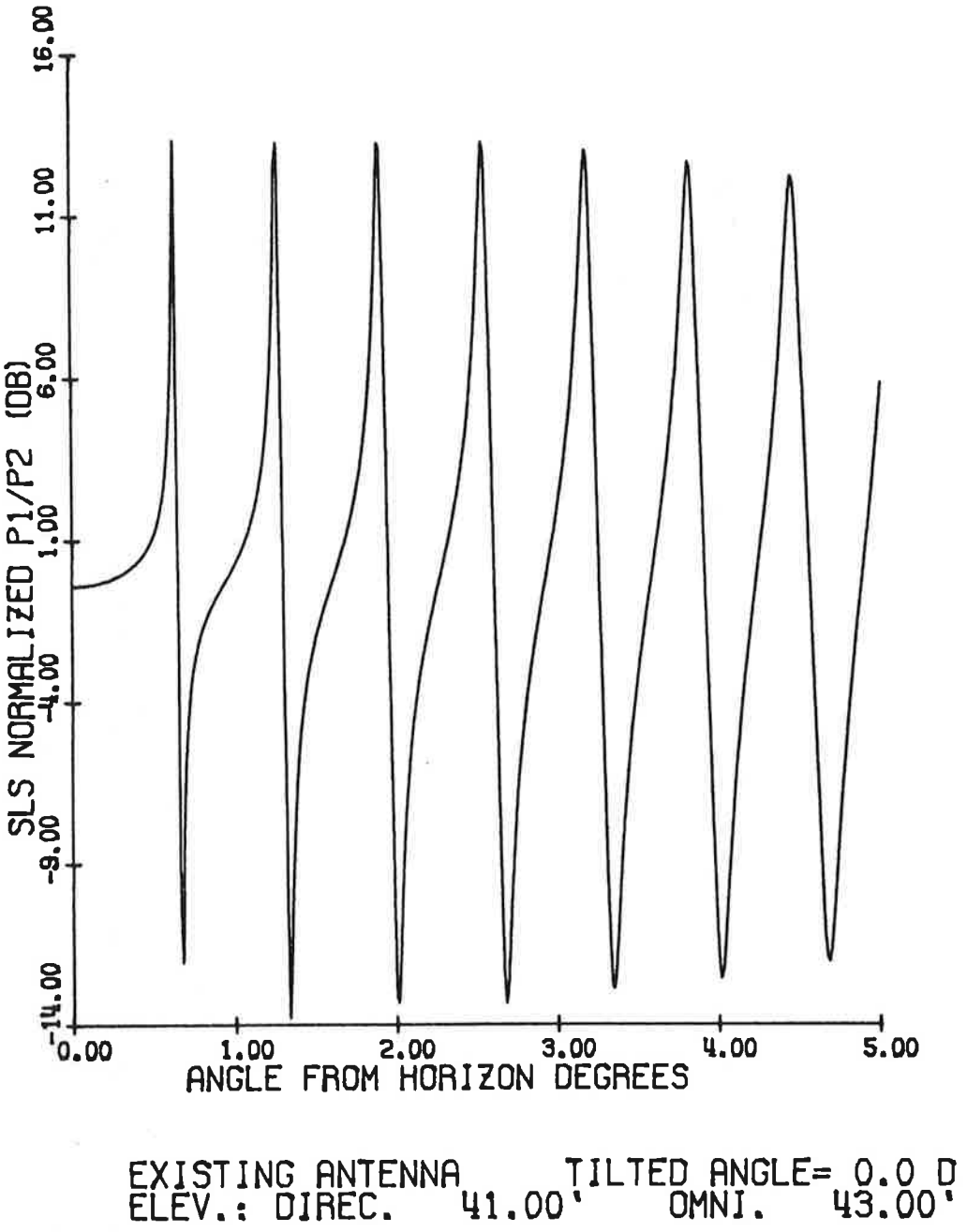

FIG. 35a: Normalized pulse ratio as a function of θ.

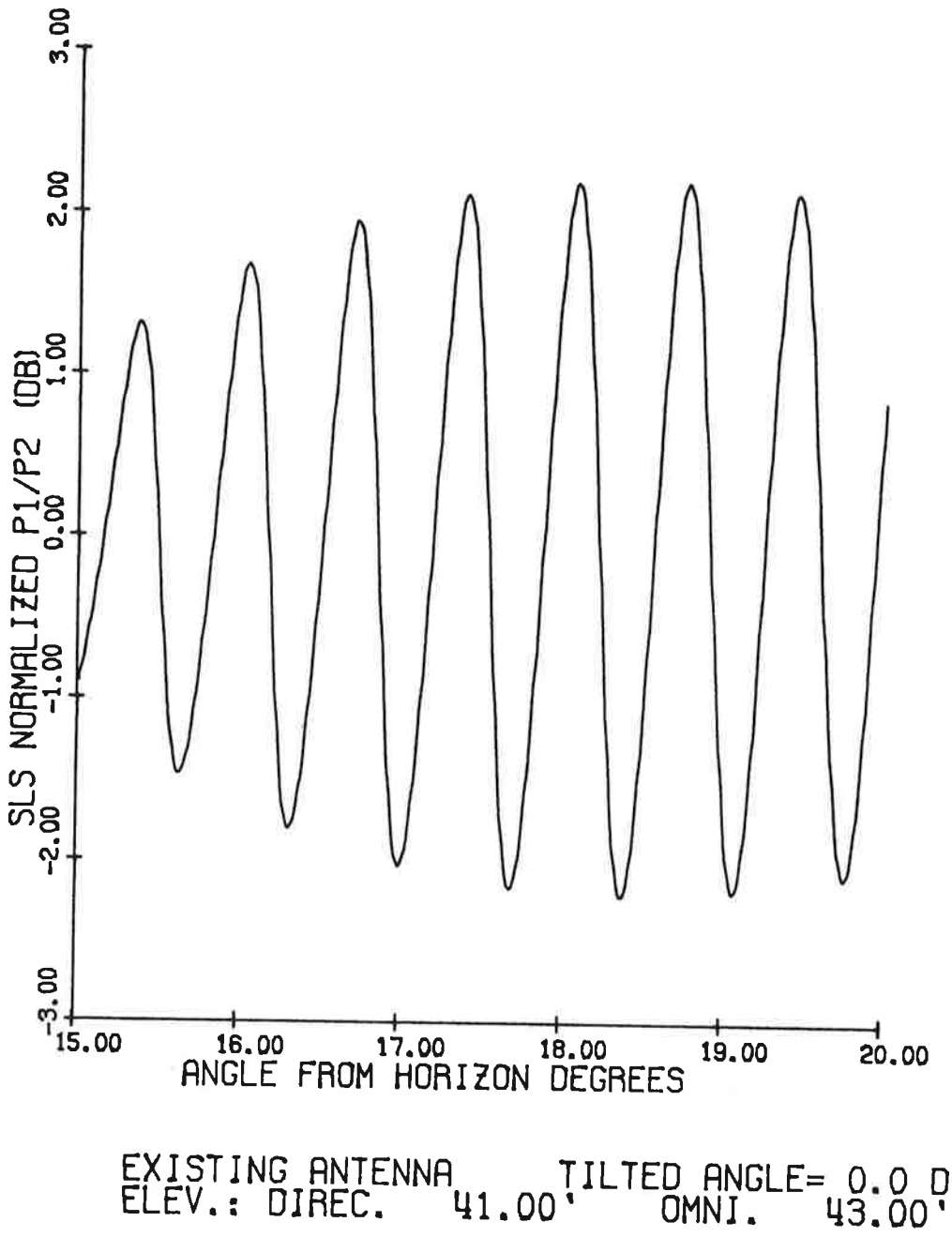

FIG. 35d: Normalized pulse ratio as a function of θ.

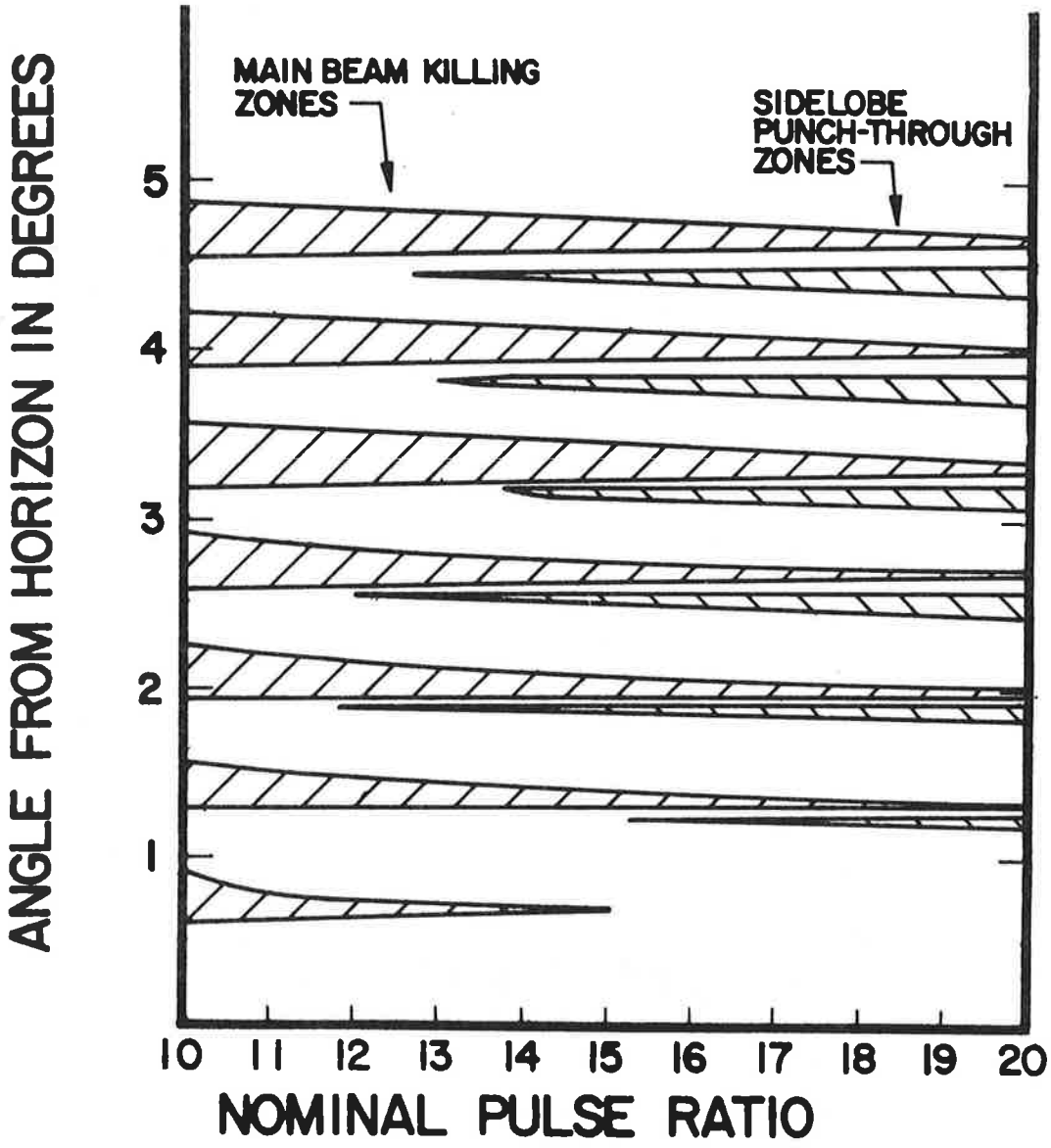

FIG. 36: Mainbeam killing and sidelobe punch-through zones as functions of the nominal pulse ratio for the existing antenna. H_d = 41', H_o = 43', f = 1030 MHz, a = 9dB, b = 0dB, L = -25dB.

Figure 37 shows the effective beamwidth as a function of θ for the range $0 \leq \theta \leq 5^{o}$. It is anticipated that for this antenna the beamwidth will continue to fluctuate for θ values up to about 20^{o}.

Figure 38 shows the number of replies as a function of θ for the range $0 \leq \theta \leq 5^{o}$. The free space value of the number of replies is about 15. The number of replies will fluctuate for θ values up to about 20^{o}.

The coverage diagram is shown in Fig. 39. The deepest minimum range is 4.8 NM and occurs at $\theta = 0.65^{o}$. The first maximum range is 76 NM and occurs at $\theta \simeq 0.35^{o}$. The lobing structure of the coverage diagram persists up to about $\theta \simeq 20^{o}$. For $\theta > 20^{o}$ the departures from the free space diagram are negligible. In Figure 39, for clarity, only the free space range and the maximum and minimum range curves are shown for $\theta > 10^{o}$.

4.2.5 Hazeltine E-Scan Antenna

This is a special beacon antenna with coincident phase centers of the directional and omnidirectional antennas. The heights of the two phase centers are $H_d = H_0 = 16'$. The vertical aperture of the antenna is 8'.

Figure 40 shows the $P1(\theta)$, $P2(\theta)$ pulses as functions of θ where the 0 dB level refers to the maximum $P1(\theta)$ level in the free space case. As can be seen from Fig. 40, the lobing structures of the $P1(\theta)$, $P2(\theta)$ curves are identical for the present case, their levels differ by the nominal value of 18 dB. As a result, the pulse ratio function $K(\theta)$ is equal to K_0 for all angles θ. The effective beamwidth and the number of replies are equal to their free space values which are 4^{o} and 16 respectively.

The coverage diagram of the antenna is shown in Fig. 41.

4.3 Numerical Results for Enroute Installations

In this section numerical results are given for the performance of enroute ATCRBS using different antenna systems.

4.3.1 Westinghouse Array Antenna

The phase centers of the directional and omnidirectional antennas are $H_d = 82'$ and $H_o = 90'$ so that the two are vertically displaced by 8'. The vertical aperture of the antenna is 8'.

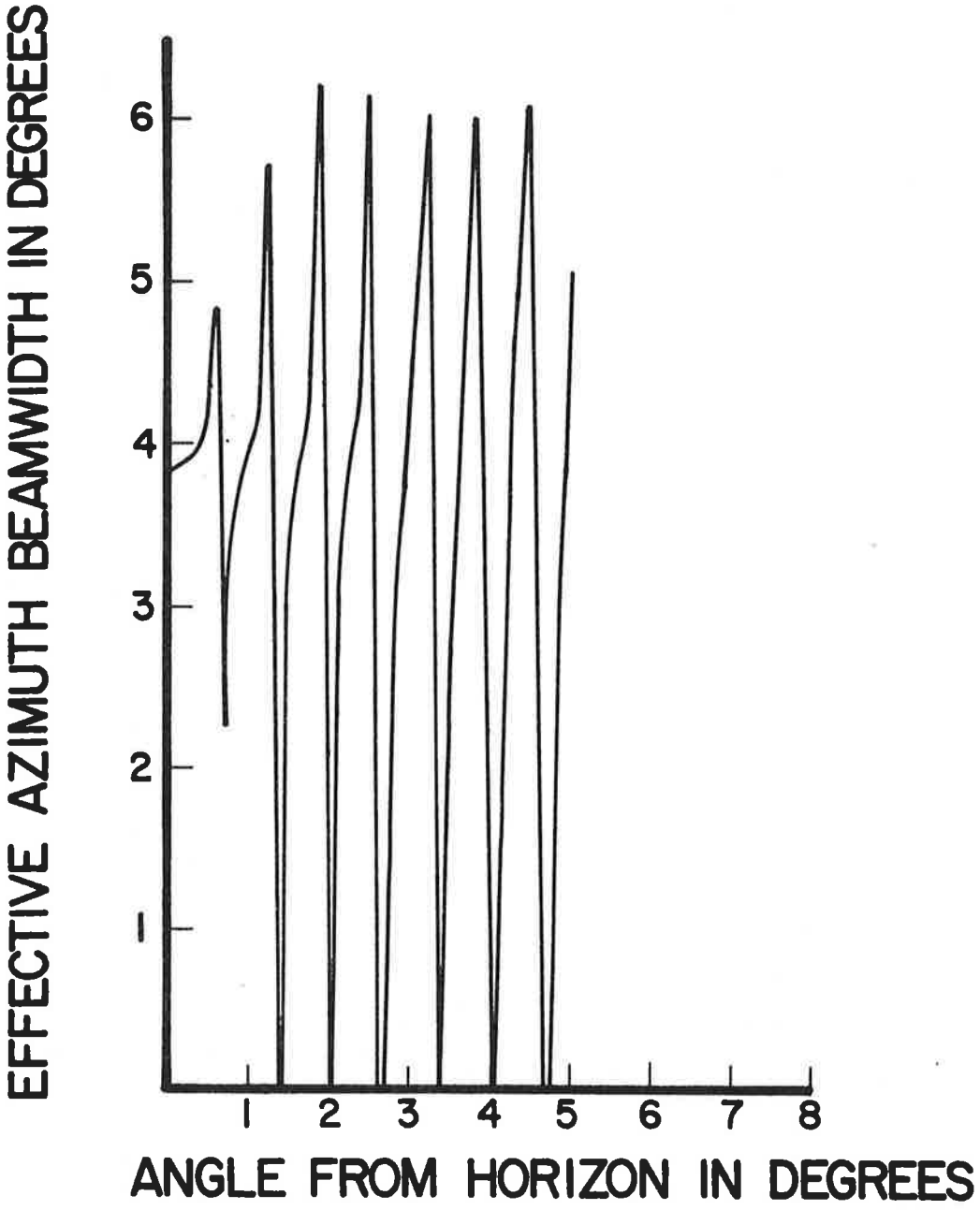

FIG. 37: Effective azimuth beamwidth as a function of angle from the horizon for the existing antenna. $H_d = 41'$, $H_o = 43'$, f = 1030 MHz, nominal pulse ratio $K_o = 18$dB.

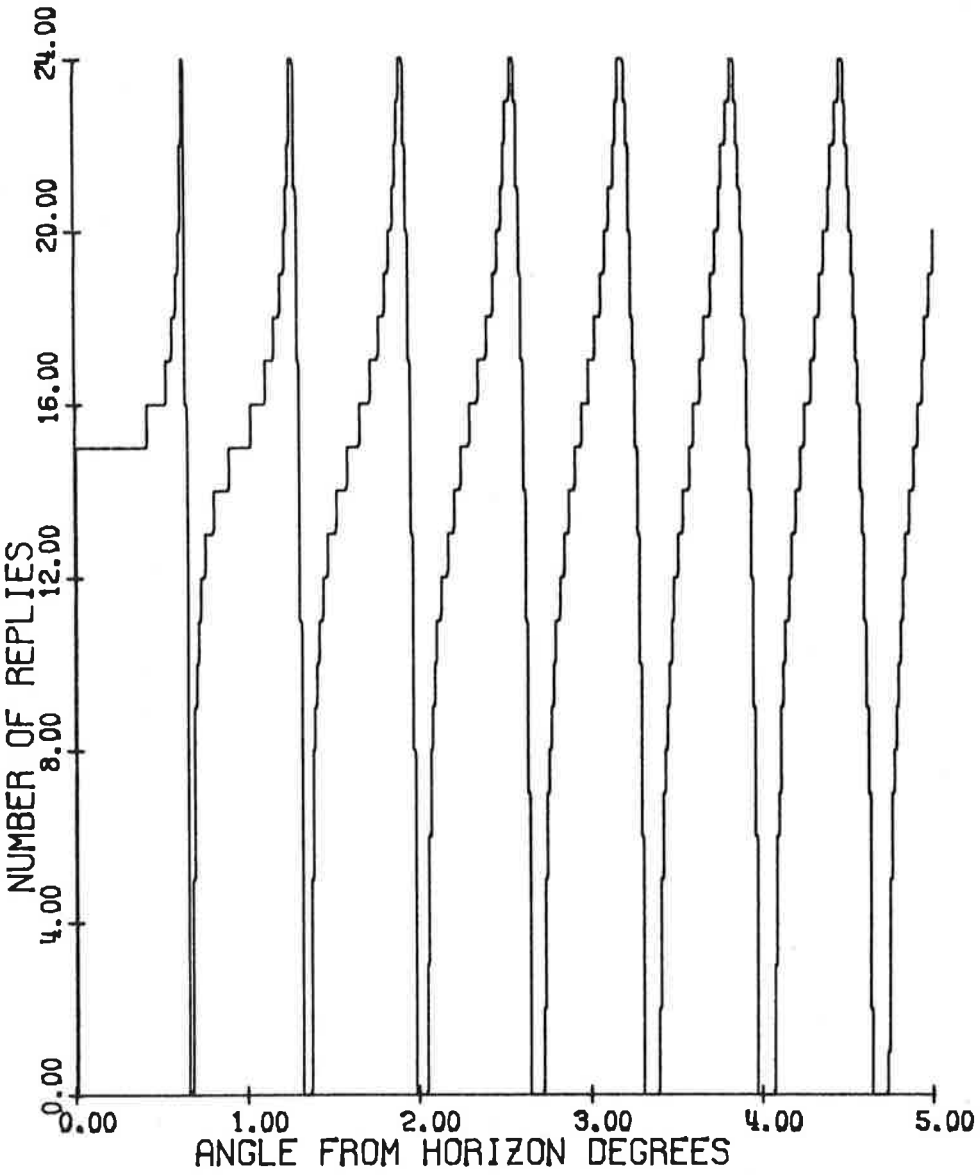

FIG. 38: Numbers of replies as a function of angle from the horizon.

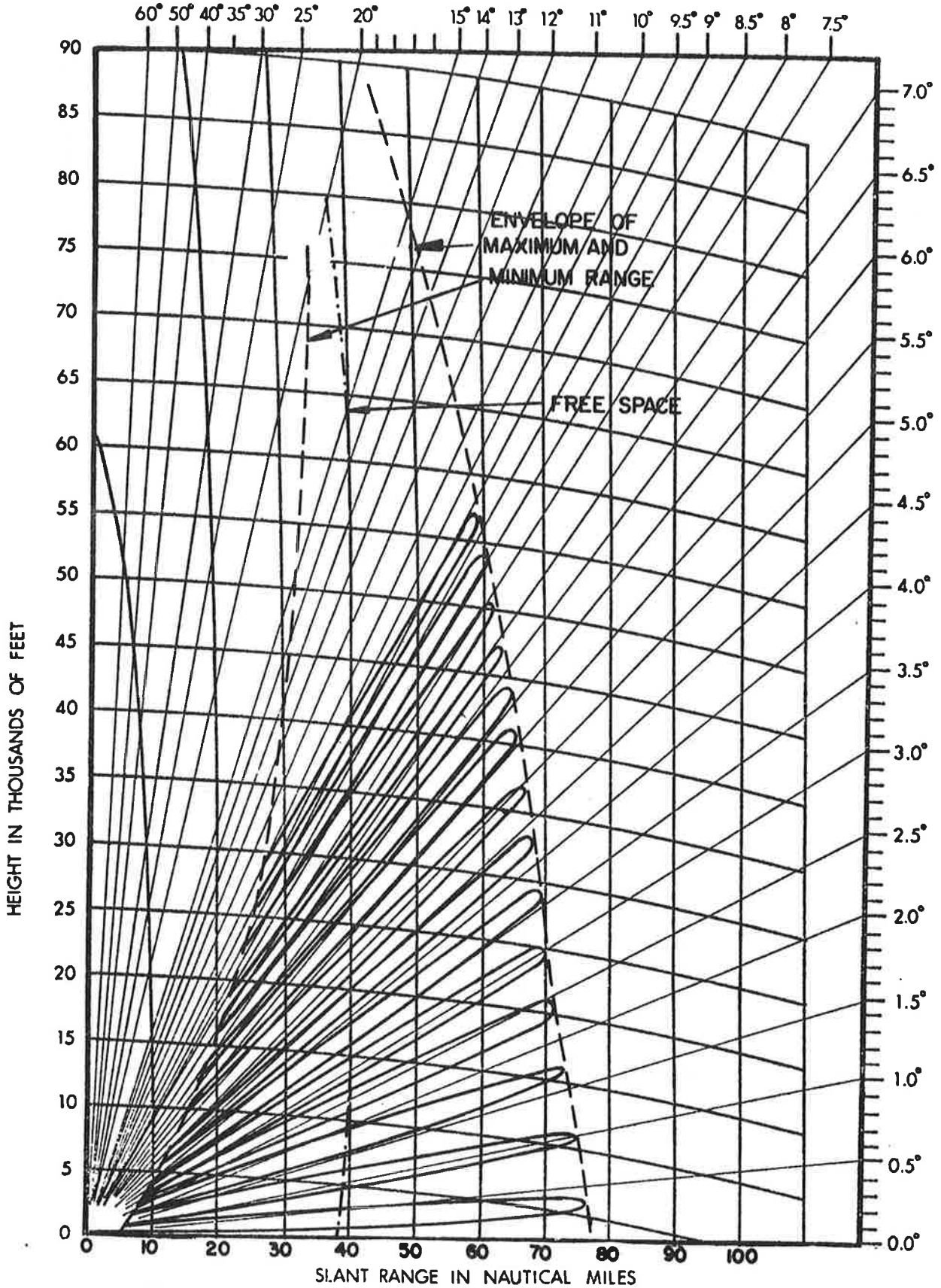

FIG. 39a: Coverage diagram for the existing "hog-trough" antenna. H_d = 41', H_0 = 43', f = 1030 MHz, maximum free space range = 40 nautical miles.

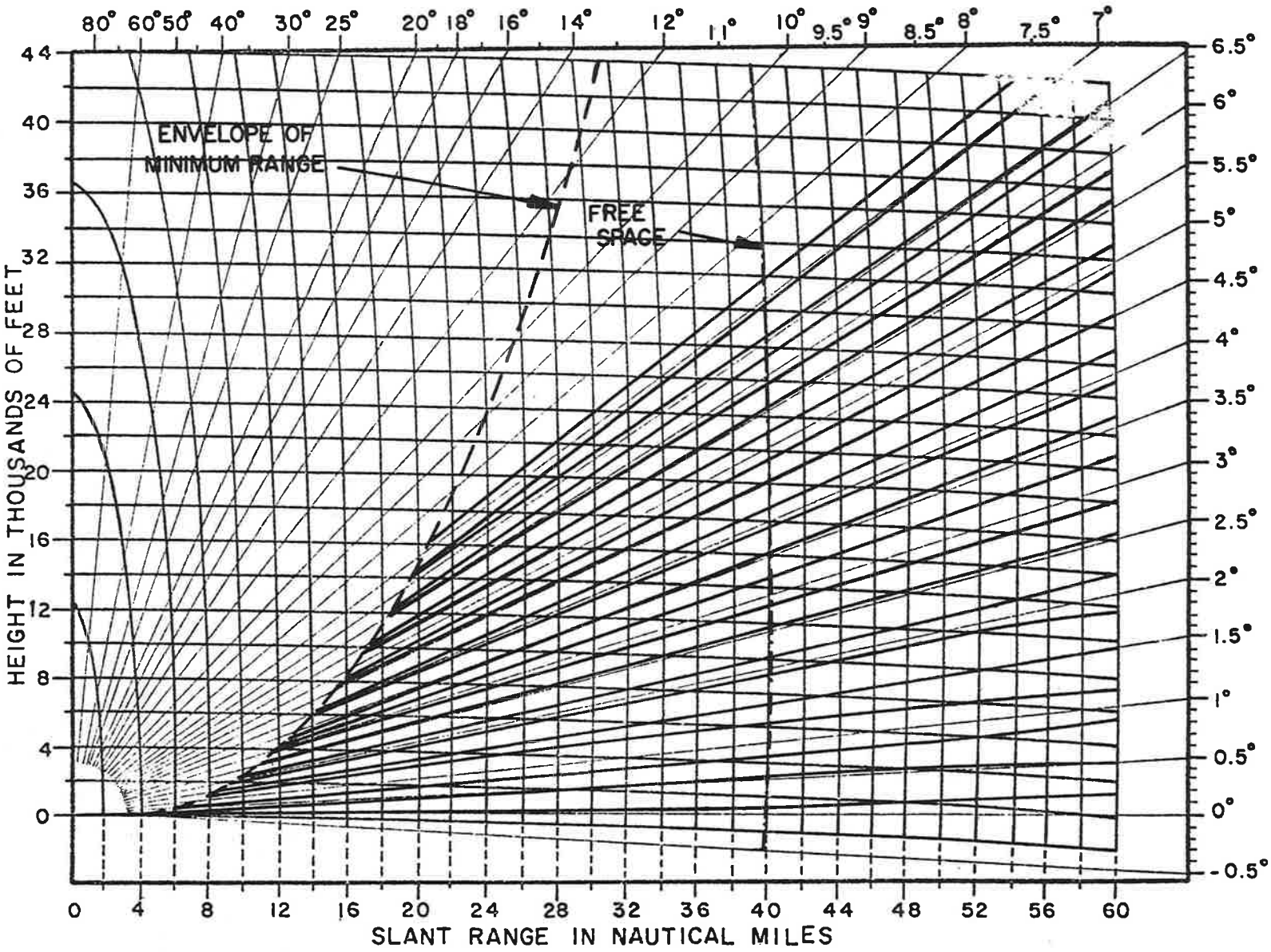

FIG. 39b: Coverage diagram on expanded scale for the existing "hog-trough" antenna. H_d = 41', H_0 = 43' f = 1030 MHz, maximum free space range = 40 nautical miles.

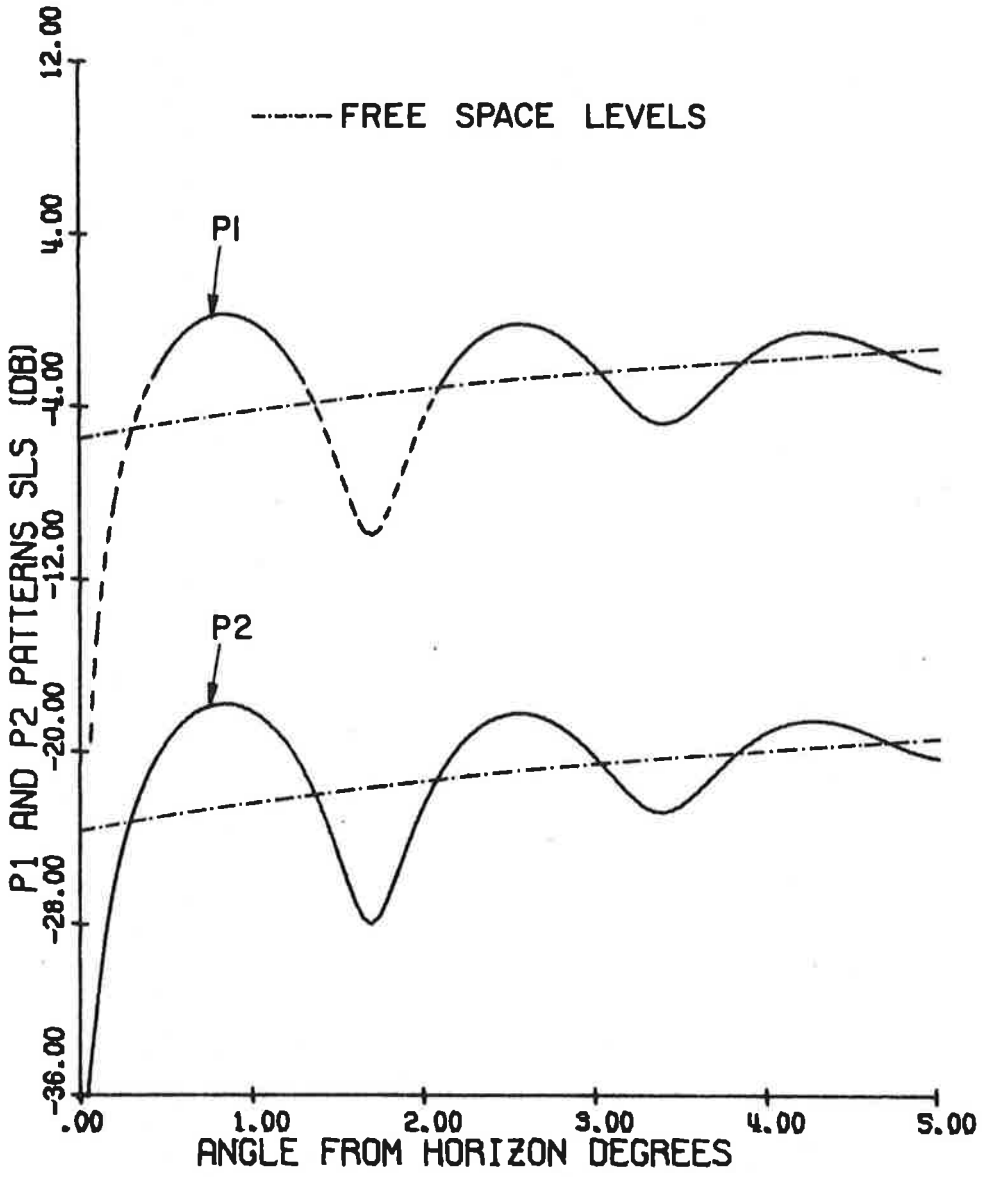

FIG. 40: P1 and P2 pulses as functions of θ.

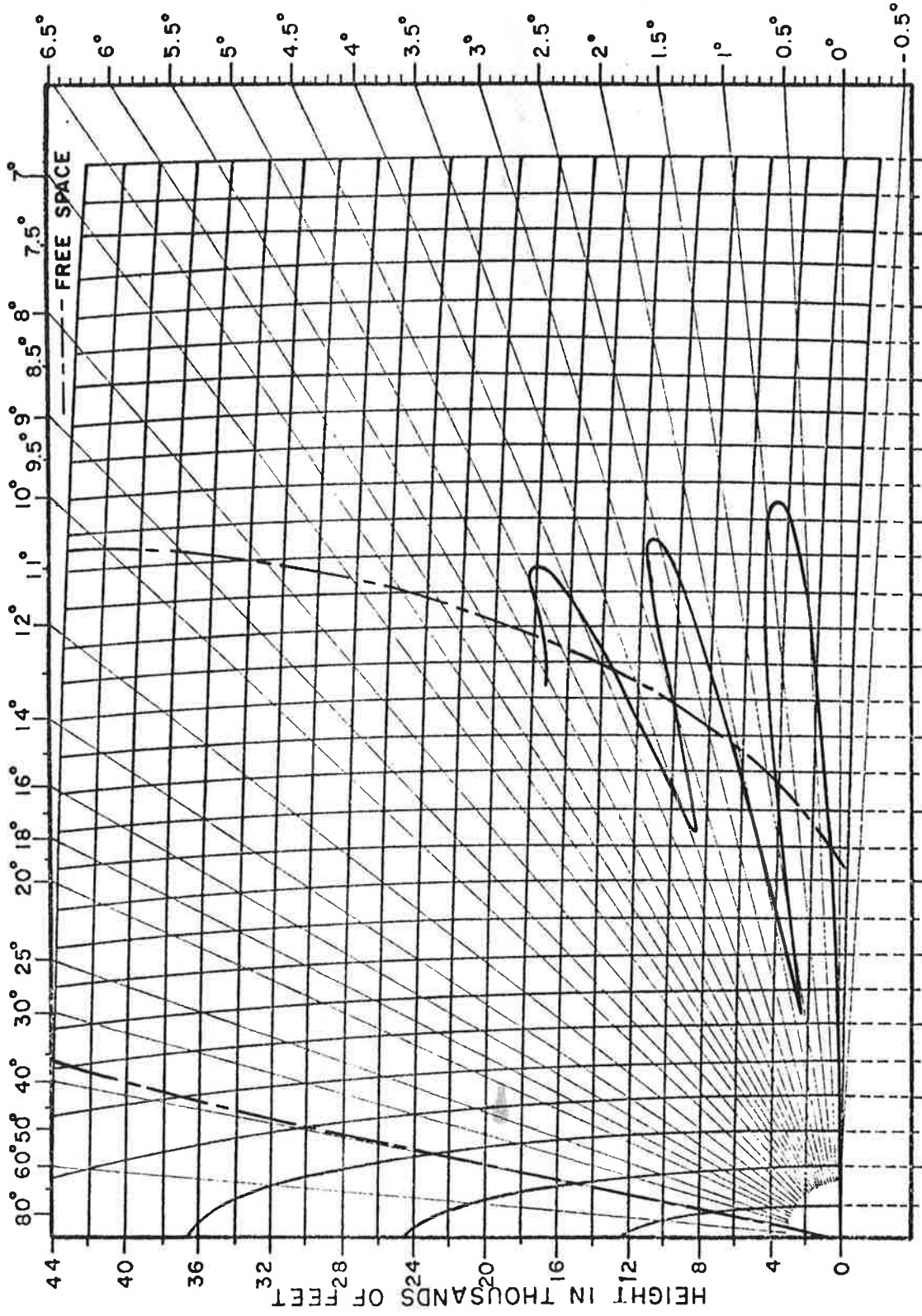

FIG. 41: Coverage diagram for the Hazeltine E-scan antenna. H_d = 16', H_o = 16', f = 1030 MHz, maximum free space range = 40 nautical miles.

Figure 42 shows the variations of P1(θ), P2(θ) pulses as functions of θ, where the 0 dB level has been adjusted to the maximum value of the P1(θ) pulse for the free space case. As compared to the terminal installation with the same antenna (Fig. 16), in the enroute case the number of lobings in the same range is much greater. This is because of the greater height of the antennas used in the enroute case. For $\theta > 4.5^{o}$ the curves assume their free space values.

Figure 43 shows the pulse ratio as a function of θ. For $\theta \gtrsim 3^{o}$ the pulse ratio assumes the nominal ratio in free space which is 18dB. The maximum departures of the pulse ratio from its nominal free space ratio are +10.3dB at 0.3^{o} and -8.1dB at 0.35^{o}.

Figure 44 shows the mainbeam killing and sidelobe punch-through zones as functions of the nominal pulse ratio K_0. Comparing Figs. 18 and 44, it is found that the number of both zones are increased by increasing the antenna height in the enroute case.

Figure 45 gives the effective beamwidth as a function of θ for $K_0 = 18$dB and a = 9dB. The effective beamwidth varies between 0.65^{o} and 5.7^{o}. The variations are stabilized above $\theta = 4.5^{o}$ to about 3.9^{o}. The number of replies N as a function of θ is shown in Fig. 46. For $\theta > 4.5^{o}$ the number of replies assumes the value ~ 31 appropriate for the free space case. The number of replies varies between N = 5 and N = 45.

Figure 47 gives the coverage diagram for the antenna. The maximum free space range is adjusted to be 200 nautical miles. It can be seen from Fig. 47 that the range of the first minimum is about 41.4 NM while that at the first maximum is about 223.4 NM.

4.3.2 Texas Instruments Reflector Antenna

The phase centers of the directional and omnidirectional antennas for this case are 82' and 91' respectively. Thus the two phase centers are displaced by 9'.

Figure 48 shows the P1(θ), P2(θ) pulses as functions of θ, where the 0dB level is adjusted to correspond to the maximum value of the P1(θ) pulse in the free space case.

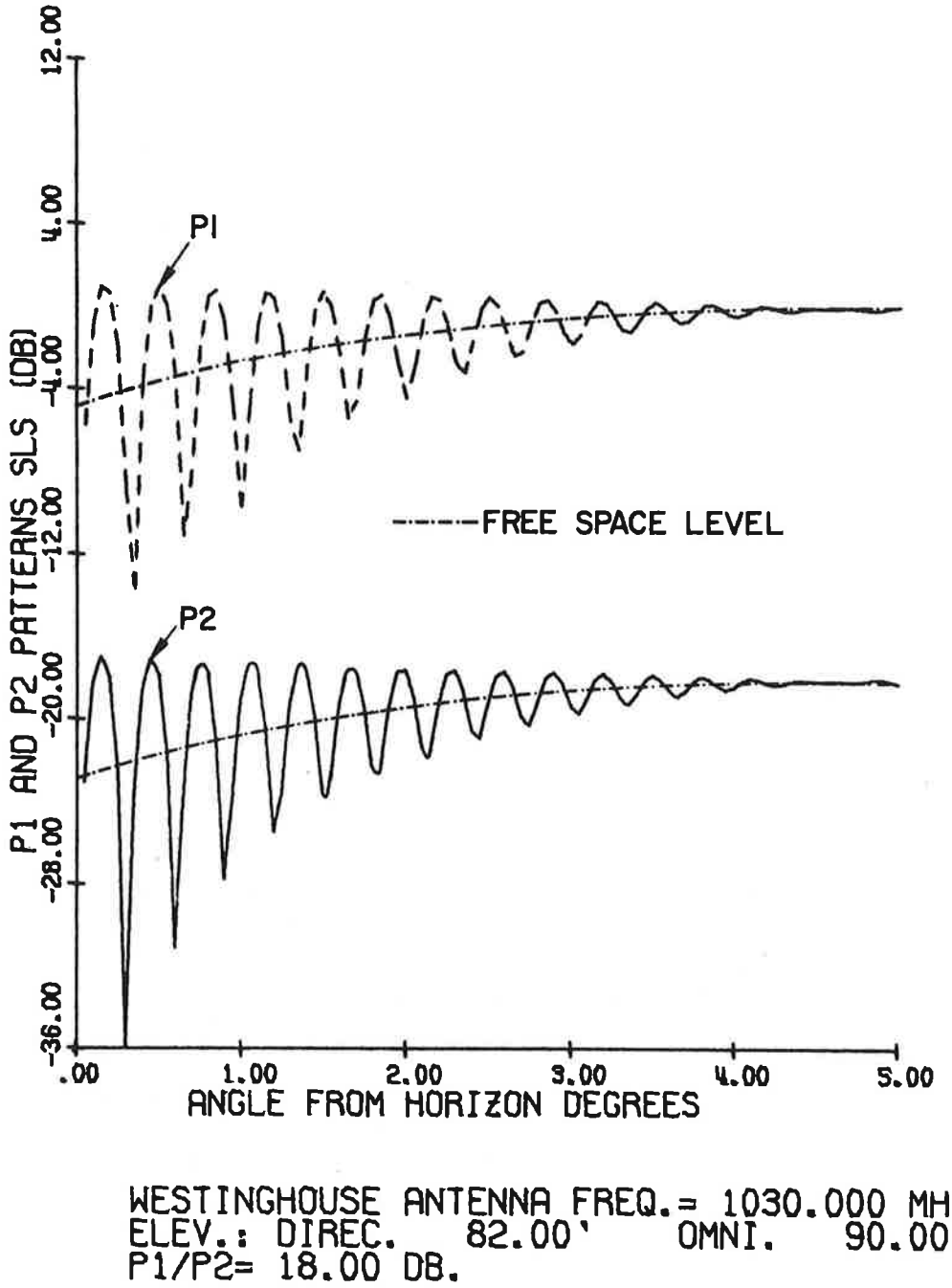

FIG. 42: P1 and P2 pulses as functions of θ.

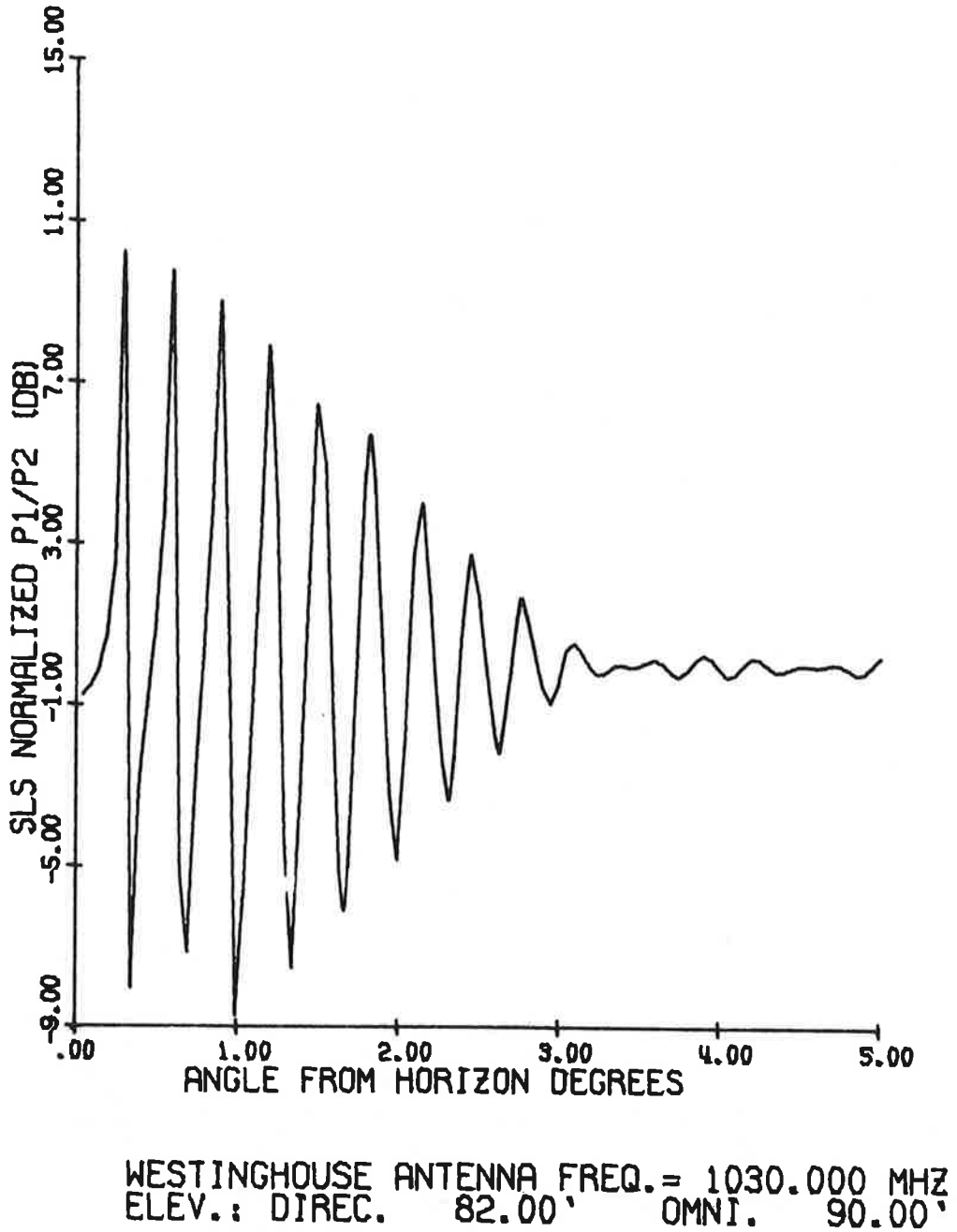

FIG. 43: Normalized pulse ratio as a function of θ.

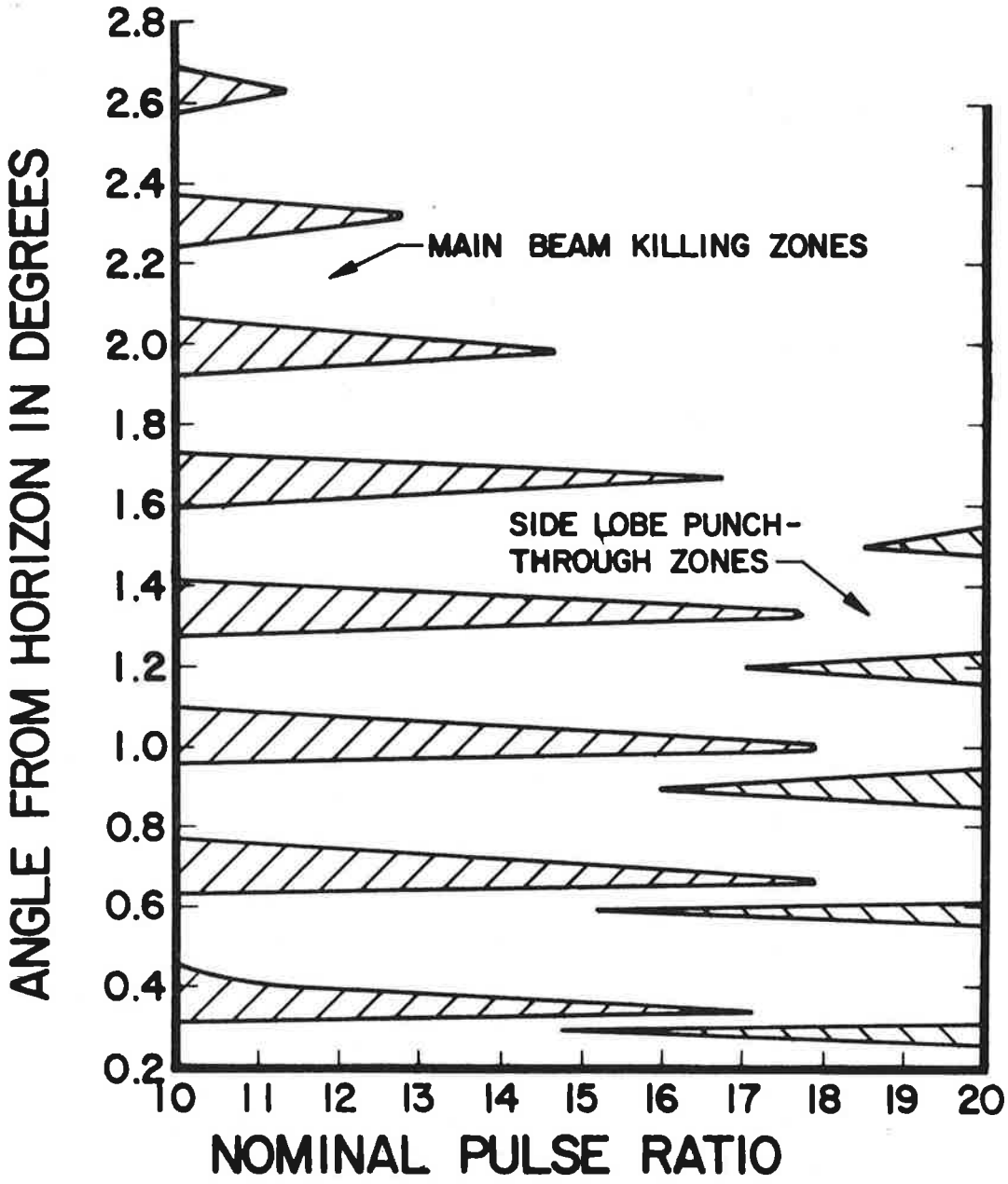

FIG. 44: Mainbeam killing and sidelobe punch-through zones as functions of the nominal pulse ratio for the Westinghouse array antenna. H_d = 82', H_o = 90', f = 1030 MHz, a = 9dB, b = 0dB, L = -25dB.

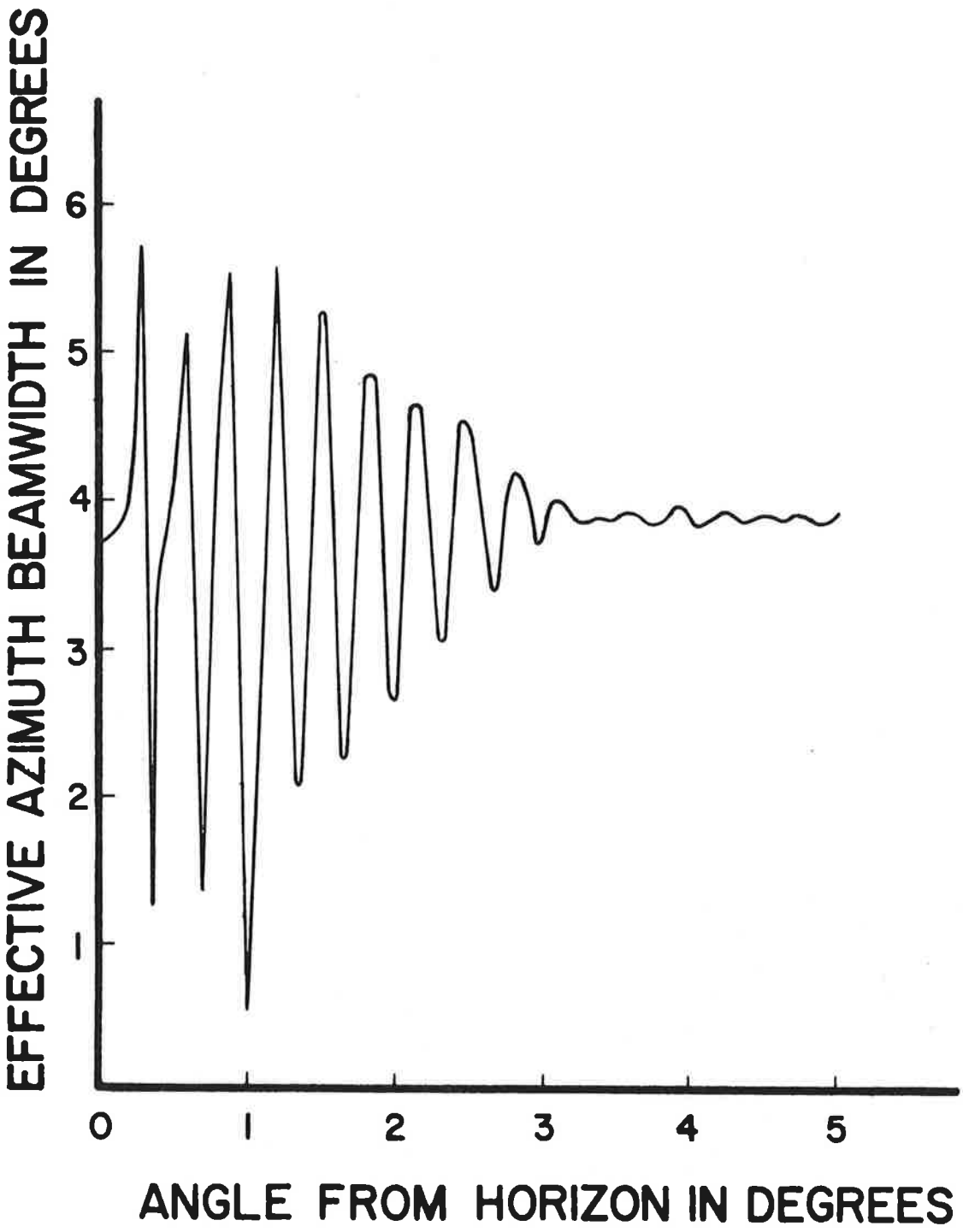

FIG. 45: Effective azimuth beamwidth as a function of angle from the horizon for the Westinghouse array antenna. H_d = 82', H_o = 90', f = 1030 MHz, nominal pulse ratio K_o = 18 dB.

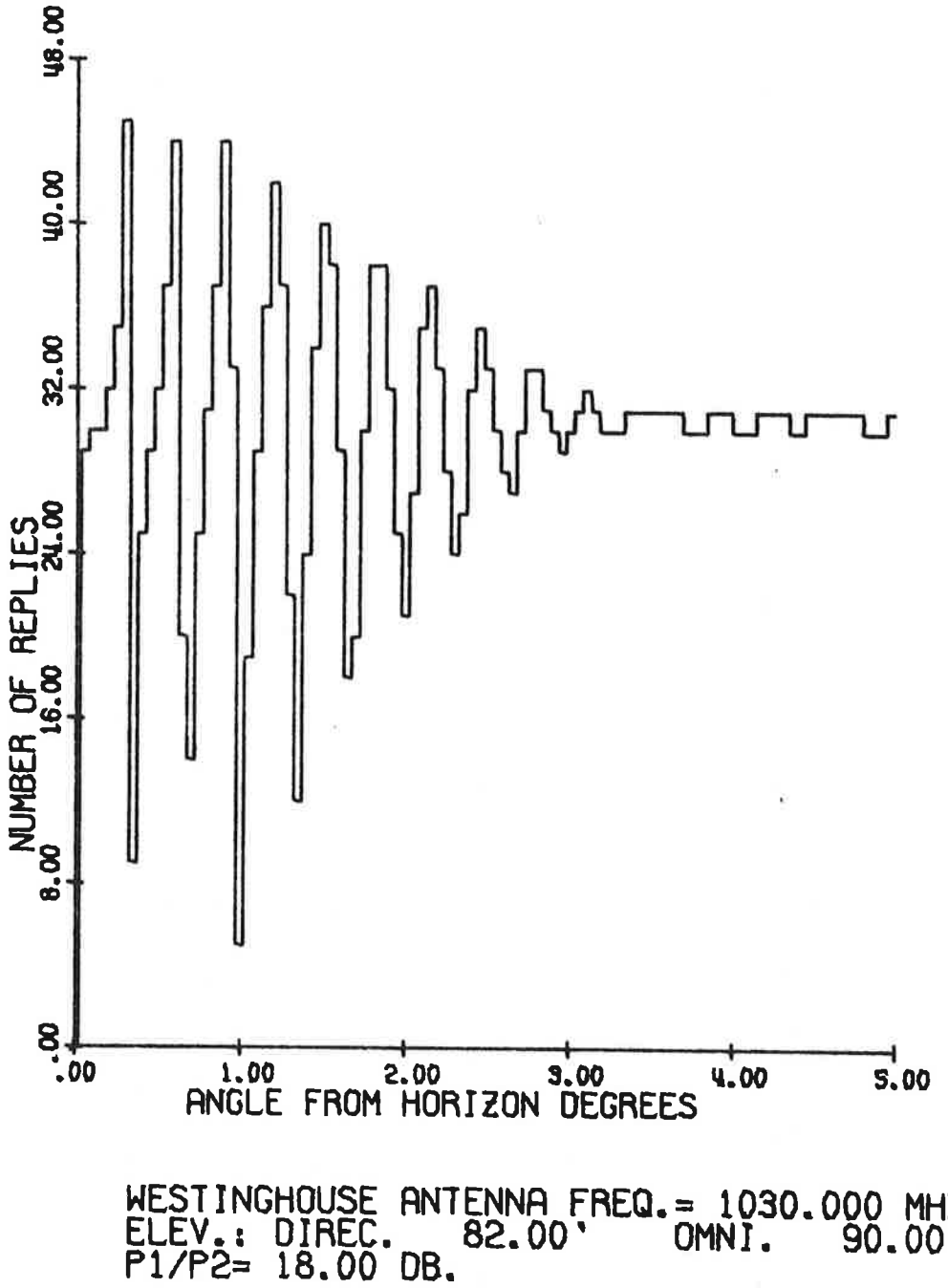

FIG. 46: Number of replies as a function of angle from the horizon.

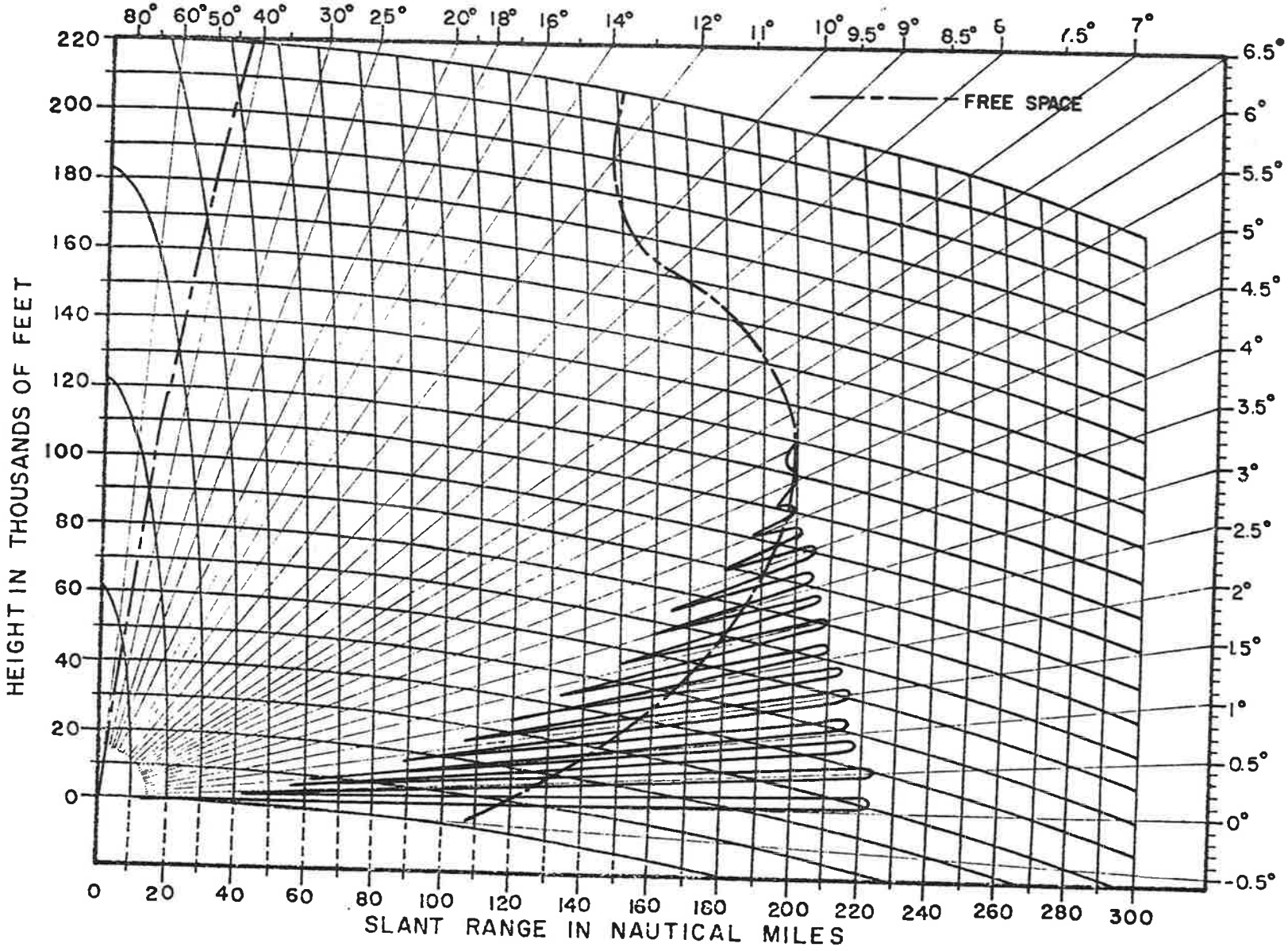

FIG. 47: Coverage diagram for the Westinghouse array antenna. H_d = 82', H_o = 90', f = 1030 MHz, maximum free space range = 200 nautical miles.

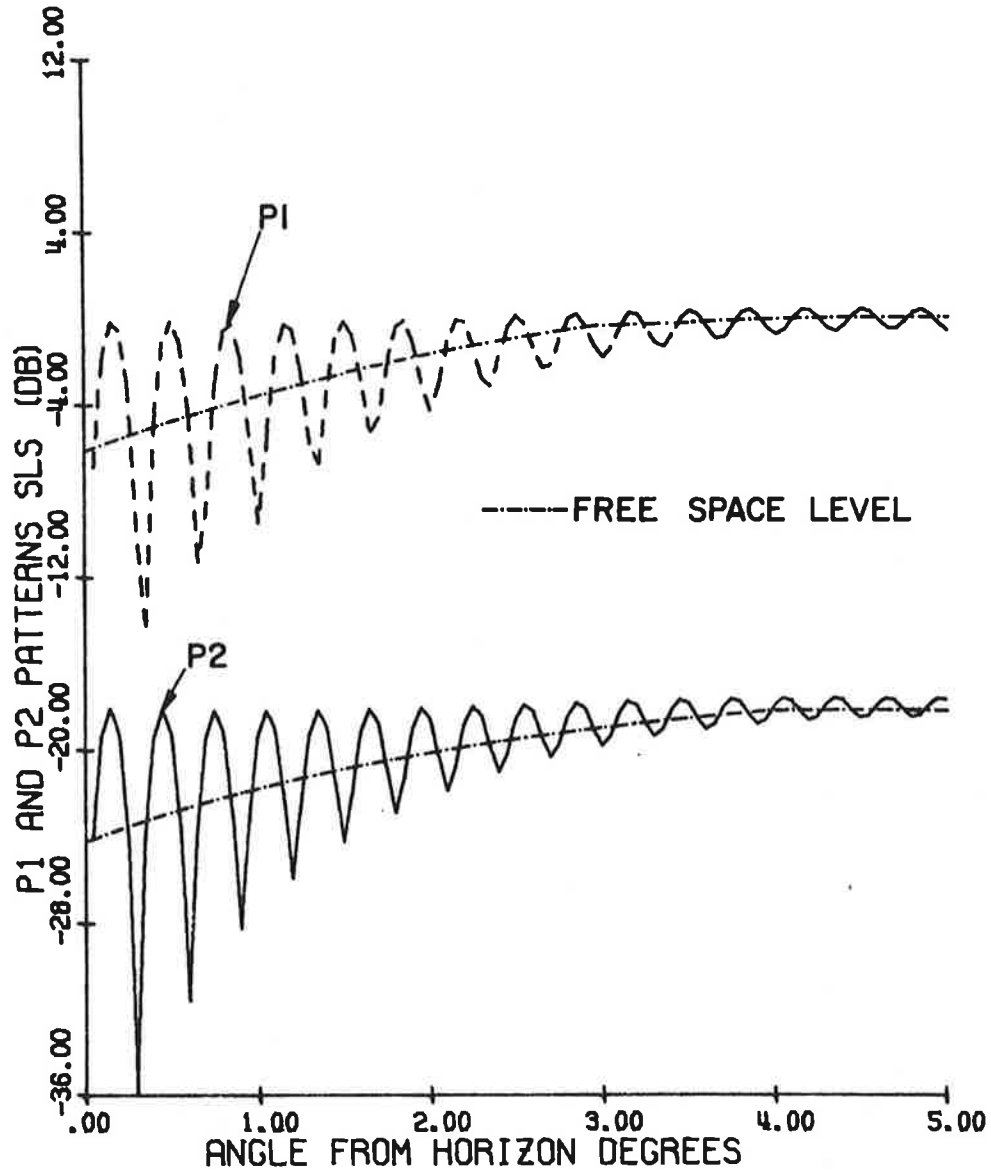

FIG. 48: P1 and P2 pulses as functions of θ.

The variation of the pulse ratio as a function of θ is shown in Fig. 49. For $\theta > 3^{o}$ the pulse ratio assumes practically the free space value.

Figure 50 shows the mainbeam killing and sidelobe punch-through zones as functions of the nominal pulse ratio K_0.

Figure 51 gives the effective azimuth beamwidth as a function of the elevation angle. The effective beamwidth assumes practically the free space value of 4^{o} for $\theta \gtrsim 3^{o}$.

Figure 52 gives the number of replies as a function of θ. For $\theta > 3^{o}$ the number of replies assumes the value ~ 32 appropriate in free space.

Figure 53 shows the coverage diagram for the antenna. The maximum free space range is adjusted to be 200 NM. The range at the first minimum is about 38.7 NM and that at the first maximum is about 196.5 NM.

4.3.3 The Existing Hog-Trough Antenna

The phase centers of the directional and omni-directional antennas are at 108' and 110' respectively. Thus the two phase centers are displaced vertically by 2', which is also the vertical aperture of each antenna.

Figure 54a shows the variation of $P1(\theta)$, $P2(\theta)$ pulses as functions of θ, with 0dB level adjusted to be the maximum value of $P1(\theta)$ in the free space case. The curves do not saturate within the range of θ considered in Fig. 54a. On comparing Fig. 54a with the corresponding terminal case (Fig. 34a) it is found that the number of lobes in the curves is much greater for the same range of θ. The lobing diagrams for the extended ranges $5^{o} \leq \theta \leq 10^{o}$, $10^{o} \leq \theta \leq 15^{o}$ and $15^{o} \leq \theta \leq 20^{o}$ are shown in Figs. 54b - 54d.

Figure 55a gives the variation of the pulse ratio as a function of θ with $0 \leq \theta \leq 5^{o}$, while Figs. 55b - 55d give the same ratio in the extended ranges of θ ($5^{o} \leq \theta \leq 10^{o}$, $10^{o} \leq \theta \leq 15^{o}$, $15^{o} \leq \theta \leq 20^{o}$).

Figure 56 gives the mainbeam killing and sidelobe punch-through zones as functions of the nominal pulse ratio. As expected compared to the terminal cases within the same range of θ, the number of zones are increased in the enroute case. In Fig. 56 the range of θ considered is $0 \leq \theta \leq 5^{o}$. The mainbeam killing and sidelobe punch-through zones in other ranges may be obtained from the corresponding pulse ratio curves.

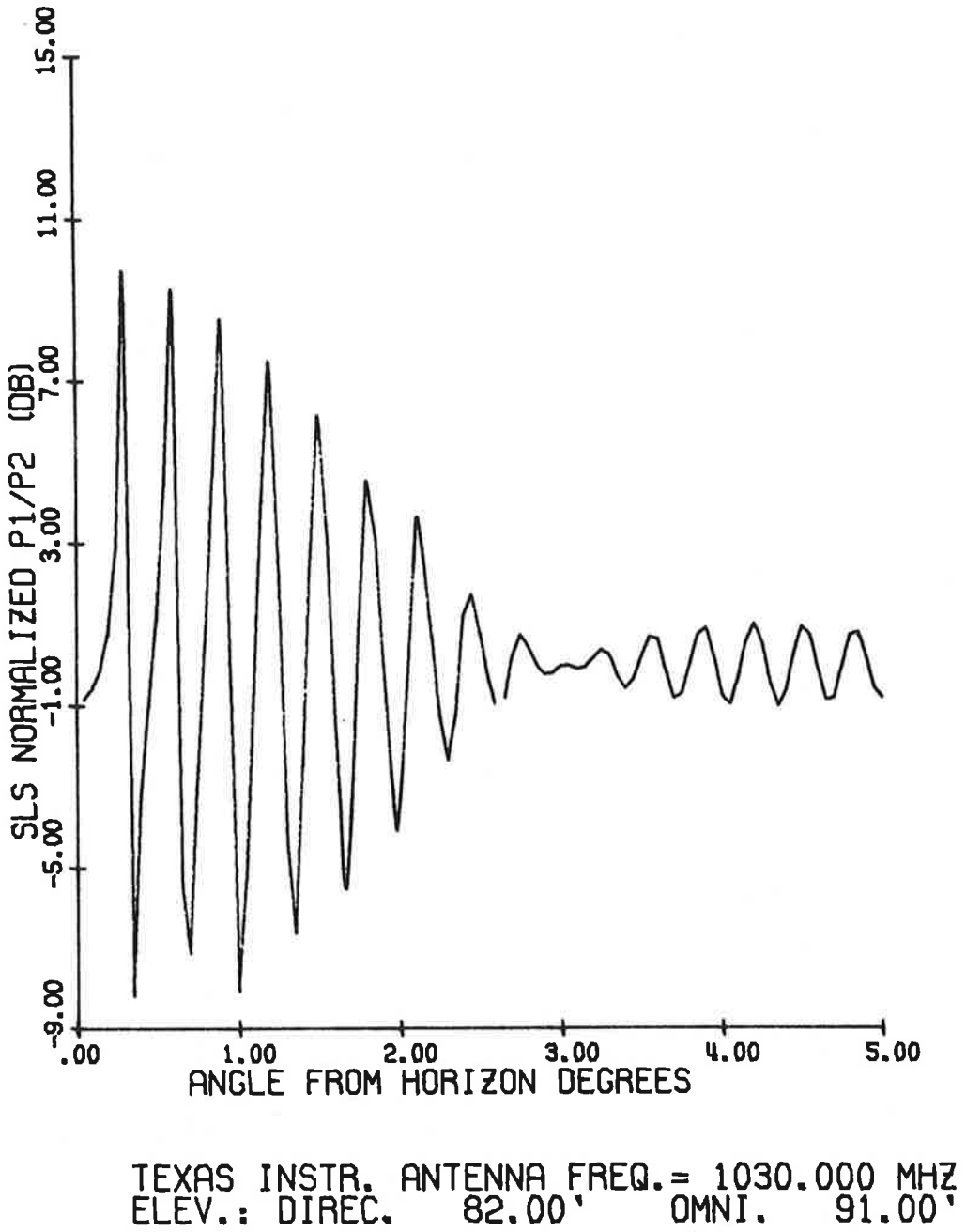

FIG. 49: Normalized pulse ratio as a function of θ.

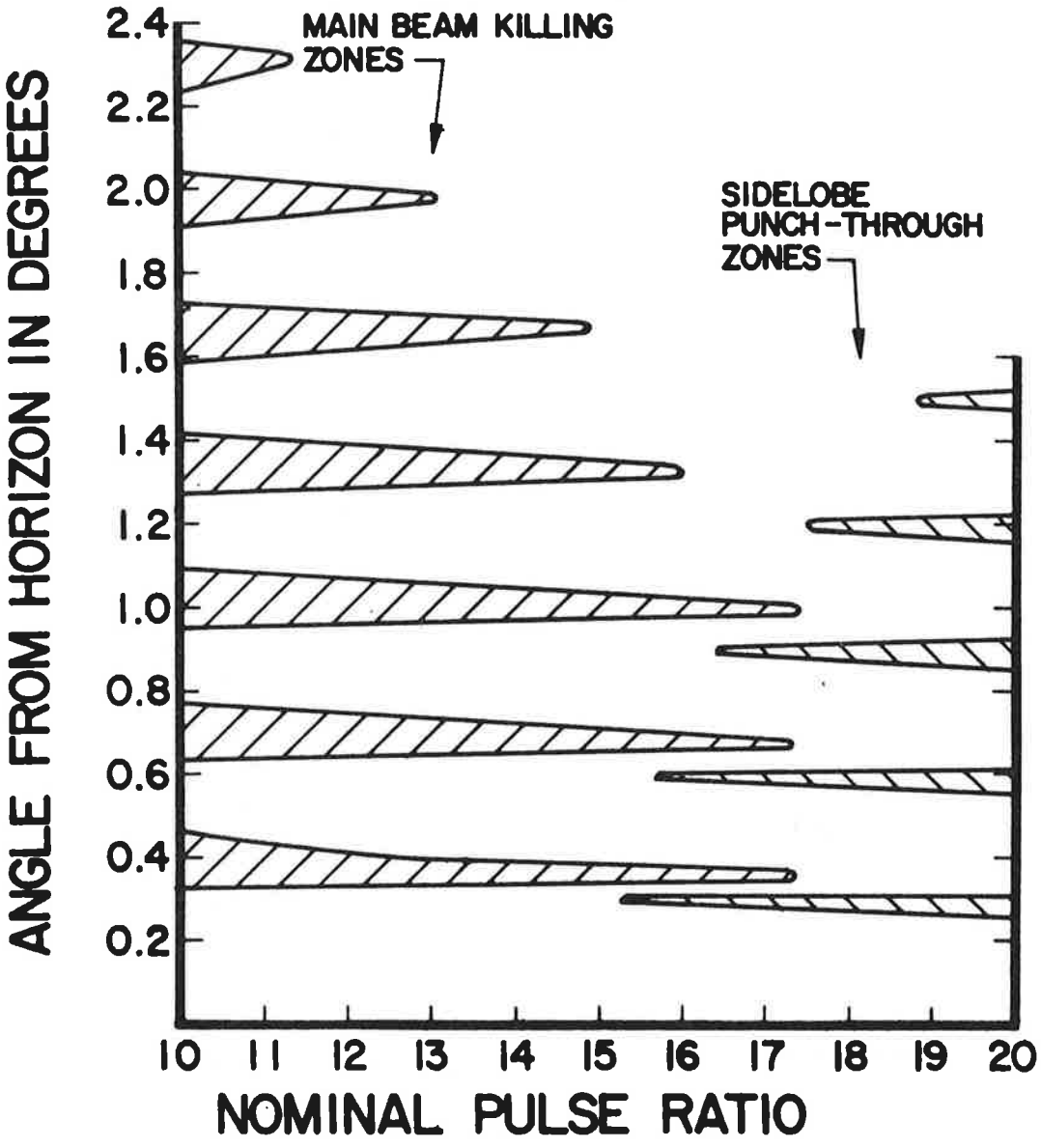

FIG. 50: Mainbeam killing and sidelobe punch-through zones as functions of the nominal pulse ratio for the Texas Instruments reflector antenna. H_d = 82', H_o = 91', f = 1030 MHz, a = 9dB, b = 0dB, L = -25dB

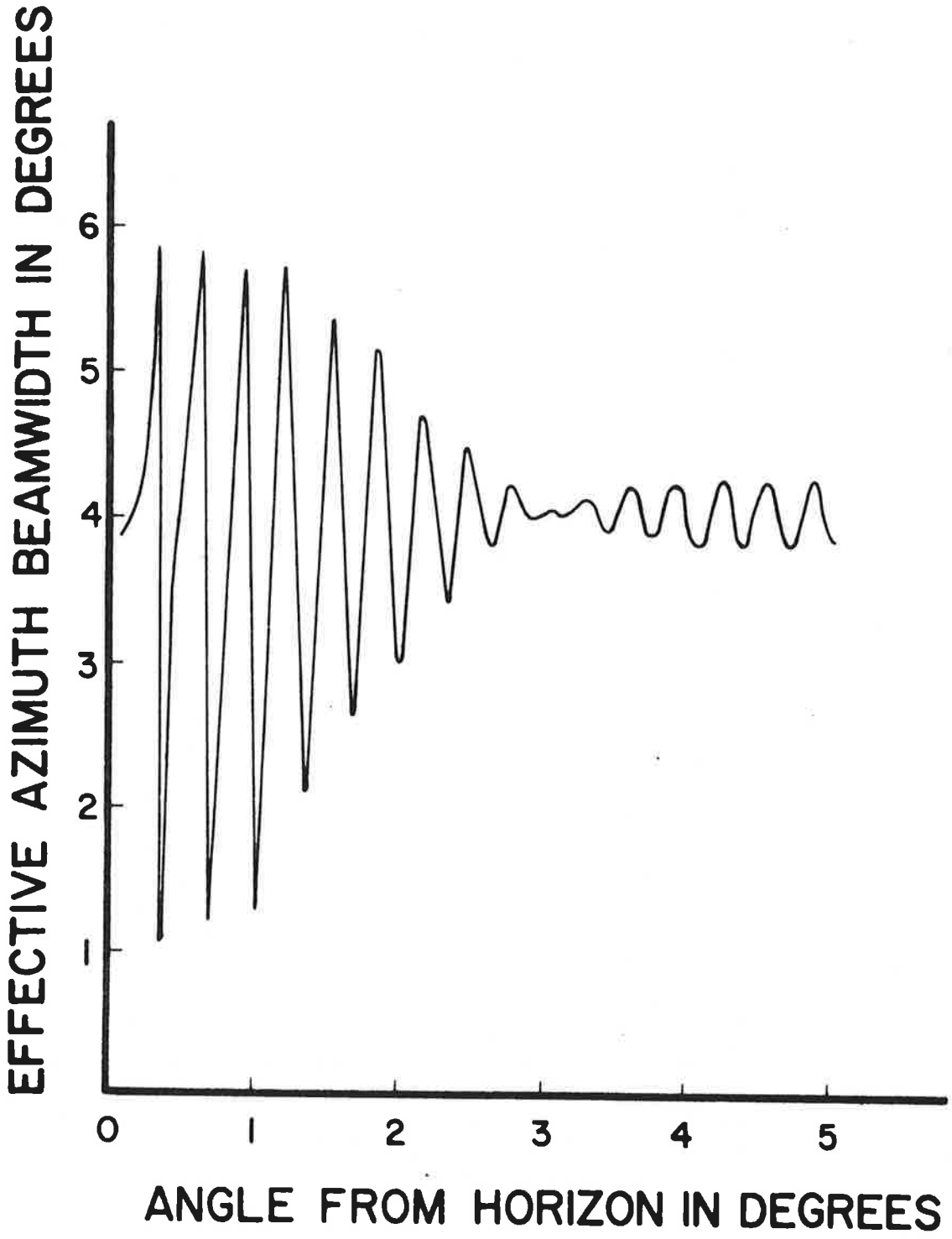

FIG. 51: Effective azimuth beamwidth as a function of angle from the horizon for the Texas Instruments reflector antenna. $H_d = 82'$, $H_o = 91'$, f = 1030 MHz, nominal pulse ratio $K_o = 18$ dB.

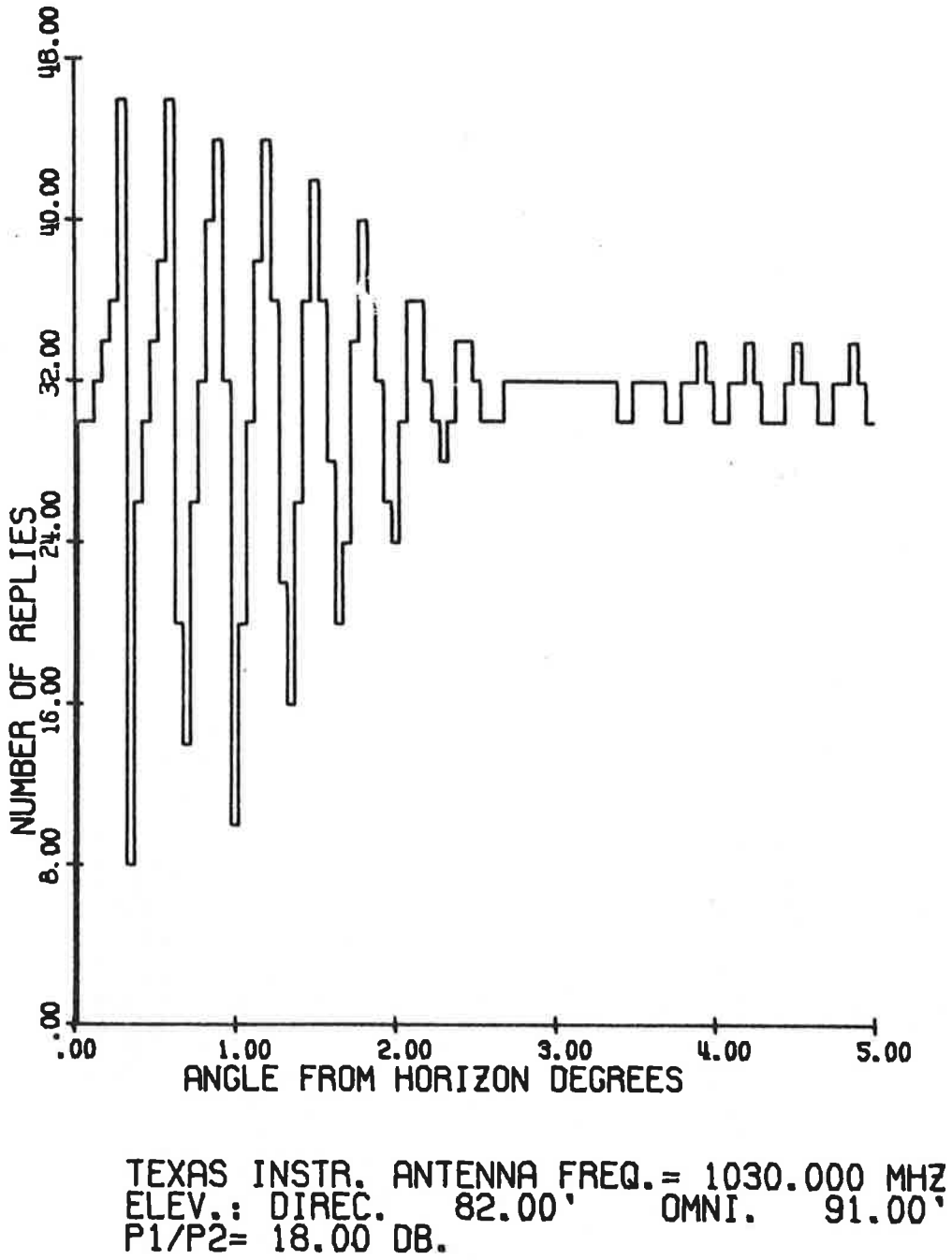

FIG. 52: Number of replies as a function of angle from the horizon.

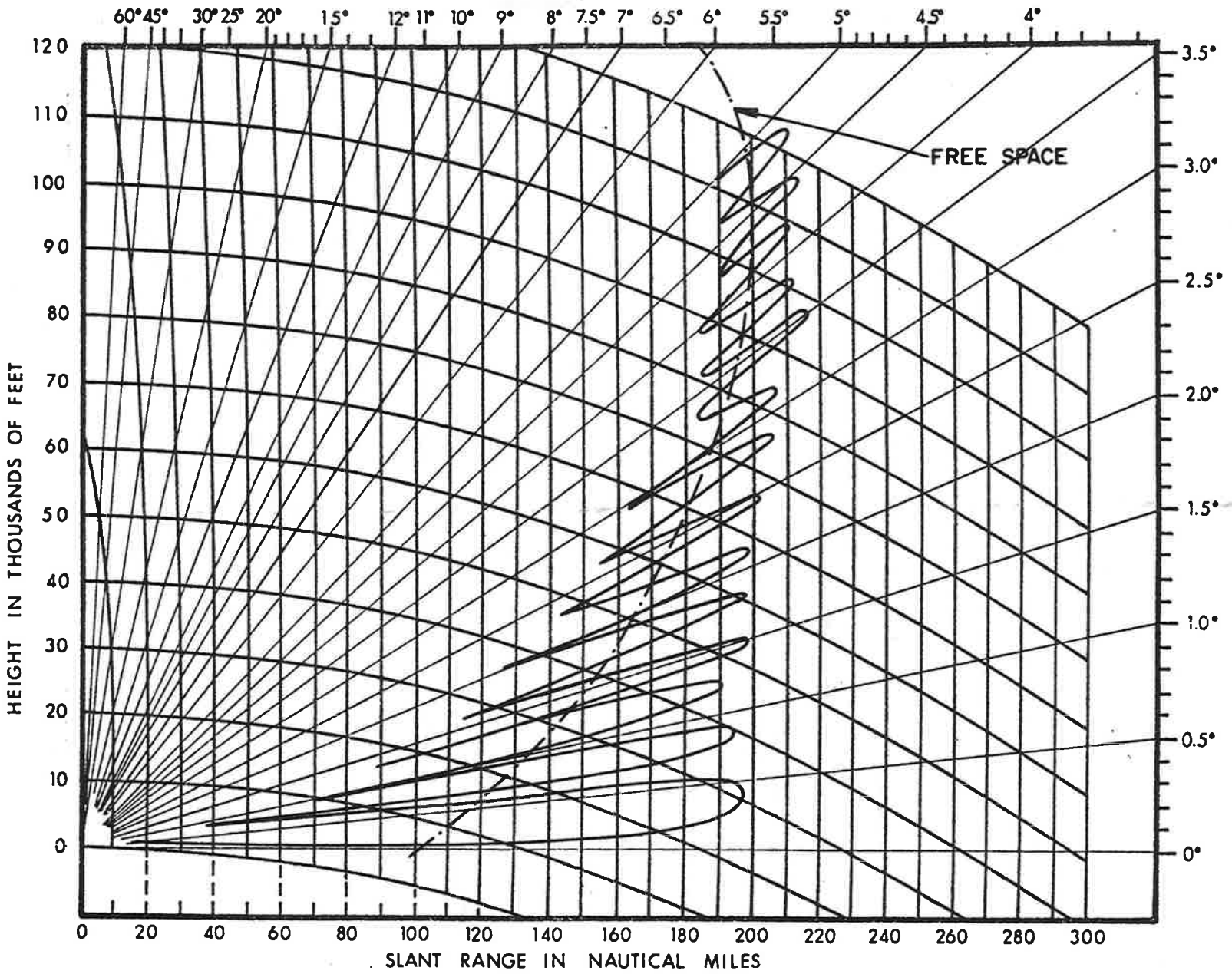

FIG. 53: Coverage diagram for the Texas Instruments reflector antenna. $H_d = 82'$, $H_o = 91'$, f = 1030 MHz, maximum free space range = 200 nautical miles.

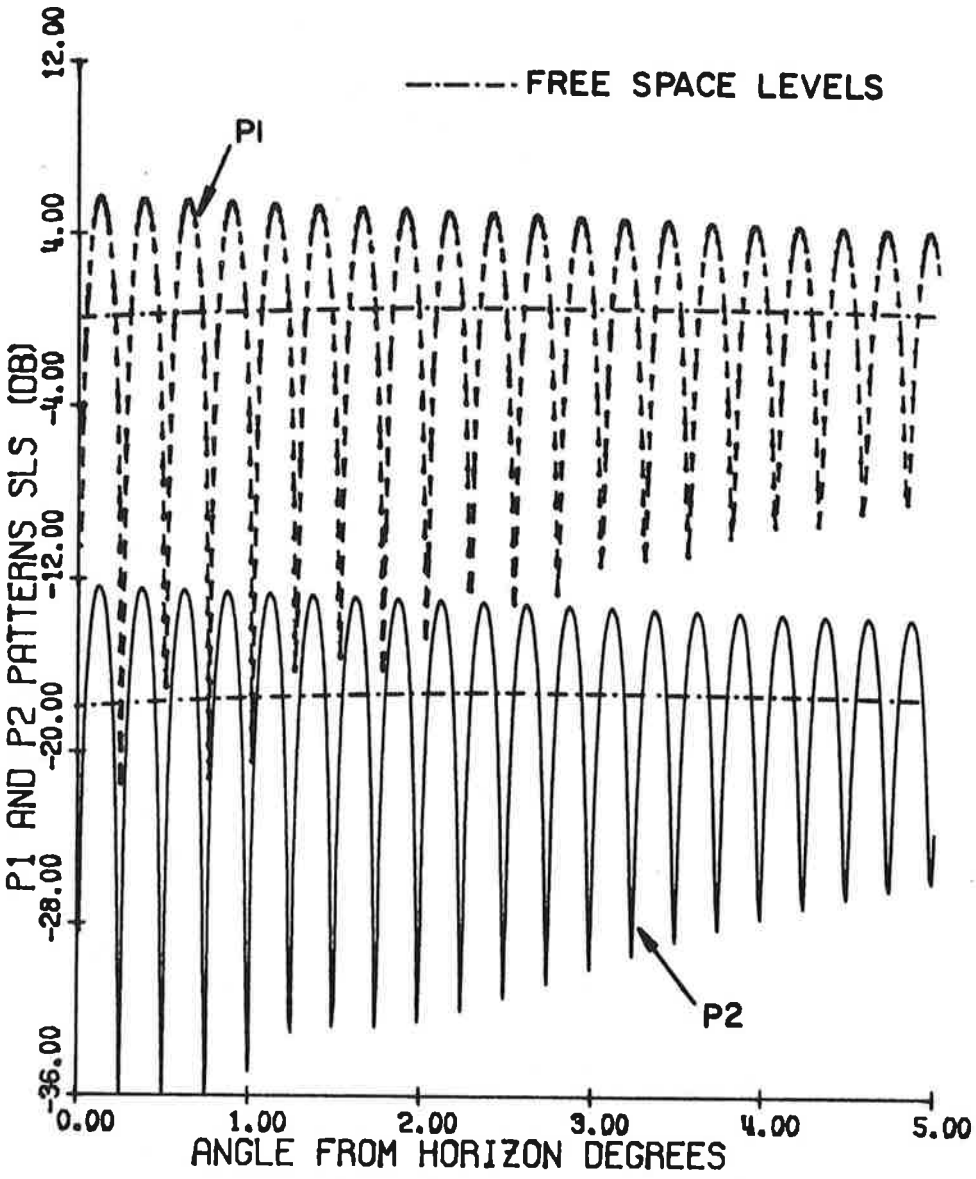

FIG. 54a: P1 and P2 pulses as functions of θ.

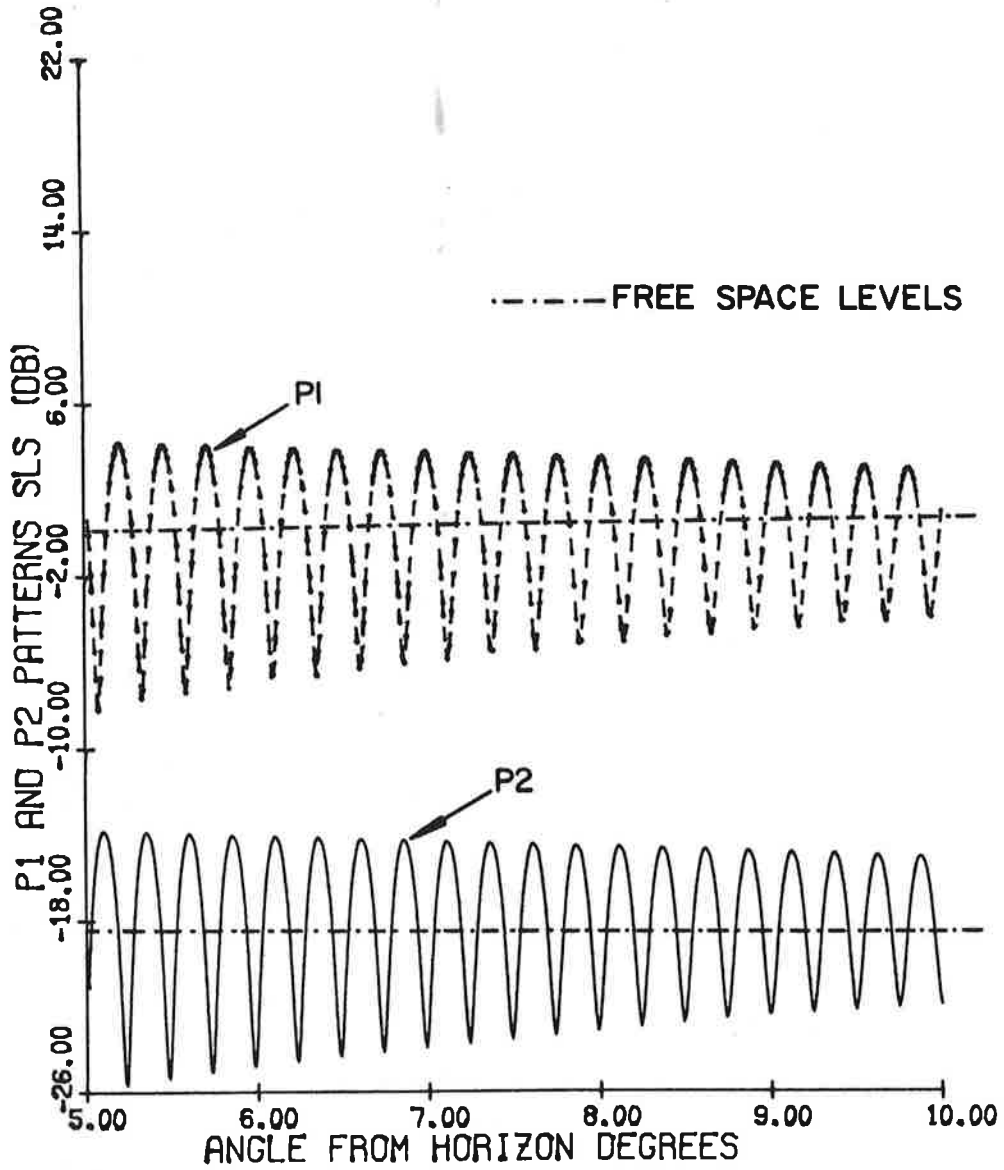

FIG. 54b: P1 and P2 pulses as functions of θ.

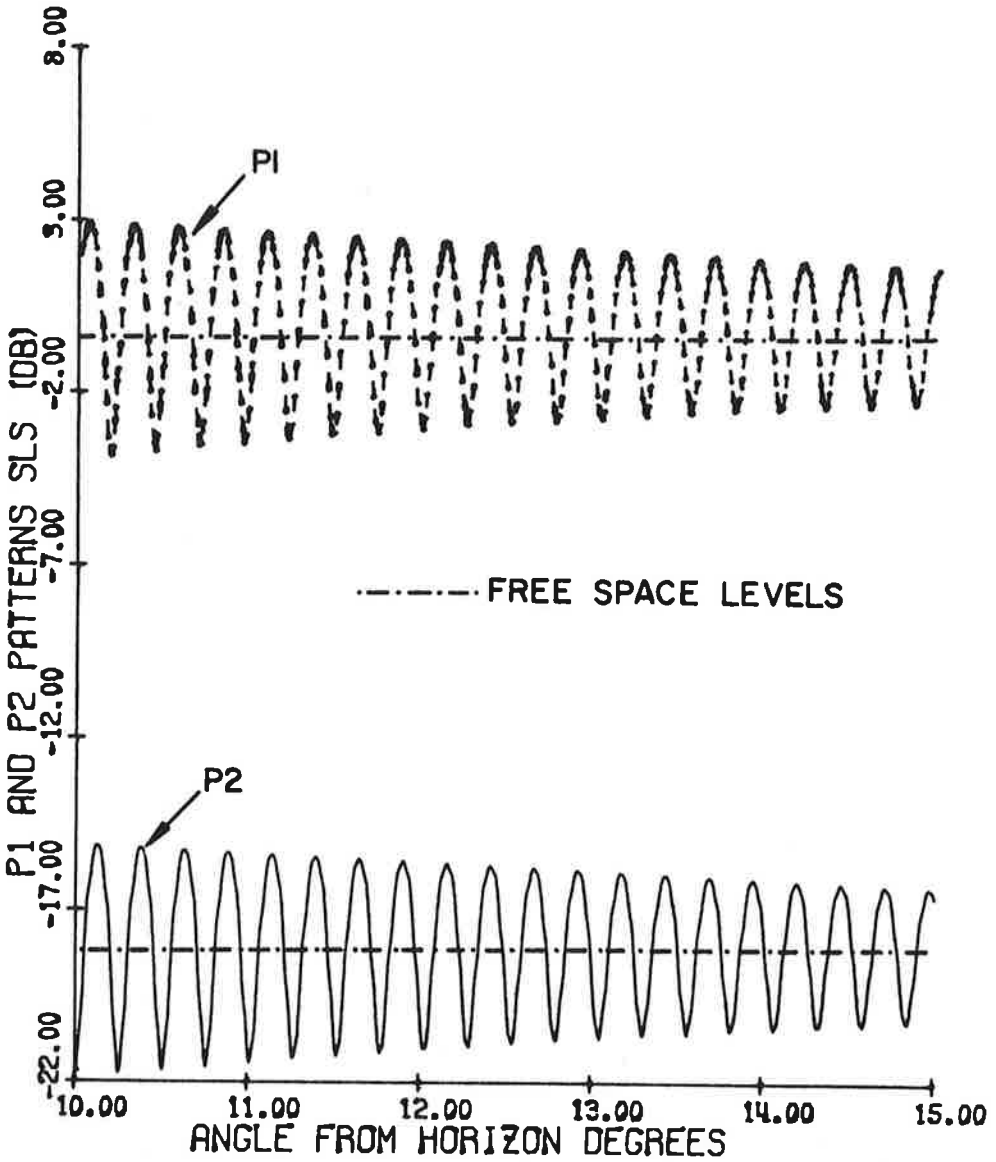

FIG. 54c: P1 and P2 pulses as functions of θ.

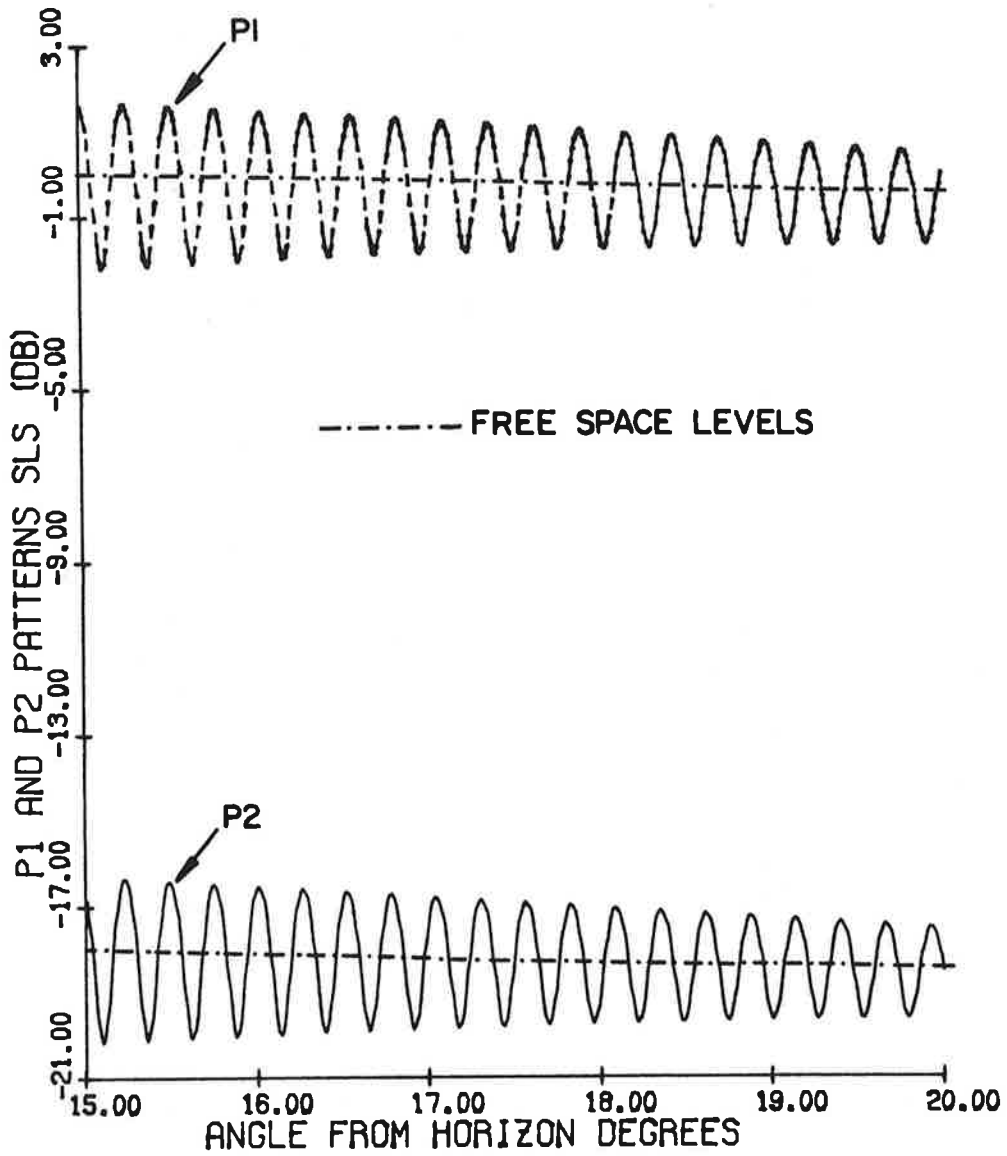

FIG. 54d: P1 and P2 pulses as functions of θ.

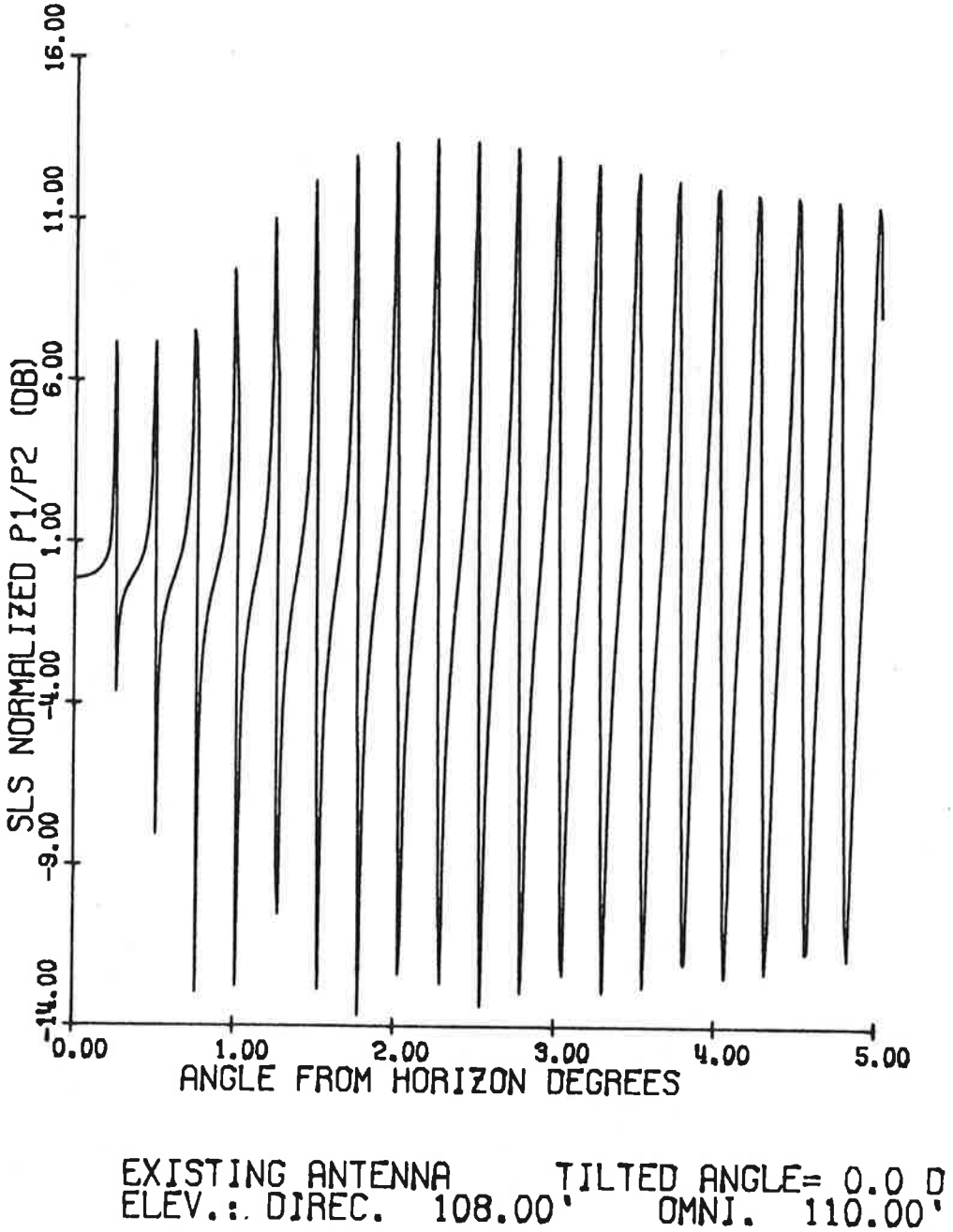

FIG. 55a: Normalized pulse ratio as a function of θ.

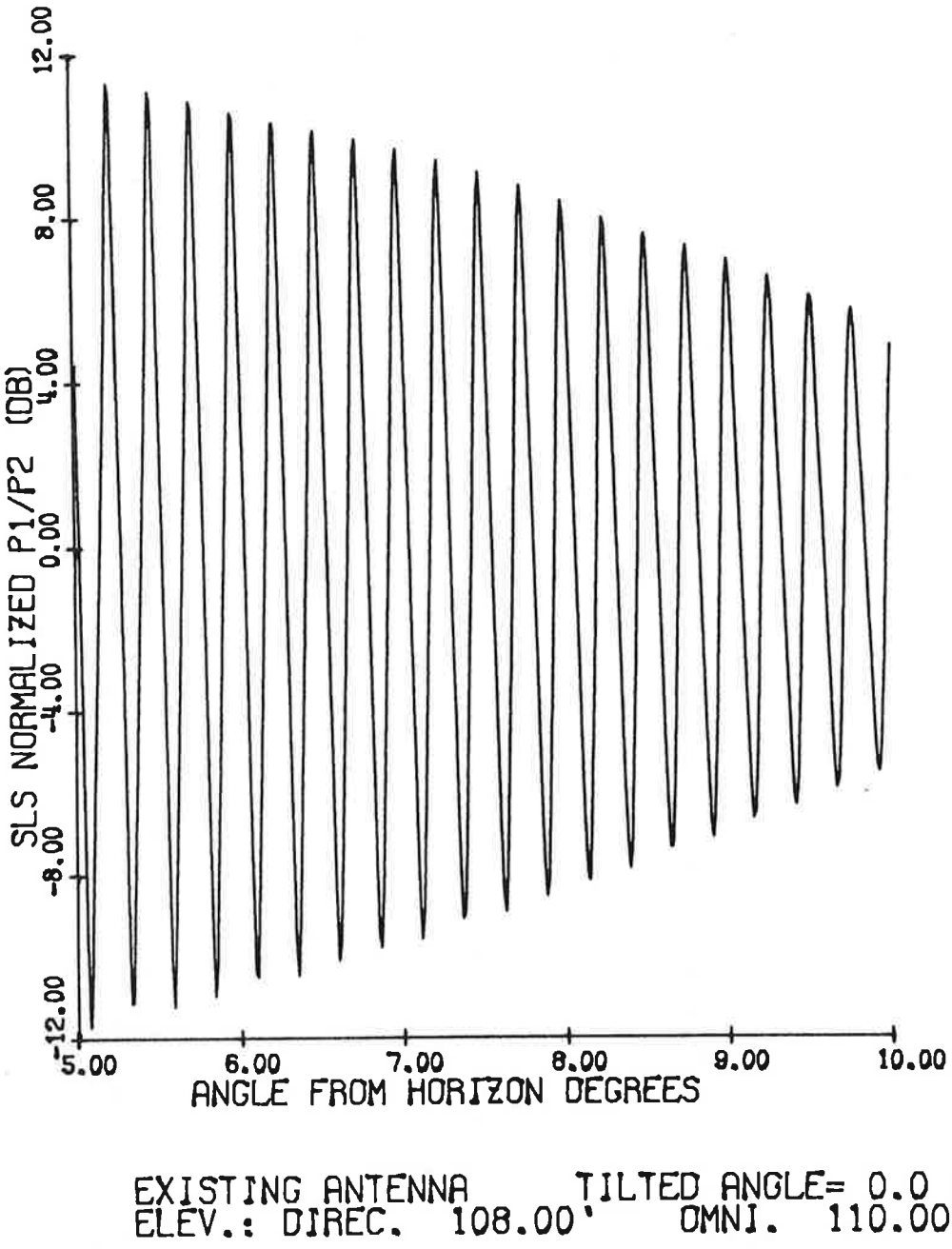

FIG. 55b: Normalized pulse ratio as a function of θ.

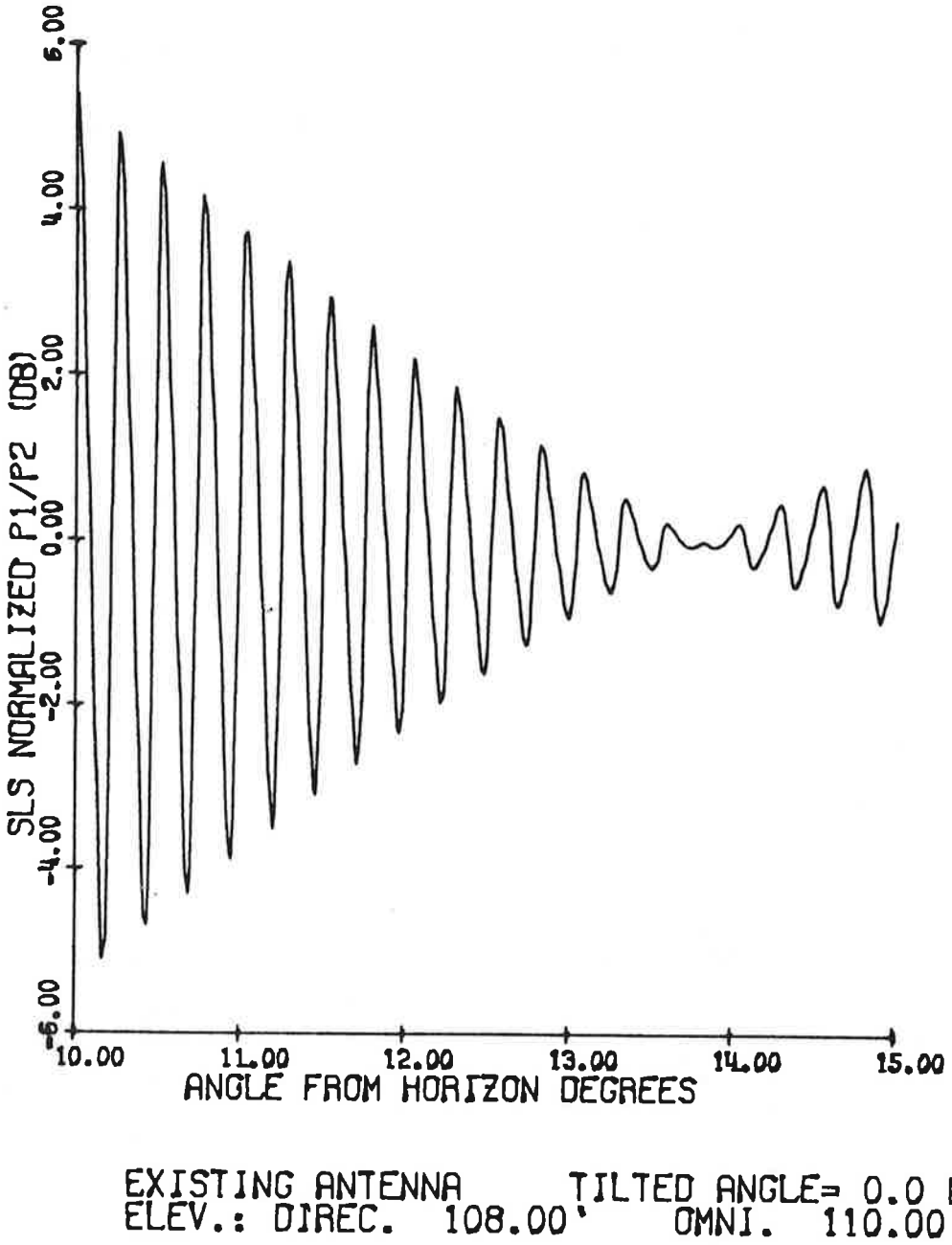

FIG. 55c: Normalized pulse ratio as a function of θ.

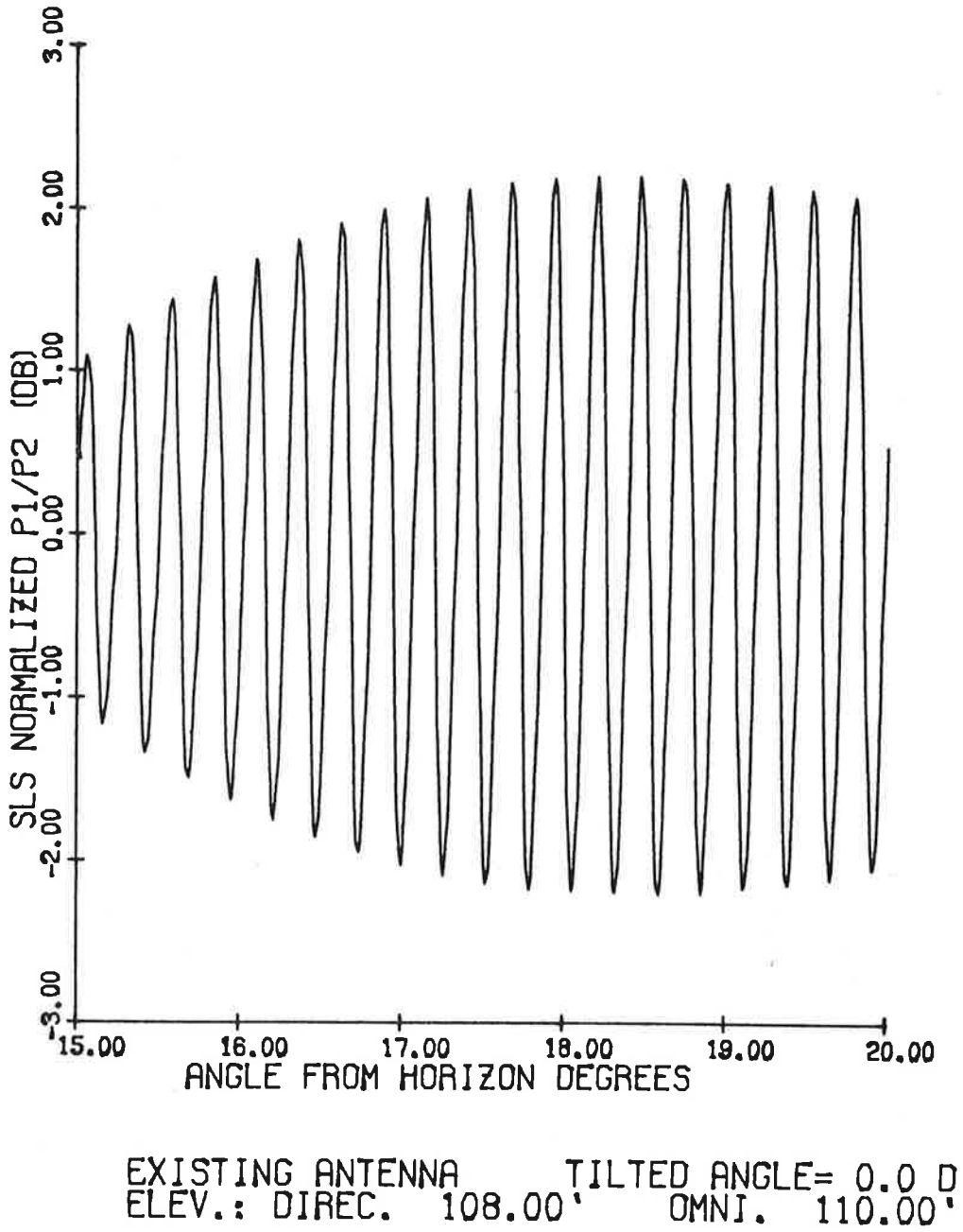

FIG. 55d: Normalized pulse ratio as a function of θ.

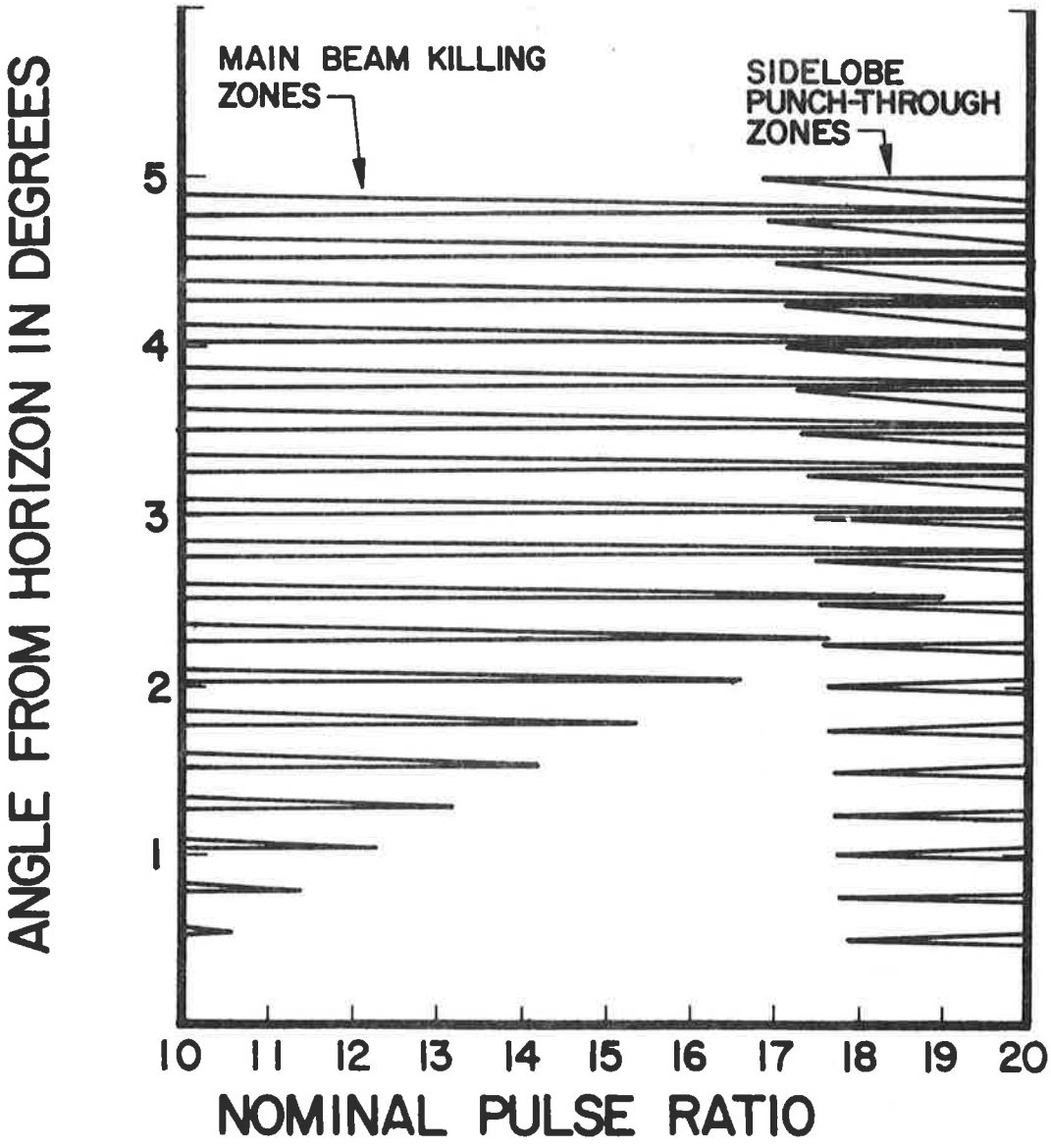

FIG. 56: Mainbeam killing and sidelobe punch-through zones as functions of the nominal pulse ratio for the existing "hog-trough" antenna. H_d = 108', H_o = 110', f = 1030 MHz, a = 9 dB, b = 0 dB, L = -25 dB.

Figure 57 gives the effective beamwidth as a function of θ in the range $0 \leq \theta \leq 5^{o}$. The stabilized value of the effective beamwidth is about 3^{o} which occurs for $\theta > 20^{o}$.

Figure 58 gives the number of replies as a function of θ in the range $0 \leq \theta \leq 5^{o}$. The number of replies varies between N = 0 and N = 43 with the stabilized value of N = 30, which occurs at $\theta > 20^{o}$.

The coverage diagram is shown in Fig. 59. The maximum free-space range is adjusted to be 200 NM. At the first minimum the range is found to be 16.8 NM and at the first maximum the range is 368.4 NM.

4.3.4 Texas Instruments Fix Antenna

The phase centers of the directional and omnidirectional antennas for this case are 92' and 112' respectively. The two phase centers are displaced by 20'.

Figure 60 shows the P1(θ), P2(θ) pulses as functions of θ where the 0 dB level corresponds to the maximum P1(θ) pulse level in the free space case. For $\theta > 3.5^{o}$ the curves assume the free space values.

Figure 61 shows the pulse ratio as a function of θ. For $\theta \geq 3.5^{o}$ the pulse ratio assumes the free space value. The maximum departures from the nominal value is +11 dB in one direction and -13.3 dB in the other.

The mainbeam killing and sidelobe punch-through zones as functions of the nominal pulse ratio are shown in Fig. 62. For $14\,\text{dB} \leq K_0 \leq 20\,\text{dB}$, both zones exist within $0 < \theta \leq 0.94^{o}$.

The effective beamwidth as a function of θ is shown in Fig. 63, for $K_0 = 18\,\text{dB}$ and a = 9 dB. For $\theta \geq 3^{o}$ the effective beamwidth assumes the constant value of 2.6^{o}.

The number of replies as a function of θ is shown in Fig. 64. For $\theta > 3^{o}$ the number assumes a constant value of 20 appropriate for free space. The number of replies varies between 0 and 30.

Figure 65 shows the coverage diagram where the maximum free space range is adjusted to be equal to 200 nautical miles. The range at the first minimum is about 30 NM and that at the first maximum is about 232 NM. For $\theta > 3^{o}$, the range may be assumed to be the same as the free space value.

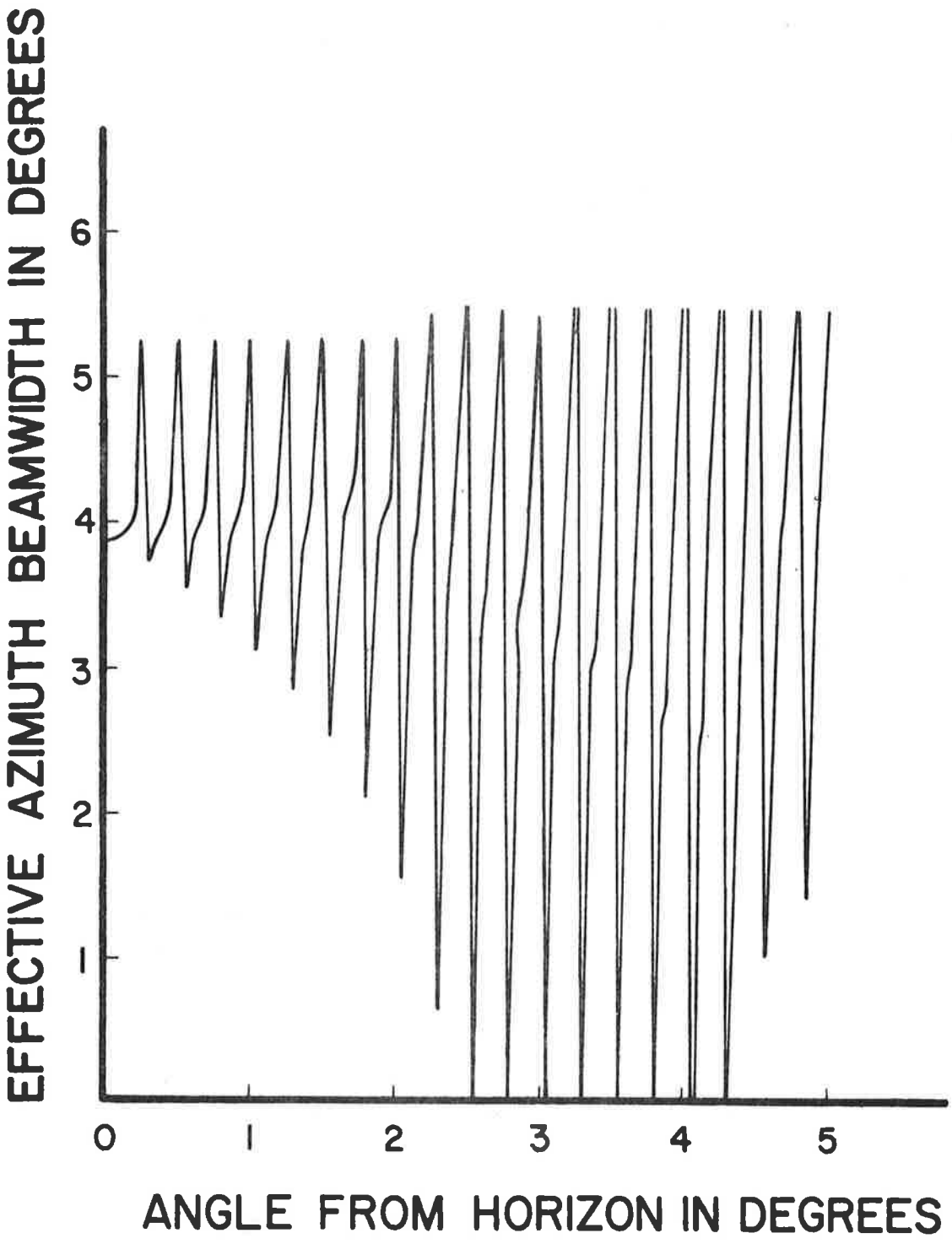

FIG. 57: Effective azimuth beamwidth as a function of angle from the horizon for the existing "hog-trough" antenna. H_d = 108', H_o = 110', f = 1030 MHz, nominal pulse ratio K_o = 18 dB.

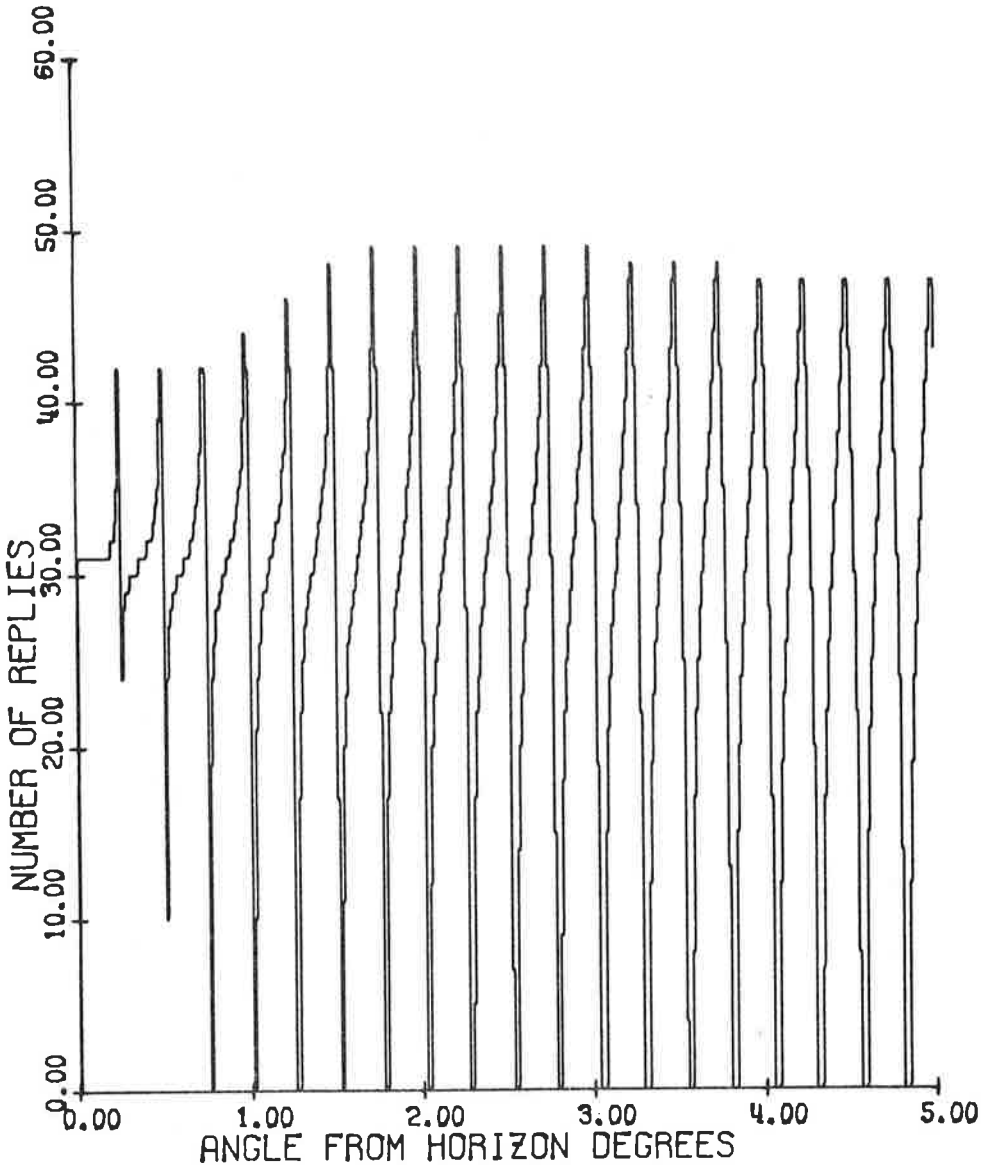

FIG. 58: Number of replies as a function of angle from the horizon.

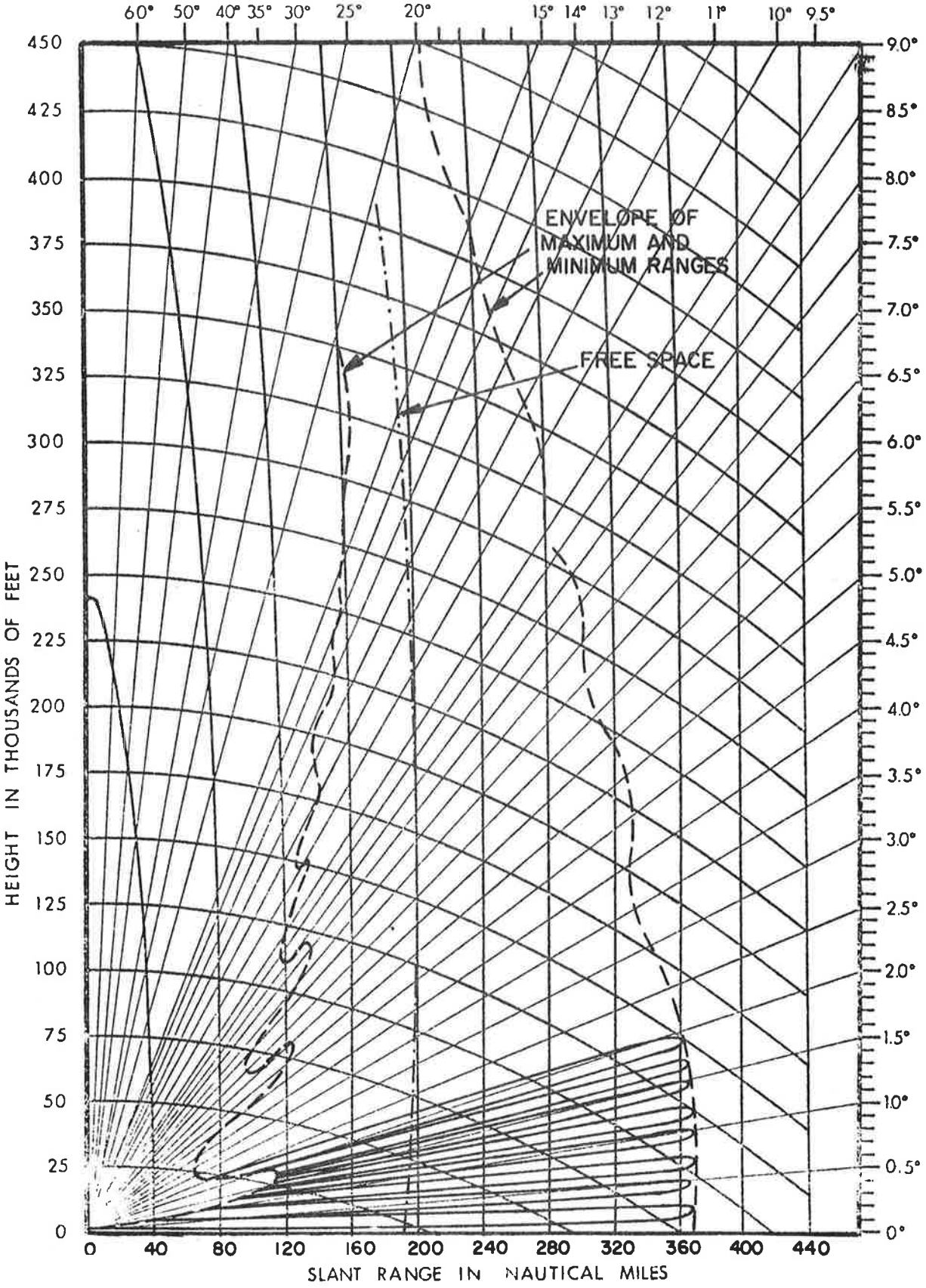

FIG. 59a: Coverage diagram for the existing "hog-trough" antenna. H_d = 108', H_0 = 110', f = 1030 MHz, maximum free space range = 200 nautical miles.

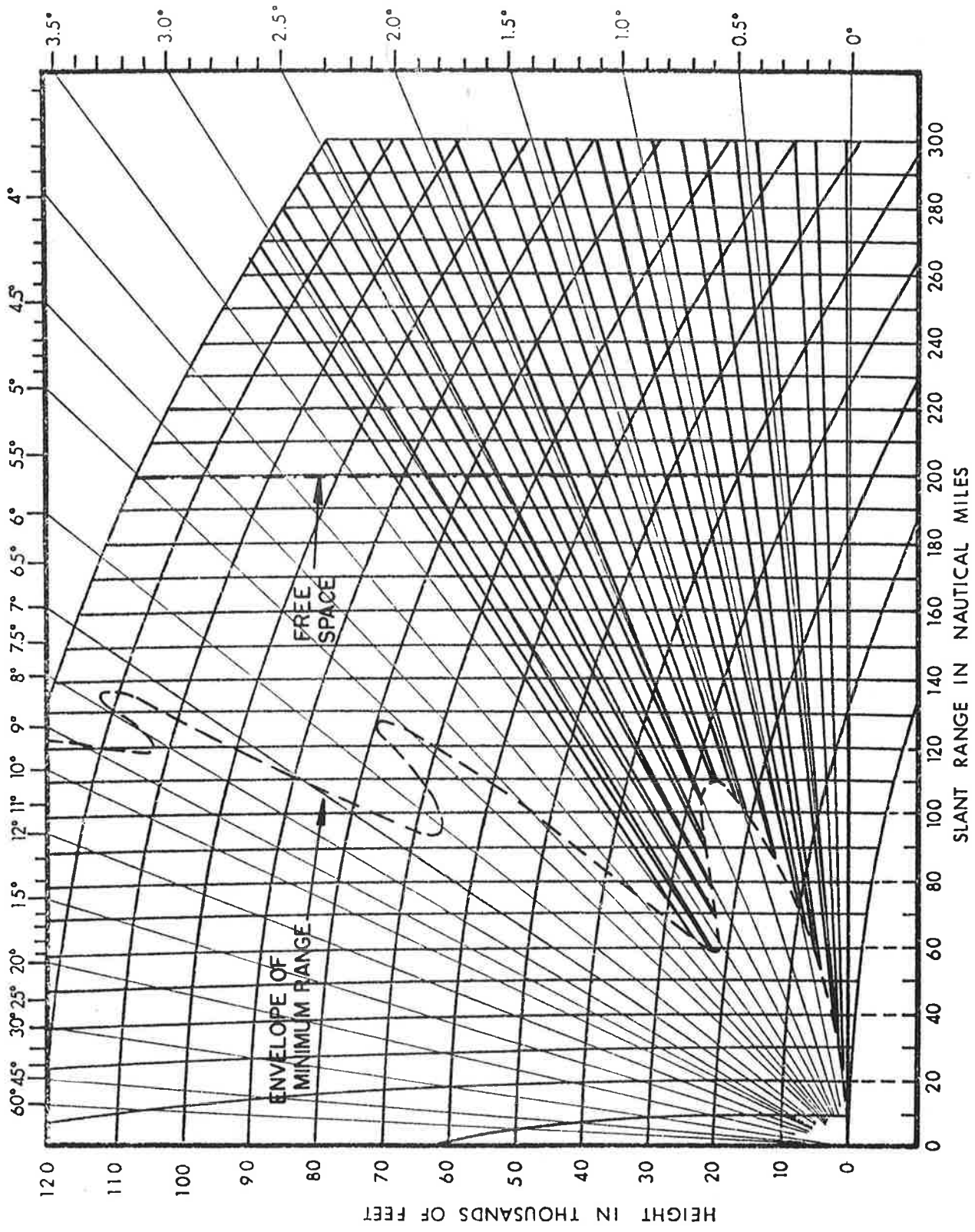

FIG. 59b: Coverage diagram on expanded scale for the existing "hog-trough" antenna. H_d = 108', H_0 = 110', f = 1030 MHz, maximum free space range = 200 nautical miles.

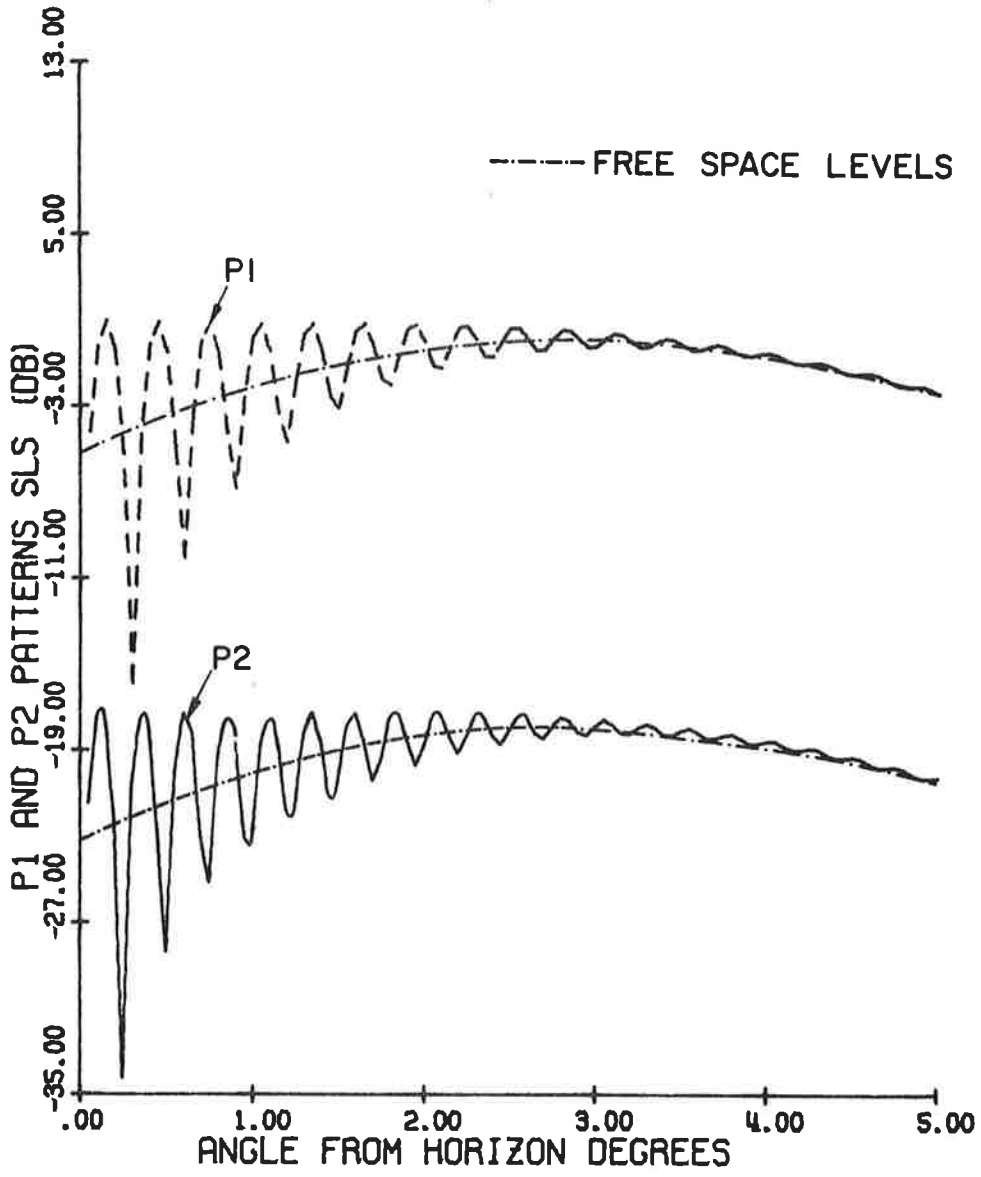

FIG. 60: P1 and P2 pulses as functions of θ.

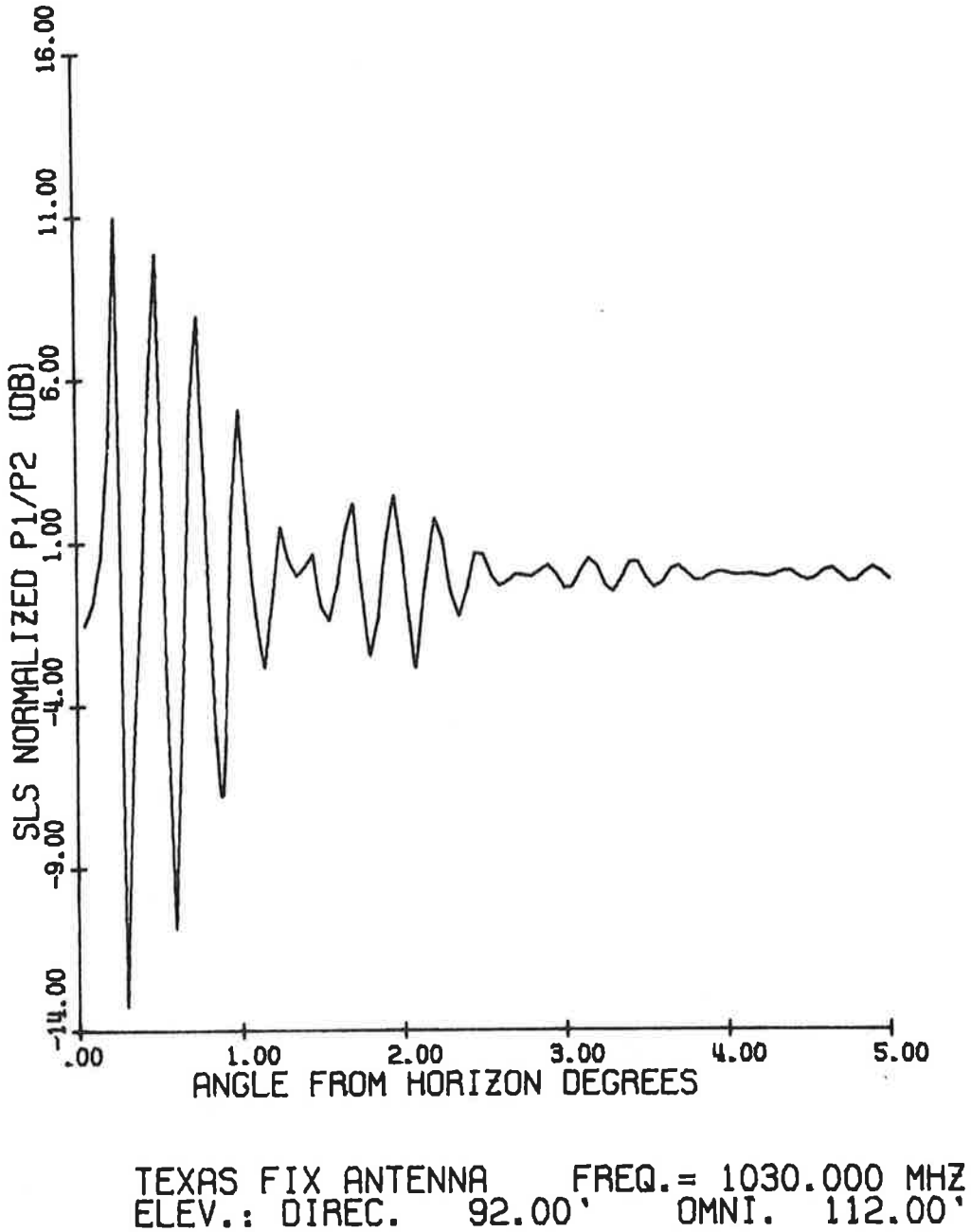

FIG. 61: Normalized pulse ratio as a function of θ.

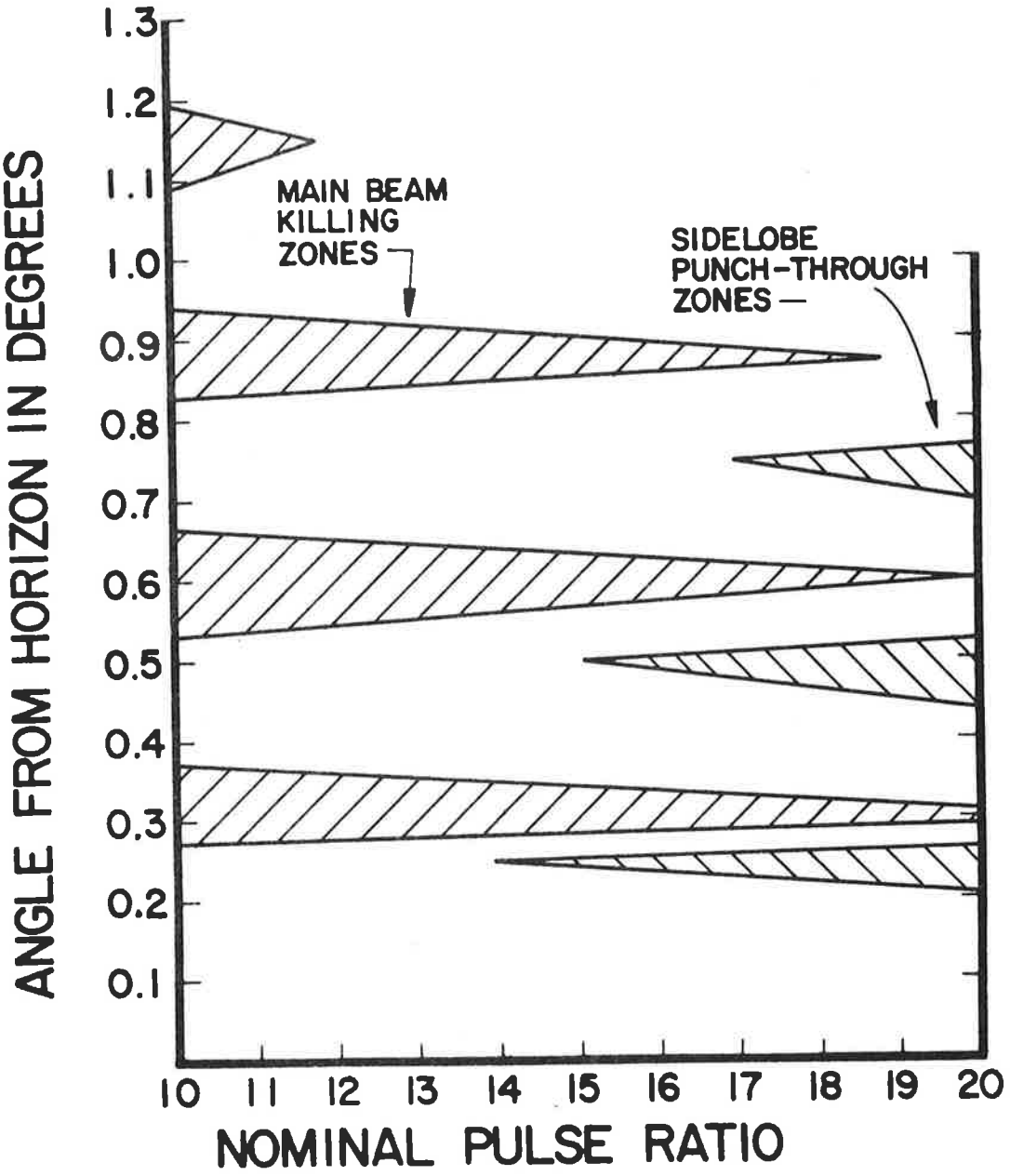

FIG. 62: Mainbeam killing and sidelobe punch-through zones as functions of the nominal pulse ratio for the TI Fix antenna. H_d = 92', H_o = 112', f = 1030 MHz, a = 9dB, b = 0dB, L = -25dB.

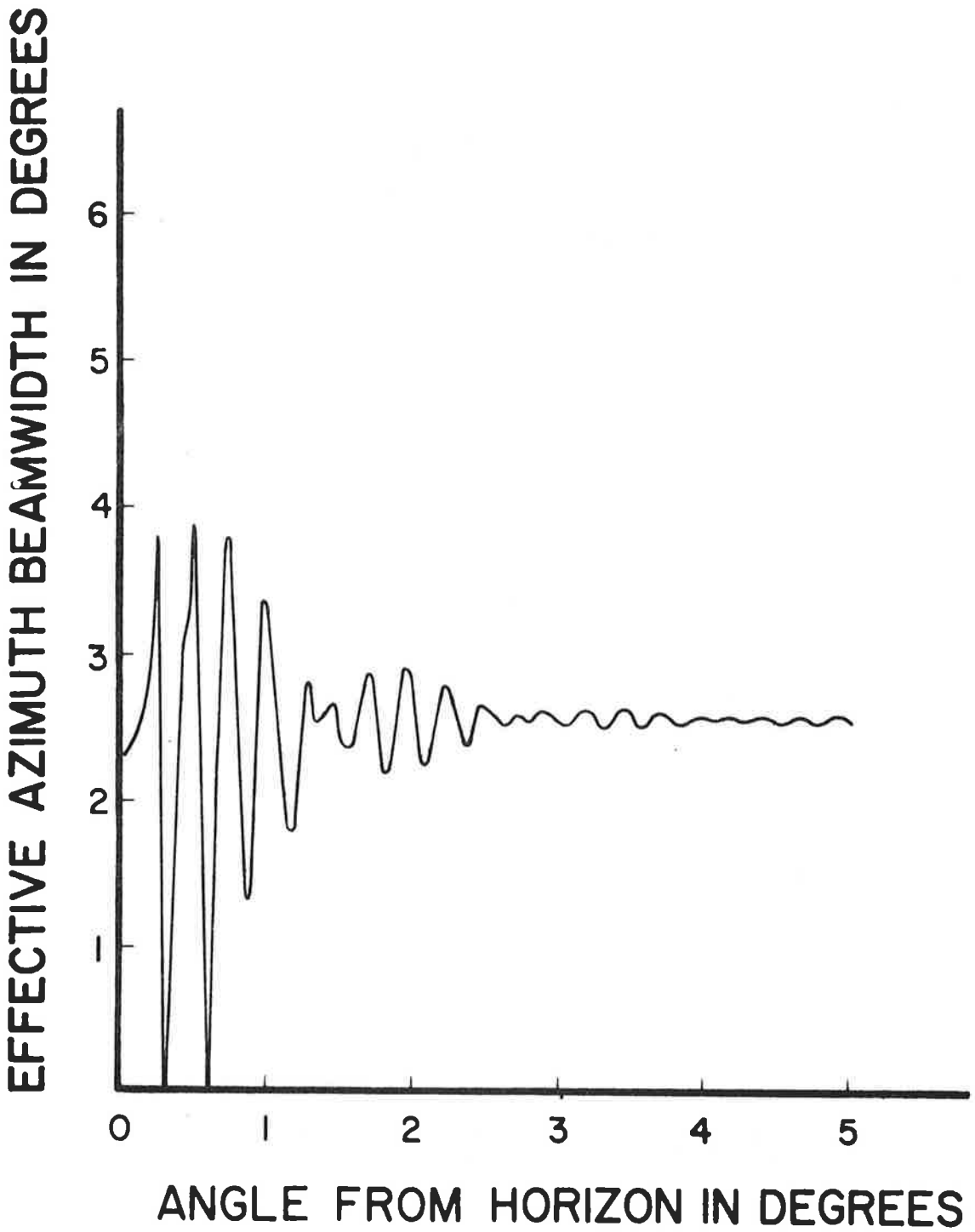

FIG. 63: Effective azimuth beamwidth as a function of angle from the horizon for the TI Fix antenna. H_d = 92', H_o = 112', f = 1030 MHz, nominal pulse ratio K_o = 18 dB.

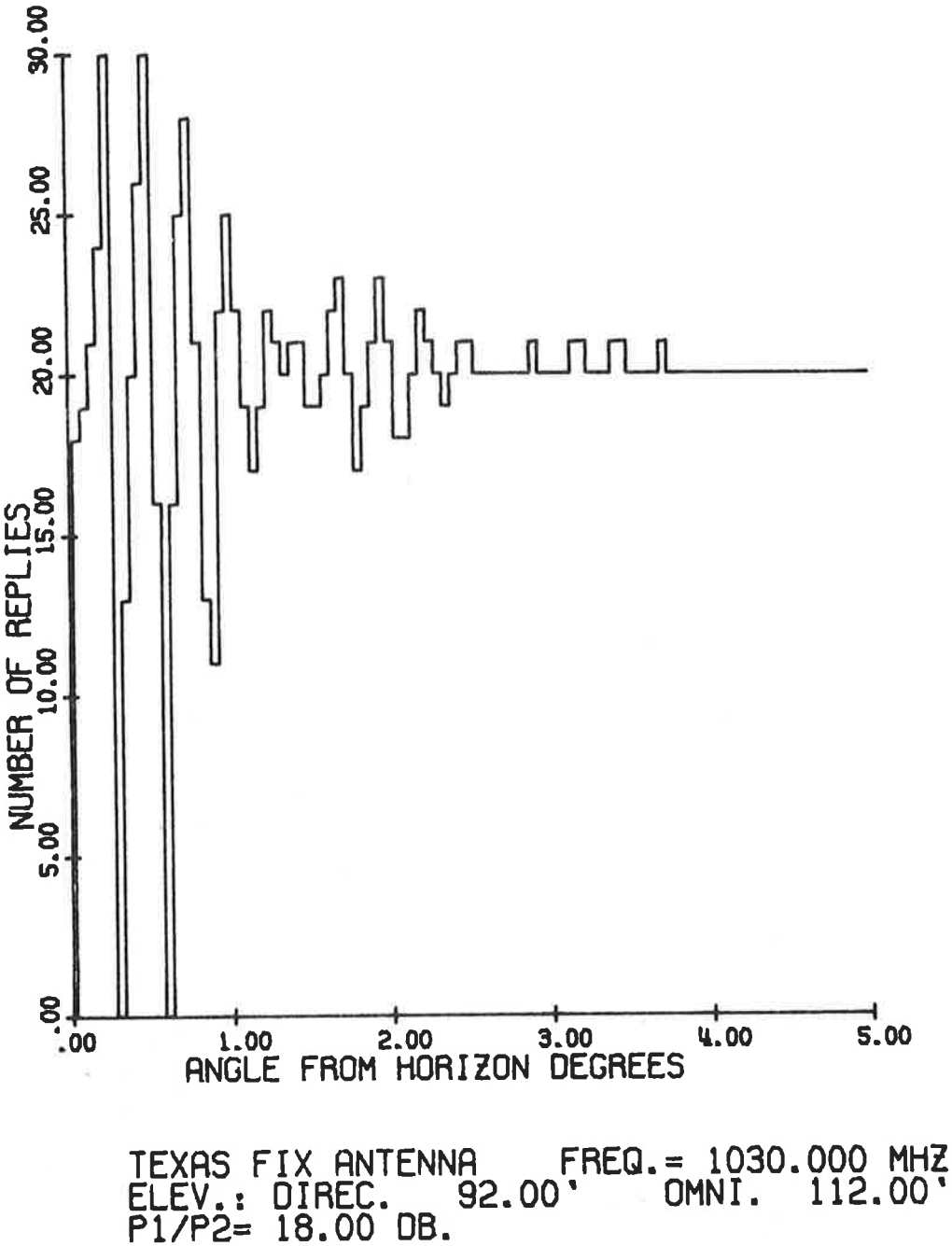

FIG. 64: Number of replies as a function of angle from the horizon.

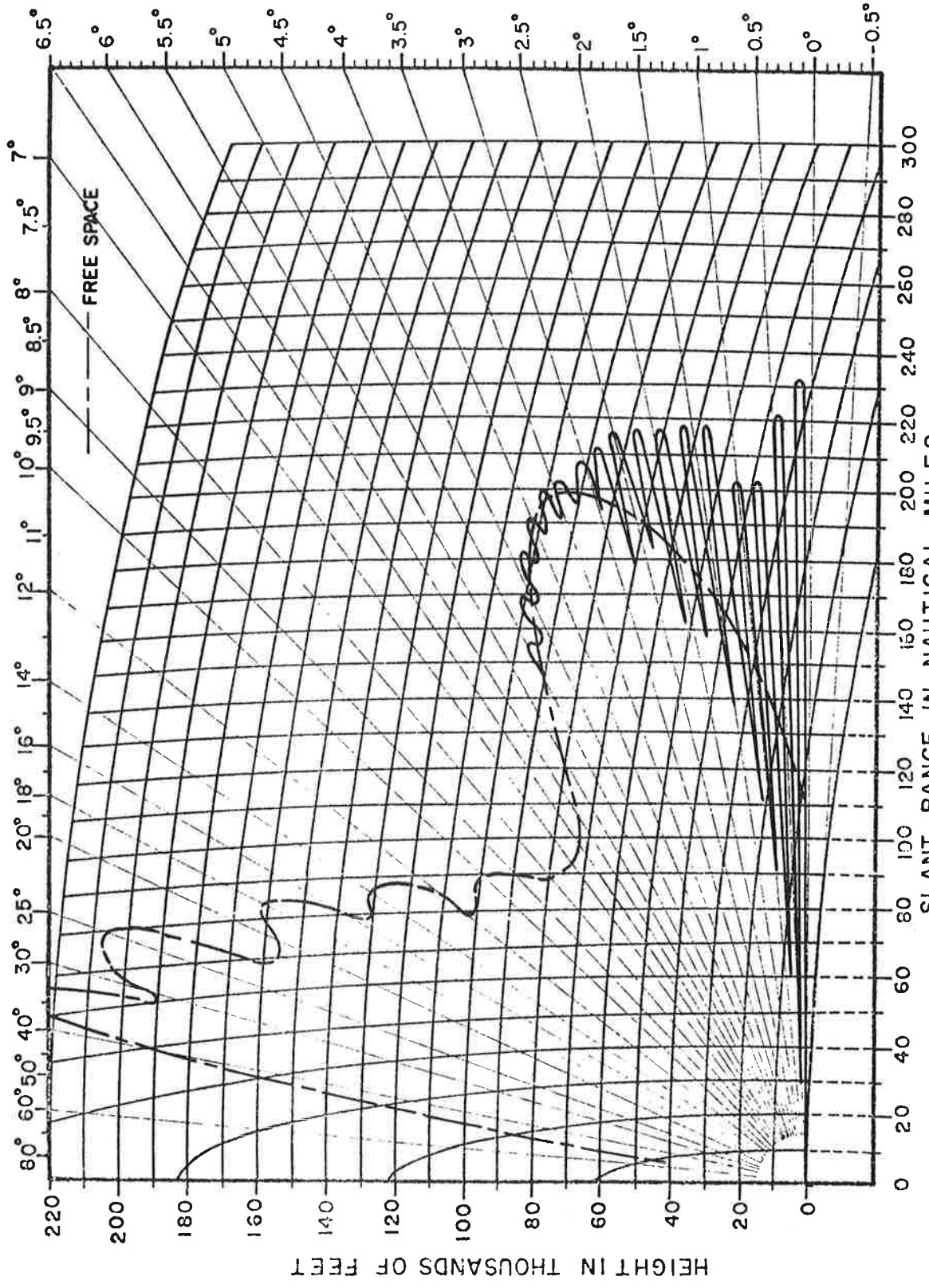

FIG. 65: Coverage diagram for the TI Fix antenna. H_d = 92', H_o = 112', f = 1030 MHz, maximum free space range = 200 nautical miles.

4.3.5 NADIF Fix I Antenna

The phase centers of the directional and omnidirectional antennas are located at 92' and 112' respectively. The two phase centers are displaced by 20'. The system uses the Texas Instruments omnidirectional antenna.

The NADIF Fix I directional antenna differs from the Texas Fix directional antenna only in the primary source for the reflector so that its vertical plane pattern is slightly different from that of the latter. The free space elevation plane patterns of the directional and omnidirectional antennas are assumed to be the same.

Figure 66 shows P1(θ), P2(θ) pulses as functions of θ where the 0 dB level is adjusted to be the maximum value of P1(θ) in the free space case. For practical purposes the two curves assume their free space values for $\theta \geq 3^{o}$.

Figure 67 shows the pulse ratio as a function of θ.

The mainbeam killing and sidelobe punch-through zones as functions of the nominal pulse ratio as shown in Fig. 68. For $13.4 \leq K_0 \leq 18.9$ dB, both the zones exist for $0.2^{o} \leq \theta \leq 1^{o}$.

The effective beamwidth as a function of θ is shown in Fig. 69. The stabilized value of the beamwidth is about 2.6^{o}.

The number of replies as a function of θ is shown in Fig. 70. The free space value of the number of replies is 20.

The coverage diagram for the antenna is shown in Fig. 71 where the maximum free space range is adjusted to be equal to 200 nautical miles. The range at the first minimum is about 30 NM and that at the the first maximum is about 252 NM.

4.3.6 NADIF Fix II Antenna

The heights of the phase centers of the directional and omnidirectional antennas are 92' and 111' respectively, so that they are displaced vertically by 19'. The Westinghouse omnidirectional antenna is used.

Figure 72 shows the P1(θ), P2(θ) pulses as functions of θ where the 0 dB level is adjusted to be the maximum P1(θ) pulse in the free space case. The two curves assume free space values for $\theta \gtrsim 3^{o}$.

Figure 73 gives the pulse ratio as a function of θ.

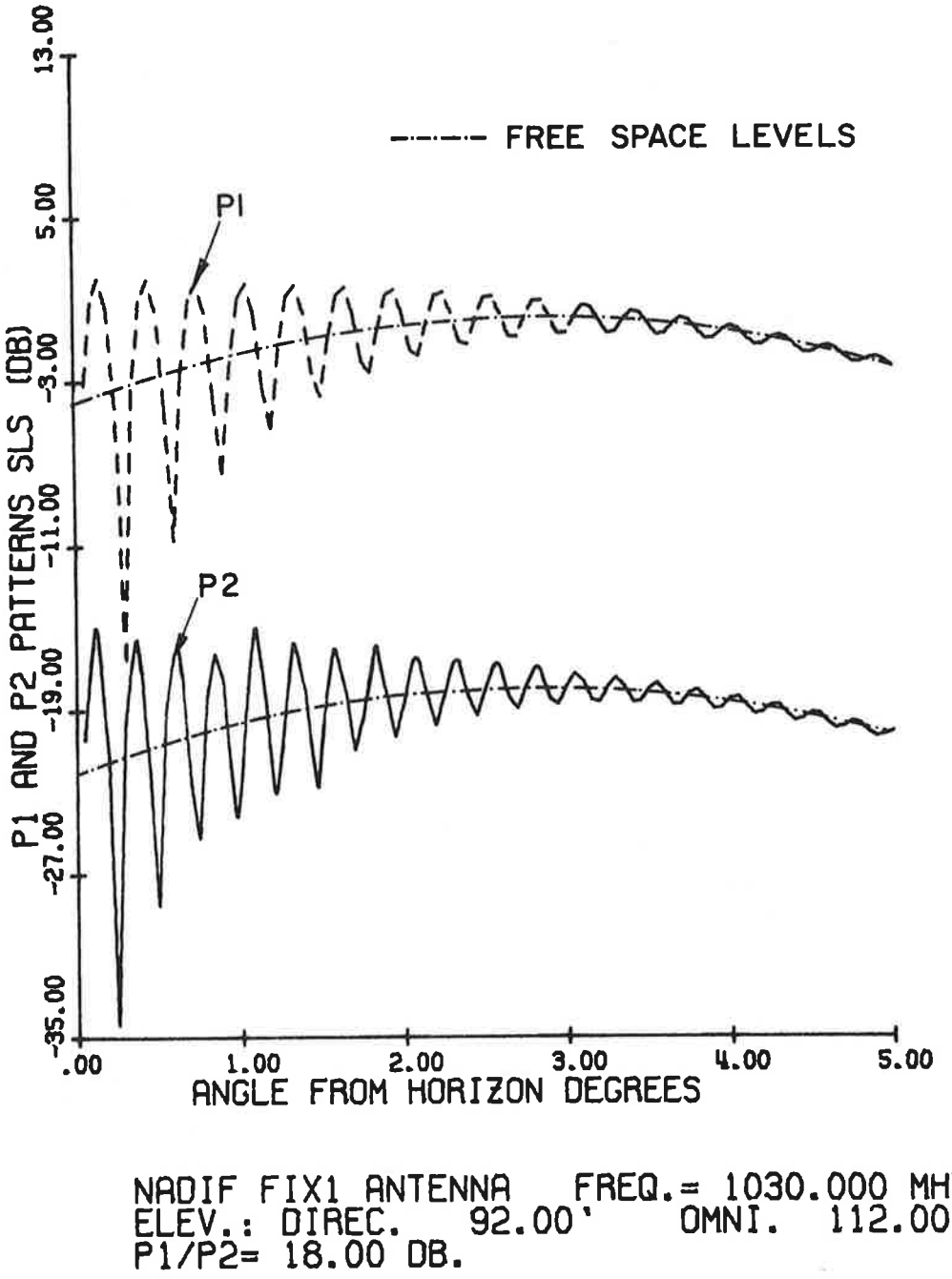

FIG. 66: P1 and P2 pulses as functions of θ.

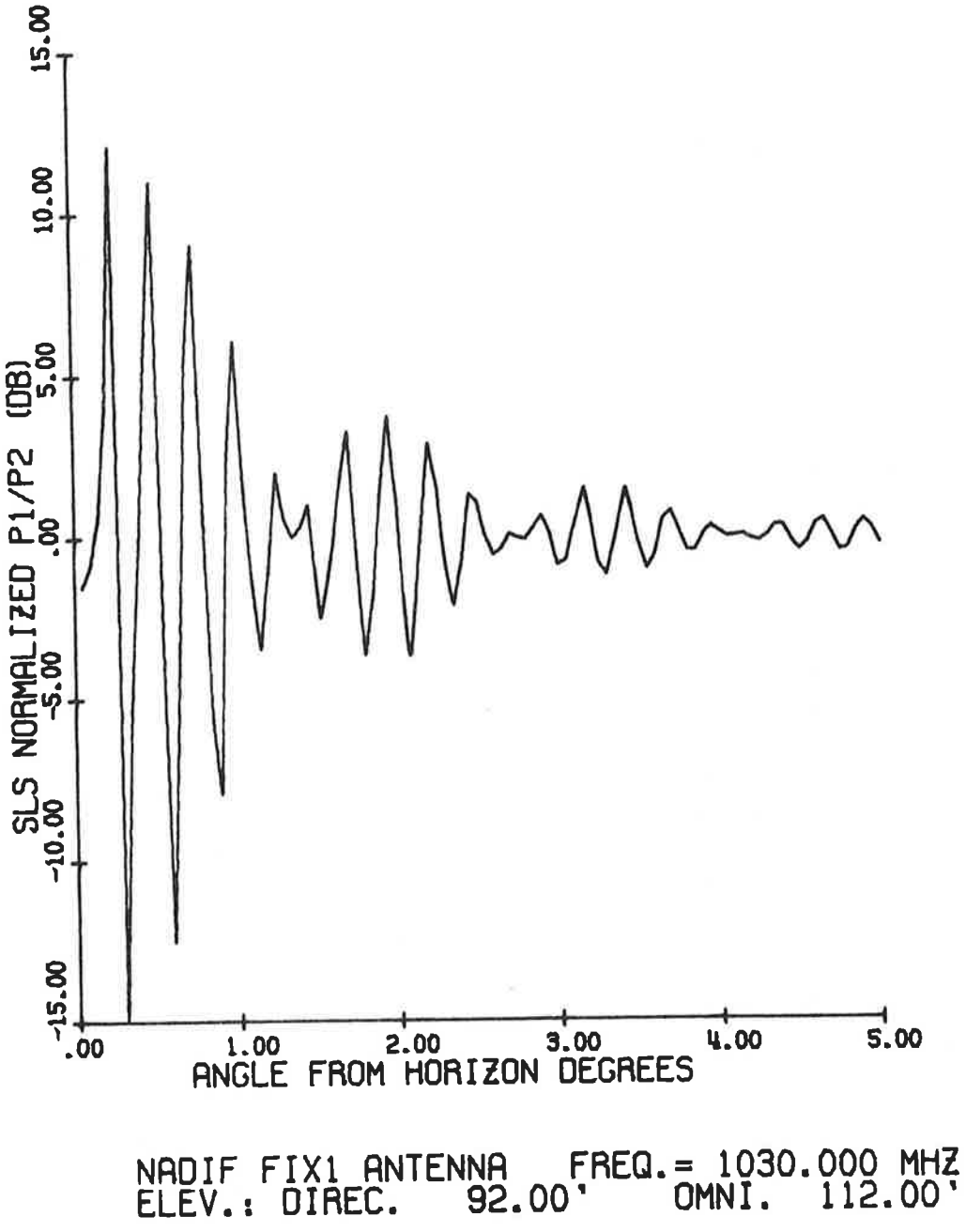

FIG. 67: Normalized pulse ratio as a function of θ

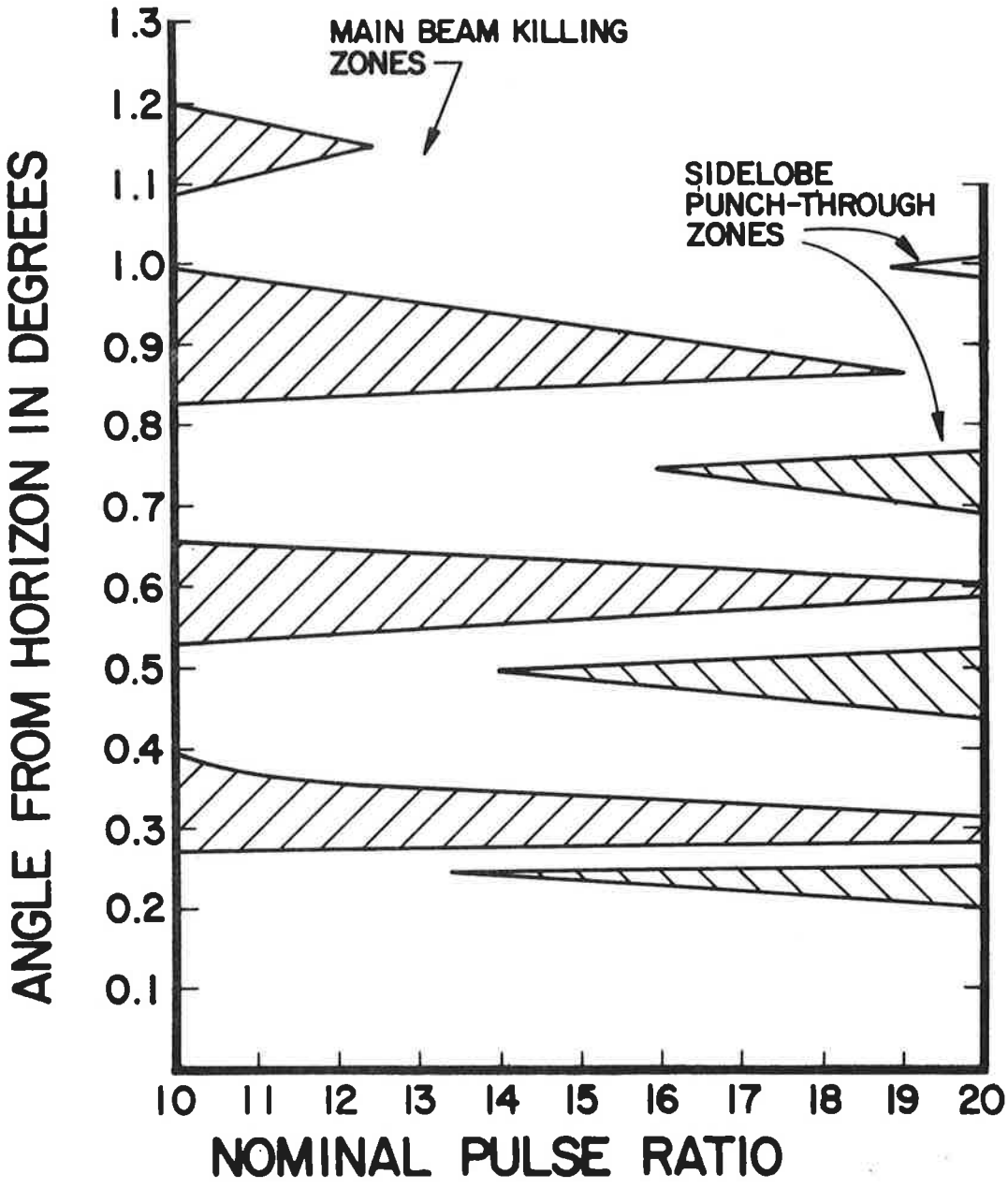

FIG. 68: Mainbeam killing and sidelobe punch-through zones as functions of the nominal pulse ratio for the NADIF FIX I antenna: H_d = 92', H_o = 112', f = 1030 MHz, a = 9dB, b = 0dB, L = -25dB.

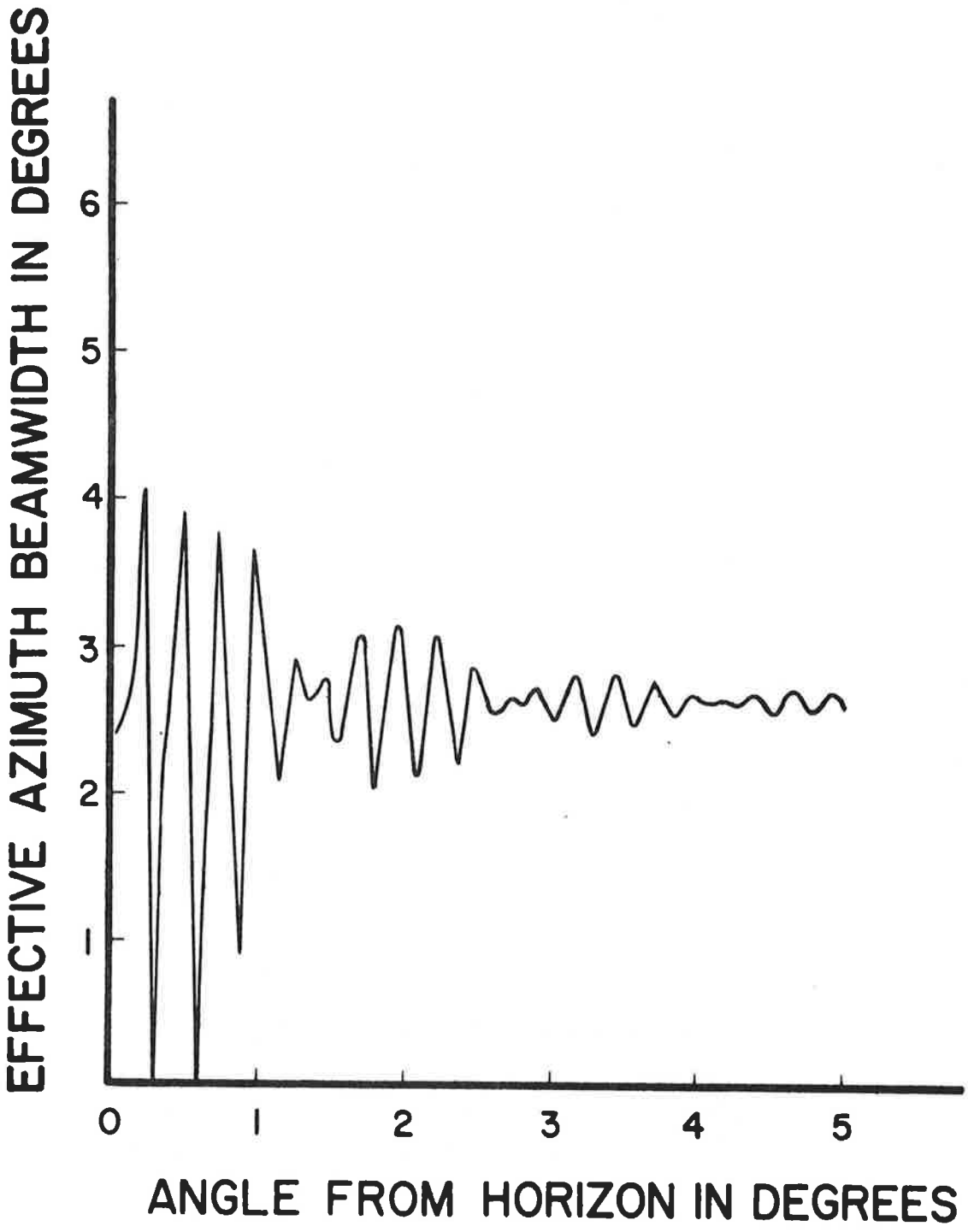

FIG. 69: Effective azimuth beamwidth as a function of angle from the horizon for the NADIF FIX I antenna. H_d = 921, H_o = 112', f = 1030 MHz, nominal pulse ratio K_o = 18 dB.

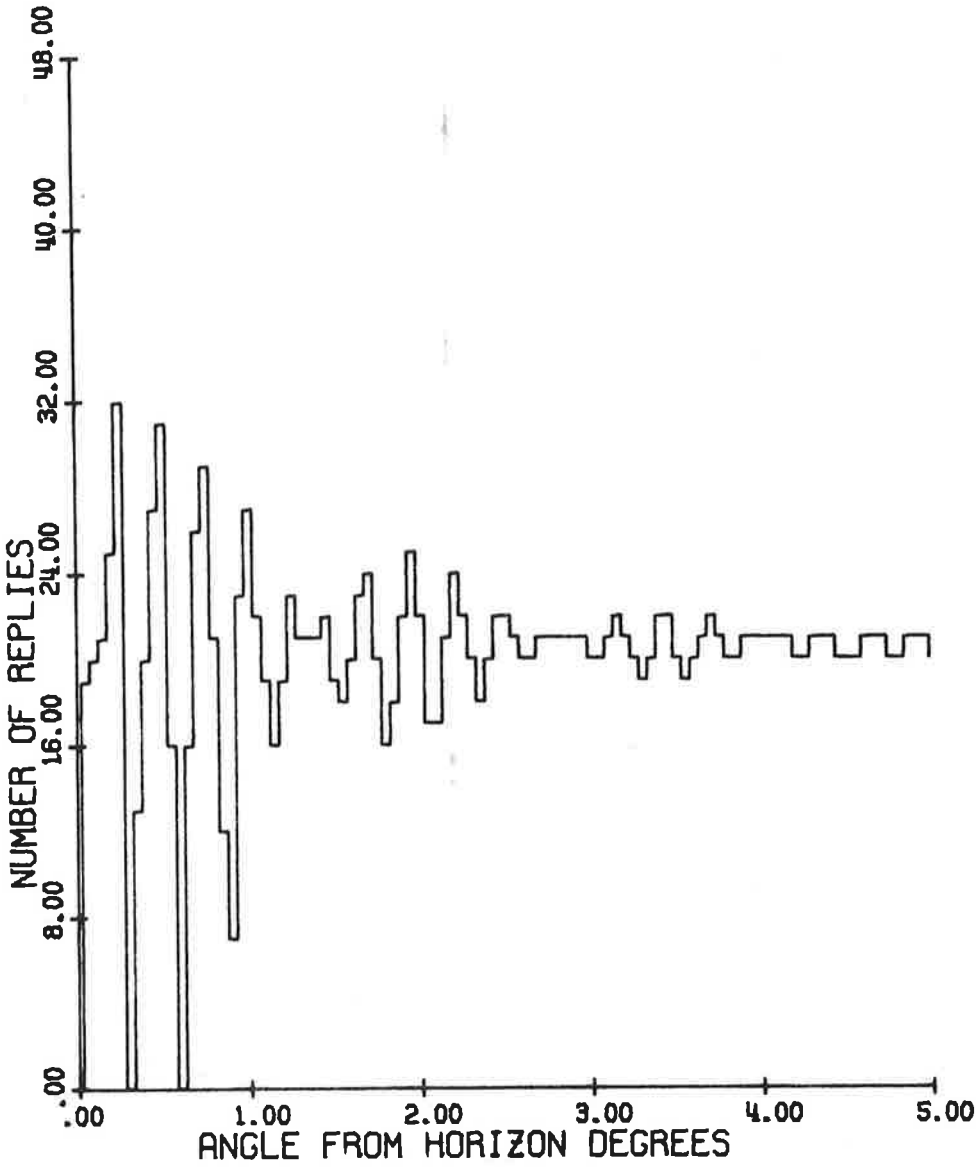

FIG. 70: Number of replies as a function of angle from the horizon.

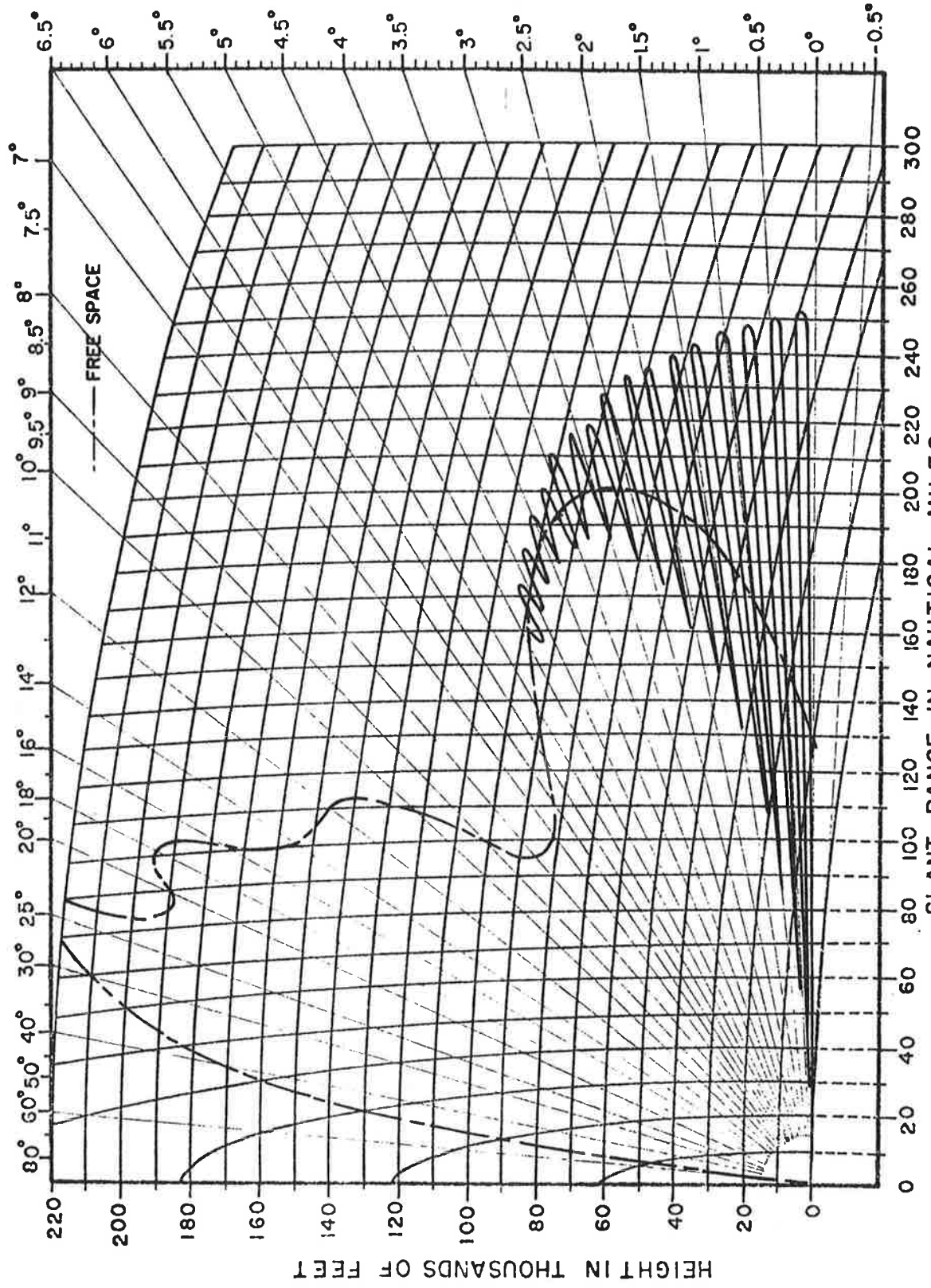

FIG. 71: Coverage diagram for the NADIF FIX I antenna, H_d = 92', H_o = 112', f = 1030 MHz, maximum free space range = 200 nautical miles.

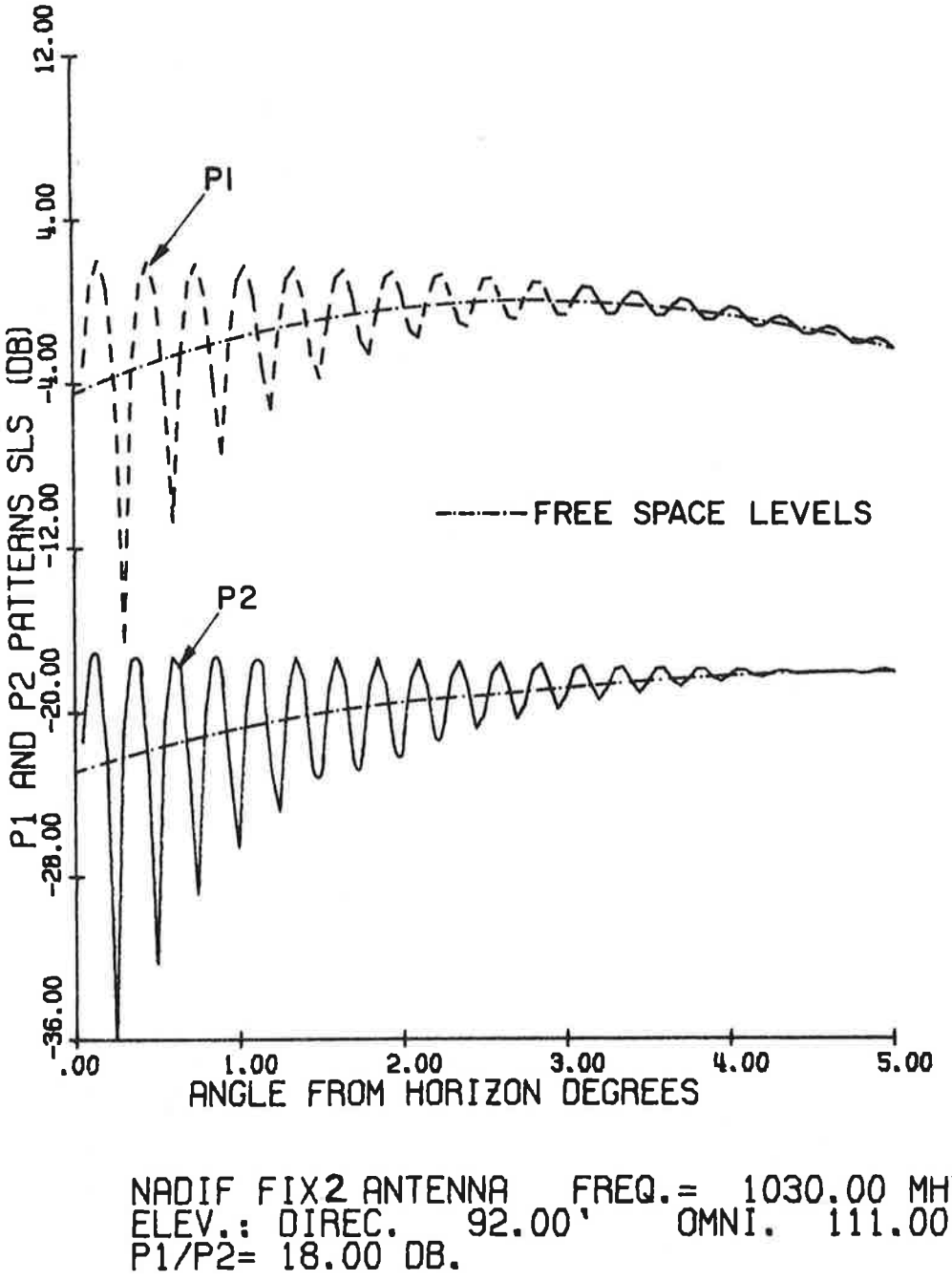

FIG. 72: P1 and P2 pulses as functions of θ.

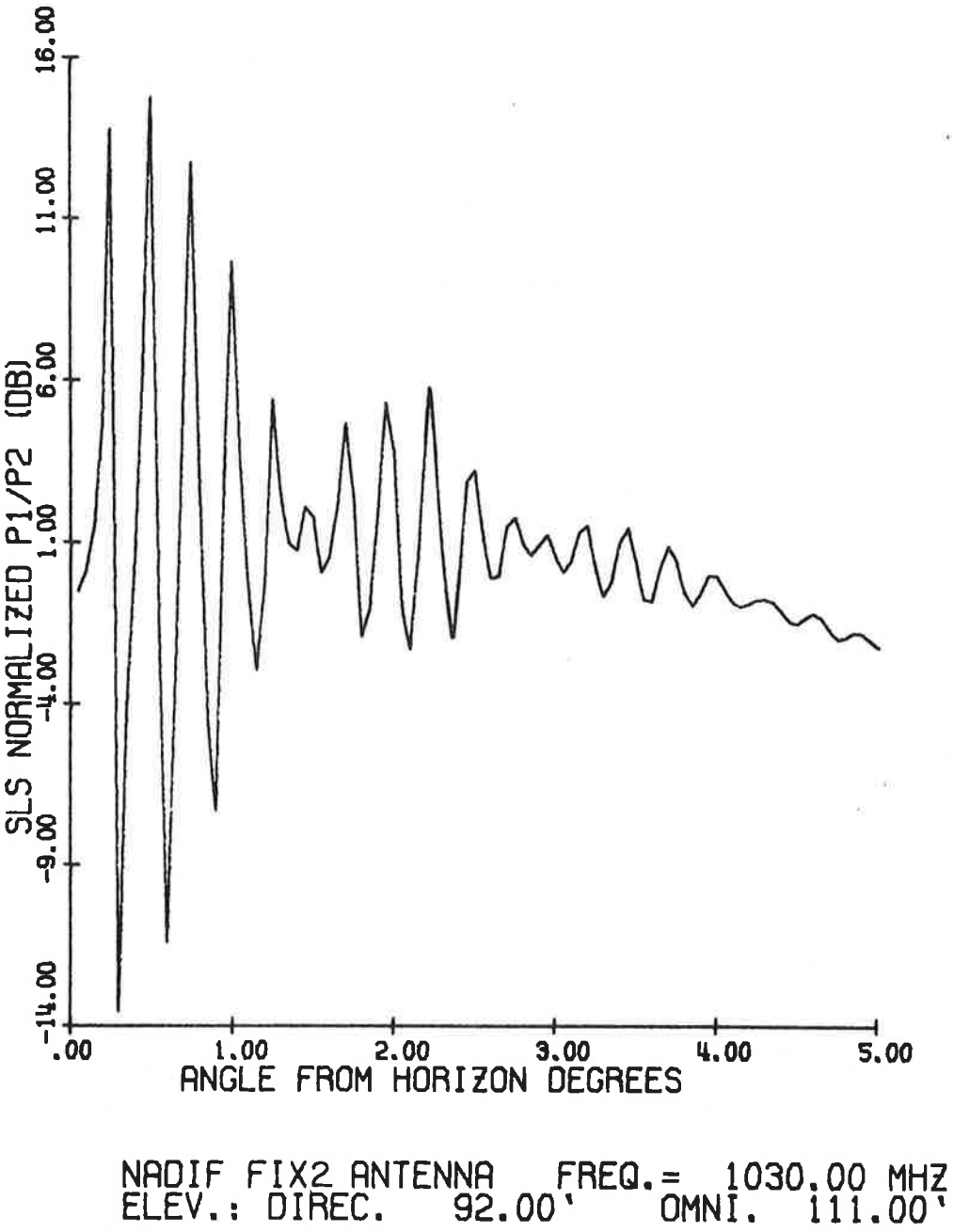

FIG. 73: Normalized pulse ratio as a function of θ.

The mainbeam killing and sidelobe punch-through zones as functions of the nominal pulse ratio are shown in Fig. 74. Both the zones exist for $12.2\,\text{dB} \leq K_0 \leq 20\,\text{dB}$ within the range of θ, $0.2^\circ \leq \theta \leq 0.7^\circ$.

The effective beamwidth as a function of θ is shown in Fig. 75.

The number of replies as a function of θ is shown in Fig. 76. The free space value of the number of replies is about 20.

Figure 77 shows the coverage diagram where the free space maximum range is adjusted to be equal to 200 nautical miles. The range at the first minimum is found to be 30 NM while that at the first maximum is found to be 252 NM.

4.3.7 NADIF Fix III Antenna

The heights of the phase centers of the directional and omnidirectional antennas are 92' and 110' respectively, so that the two phase centers are displaced by 18'. It uses the existing small aperture omnidirectional antenna.

Figure 78 shows the P1(θ), P2(θ) pulses as functions of θ where the 0 dB level is adjusted to be the maximum value of the P1(θ) pulse in the free space case. The P1 curves assumes its free space value for $\theta > 3^\circ$. Due to the small vertical aperture of the omni antenna, the P2 curve oscillates beyond $\theta = 5^\circ$.

Figure 79 gives the pulse ratio as a function of θ.

The mainbeam killing and sidelobe punch-through zones as functions of the nominal pulse ratio are shown in Figures 80a and 80b.

The effective azimuth beamwidth as a function of θ is shown in Fig. 81.

The number of replies as a function of θ is shown in Fig. 82. The free space value of the number of replies is 20.

The coverage diagram for this antenna is the same as that of the NADIF Fix II antenna and is shown in Fig. 77, where the maximum range in the free space case is adjusted to be equal to 200 nautical miles. The range at the first minimum is found to be 30 NM and that the the first maximum is found to be 252 NM.

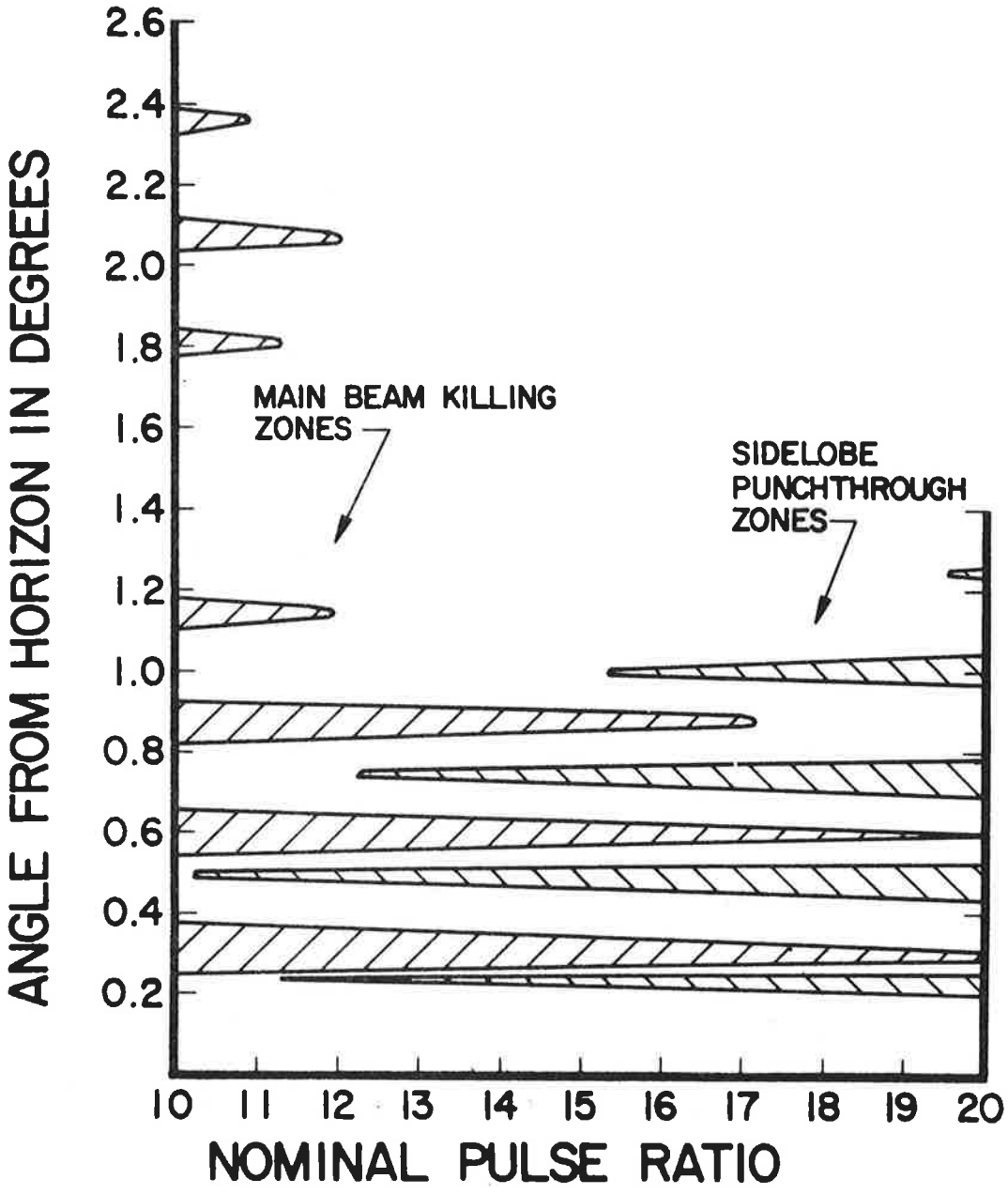

FIG. 74: Mainbeam killing and sidelobe punch-through zones as functions of the nominal pulse ratio for NADIF FIX II antenna. H_d = 92', H_o = 111', f = 1030 MHz, a = 9dB, B = 0dB, L = -25dB.

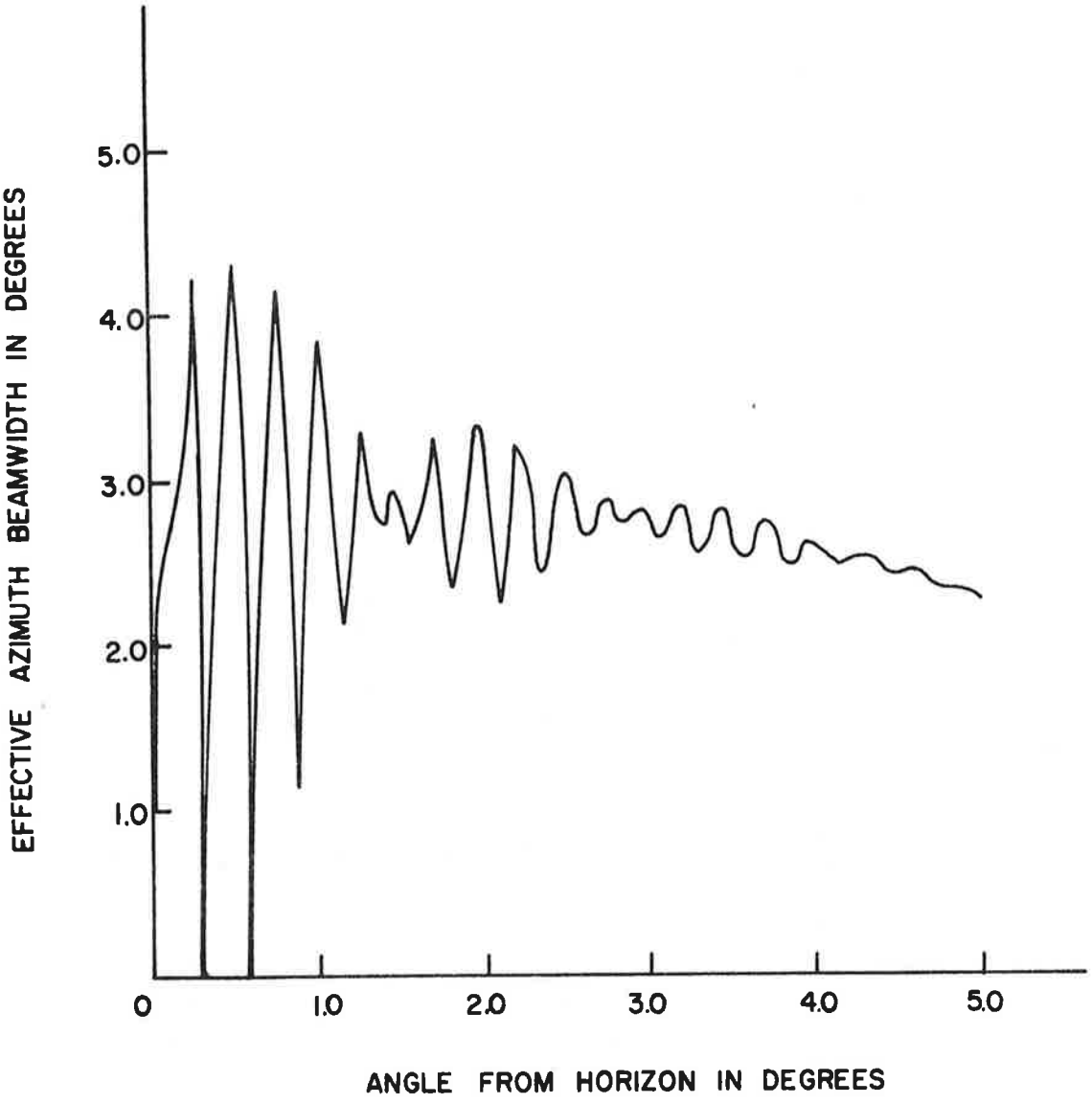

FIG. 75: Effective azimuth beamwidth as a function of angle from the horizon for NADIF FIX II antenna. H_d = 92', H_o = 111', f = 1030 MHz, nominal pulse ratio K_o = 18 dB.

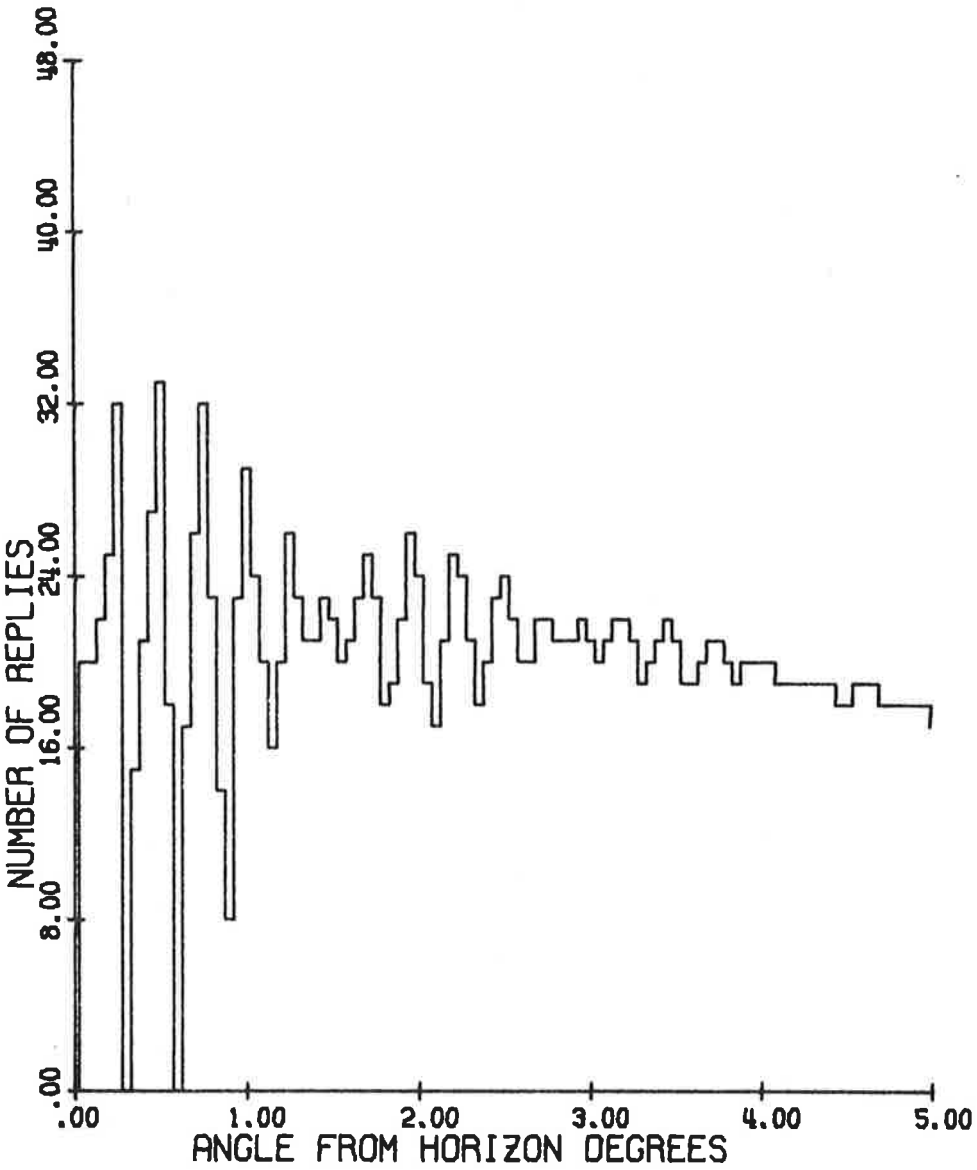

FIG. 76: Number of replies as a function of angle from the horizon.

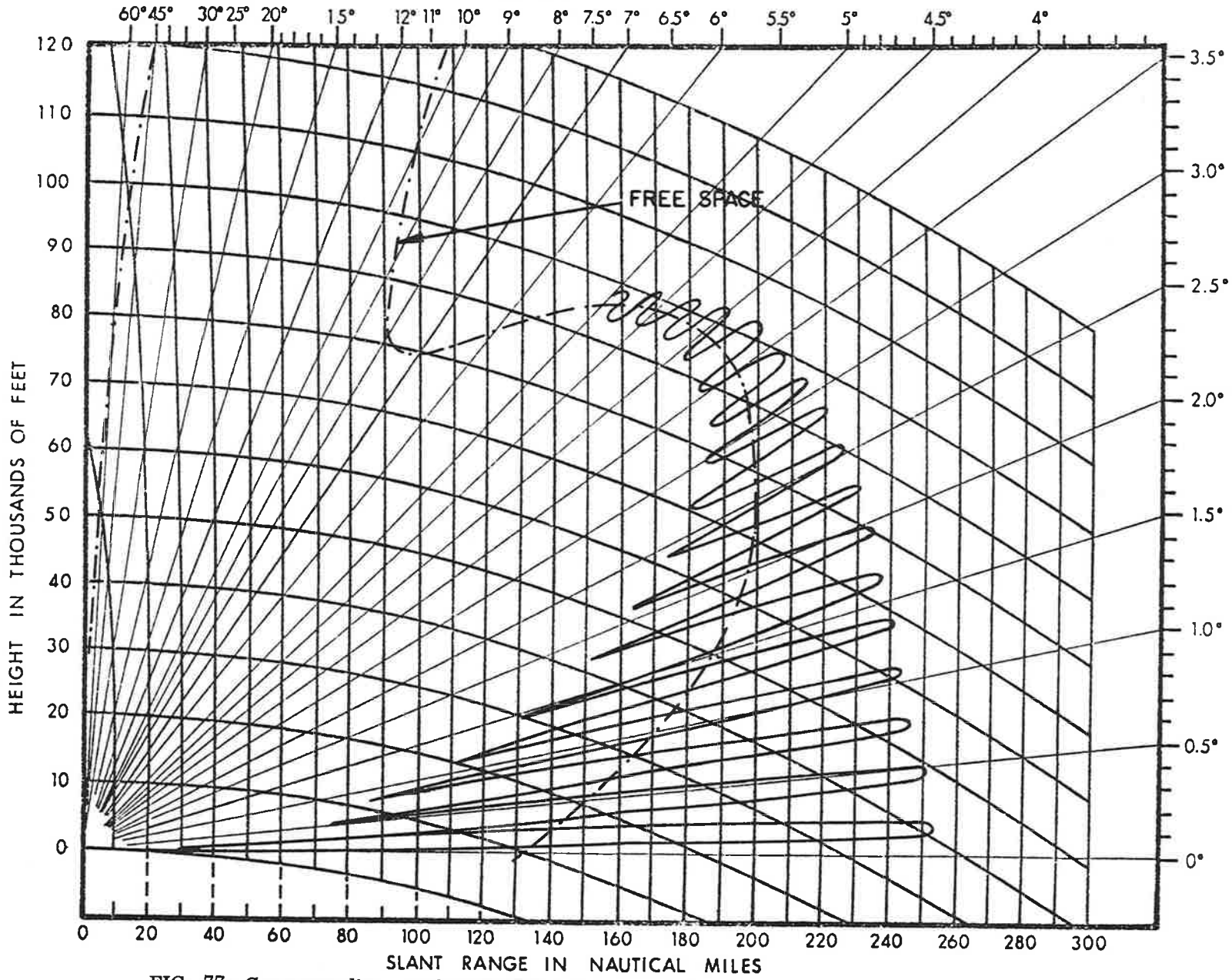

FIG. 77: Coverage diagram for the NADIF Fix I, II and III antennas. H_d = 921, H_o = 111', f = 1030 MHz, maximum free space range = 200 nautical miles.

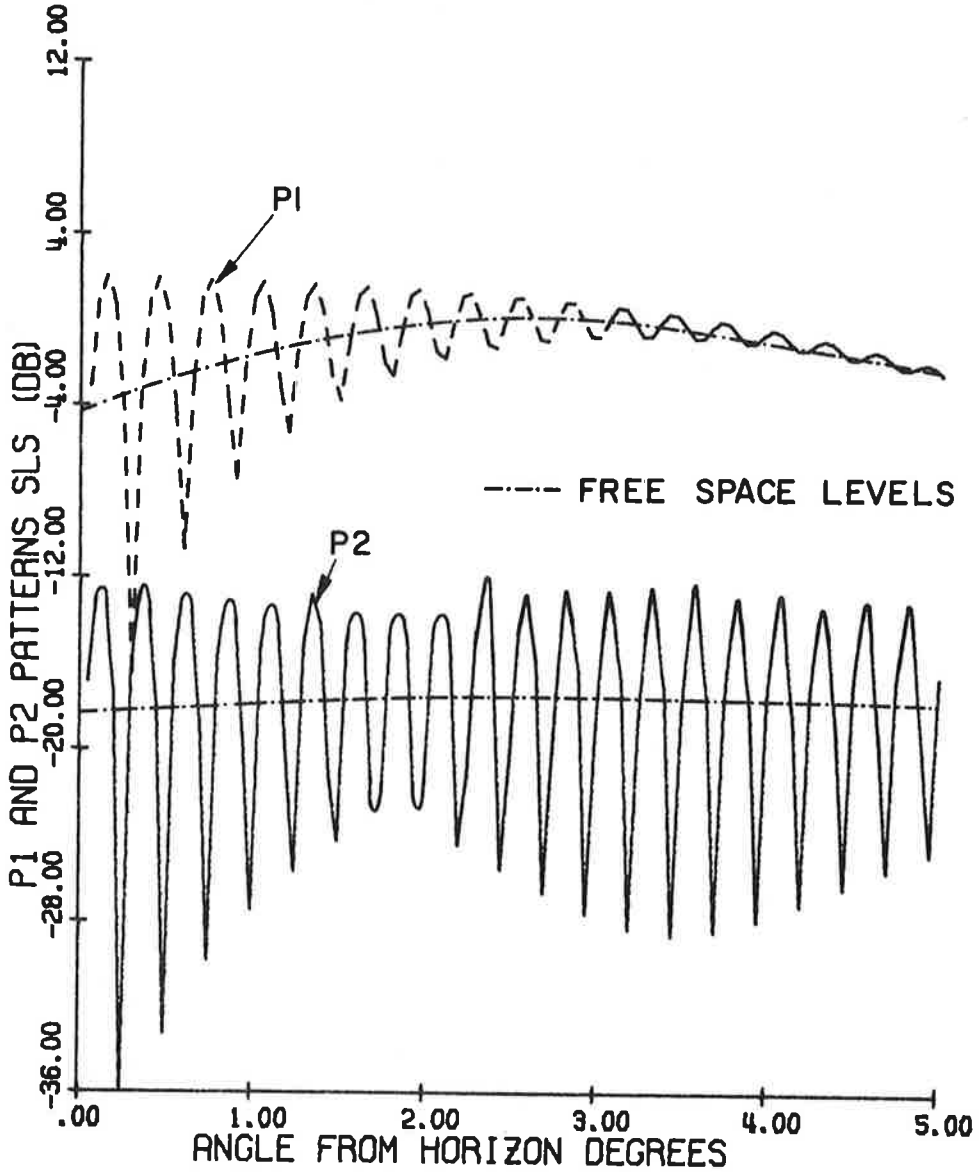

FIG. 78: P1 and P2 pulses as functions of θ.

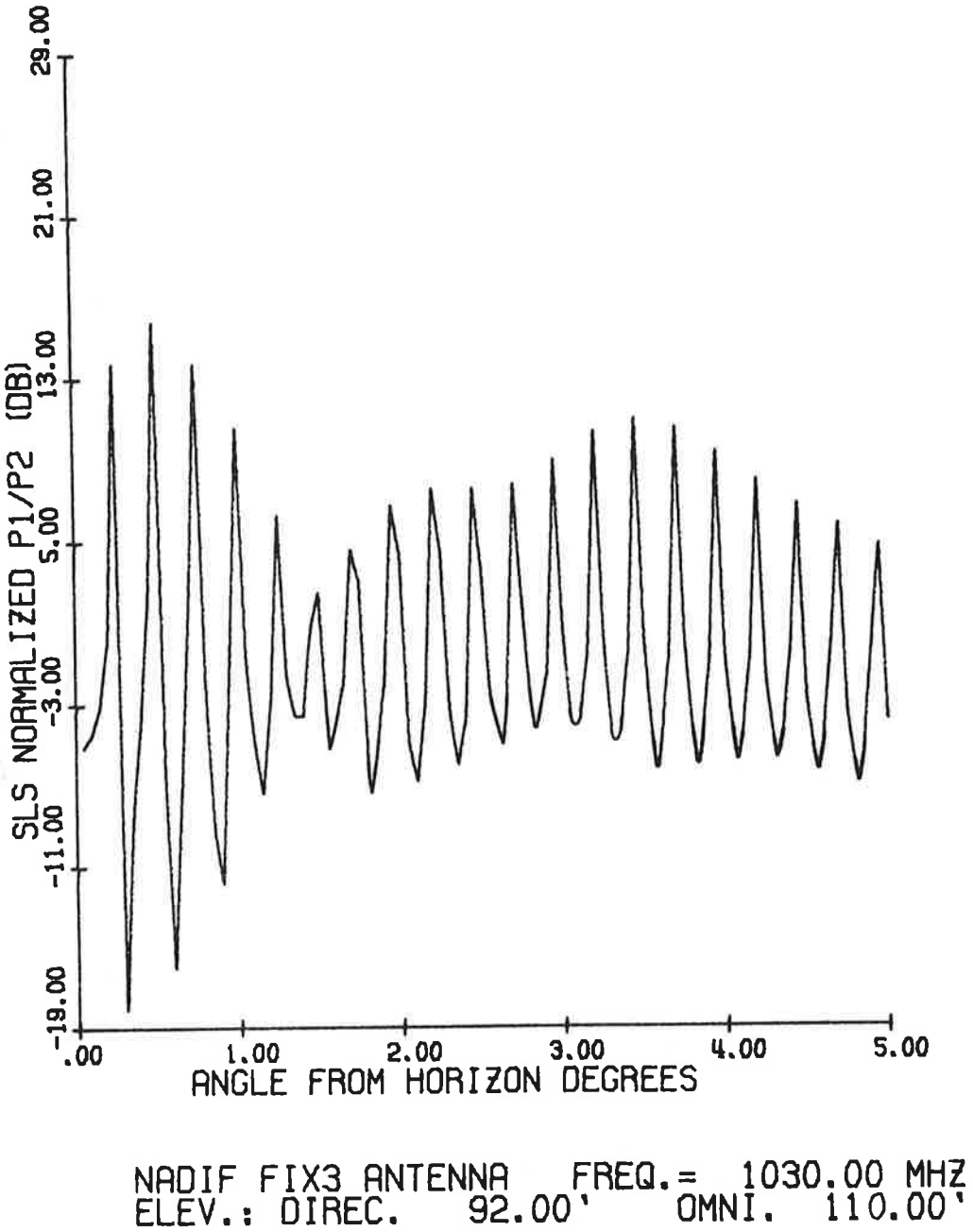

FIG. 79: Normalized pulse ratio as a function of θ.

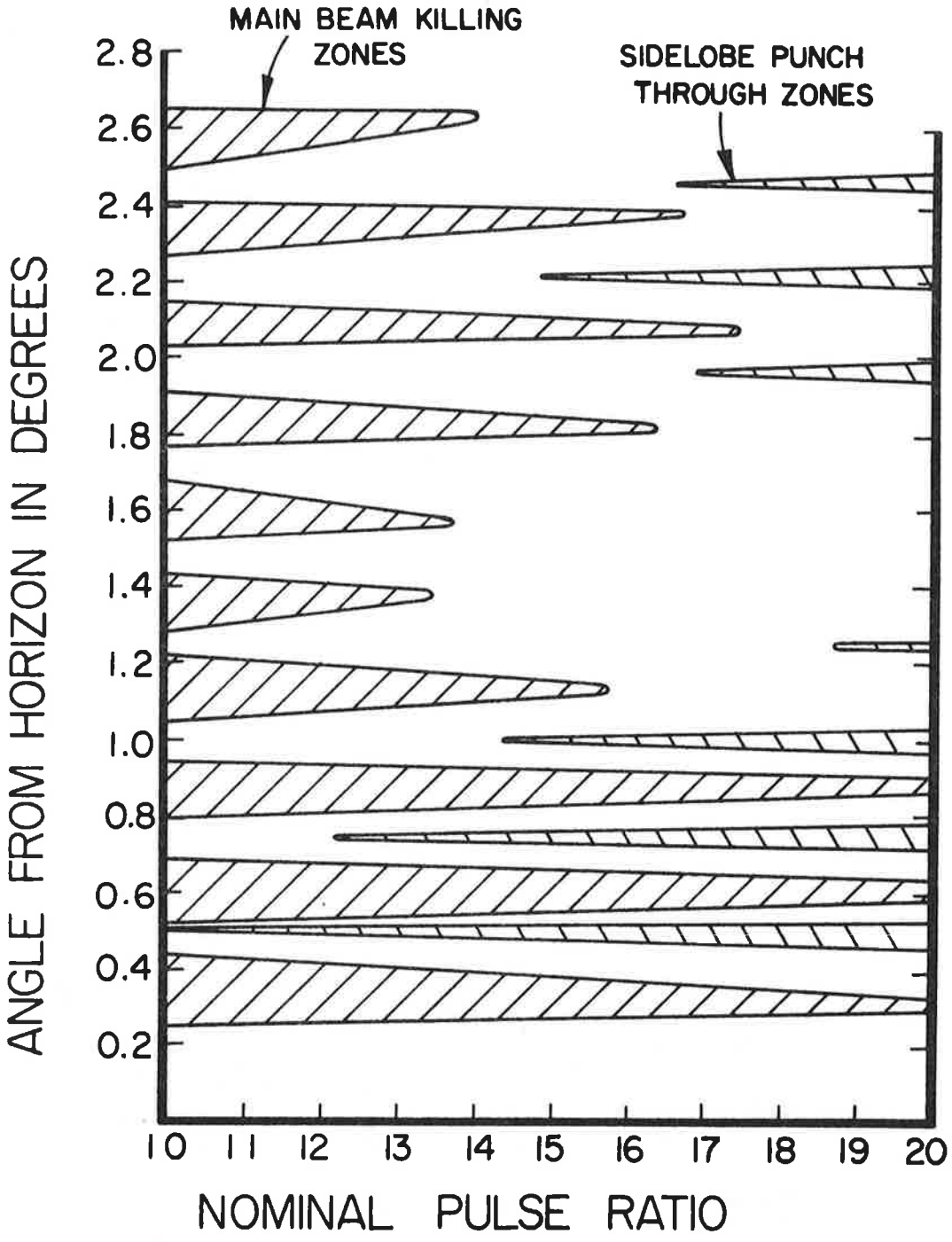

FIG. 80a: Mainbeam killing and sidelobe punch-through zones as functions of nominal pulse ratio for the NADIF FIX III antenna. H_1 = 92', H_0 = 110', f = 1030 MHz, a = 9 dB, b = 0 dB, L = -25 dB.

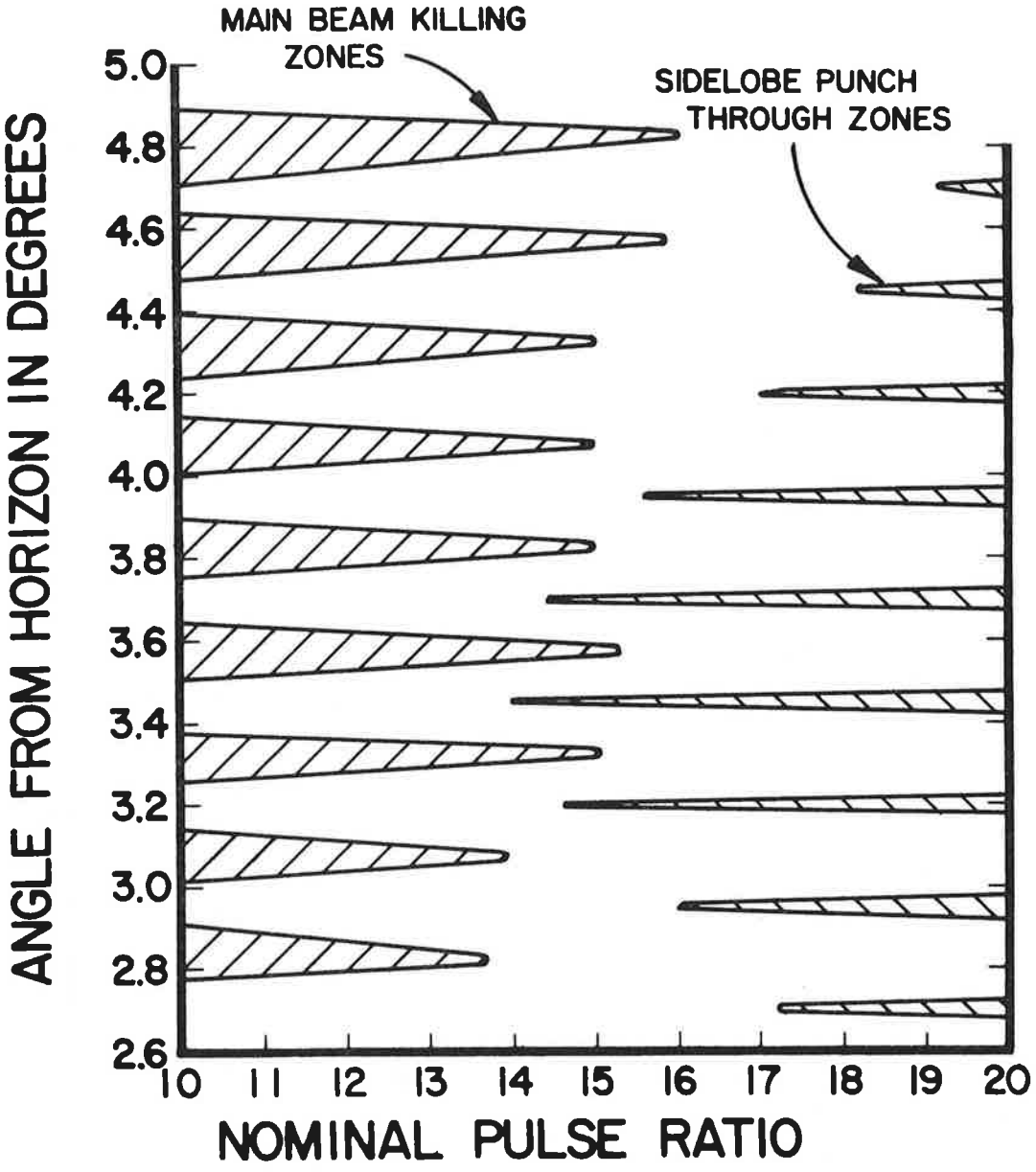

FIG. 80b: Mainbeam killing and sidelobe punch-through zones as functions of the nominal pulse ratio for the NADIF FIX III antenna. H_d = 92', H_o = 110', f = 1030 MHz, a = 9 dB, b = 0 dB, L = -25 dB.

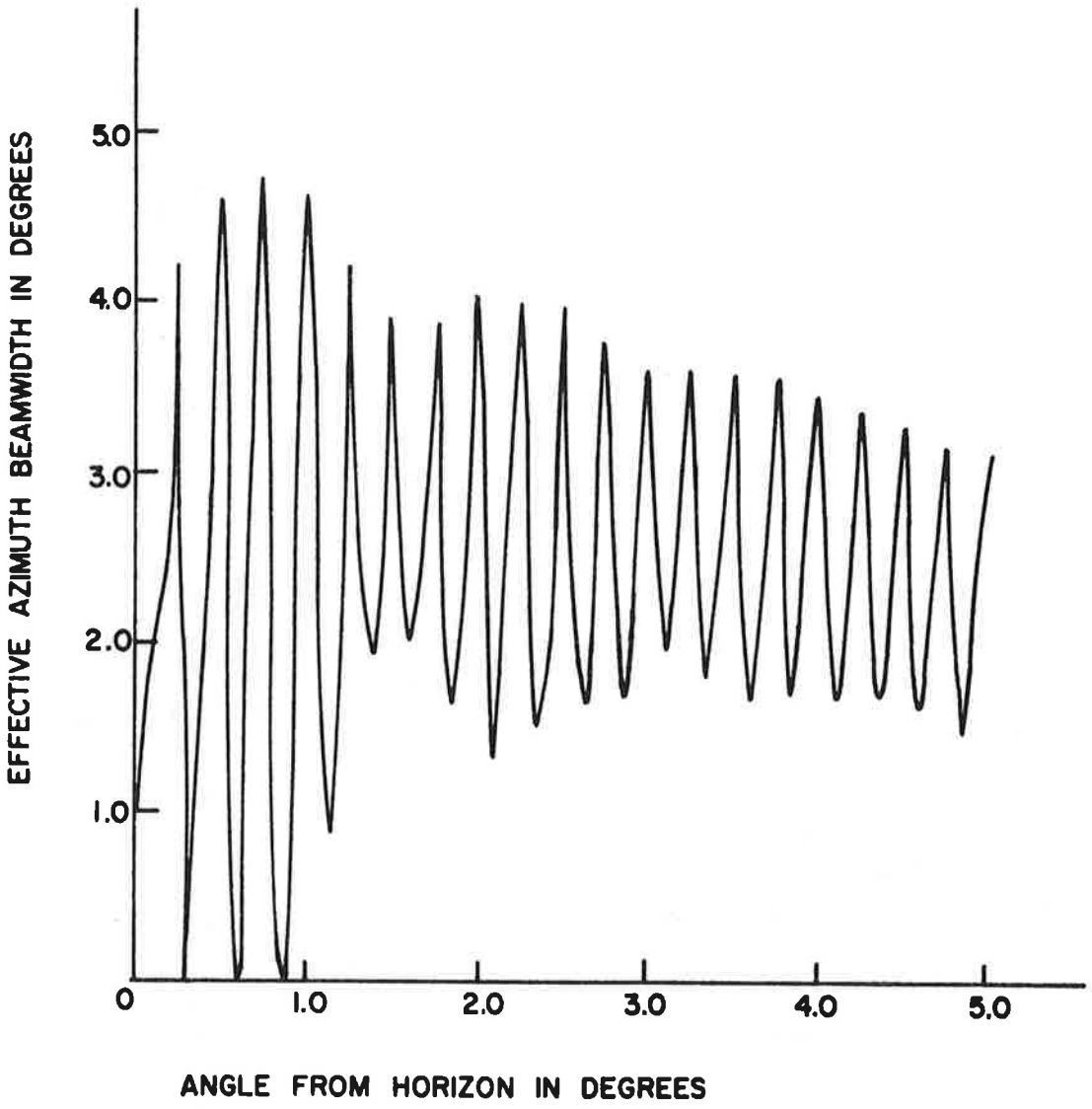

FIG. 81: Effective azimuth beamwidth as a function of angle from the horizon for NADIF FIX III antenna. H_d = 92', H_o = 110', f = 1030 MHz, nominal pulse ratio K_o = 18 dB.

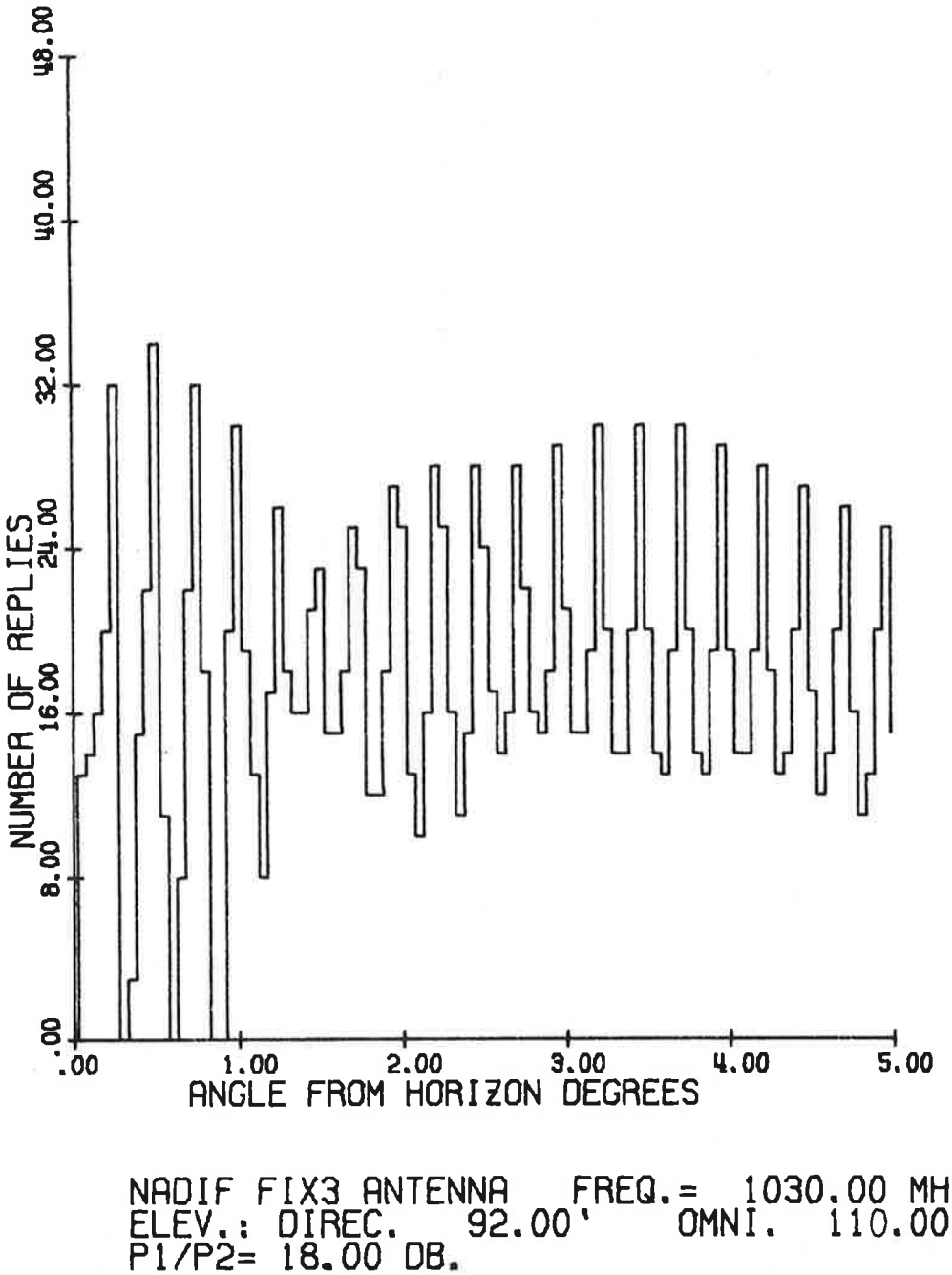

FIG. 82: Number of replies as a function of angle from the horizon.

5. GENERAL DISCUSSION

Detailed numerical results for the SLS mode performance of ATCRBS using different antennas have been given in Section 4. In the present section we give a short discussion of some of the results.

5.1 Summary of Important Results

Some of the selected results for the important parameters characterizing the overall performance of the ATCRBS are shown in Table 9. The table is prepared so that the various antennas involved may be compared with each other on the basis of different performance criteria. The different symbols used in Table 9 are explained as follows.

N_{MB} is the number of mainbeam killing zones in $0 \leq \theta \leq 5^{o}$ for nominal pulse ratio $K_0 = 18$dB and the threshold level a = 9dB.

N_{SL} is the number of sidelobe punch-through zones in $0 \leq \theta \leq 5^{o}$ for nominal pulse ratio $K_0 = 18$dB, threshold level b = 0dB and sidelobe level L = -25dB.

N_{max} is the maximum number of replies in $0 \leq \theta \leq 5^{o}$.

N_{min} is the minimum number of replies in $0 \leq \theta \leq 5^{o}$.

N_0 is the number of replies in free space.

R_{max} is the maximum range in nautical miles for ATCRBS in the presence of ground.

R_{min} is the minimum range in nautical miles for ATCRBS in the presence of ground.

R_0 is the maximum range in nautical miles for ATCRBS in free space.

5.2 General Discussion

Except for the existing hog-trough and Hazeltine open array antennas, it is found that the lobings in the elevation plane patterns of all other antennas in the presence of ground take place mostly in the region $\theta < 5^{o}$. For $\theta > 5^{o}$ the patterns above ground assume essentially the corresponding free space values. This is

6. REFERENCES

[1] A. Ashley, C. F. Phillips and A. A. Simolunas, "System capability of air traffic control radar beacon system", Department of Transportation Air Traffic Control Advisory Committee, Vol. 2, pp. 287-300, 1969. See also, N. K. Shaw and A. A. Simolunas, "System capability of air traffic control radar beacon system", Proc. IEEE, Vol. 58, No. 3, pp. 399-407, 1970.

[2] A. Ashley and J. S. Perry, "Beacons", in Chapter 38 of Radar Handbook (M. Skolnik, Ed.), McGraw-Hill Book Co., New York, pp. 38-1 - 38-33, 1970.

[3] P. R. Drouilhet, "The development of the ATC radar beacon system: past, present and future", IEEE Trans. on Communications, Vol. COM-21, No. 5, pp. 408-421, 1973.

[4] B. M. Poteat, W. B. Evans, A. W. Markusan, K. W. Connor, K. F. Horenkamp, D. Davis, and D. R. Logan, "ATCRBS antenna modification kit: Phase I", Westinghouse Defense and Electronic Systems Center, Systems Development Division, Baltimore, Maryland, July 25, 1973.

[5] P. Richardson, et al., "Air traffic control radar beacon system (ATCRBS): Phase I final engineering report", Texas Instruments Incorporated, Dallas, Texas, October 1973.

[6] V. Mazzola, P. W. Hannan, E. M. Newman and P. Kendrick, "ATCRBS antenna modification kit, Phase 1", Engineering Report No. 10991, Hazeltine Corporation, Greenlawn, New York, 1973.

[7] Frank LaRussa, Private communication, 1974.

[8] R. J. Giannini, J. H. Gutman and P. W. Hannan, "A cylindrical phased-array antenna for ATC interrogation", Microwave Journal, Vol. 16, No. 10, pp. 46-49, 1973.

[9] P. M. Woodward, "Method of calculating the field over a plane aperture required to produce a given polar diagram", J. Inst. Elect. Eng., Vol. 93, No. 10, Pt. IIIA, pp. 1554-1558, 1946. See also, P. M. Woodward and J. D. Lawson, "The theoretical precision with which an arbitrary radiation pattern may be obtained from a source of finite size", J. Inst. Elect. Eng., Vol. 95, No. 37, Pt. III, pp. 363-371, 1948.

[10] J. A. Stratton, "Electromagnetic Theory", McGraw-Hill Book Co., New York, pp. 490-497, 1941.

APPENDIX A
COMPUTER PROGRAM FOR IBM-360, MODEL 67

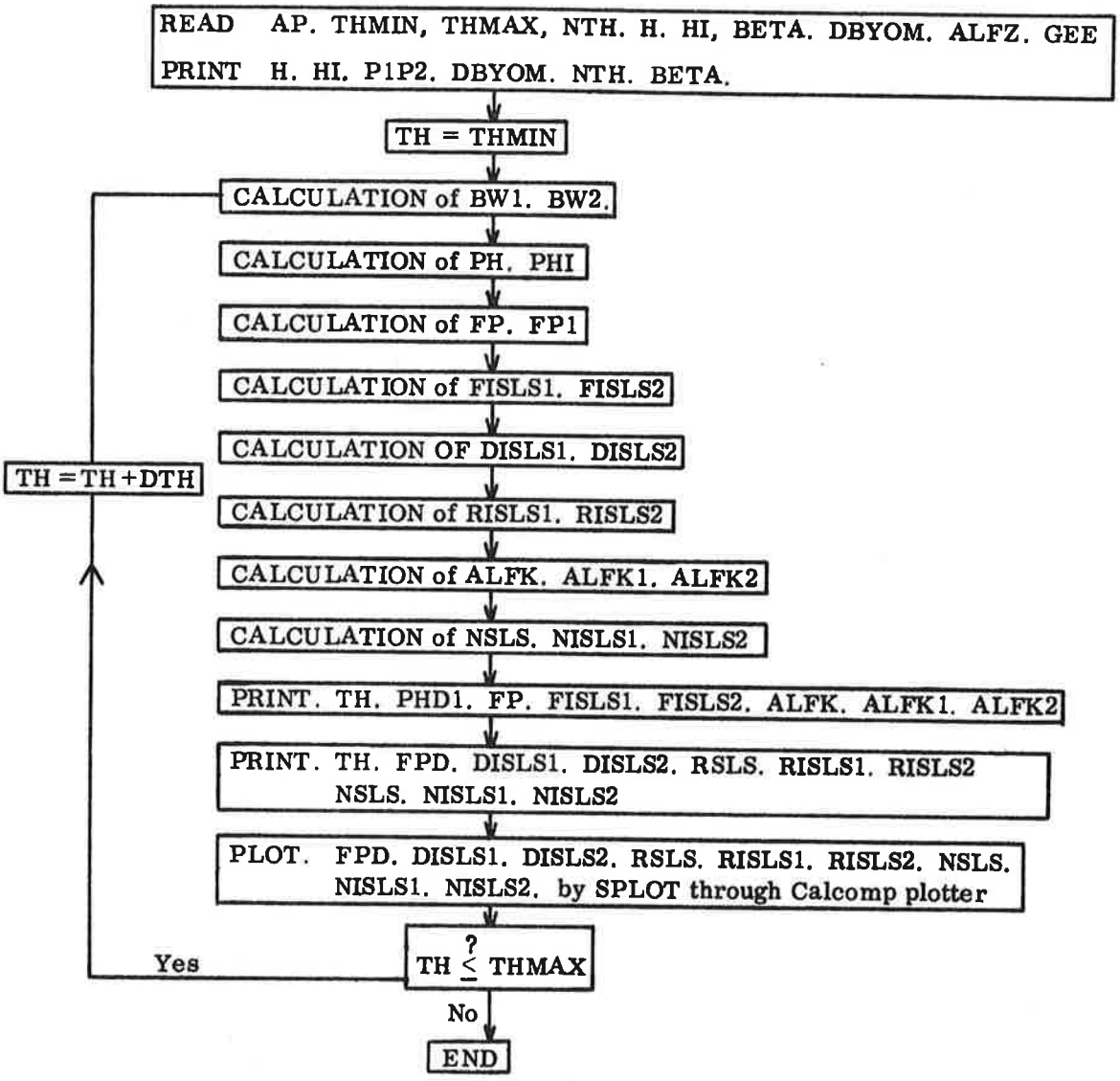

FIG. A-1: Flow diagram for the main program.

List of Some of the Symbols Used

ABS = Absolute value

ALFK = $\alpha_{eff}(\theta)$SLS

ALFK1 = $\alpha_{max}(\theta)$

ALFK2 = $\alpha_{min}(\theta)$

ALOG10 = Log 10

BETA = β

DISLS1 = 20 log 10 (FISLS1)

DISLS2 = 20 log 10 (FISLS2)

DR = $\pi/180.0$

DTH = (THMAX - THMIN)/(NTH - 1)

FISLS1 = P1 max(θ)

FISLS2 = P1 min(θ)

FP = P1(θ)SLS for H

FPD = 20 log 10 (FP)

FP1 = P1(θ)SLS for H1. FPD1 = 20 log 10 (FP1)

NSLS = N(θ)SLS

NISLS1 = $N_{max}(\theta)$

NISLS2 = $N_{min}(\theta)$

PH = Fd(θ)

PHD = 20 log 10 PH

PHDI = 20 log 10 PHI

PHI = Fd(-θ)

PI = π

REF = $\rho(\theta)$

RISL1 = DISLS1 - FPD1

RISLS2 = DISLS2 - FPD1

RSLS = PFD - FPD1

SIN1 = specified for each antenna

SQRT = Square root

TH = θ

Main Program

```
C   *** PROGRAM TO ANALIZE THE PERFORMANCE OF BEACON SYSTEMS ***
C
C    *** INPUT QUANTITIES :
C      AP        ANTENNA TYPYE;
C                1    WESTINGHOUSE ANTENNA
C                2    TEXAS INSTRUMENTS ANTENNA
C                3    HAZELTINE ANTENNA
C                4    EXISTING ANTENNA
C                5    NADIR FIX1 ANTENNA
C                6    TEXAS FIX ANTENNA
C                7    HAZELTINE ESCAN ANTENNA
C      THMAX     UPPER LIMIT FOR ELEVATION ANGLE IN PATTERN CALCULATION
C      THMIN     LOWER LIMIT FOR ELEVATION ANGLE IN PATTERN CALCULATION
C      BETA      TILTED ANGLE
C      NTH       NUMBER OF POINTS BETWEEN HORIZONTAL AND THMAX
C      H         ELEVATION OF DIRECTIONAL ANTENNA
C      H1        ELEVATION OF OMNIDIRECTIONAL ANERNNA
C      P1P2      RATIO OF P1 PULSE TO P2 PULSE AMPLITUDES IN DB
C      DBYOM     RATIO OF THE PORTION OF P1 PULSE RADIATED BY THE
C                DIRECTIONAL ANTENNA TO THAT RADIATED BY THE
C                OMNIDIRECTIONAL ANTENNA FOR ISLS CASE
C      ALFZ      NOMINAL BEAMWIDTH
C      GEE       CONSTANT RELATED TO THE SPEED OF ROTATION
       DIMENSION A(7),C(15,8)
       INTEGER AP
       DATA A /4.3738,1.7039,0.4554,1.1086,0.2644,0.6346,0.8108/
       DATA C /-64.85,-135.06,13.02,-64.55,-151.88,-47.04,-91.27,8*0.0,
      10.084,0.080,0.500,1.000,0.300,0.860,0.790,0.860,0.960,0.540,
      20.230,0.120,0.060,2*0.0,
      30.500,1.000,0.885,0.530,11*0.0,
      40.084,0.51,0.966,0.780,0.045,10*0.0,
      50.01,0.094,0.635,0.99,0.53,0.542,0.515,0.515,0.43,0.465,0.437,
      60.327,0.302,0.217,0.153,
      70.01,.039,.561,.995,.482,.45,.435,.42,.355,.417,.342,.35,.334
      8,.24,.12,
      90.079,0.072,0.03,0.53,0.915,0.945,0.845,0.845,0.315,0.034,5*0.0/
       READ(5,200) AP,THMIN,THMAX,NTH,H,H1,BETA,P1P2,DBYOM,ALFZ,GEE
       IF(NTH.GT.401) NTH=401
       IF (THMAX.GT.90.0) THMAX=90.0
C   *** OPERATING FREQUENCY : F=1030.0 MHZ
       F=1030.0
       PI=3.14159265
       DR=0.017453292
       PP1=-36.0
       PP2=0.0
       RAT1=-15.00
       RAT2=15.000
       NOPMIN=000
       NOPMAX=030
       CONST=4.*PI*F/11808.0
       P1P2=ABS(P1P2)
       DBYOM=ABS(DBYOM)
       QISLS=1.0/(10.0**(DBYOM/20.0))
       BW1=2.32-1./(10.0**((P1P2-DBYOM)/20.0))
       BW2=7.64-BW1
       BW1=20.0*ALOG10(BW1)
       BW2=20.0*ALOG10(BW2)
       DTH=(THMAX-THMIN)/(NTH-1)
       WRITE (6,212)
       GO TO (1,2,3,4,5,6,7), AP
```

main program (cont'd)

```
1     WRITE (6,201) BETA
      WRITE (7,201) BETA
      NS=7
      B=2.*5.4*F/11808.0
      GO TO 8
2     WRITE (6,202) BETA
      WRITE (7,202) BETA
      NS=13
      K1=3
      SIN1=0.07846
      GO TO 8
3     WRITE (6,203) BETA
      WRITE (7,203) BETA
      NS=4
      K1=1
      SIN1=0.22495
      GO TO 8
4     WRITE (6,204) BETA
      WRITE (7,204) BETA
      NS=5
      K1=3
      SIN1=0.47767
      GO TO 8
5     WRITE (6,205) BETA
      WRITE (7,205) BETA
      NS=15
      K1=3
      SIN1=0.0583
      GO TO 8
6     WRITE (6,206) BETA
      WRITE (7,206) BETA
      NS=15
      K1=3
      SIN1=0.0583
      GO TO 8
7     WRITE (6,207) BETA
      WRITE (7,207) BETA
      NS=10
      K1=4
      SIN1=0.11942
8     WRITE(6,208) H,H1,P1P2,DBYDM
      WRITE(7,209) H,H1,P1P2,DBYDM,P1P2,NTH
      H=12.0*H
      H1=12.0*H1
      DO 14 N=1,NTH
      TH=THMIN+(N-1)*DTH
      THETA=TH*DR
      SINTH=SIN(THETA)
      SQRT1=SQRT(2.+SINTH**2)
      REF=(3.*SINTH-SQRT1)/(3.*SINTH+SQRT1)
       TB=(TH-BETA)*DR
      SINTB=SIN(TB)
      COSTB=COS(TB)
      TC=(TH+BETA)*DR
      SINTC=SIN(TC)
      COSTC=COS(TC)
      IF (AP.EQ.1) GO TO 11
C ***FREE SPACE PATTERN FOR ALL EXPECT WESTINGHOUSE
      ARG1=SINTB/SIN1
      ARGN=SINTC/SIN1
```

main program (cont'd)

```
      PH=0.0
      PH1=0.0
      DO 10 K=1,NS
      ARG=PI*(ARG1-K+K1)
      IF (ABS(ARG).LE.0.0349) GO TO 9
      PH=PH+C(K,AP)*SIN(ARG)/ARG
      GO TO 101
    9 PH=PH+C(K,AP)
  101 ARGM=PI*(K1-K-ARGN)
      IF (ABS(ARGM).LE.0.0349) GO TO 102
      PH1=PH1+C(K,AP)*SIN(ARGM)/ARGM
      GO TO 10
  102 PH1=PH1+C(K,AP)
   10 CONTINUE
      GO TO 13
C ***FREE SPACE PATTERN FOR WESTINGHOUSE
   11  COSTH=COS(THETA)
      ARG2=PI*COSTB/2.
      ARG3=PI*SINTB/2.0
      PHZ=SIN(ARG2)*COS(ARG3)/COSTB
      AR2=PI*COSTC/2.0
      AR3=PI*SINTC/2.0
      PHX=SIN(AR2)*COS(AR3)/COSTC
      PH=PHZ*5.4201
      PH1=5.4201*PHX
      DO 12 K=1,NS
      ARG4=K*PI*B*SINTB
      ARGL=K*PI*B*SINTC
      PH=PH+2.*PHZ*A(K)*COS(ARG4+DR*C(K,AP))
      PH1=PH1+2.*PHX*A(K)*COS(DR*C(K,AP)-ARGL)
   12 CONTINUE
      PH=PH/15.686
      PH1=PH1/15.686
   13 IF (ABS(PH).LE.0.016035) GO TO 103
      PHD=20.0*ALOG10(ABS(PH))
      GO TO 104
  103 PHD=-36.00
  104 IF(ABS(PH1).LE.0.016035) GO TO 105
      PHD1=20.0*ALOG10(ABS(PH1))
      GO TO 106
  105 PHD1=-36.00
  106 IF (H.LE.0) GO TO 14
      ETA=PH1*REF/PH
      ARG5=CONST*H*SINTH
      FP=PH*SQRT(1.+ETA**2+2.*ETA*COS(ARG5))
      IF (FP.LE.0.016035) GO TO 107
      FPD=20.0*ALOG10(FP)
      GO TO 108
  107 FPD=-36.0
  108  IF (H1.LE.0.0) GO TO 14
      ARG6=CONST*H1*SINTH
      FP1=PH*SQRT(1.+ETA**2+2.*ETA*COS(ARG6))
      IF (FP1.LE.0.016035) GO TO 109
      FPD1=20.0*ALOG10(FP1)
      FPD2=FPD1-P1P2
      IF (FPD2.LE.-36.00) FPD2=-36.00
      GO TO 110
  109 FPD1=-36.0
      FPD2=FPD1
  110 FISLS1=FP+QISLS*FP1
```

SPLOT

```
      DIMENSION X(401),X1(800),X2(800),X3(800)
      DIMENSION Y1(401),Y2(401),Y3(401),Y4(401),Y5(401),Y6(401),Y7(401)
      REAL NR1,NR2,NR3
      DIMENSION NR1(800),NR2(800),NR3(800)
      DIMENSION T1(10),T2(10),T3(15),T4(10),T5(10)
      DIMENSION XPRINT(10),YPRNT1(10),YPRNT2(10),YPRNT3(10),YPRNT4(10)
      READ (5,21,END=500) (T1(I),I=1,10)
      READ (5,21) (T2(I),I=1,10)
      READ (5,24) (T3(I),I=1,14)
      READ (5,21) (T4(I),I=1,10)
      READ (5,21) (T5(I),I=1,10)
      READ (5,21) (XPRINT(I),I=1,8)
      READ (5,21) (YPRNT1(I),I=1,8)
      READ (5,21) (YPRNT2(I),I=1,8)
      READ (5,21) (YPRNT3(I),I=1,9)
      READ (5,21) (YPRNT4(I),I=1,8)
      READ (5,22) N
      M1=1
      M2=1
      M3=1
      DO 3 I=1,N
      READ (5,23) X(I),Y1(I),Y2(I),Y3(I),Y4(I),Y5(I),Y6(I),Y7(I)
     1,NNR1,NNR2,NNR3
      IF(I.NE.1) GO TO 100
      NR1(1)=NNR1
      NR2(1)=NNR2
      NR3(1)=NNR3
      X1(1)=X(I)
      X2(1)=X(I)
      X3(1)=X(I)
  100 IF((NNR1.EQ.NR1(M1)).AND.(I.NE.N)) GO TO 1
      M1=M1+1
      X1(M1)=(X(I)+X(I-1))/2.0
      NR1(M1)=NR1(M1-1)
      M1=M1+1
      X1(M1)=X1(M1-1)
      NR1(M1)=NNR1
    1 IF((NNR2.EQ.NR2(M2)).AND.(I.NE.N)) GO TO 2
      M2=M2+1
      X2(M2)=(X(I)+X(I-1))/2.0
      NR2(M2)=NR2(M2-1)
      M2=M2+1
      X2(M2)=X2(M2-1)
      NR2(M2)=NNR2
    2 IF((NNR3.EQ.NR3(M3)).AND.(I.NE.N)) GO TO 3
      M3=M3+1
      X3(M3)=(X(I)+X(I-1))/2.0
      NR3(M3)=NR3(M3-1)
      M3=M3+1
      X3(M3)=X3(M3-1)
      NR3(M3)=NNR3
    3 CONTINUE
      CALL PLT(X(2),Y1(2),N-1,X(2),Y2(2),N-1,0.0,0.0,0.0,0,XPRINT(1),
     1YPRNT1(1),T1(1),T2(1),T4(1))
      CALL PLT(X(2),Y1(2),N-1,X(2),Y3(2),N-1,X(2),Y4(2),N-1,XPRINT(1)
     1,YPRNT2(1),T1(1),T2(1),T3(1))
      CALL PLT(X(2),Y5(2),N-1,0.0,0.0,0,0.0,0.0,0,XPRINT(1),YPRNT3(2),
     1T1(1),T2(1),T5(1))
      CALL PLT(X(2),Y5(2),N-1,X(2),Y7(2),N-1,0.0,0.0,0,XPRINT(1),
     1YPRNT3(1),T1(1),T2(1),T3(5))
```

SPLOT (cont'd)

```
      CALL PLT(X1(1),NR1(1),M1,0.0,0.0,0,0.0,0.0,0,XPRINT(1),YPRNT4(1)
     1,T1(1),T2(1),T4(1))
      CALL PLT(X2(1),NR2(1),M2,X3(1),NR3(1),M3,0.0,0.0,0,XPRINT(1),
     1YPRNT4(1),T1(1),T2(1),T3(1))
21    FORMAT(10A4)
22    FORMAT (I4,/)
23    FORMAT (8E12.4,7X,I3,9X,I3,8X,I3)
24    FORMAT (14A4)
500   STOP
      END
      SUBROUTINE PLT(X1,Y1,N1,X2,Y2,N2,X3,Y3,N3,XPRINT,YPRINT,T1,T2,T3)
      DIMENSION X1(800),X2(800),X3(800)
      DIMENSION Y1(800),Y2(800),Y3(800)
      DIMENSION XPRINT(10),YPRINT(10),T1(10),T2(10),T3(10)
      CALL PLTXMX(10.0)
      CALL PSCALE(5.0,1.0,XMIN,DX,X1,N1,1,X2,N2,1,X3,N3,1)
      CALL PSCALE(5.0,1.0,YMIN,DY,Y1,N1,1,Y2,N2,1,Y3,N3,1)
      CALL PLTOFS(XMIN,DX,YMIN,DY,3.0,3.0)
      CALL PAXIS(3.0,3.0,XPRINT,-30,5.0,0.0,XMIN,DX,1.0)
      CALL PAXIS(3.0,3.0,YPRINT,30,6.0,90.0,YMIN,DY,1.0)
      CALL PLTREC
      IF (N1.EQ.0) GO TO 1
      CALL PLINE(X1,Y1,N1,1,0,0,1.0)
1     IF (N2.EQ.0) GO TO 2
      CALL PDSHLN(X2,Y2,N2,1,0.1,1.0)
2     IF (N2.EQ.0) GO TO 3
      CALL PCTRLN(X3,Y3,N3,1,1.0)
3     CL=PSYMLN(0.15,30)
      CALL PSYMB(5.25-CL/2.,2.0,0.15,T1,0.0,40)
      CALL PSYMB(5.25-CL/2.,1.8,0.15,T2,0.0,40)
      CALL PSYMB(5.25-CL/2.,1.6,0.15,T3,0.0,40)
      CALL PLTEND
      RETURN
      END
```

APPENDIX B
REPORT OF INVENTIONS

A diligent review of the work performed under this contract has revealed no new innovation, discovery, improvement or invention.